4-1998

Groundwater Hydraulics and Slope Stability Analysis: Elements for Prediction of Shoreline Recession

William W. Montgomery
Western Michigan University

GROUNDWATER HYDRAULICS AND SLOPE STABILITY ANALYSIS: ELEMENTS FOR PREDICTION OF SHORELINE RECESSION

by

William W. Montgomery

A Dissertation
Submitted to the
Faculty of The Graduate College
in partial fulfillment of the
requirements for the
Degree of Doctor of Philosophy
Department of Geology

Western Michigan University
Kalamazoo, Michigan
April 1998

GROUNDWATER HYDRAULICS AND SLOPE STABILITY ANALYSIS: ELEMENTS FOR PREDICTION OF SHORELINE RECESSION

William W. Montgomery, Ph.D.

Western Michigan University, 1998

Studies documenting the roles that geologic materials and groundwater play in Great Lakes bluff recession are rare. This study reports findings concerning relationships between bluff lithology, bluff hydrology, and bluff recession along a 10-mile stretch of eastern Lake Michigan shoreline in heterogeneous Pleistocene deposits. According to a newly-developed, field-tested, GIS-based methodology, bluffs in the study area can be characterized lithologically as sand, clay, or mixed sand/clay, and can be characterized hydrologically as exhibiting either high head or low head

Geotechnical analysis indicates that Atterberg limits, index properties, consolidation state, and drainage conditions affect the shear strength of bluff materials. Silty grey diamicton, a major constituent of clay-dominated bluffs, exhibits high undrained shear strength, and $\phi' = 28^{o}$. Laminated, fine-grained clay, a major constituent of mixed sand/clay bluffs, has very low undrained shear strength, and $\phi' = 20^{o}$. Sandy bluffs in the study area exhibit a range of effective stress failure envelope angles: $34^{o} < \phi' < 43^{o}$.

Comparison of bluff characterization with historical recession patterns indicates that bluff lithology and hydrology influence recession. Mixed sand/clay bluffs with high hydraulic head were found to have receded up to 100 feet (30.0 m) over the long term (1938 to 1996), whereas bluffs characterized as all clay or all

sand receded 50 feet (15.0 m) or less during this time. Over the short term (1989 to 1996), a period in which Lake Michigan water levels were not unusually high, mixed sand/clay bluffs were the only ones in the study area to show measurable retreat (> 4 feet, 1.2 m).

Results of Factor of Safety analyses performed upon bluffs at six field sites suggest that effective stress-based analyses that reflect long-term, drained conditions may be most appropriate in modeling recession in sandy bluffs of both high and low head, mixed sand/clay bluffs of both high and low head, and diamicton bluffs with high head. Diamicton bluffs with low head are apparently not destablilzed by groundwater; in this case, total stress-based Factor of Safety analysis may be an alternative method for modeling recession.

INFORMATION TO USERS

This manuscript has been reproduced from the microfilm master. UMI films the text directly from the original or copy submitted. Thus, some thesis and dissertation copies are in typewriter face, while others may be from any type of computer printer.

The quality of this reproduction is dependent upon the quality of the copy submitted. Broken or indistinct print, colored or poor quality illustrations and photographs, print bleedthrough, substandard margins, and improper alignment can adversely affect reproduction.

In the unlikely event that the author did not send UMI a complete manuscript and there are missing pages, these will be noted. Also, if unauthorized copyright material had to be removed, a note will indicate the deletion.

Oversize materials (e.g., maps, drawings, charts) are reproduced by sectioning the original, beginning at the upper left-hand corner and continuing from left to right in equal sections with small overlaps. Each original is also photographed in one exposure and is included in reduced form at the back of the book.

Photographs included in the original manuscript have been reproduced xerographically in this copy. Higher quality 6" x 9" black and white photographic prints are available for any photographs or illustrations appearing in this copy for an additional charge. Contact UMI directly to order.

UMI

A Bell & Howell Information Company
300 North Zeeb Road, Ann Arbor MI 48106-1346 USA
313/761-4700 800/521-0600

ACKNOWLEDGMENTS

In a multidisciplinary study such as this, many parties contribute to a successful outcome. I am indebted to my research advisors, Dr. Ron Chase, Dr. Vic Torrey, Dr. Alan Kehew, and Dr. Duane Hampton for their technical guidance and constructive criticism throughout the research and reporting process. I am also extremely grateful to Dr. Lawson Smith, who buoyed my spirits with his counsel and contributed intellectually at critical junctures during the early stges of the research. Ms. Joan Pope of the Waterways Experiment Station was particularly encouraging during the research process as well. Special thanks also go to Mr. Greg Anderson of the WMU GIS Research Center, without whose help the enclosed GIS characterization maps would have suffered immensely.

Many U.S. Army Corps of Engineers personnel provided assistance at the Waterways Experiment Station during geotechnical testing (David Bennett, Una Sanders, James Lowe, and John Peters) and Factor of Safety computer analysis (Wipawi Vanadit-Ellis and Earl Edris), and in the Detroit District during GIS airphoto analysis (Roger Gauthier, Lisa Jipping, Bill Kempisty, David Gerczak, Lyle Thompson, and Rob Ferguson). Mateco Drilling Co. personnel (Lisa, Dale, Steve, and Joyce Elliott, and especially Steve Rempalski) provided very professional service and technical expertise during the drilling, sampling, and finishing of piezometers. Thanks are also due to Dr. Russell Harmon and the U.S. Army Research Office (Grant Number DAAH04-96-1-0064) for supporting this research.

Without the enlightened foresight and encouragement of a number of Lake Michigan bluff residents, this study would not have been well-grounded in field data.

Thanks go to Mr. Wm. Erby Smith (Wau-Ken-A), Mr. Peter Brown and Mr. Andrew Marks (Miami Park), Mr. Bill Nelson of the Allegan County Road Commision (116th Avenue), Mr. Jack Pettet (Fabun Road and West Side County Park), Mr. Milton Haan of the Allegan County Parks Department, and Verne Cappell and Dan Zentello (Consumers Power, now Consumers Energy) for facilitating access to the six field sites that continue to yield valuable data.

The most enlightened foresight, however, was exhibited by my family and friends during this process. They recognized my need to accomplish this step in my development, and their support was unwavering. To my son Evan and my daughter Katie, I will be forever grateful that you allowed me to show you how to climb a mountain and then helped me do it. To my mother Evelyn and my father Bill, I will be forever grateful that you have never ceased to believe in me. To my wife Marcia, I will simply be forever grateful.

William W. Montgomery

TABLE OF CONTENTS

CHAPTER

CHAPTER

CHAPTER

CHAPTER

LIST OF TABLES

LIST OF FIGURES

List of Figures—continued

CHAPTER I

INTRODUCTION

Statement of the Problem

Coastal areas often combine beautiful settings with complex geology. The former attracts large numbers of people while the latter complicates interpretations of systems and processes. There is increasing population pressure being applied along all of America's coastlines, and the Great Lakes are no exception (Williams, 1991). With increasing population density, adverse effects of natural processes such as shoreline recession become magnified and cause great public concern.

The Great Lakes are of particular interest in this context. First, much of their shoreline length is composed of glacial materials that are relatively susceptible to erosion and recession. Second, as recipients of drainage from a huge watershed, some of the Great Lakes have been subject to significant (up to 6 feet) swings in lake level in modern history. When high storm and wave activity are superimposed upon periods of high lake level there is clear evidence of wave-induced removal of shoreline material, and a panic mentality often sets in with resulting public outcry.

An unfortunate consequence of the cyclicity of lake level rise and fall is that it has tended to result in cyclic shoreline recession research (Meadows et al., 1991). Classic research was triggered by high lake levels in the 1950s (e.g., Powers, 1958) and 1970s (Davis, 1976; Hands, 1979, 1980), but much of it was directed on nearshore processes involving wave and current interaction with mobile sand. More recently, research efforts directed toward a better understanding of the role of

geologic framework in shoreline recession has been undertaken by some researchers (e.g., Nairn, 1992; Boyd, 1992; Davidson-Arnott, 1986), especially with respect to the interaction of waves and currents with cohesive and non-cohesive substrates in the Great Lakes. These workers have advanced arguments suggesting that long-term recession may not be directly tied to lake level. They also suggest that times of low lake level do not guarantee a halt in recession.

Field observations confirm that shoreline recession does not halt during times of lower lake level; bluff recession continues to occur on many segments of the Lake Michigan shore during these times. However, due in part to cyclic research, a gap remains in our knowledge base concerning coastal evolution in the Great Lakes during times of lower lake level. With 1989-96 lake levels down from historic highs, this is an excellent time to identify and study factors other than wave and current-induced erosion that play a role in ongoing shoreline recession in the Great Lakes.

Research Goals

This research is designed to focus on the roles that groundwater and lithology play in recession along Great Lakes shorelines composed of glacial materials. Prediction of where and when recession is likely to occur may be improved if these factors are better understood. In particular, geologic/hydrologic mapping, determination of geotechnical properties, and civil engineering principles and techniques may be utilized to produce a recession prediction methodology that may have wide applicability in glaciated terranes. There are several specific goals that have driven this research.

Develop a GIS-Compatible Characterization of Bluff Lithology and Hydrology

One goal of this study is to develop a bluff characterization methodology that can take full advantage of readily available lithologic and hydrologic data. It is hypothesized that adequate characterization of bluff geology and hydrogeology for the purposes of recession prediction can be achieved through a combination of traditional field mapping and analysis of subsurface well data. A methodology that can take full advantage of these data in lieu of obtaining expensive proprietary data (e.g., through drilling) would be very cost-effective, and cost-effectiveness could in turn promote utilization of the methodology in other areas. Geographic Information System (GIS) technology was used to facilitate bluff lithologic/hydrologic characterization in this study (Montgomery et al., 1996a).

Improve Understanding of Failure Mechanics

Another important goal of this study is to gain insight into the timing and mechanics of Lake Michigan bluff failure. It is hypothesized that different lithologic/hydrologic conditions produce different rates and mechanisms of failure. Six field sites interpreted to represent different lithologic/hydrologic conditions were selected for field study. Drilling and geotechnical sampling were conducted at these sites, and long-term monitoring of groundwater conditions and slope failure is underway in order to improve understanding of timing, rates, and geometries of failure in these settings (Chase et al., 1997).

Determine Geotechnical Controls on Bluff Failure

Another goal of this study is to utilize civil engineering-based limit equilibrium analysis as a tool in recession prediction. This technique has been used

with some success in previous studies of shoreline recession in the Great Lakes (Edil and Vallejo, 1977; Quigley and Gelinas, 1976), but it requires geotechnical data from undisturbed subsurface soil samples. Undisturbed soil samples of different lithologies were retrieved at the six field sites, and extensive geotechnical testing was performed at the United States Army Corps of Engineers Waterways Experiment Station. The geotechnical information generated and analyzed for this study is the first of its kind from the eastern shore of Lake Michigan. It allowed for the testing of the hypothesis that geotechnical properties, in conjunction with certain hydrologic conditions, exert a strong and perhaps unique control on shoreline recession (Montgomery et al., 1996b).

Determine Historical Bluff Recession Patterns and Their Relation to Bluff Lithology and Hydrology

Previous determination of recession rates on the eastern shore of Lake Michigan has been performed by Buckler (1987), Buckler and Winters (1975, 1983), Seibel (1972), and Powers (1958), among others. However, the recent application of GIS technology to shoreline change analysis (Johnson and Johnston, 1995; Law et al., 1991) has improved the prospect of greater accuracy and precision in analysis of Great Lakes shoreline recession. High-resolution airphoto analysis of both short-term (1989-1996) and long-term (1938-1996) bluffline recession was undertaken in three subareas of the overall study area. In conjunction with the GIS-based lithologic/hydrologic bluff characterization, GIS-based airphoto analysis allowed for a detailed comparative study to be performed in order to test the hypothesis that lithology and hydrology play unique roles in determining rates and locations of shoreline recession (Montgomery et al., 1997).

Study Area

A strip of western Allegan County, Michigan shoreline approximately 10 miles (16 km) long between the cities of South Haven and Saugatuck was chosen as the study area (Figure 1). This area is optimum for study for a number of reasons.

The stratigraphy of the study area is diverse and variable. It is representative of glacial deposits present throughout the Great Lakes. Lithologically, the study area is composed of dominantly sand, dominantly clay, or mixed sand / clay bluffs. Hydrologically, there is sufficient well control to create hydraulic head maps of reasonable accuracy. These wells serve an additional purpose in that they provide lithologic data both in areas of covered slope and below lake level. Lithologic data below lake level can provide for characterization of subaqueous nearshore geology, which is required for accurate modeling of recession of both cohesive and cohesionless shore types (Philpott, 1984; Nairn, 1992).

There are some individual groins and seawalls in parts of the study area, but there are no massive engineering structures present. The individual groins and seawalls in the study area probably have had some local impact on recession rates on short temporal scales, but their general state of disrepair is indicative of their ineffectiveness over the long term. As such, their impact on 1938-1996 long-term recession patterns is believed to be minimal. Furthermore, inspection of 1938 air photos reveals that, at least in the areas of detailed airphoto analysis, these devices were not even present in 1938.

In summary, the study area is an excellent microcosm of Great Lakes shorelines composed of complex combinations of glacial geology and hydrology. It has sufficient population density to provide adequate well control, but the shoreline is not engineered to the degree that it responds unnaturally to physical processes.

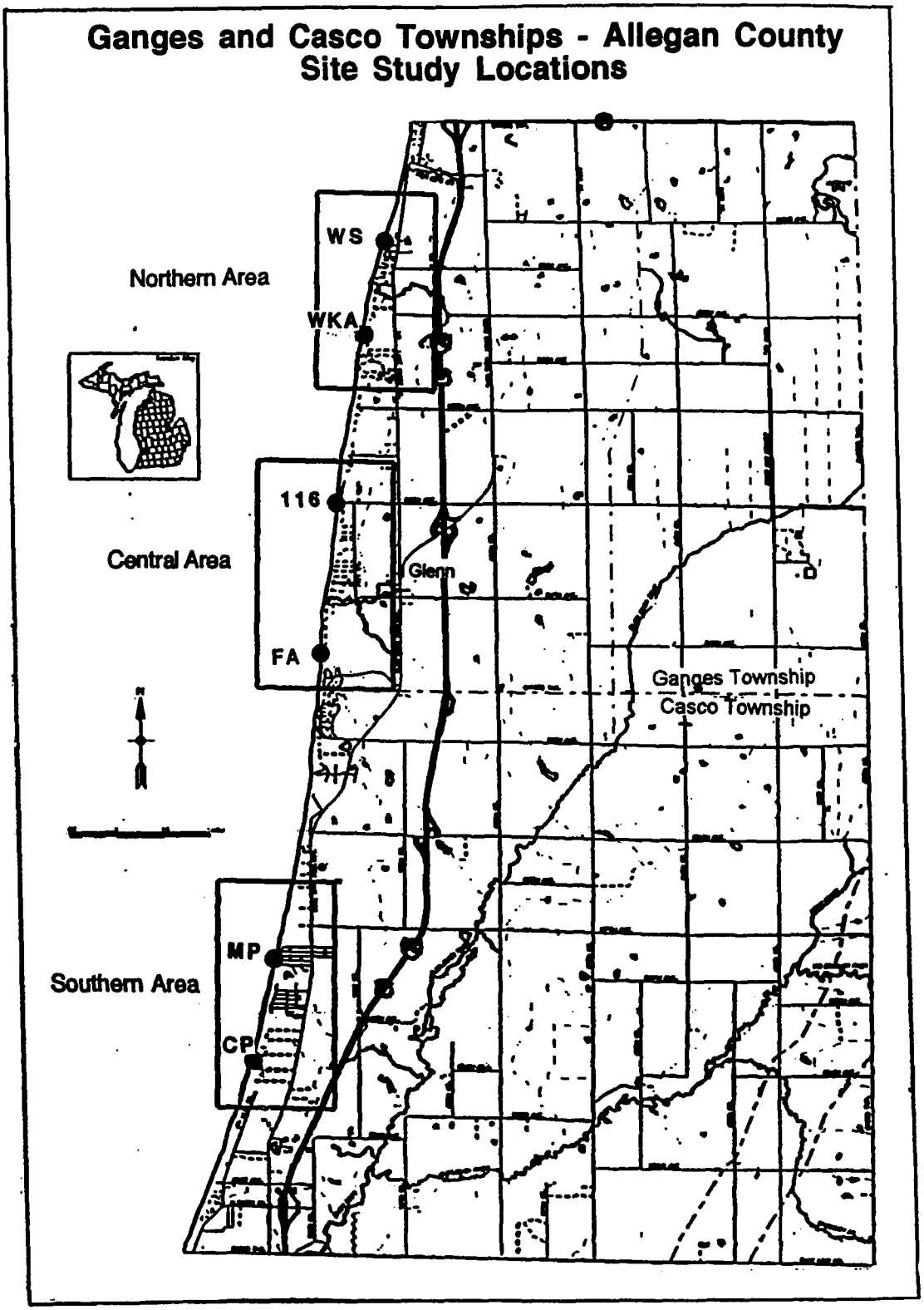

Figure 1. Map of Study Area Showing Locations of Monitoring Sites and Areas of Historical Bluff Recession Analysis.

Furthermore, logistics are favorable for the monitoring of slope failure and groundwater conditions on a weekly or bi-weekly basis, a frequency which is unprecedented in studies of Great Lakes shoreline recession.

Regional Geologic/Hydrologic Setting

Geologically, the study area is classified as part of the Lake Border Morainic System (Farrand and Bell, 1982; Hansel, 1985; Monaghan and Larson, 1986) (Figure 2). Lake Michigan abuts and overlaps the moraine in the study area. Deposits include fine- to medium-grained, buff-colored, laminated to cross-bedded quartzose sand interbedded with very fine-grained, laminated, reddish brown, often varved clay; and reddish-brown to gray to blue-gray diamicton containing clasts ranging in size from clay to boulders. Environments of deposition for the sand are interpreted to range from lacustrine to fluvial-deltaic, while the very fine-grained clay is interpreted to have been deposited in lacustrine environments.

The diamicton occurs in several layers or sheets in the study area, varying in thickness from less than 3 feet (0.91 m) to 20 feet (6.1 m) or more. Pebble- and boulder-sized clasts in the diamicton are of variable lithology, including what are interpreted to be Paleozoic carbonates and sandstones and Precambrian igneous and metamorphic rocks. Local clast orientation in one diamicton layer was measured by Chase (1990). The composition and texture of the diamicton layers is consistent with an interpreted glacial origin. In some exposures in the southern part of the study area, low-angle thrust faults and overturned bedding are interpreted to be present, but in most of the study area it is difficult to see internal structure and bedding in the diamicton.

The stratigraphy of the area is complex. Chase (1990) has mapped the area in detail, while Monaghan and Larson (1986) and Monaghan (1990) have focused on

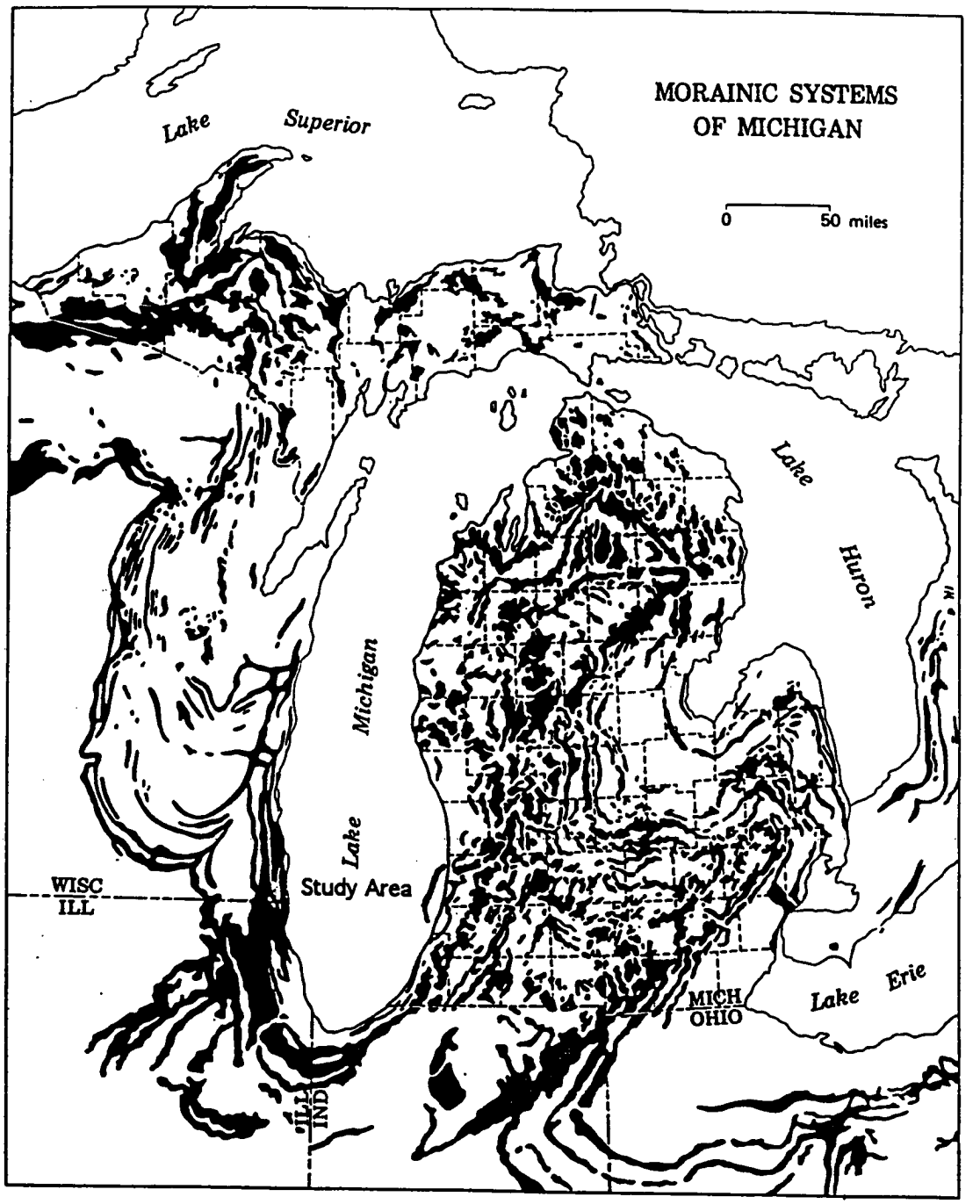

Figure 2. Location of Study Area in the Context of Regional Morainic Systems (after Farrand and Bell, 1982).

the dating and correlation of the diamicton layers to other areas in the Great Lakes. Within the study area, Monaghan and Larson (1986) designated a type section for the Glenn Shores till (Figure 3), the oldest diamicton exposed in the study area. Radiocarbon dates from organic material from lacustrine deposits immediately above the Glenn Shores till cluster for the most part in the range of 37,000 - 48,000 years BP (Monaghan and Larson, 1986).

The Glenn Shores type section contains two younger diamictons as well: the Ganges and Saugatuck tills (Figure 3). Along the length of the Lake Michigan bluffs in the study area, it is these two younger diamictons that are most commonly exposed, while the Glenn Shores till is interpreted to have been penetrated at depths below lake level in some wells.

The two younger diamictons are interpreted to record late Wisconsinan (Michigan Subepisode; Johnson et al., 1997) ice advances from the Lake Michigan lobe of the Pleistocene Laurentide ice sheet. Monaghan and Larson (1986) suggest that the advance that deposited the Ganges till in the study area formed the Tekonsha Moraine further east in south-central Michigan, whereas the later advance that deposited the Saugatuck till in the study area formed both the Kalamazoo Moraine (near Kalamazoo, MI) and the Lake Border Moraine as well. The time of formation of the Lake Border Morainic System is interpreted to be about 14,000 years BP (Hansel et al., 1985; Gephardt et al., 1982, 1983).

Although the Saugatuck and Ganges tills represent the most readily identifiable surface mapping units on the bluff face, there is extreme lateral variation within the study area (Chase, 1990). At times it becomes very difficult to distinguish one diamicton from another or laterally correlate overlying or underlying sequences. Difficulty in surface correlation and mapping stems from complex stratigraphy and poor exposure. Poor exposure sometimes is a function of

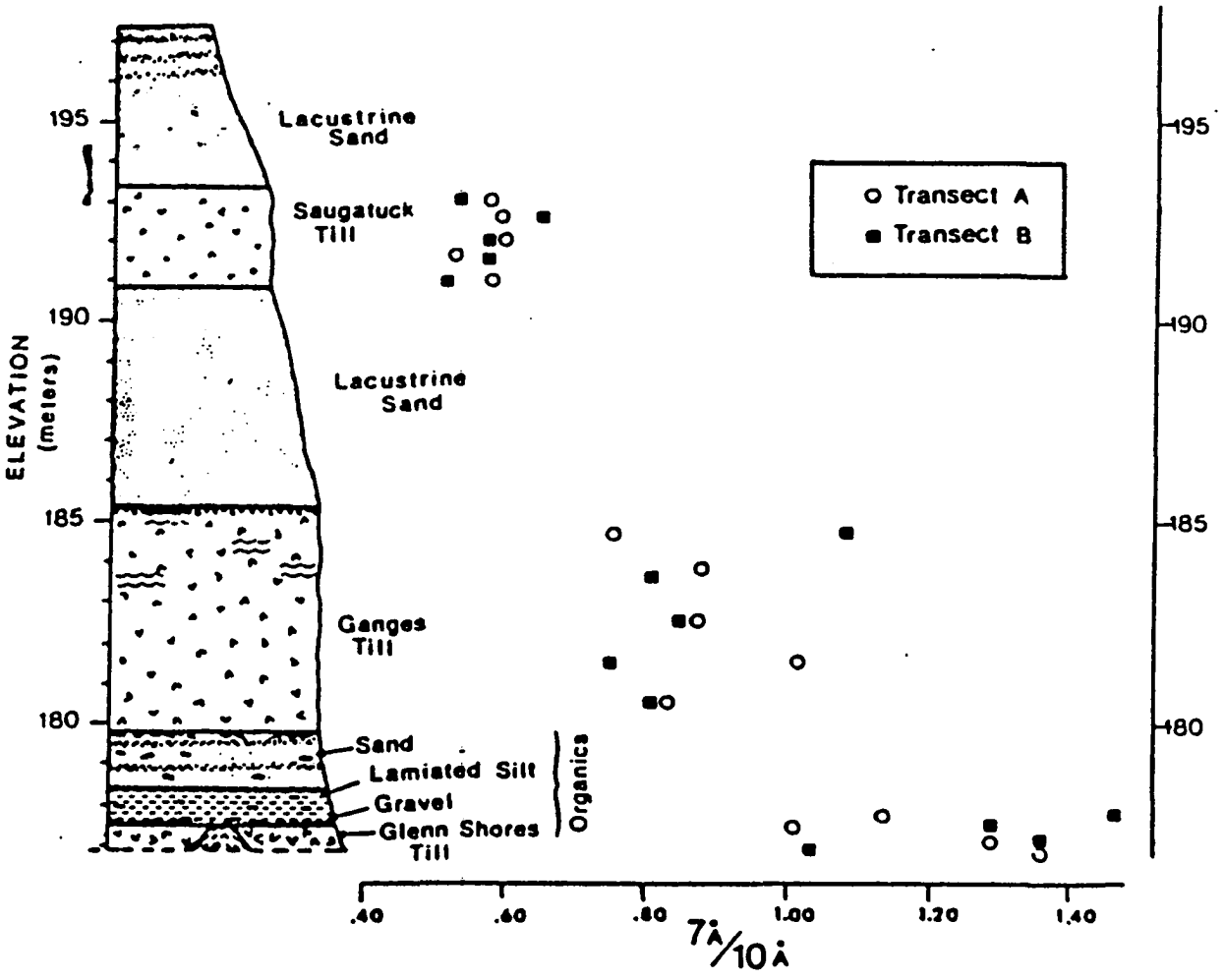

Figure 3. Schematic Stratigraphic Column of Study Area (after Monaghan and Larson, 1986).

vegetation, but it is often further complicated by the presence of a clay armor that covers much of the bluff face. This cover originates from upper bluff diamicton, and results from cyclic wetting, fluidized flow, and subsequent drying of the mobilized clay as it moves downslope. Stratigraphic correlation is also complicated by the presence of displaced slump blocks which are often weathered and eroded.

In terms of the hydrogeology of the area, it appears that there are three main aquifer systems present: shallow, intermediate, and deep. The term "system" is used here because subsurface correlation of aquifers and mapping of hydraulic head suggests that there may be hydraulic communication between individual aquifers in each of the three main systems. In the shallow aquifer system, it is probable that there are multiple perched aquifers at the bluff face.

The simplest way to bracket the hydrostratigraphy of the area is to consider the apparent aquifer/aquitard pairs of Figure 3. In general terms the shallow aquifer system can be described as occurring above the stratigraphically youngest Saugatuck till, the intermediate aquifer system occurs between the Saugatuck and Ganges tills, and the deep aquifer system occurs between the Ganges and Glenn Shores tills. New radiocarbon age dates acquired during this study support this general stratigraphic zonation. Wood fragments recovered from what is interpreted to be the deep aquifer in the southern part of the study area have been dated at 32,680 +/- 500 years BP. This date is slightly younger than those reported by Monaghan and Larson (1986) for organic material immediately above the Glenn Shores till, and thus is consistent with the hydrostratigraphic zonation implied by Figure 3. Detailed subsurface correlation and mapping performed throughout the study area suggest that this zonation is very likely an oversimplification of the area's true hydrostratigraphy, but it represents a good starting point nonetheless.

CHAPTER II

PREVIOUS WORK

Studies of shoreline recession in the Great Lakes date back at least to the mid-19th century (Andrews, 1870; Chamberlin, 1877; Goldthwait, 1907). From the beginning, published estimates of recession rates along various Great Lakes shorelines have varied widely in both time and space. Powers (1958) performed a pioneering, comprehensive attempt to characterize both geomorphology and recession on the Lake Michigan shore. He field-mapped and characterized the entire Lake Michigan shore in terms of lithology and shore type, and measured, either on the ground or through the use of 1938 air photos, a total of 134 bluffline positions relative to quarter-section points. He then compared those measurements to Government Land Office survey measurements to the "meander line" (never clearly defined) made in 1831, and derived long-term recession rates. Powers noted that previous estimates of recession by earlier workers such as Goldthwait (1907) and Chamberlin (1877) were substantially higher than what he had found. He suggested "it was apparent that such men ... considered only shore segments of unusually severe erosion" (p. 91). Seven of Powers' sites are located in this study's Allegan County, Michigan field area. He calculated recession rates for these sites of 1.03 to 2.03 feet per year for the period 1831 to 1956-57.

Powers (1958) enumerated a number of factors that he believed controlled or influenced recession (p. 85). Some or all of them are often cited in the literature as important factors in recession: (a) height of backland above mean lake level; (b) materials composing backland and landface, whether weak or strong; (c) abundance

and coarseness of beach materials; (d) exposure to lake storms and waves; (e) protective structures built by man ; (f) level of Lake Michigan; and (g) unusual storms of great severity.

Powers went on to state that the most time-variant factors are the last two, lake level and severe storms. Further, he claimed, "without exception, accelerated shore erosion has taken place during times of high water, while during low water, beaches have widened and wave attack on the landface has been much less effective" (p. 86).

E. A. Seibel (1972) performed his Ph.D. fieldwork at several sites on Lakes Michigan and Huron. His Glenn site encompasses a stretch of Allegan County shoreline that has also been studied in detail for this work. Using photography over several time periods from 1938 to 1970 and hand-caliper measurement techniques, he determined recession rates from 1 to 5 feet per year in this area. In general, Seibel found, as did Powers (1958), that average recession rates increased with increased lake level and the passing of large storms.

W. R. Buckler (1973), in conjunction with H. A. Winters (Buckler and Winters, 1975), attempted to correlate several different factors to recession rates. He revisited, remeasured, and performed a 1956-73 airphoto analysis at eight of Powers' sites, including one in Allegan County (No. 4; Powers' No. 106), where he found no recession during this time (Buckler, 1973). Buckler concluded that factors such as bluff height, slope, hydrology, composition, and trend of the shoreline could not be positively correlated with recession trends at Powers' sites. The presence of vegetation and a wide beach correlated with less recession, but he was ambiguous (e.g., 1973 vs. 1975) as to whether or not there was a causal relationship between these factors and recession. He observed what he thought were opposite tendencies (development toward a smooth coastline on one hand but

differential recession rates on the other), and suggested that lateral variation in nearshore hydrographic processes (waves and currents) controlled lateral variation in recession rates, as opposed to lateral variation in geomorphology.

Later work by Buckler (1987), also in conjunction with others (Buckler and Winters, 1983; Buckler et al., 1988), included updated airphoto analysis (through 1986) of the southeastern Lake Michigan shore. He emphasized, as others before him, the fact that large variations in Lake Michigan bluff recession rates exist both temporally and spatially. Ignoring differences in site geomorphology or lithology, he utilized widely-varying recession rate data from 20 sites in four southwestern Michigan counties to calculate an average short-term, high-water recession rate of 6.07 feet per year during 1977-86 and an average long-term recession rate of 1.65 feet per year for 1831 to 1986. He noted a possible relationship in recession to shoreline orientation and fetch distance; that is, the more perpendicular the shoreline to a long fetch, the higher the recession rate. He concluded in his 1988 analysis that, in the short term with high lake level, bluffs with bases composed of till or lacustrine clay "responded less rapidly to recessional influence than did bluffs containing basal sands" (1988, p. 58). But in the long term, he saw no difference between these two bluff types. In contrast, "sand dune encompassed bluffs were discovered to be receding at significantly lower long-term rates than were bluffs composed of non-dune sediments" (1988, p. 52).

R. A. Davis performed much research on sediment transport and nearshore profile change in the early and mid-1970s on the eastern shore of Lake Michigan under the auspices of the U.S. Army Corps of Engineers (USACE). Numerous reports (Davis and Fox, 1971; Davis, 1976; Davis et al., 1975) documented nearshore profile change with the passing of storms, increasing wave energy, and decreasing wave energy. He saw clear changes in terms of offshore bar migration over the short

term, and was able to document seasonal profile change similar to that seen on open ocean coasts in the longer term.

Birkemier (1980, 1981) documented coastal change south of Allegan County, while Hands (1979, 1980, 1981) focused on some of Davis' earlier areas to the north in Manistee County. Hands utilized the eastern shore of Lake Michigan as a test bed for determining the validity of the Bruun Rule (Bruun, 1962). The Bruun Rule predicts that a non-cohesive mobile sand blanket will develop a parabolic, concave-upward equilibrium profile in response to prevailing wave climate. Hands noted that open ocean coasts, because of their tidal ranges and continual profile adjustment, were not particularly well-suited to the study of the equilibrium profile, whereas Lake Michigan provided an ideal sand-rich, non-tidal setting. He found that the Bruun Rule worked quite well in predicting shoreline retreat during rising lake level in the mid-1970s, though he noted that retreat continued to occur even after lake level began to subside. He explained this apparent anomaly by suggesting that the subaerial bluff profile took some time to readjust or "catch up" to the new subaqueous equilibrium profile.

In the 1980s and 1990s, increased research efforts have been brought to bear on the role that bluff composition may play in recession (Davidson-Arnott, 1986; Philpott,1984; Boyd, 1992; Kamphuis, 1987; Nairn, 1992) primarily through work on the glacially mantled, clay-rich north shore of Lake Erie. Two compositional bluff end members have been identified. One end member is cohesionless, represented by a mobile sand blanket of infinite thickness as modeled by Bruun (1962), Dean (1977, 1983), and Hands (1980, 1983). The other end member is cohesive, composed primarily of clay-rich glacial till (diamicton) deposits (Philpott, 1984; Quigley and Gelinas, 1976).

An important consequence of cohesive bluff composition is that eroded material is primarily clay-sized (very fine-grained) and easily transported out of the nearshore littoral system permanently. Therefore, ongoing erosion of cohesive bluffs may not contribute the volume of sand supply necessary to build and maintain beaches, which serve as important buffers to incoming wave energy. With no beach present at the base of a bluff, wave energy can impinge more forcibly upon both the nearshore and the foreshore and cause increased erosion.

A potentially more severe consequence emerges if an intermediate condition between the two bluff end members develops. This intermediate condition is represented by a thin, mobile sand blanket that moves back and forth like sandpaper over a cohesive substrate. Studies by Sunamura (1983) and Kamphuis (1983) indicate that sand incorporated into fluid greatly reduces the threshold shear stress requirements for submarine erosion of cohesive material. Thus, the presence of a thin sand layer can result in the downcutting and landward translation of a nearshore cohesive profile (Boyd, 1992; Nairn, 1992) with less wave energy than would be required in the absence of sand (Kamphuis, 1987). An important consequence of further downcutting and increased water depth is that more powerful waves with longer wavelengths and greater heights can carry their energy to the shoreline, potentially resulting in greater erosion.

Additional evidence that subaqueous nearshore and bluff lithology plays an important role in long-term Great Lakes shoreline retreat is provided by Jibson and Staude (1991). In a study of the Lake Michigan shoreline in Illinois, they concluded that bluff lithology was the only factor (including lake level, precipitation, and shore protection) that they could correlate with retreat rates between 1872 and 1987.

Further complicating an already complex problem are the onshore processes that lead to bluff failure. Onshore failure processes in the form of landslides, mudflows, rill/gully erosion, and hillside creep (Sterrett, 1980; Quigley et al., 1977) are at work as well as submarine processes on Great Lakes shorelines. The significance of these processes is often considered as being secondary to more primary driving mechanisms such as toe erosion (Edil and Vallejo, 1977; Mickelson et al., 1977; Chapman, 1996; Sterrett, 1980) or nearshore downcutting (Boyd, 1992; Nairn, 1992; Davidson-Arnott and Ollerhead, 1995). Onshore failure mechanisms are often considered as serving to drive a bluff back toward an equilibrium condition after some form of wave-induced erosion has caused oversteepening of the bluff face.

Some form of limit equilibrium analysis (e.g., Bishop, 1955) has been used by civil engineers since the time of Coulomb to calculate or otherwise estimate conditions of slope failure (or stability) that either exist naturally or are anthropomorphically induced. Limit equilibrium analysis involves the identification and quantification of factors that act to drive and resist slippage along a defined failure surface followed by calculation of the ratio of the sum of stresses resisting failure (shear strength) to the sum of stresses driving failure (shear stress) acting along this plane. The ratio is known as the Factor of Safety (FS) (McCarthy,1993). Accurate identification of these factors requires adequate knowledge of external forces (e.g., weight) and quantification of internal geotechnical parameters such as shear strength, internal angle of friction, and cohesion. These parameters are determined via standardized testing procedures (USACE, 1986) that have been developed by soil mechanicists.

Limit equilibrium analysis has been used to aid in the understanding and prediction of bluff failure by two main groups of researchers in the Great Lakes.

Slope failure or evolution models in the Great Lakes have been developed for the north shore of Lake Erie by Canadians (Gelinas, 1974; Gelinas and Quigley, 1973; Quigley and Gelinas, 1976; Quigley et al., 1977) and for the western shore of Lake Michigan by Wisconsin researchers (Edil, 1974, 1975; Edil and Haas, 1980; Edil and Vallejo, 1977, 1980; Edil and Bosscher, 1988; Edil et al., 1977; Mickelson et. al., 1977). As expected, most of the published information on geotechnical parameters of glacial deposits of the Great Lakes is from these researchers as well (Edil, 1974, 1975; Edil and Vallejo, 1977; Quigley et al., 1977). Currently, little geotechnical data for glacial deposits of the eastern shore of Lake Michigan are available. A limited amount of information was found in the form of boring logs for highway bridges (which provide some lithologic descriptions and blow counts) through the Department of Transportation in Michigan, but this information is inadequate for rigorous quantitative analysis.

Edil and Vallejo (1977) proposed models of slope evolution at Kewaunee and Port Washington, Wisconsin. The bluffs vary in height from 25-100 feet (7.5-30 m), and are composed of silty glacial diamicton and lacustrine deposits. They zoned the bluff into top, intermediate, and toe zones, and described the failure processes occurring in each zone. In terms of overall bluff evolution, they stressed that the two most important processes in the initiation of mass movement were physical degradation of the bluff face and toe erosion. Physical degradation of the bluff face due to solifluction and slumping - perhaps triggered by "spring waters" (p. 4) - led to an accumulation of material at the bluff toe, while toe erosion by wave activity led to the removal of this accumulated material.

At Port Washington, Wisconsin, Edil and Vallejo (1977) found that the dominant failure pattern was rotational landsliding along semicircular failure planes, with a tendency for the failures to progress upslope over time. The authors

found that the Bishop Method (Bishop, 1955) of equilibrium analysis successfully predicted changes in Port Washington profiles through time when effective stress analysis was employed. Effective stress analysis yielded lower (more conservative) Factors of Safety than total stress analysis. At Kewaunee, Wisconsin, the authors found that the dominant failure pattern was translational landsliding along linear failure planes in the form of mudslides and solifluction, with both parallel and non-parallel bluff retreat resulting from these mechanisms.

Canadian research, focused on the north shore of Lake Erie in diamicton and lacustrine deposits similar to those found in Wisconsin, has led to conclusions similar to those of Wisconsin researchers. For example, Quigley et al. (1977) found Lake Erie bluff retreat rates and mechanisms to be cyclic, and suggested that they resulted from complex processes of bluff face degradation, landsliding, and toe erosion, as did Edil and Vallejo (1977). Quigley and Gelinas (1976) grouped the Lake Erie bluffs under study into three main categories in terms of modes of retreat: (1) non-eroding cliff, gradually flattening to a long-term stable geometry; (2) eroding cliff, retaining fairly constant shape and retreating at fairly constant rate due to a combination to toe erosion, toppling, and sheet sloughing; and (3) eroding cliff, cyclically changing profile due to major landslides in response to toe erosion or soil softening under conditions of decreasing effective stress.

With respect to toe erosion in particular, Quigley and Gelinas (1976) stated that rising lake level could have a profound effect on mechanisms of shoreline retreat. This is because wave attack "alters the slope failure mechanisms from a slow, flattening process controlled by effective stresses to a short term toe failure mechanism controlled primarily by geometry and undrained shear strength" (p. 169).

In summary, classic geological work in the Great Lakes from the mid-1800s to the present has suggested that elevated lake levels and singularly intense storms may be particularly responsible for accelerated rates of shoreline retreat. However, recent research from both the geological and engineering communities suggests that shoreline retreat results from a complex interplay of other variables as well. These variables include the amount of nearshore/foreshore downcutting, differences in geotechnical characteristics of materials that comprise the bluff, and the influence of groundwater in terms of slumping and sloughing on the surface and decreased effective stress in the subsurface.

CHAPTER III

METHODS OF DATA STUDY, COLLECTION, AND GENERATION

Chapter Overview

A variety of methods were employed in the study, collection, and generation of data and work products during the course of this study. A new Geographic Information System (GIS)-based methodology was developed for the utilization of existing subsurface data in the creation of new bluff characterization maps. Drilling, sampling, and groundwater monitoring operations resulted in the collection of new lithologic and hydrologic data. Laboratory testing of undisturbed samples generated new geotechnical data, the results of which were utilized in slope stability analysis. A GIS-based airphoto analysis methodology was utilized to create new high-resolution airphoto mosaics from existing air photos. Finally, a comparison of lithologic/hydrologic data and historical bluff recession data was undertaken.

Method of Bluff Characterization

Introduction

Characterization of geological materials and aquifer systems is important, because these factors influence shoreline recession. GIS technology, with its cell-based data management format, is an excellent tool for incorporation of these factors into recession analysis. Initial, study efforts focused upon the compilation, error analysis, and mapping of available lithologic and hydrologic data. Subsequently, a

GIS-based methodology was developed and employed to utilize these data in characterization of Lake Michigan bluff lithology and hydrology.

Data Sources, Compilation, and Error Analysis

Surface Data

An extensive collection of surface data has been compiled by Chase (1990; personal communication, 1996) in the form of detailed measured sections made every 200 feet along the Lake Michigan shoreline in the study area. Parameters recorded include: (a) lithology, (b) slope angles, (c) presence or absence of vegetation, (d) groundwater seeps, (e) shore protection, (f) failure conditions, (g) beach width at the time, (h) land use, (i) fracture conditions, and (j) more obvious erosion mechanisms. Field observations were also made by the author during the summers of 1994, 1995 and 1996.

Subsurface Data Sources

When in situ lithology of the bluff face is concealed, as is the case in up to 50% of the study area, surface descriptions can be problematic. Subsurface lithologic data from driller's logs generally yield less detail than surface descriptions taken from a fresh face, but subsurface well logs can be adequate for the determination of general bluff stratigraphy. Additionally, subsurface well data can augment surface observations by providing lithologic data below lake level. Finally, well data serve as an important (usually the only) source for hydrological information.

The bulk of subsurface data from wells in the study area (Figure 4) comes from water well drilling records filed at the Allegan County Board of Health.

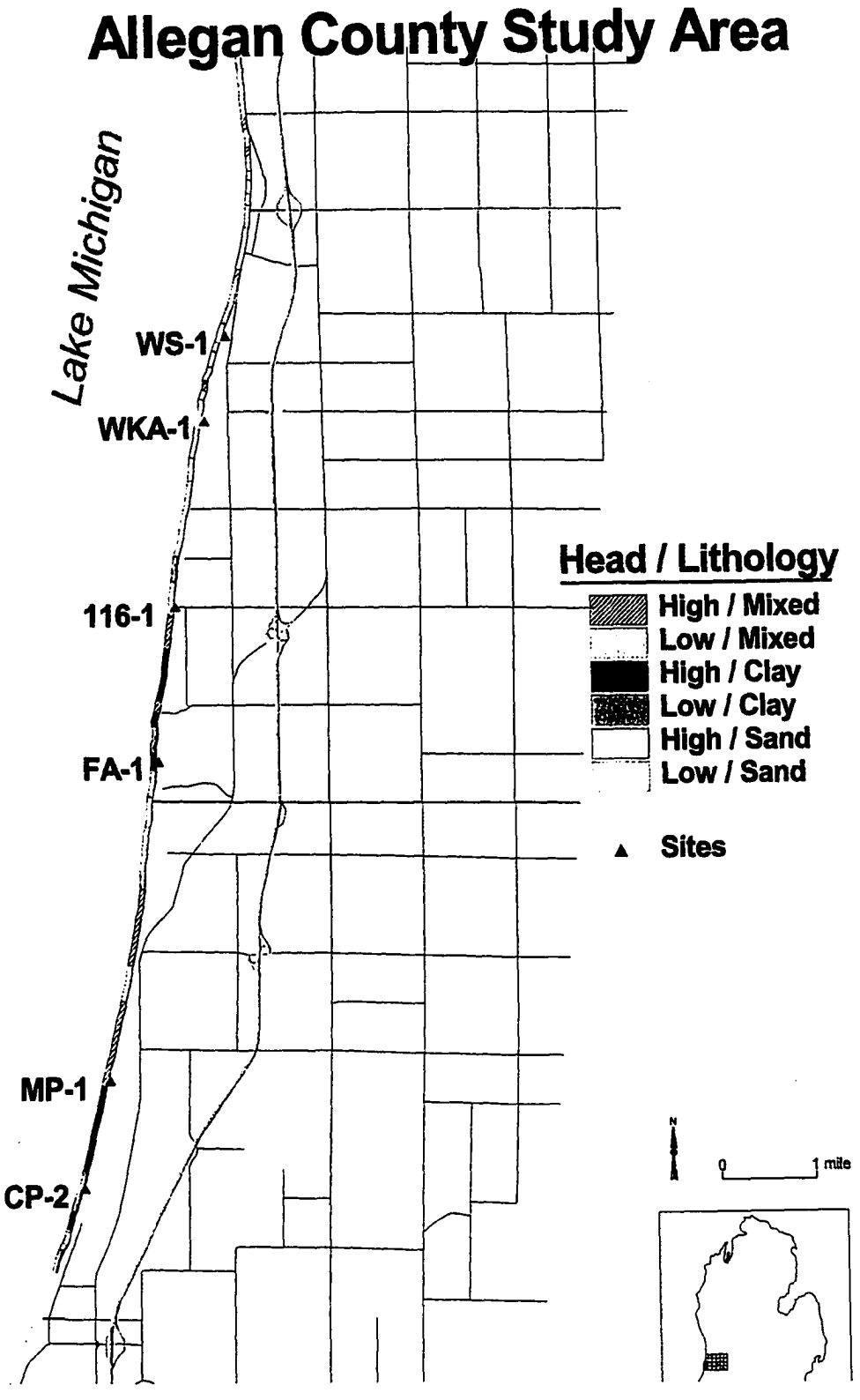

Figure 4. Locations of Water Wells Used to Delineate Shallow, Intermediate and Deep Aquifer Systems in Study Area. Monitoring Sites Include Multiple Wells. See Discussion of Aquifer Systems in Text.

Subsurface information is also available from drilling records of oil and gas wells, but the utility of these data is often limited to a reported Pleistocene-Paleozoic contact, determination of which can be difficult, especially when dark clay-rich gray diamicton overlies dark gray Mississippian Coldwater Shale.

Subsurface Data Quality

Some geologists object to the use of water well logs as subsurface data sources, because of potential errors inherent in their usage. Errors can result from inaccurate reports of well locations, inaccurate static water level measurements, and inadequate sample descriptions. One way to address the issue of sample description quality is to use nearby bluff exposures as checks. Another way to overcome problems with sample description quality and consistency is through utilization of a large volume of well control. Inconsistency in lithologic sample description is minimized with increasing amounts of well control, because anomalies are more readily identified as either real or fictitious. In the study area, over 300 well records were studied and correlated.

Accurate determination of static water level (SWL) in a wellbore and accurate spatial positioning of well locations are important to accurate mapping of hydraulic head. Accurate downhole measurement of SWL is facilitated by modern electronic water level meters that are easy to use, reliable, and accurate to 0.01 foot (0.30 cm). Error in SWL determination in a borehole is likely to be a function of lack of equilibration between the aquifer system the well penetrates and the water level recorded in the well, usually most prevalent in aquifers that exhibit low hydraulic conductivity. Water may move slowly under these conditions, and it may take a day or more for water level in a well to equilibrate to the level of either the

water table elevation (when unconfined) or the potentiometric surface (when confined) of an aquifer. In these cases, the reported SWL on a driller's log may merely represent the water level at the time of measurement, rather than the equilibrated hydraulic head.

As in the case of sample descriptions, sheer volume of well control can help minimize interpretational error caused by inaccurate SWLs, because an increased amount of well control facilitates identification of anomalies. There is the occasional case, especially in areas of little control, that an inaccurate SWL can lead to an erroneous interpretation, but this case is the exception rather than the rule.

Spatial Positioning Error of Subsurface Data

Accurate spatial positioning of well control can be achieved, if sufficient resources exist, through the use of modern computer and Global Positioning System (GPS) technology. Unfortunately, the Allegan County water well computer database suffers from extremely poor locational data, and an inordinate amount of effort would have been required to correct the database. Therefore, manual locating of wells based upon street addresses or diagrams on the well records was performed on 1:24,000 scale U.S.G.S. 7 1/2 minute series topographic maps.

These topographic maps are required by National Map Standards (Anders and Byrnes, 1991) to be accurate horizontally to +/- 40 feet (12.1 m) and vertically to +/- 10 feet (3.0 m). Even though many well locations were refined through field checks during the course of the study, especially those within the three areas of detailed airphoto analysis, it is likely that the horizontal accuracy of much of the well control in the study area is +/- 100 feet (30.3 m). Wells located on flat topography are subject to only a minor amount of vertical uncertainty in lithologic

contact position or hydraulic head because of horizontal uncertainty. However, in locations where relief may change 10 feet or more in a relatively short distance, vertical positions of lithologic contacts or head values may be subject to significant error.

Elevation Uncertainty

It was important to determine the magnitude of vertical uncertainty that could be expected to be present in maps and cross sections generated from the subsurface data. The elevations determined from topographic maps at six field sites were compared with both electronically-controlled survey elevations as well as with GPS-derived elevations.

Electronically-Controlled Elevation Surveys. A Sokkia Set 4CII Total Station was used to determine ground elevations of the bluff edge and piezometer nest at each of the six field sites (Table 1). These data are accurate to within 0.10 foot (0.003 m). They indicate that the topographic maps are accurate to within two feet at three sites, three feet at two sites, and seven feet at the sixth site.

Global Positioning System (GPS) Elevation Surveys. GPS-derived elevations were acquired using a pair of Magellan ProMark X-CP receivers operated in differential mode. Differential mode was necessary in order to minimize error due to dithering of satellite signals. At each of the six sites, five to seven 10-minute, continuously-recorded occupations were made. These occupations were then averaged to produce a ground elevation for that site. All occupations fell within +/- 1.5 feet (0.45 m) of the calculated average elevation at each site (Sauck and

Table 1

Field Site Elevation Data Acquired With Sokkia Total Station

Field Site Elevation Data					
Site	Well	TOC wrt GL (ft)	Elev TOC (ft abv MSL)		
WS	1	-0.24	623.33		
	2	-0.48	623.42		
	3	-0.19	623.54		
WKA	1	0.75	620.52		
	2	Not Msrd	620.94		
116	1	0.50	640.54		
	2	Not Msrd	640.53		
	3	Not Msrd	640.38		
FA	1	Not Msrd	622.89		
	2	Not Msrd	623.01		
	3	0.60	623.28		
MP	1	Not Msrd	670.36		
	2	Not Msrd	670.56		
	3	0.75	670.55		
CP	1	Not Msrd	660.20		
	2	Not Msrd	659.96		
	3	0.75	660.27		
Procedure:	Sokkia Set 4C Total Station used 11-29 and 11-30-97.				
	Shoot to lake level and TOC from bluff edge.				
	Accurate to +/- 0.10 ft. Reference elev = Mean L. Mich. above MSL.				
	Elev L. Mich 11-29 = 580.25 ft; elev L. Mich 11-30 =580.35 ft. (USACE-Det Dist)				
	All SWL data measured from east side TOC.				
					WWM 3-98

Montgomery, unpublished data). GPS-derived average elevations were within 10 feet (3.0 m) of the elevation indicated by the topographic maps at all but one site.

Reformatting of Subsurface Data

Well records were reformatted from purely written descriptions to a visual lithologic strip log format through the construction of a scaled (1 inch = 20 feet) (2.54 cm = 6.1 m) grain-size column for each driller's log. This provided a visual means of correlation between lithologic logs as well as a basis for correlation with natural gamma ray wireline logs that were obtained during the course of the study. Natural gamma ray logs record the natural radioactivity emanating from soil and rocks. Clay minerals, because of their platy, layered structure, tend to hold more radioactive elements in their crystal lattices than do minerals like quartz. Therefore, fine-grained soils and rocks usually emit high radioactivity, while coarse-grained silica-rich materials usually emit low radioactivity. The grain-size column on a lithologic strip logs therefore visually mimics a gamma ray curve, which greatly facilitates log correlation.

Cross Section Network Construction

A network of cross sections was constructed (Figure 5) using the reformatted subsurface well records in order to develop the geologic framework required for adequate characterization of bluff geology and hydrology. The cross section network consists of a long (~10 miles; 16 km) regional line (Figure 6) along the Lake Michigan shore with a series of shorter (1-2 miles; 1.6-3.2 km) east-west trending segments (Figures 7 and 8). The regional north-south cross section was the most critical line in the network. This line was generated primarily from

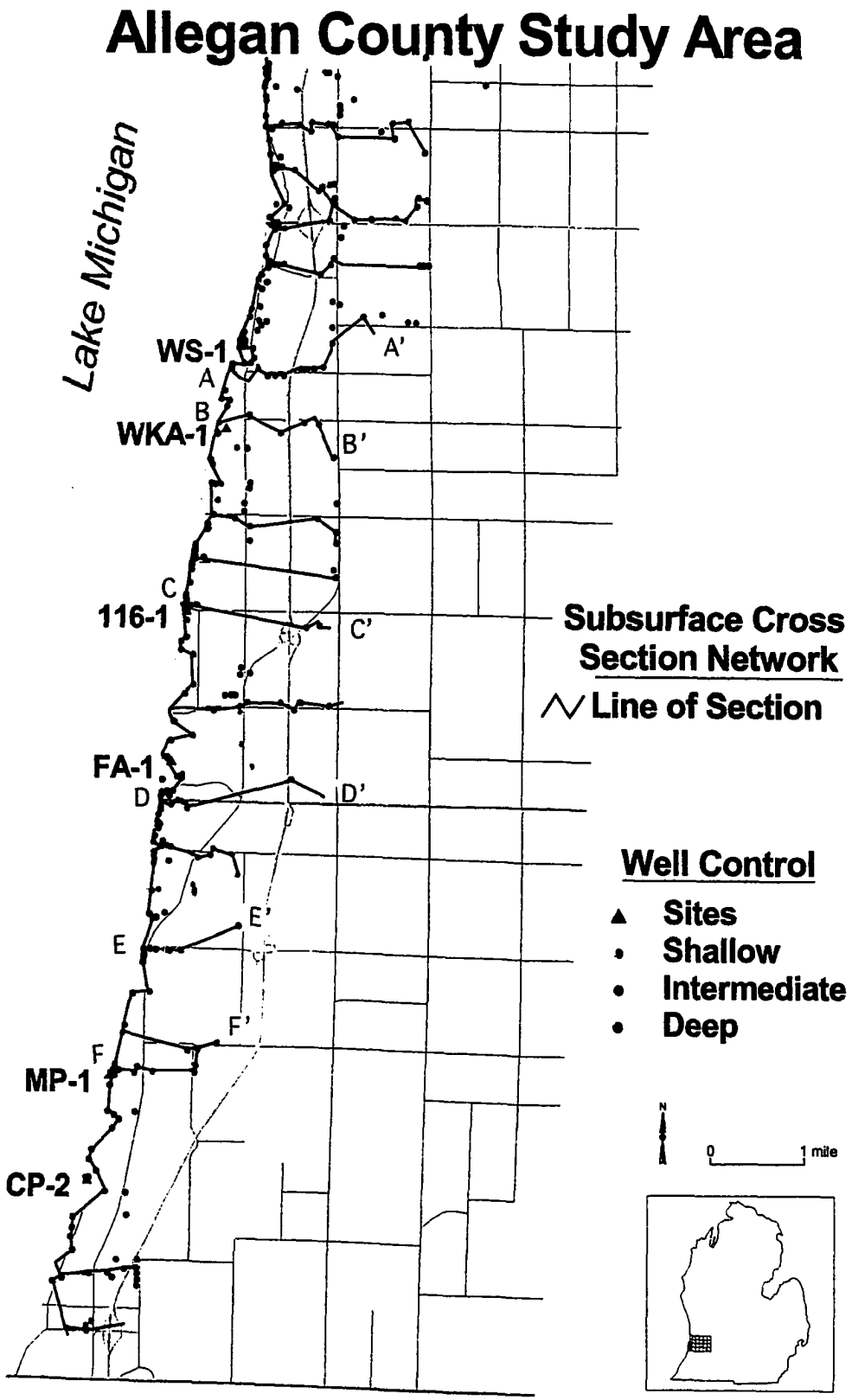

Figure 5. Subsurface Cross Section Network Used to Delineate Aquifer Systems in Study Area.

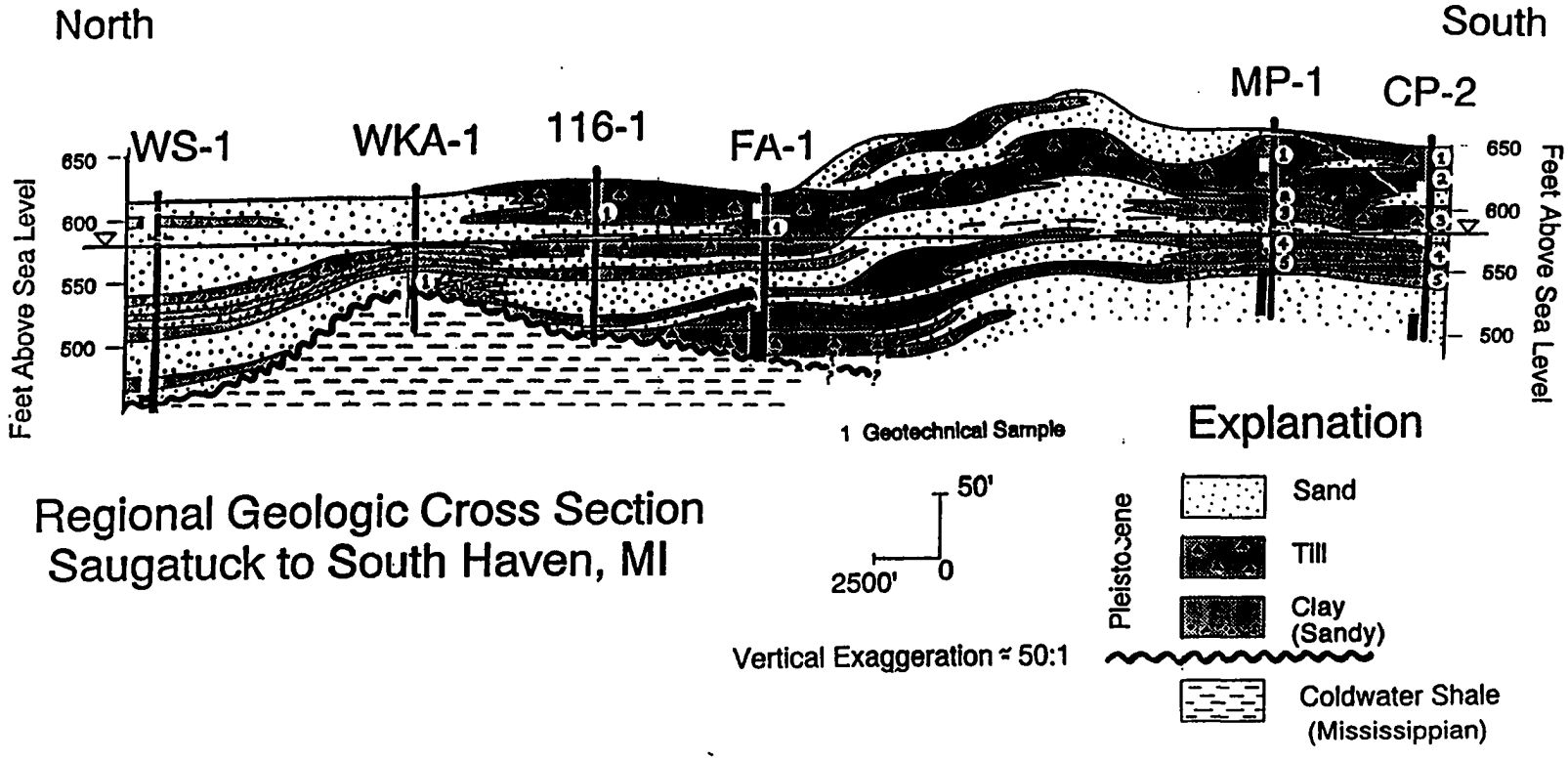

Figure 6. Regional North-South Geologic Cross Section Along Lake Michigan Shore. See Figure 5. for Location.

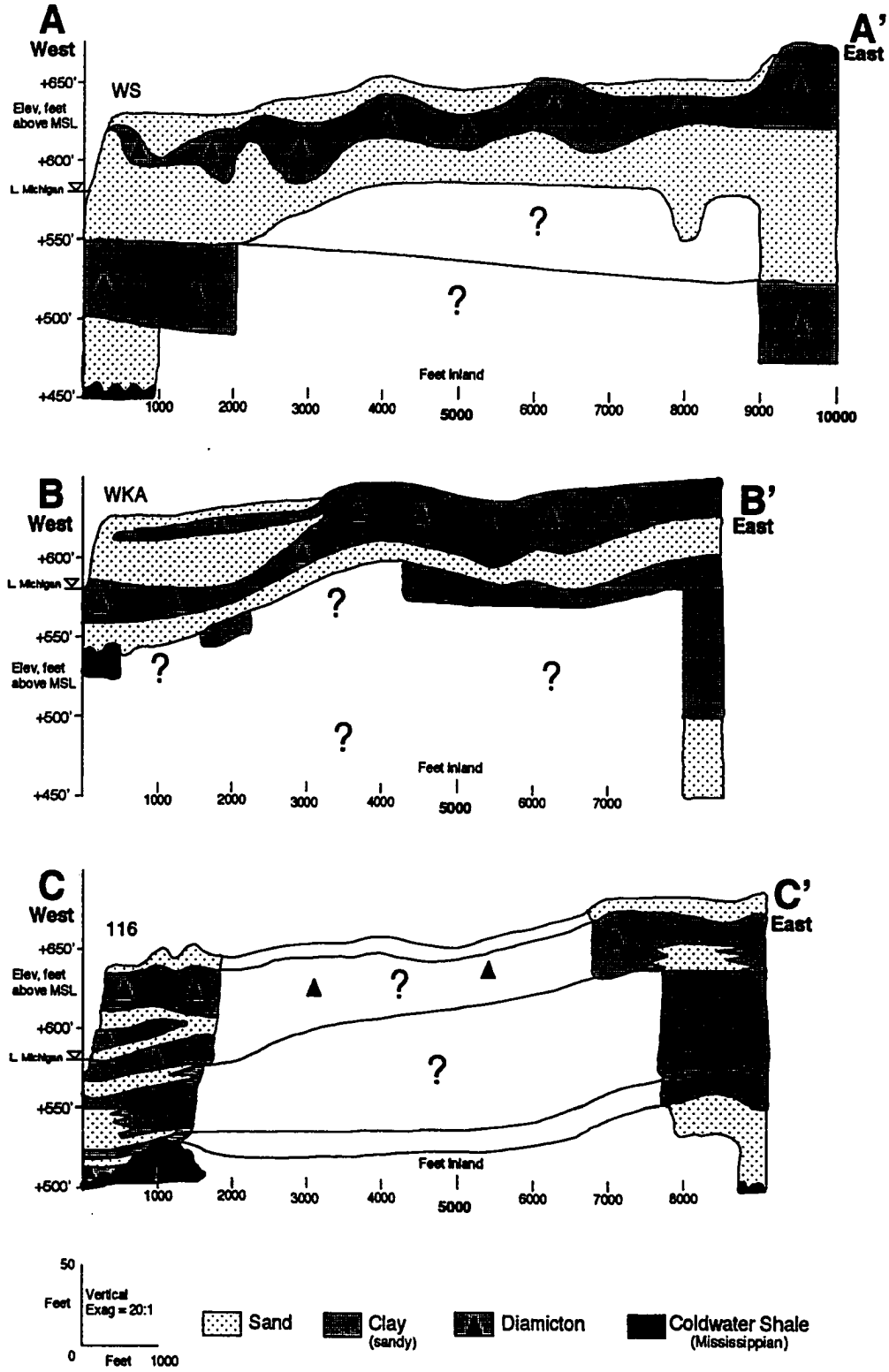

Figure 7. East-West Geologic Cross Sections A-A' to C-C'. See Figure 5 for Locations.

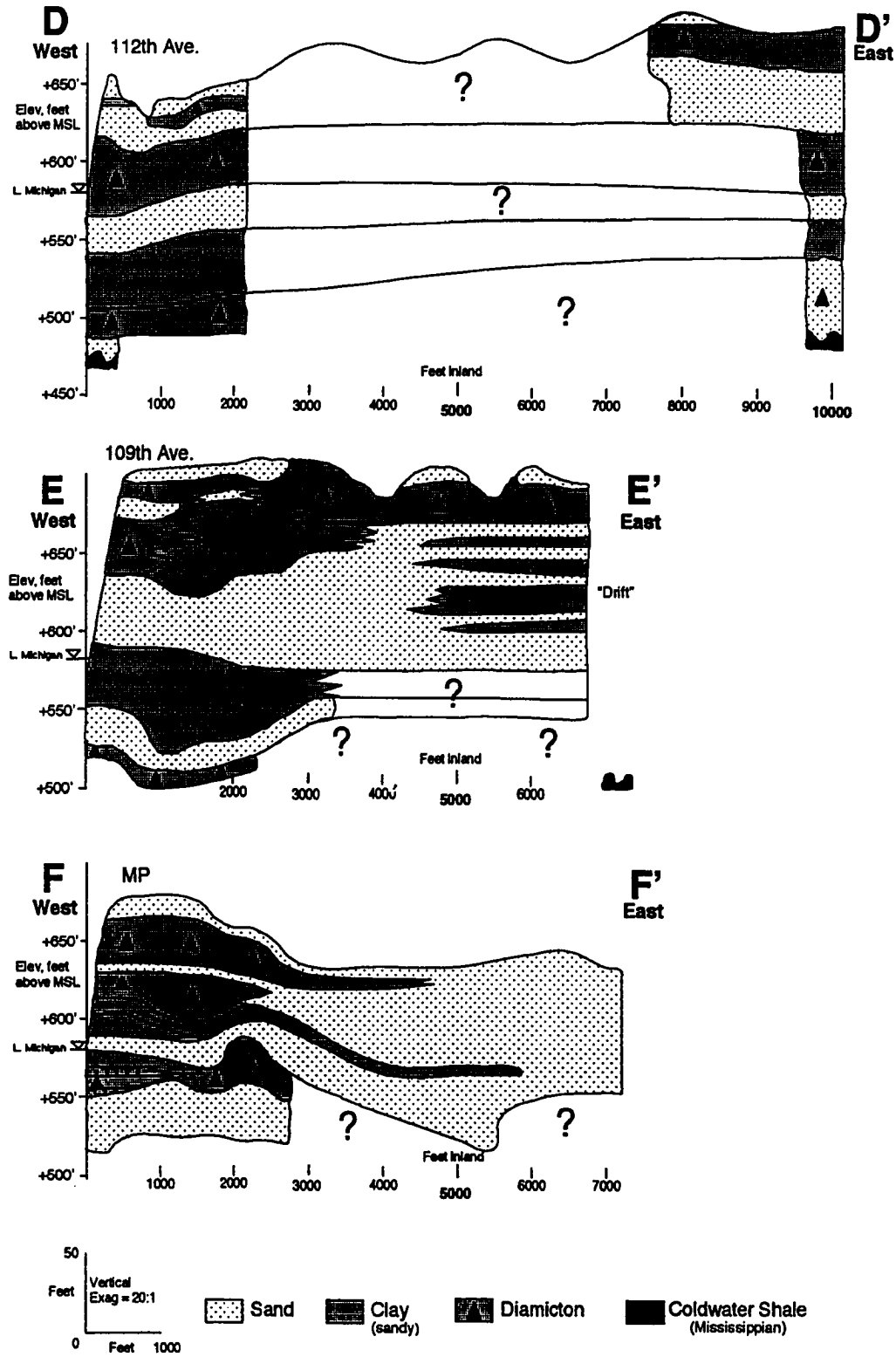

Figure 8. East-West Geologic Cross Sections D-D' to F-F'. See Figure 5 for Locations.

subsurface well control, but because of its proximity to the bluff face, it could be checked against the surface work of Chase (1990; 1996, personal communication) and field observations of the author. Subsurface and surface data were generally found to be consistent.

Method for Characterization of Bluff Lithology

A methodology for characterization of bluff lithology was developed with the consideration that subsurface well logs in Allegan County are reliable indicators of three primary lithotypes: (1) sand, (2) clay, and (3) mixed sand/clay lithologies (Figure 9). This characterization reflects the level of detail present in the subsurface data base; and is also consistent with what is often generally observed on the bluff face (Chase, 1990; 1996, personal communication). Using the regional north-south cross section as the primary data source, checked with the surface data of Chase (1990) and traverses by the author, the bluff face along the shoreline was partitioned into cell segments, each segment representative of the major bluff lithology present according to the characterization system. Cell boundaries were digitized into an Arc/Info system at the Western Michigan University GIS Research Center from a 1:24,000 - scale topographic base map to produce a characterization map of bluff lithology (Figure 10).

Method for Characterization of Bluff Hydrology

In order to adequately assess and characterize the bluff hydrology of the study area, groundwater flow had to be determined. Groundwater flow is governed by the principle that water moves from high total hydraulic head to low total hydraulic head. Total hydraulic head in a well or piezometer is composed of two components:

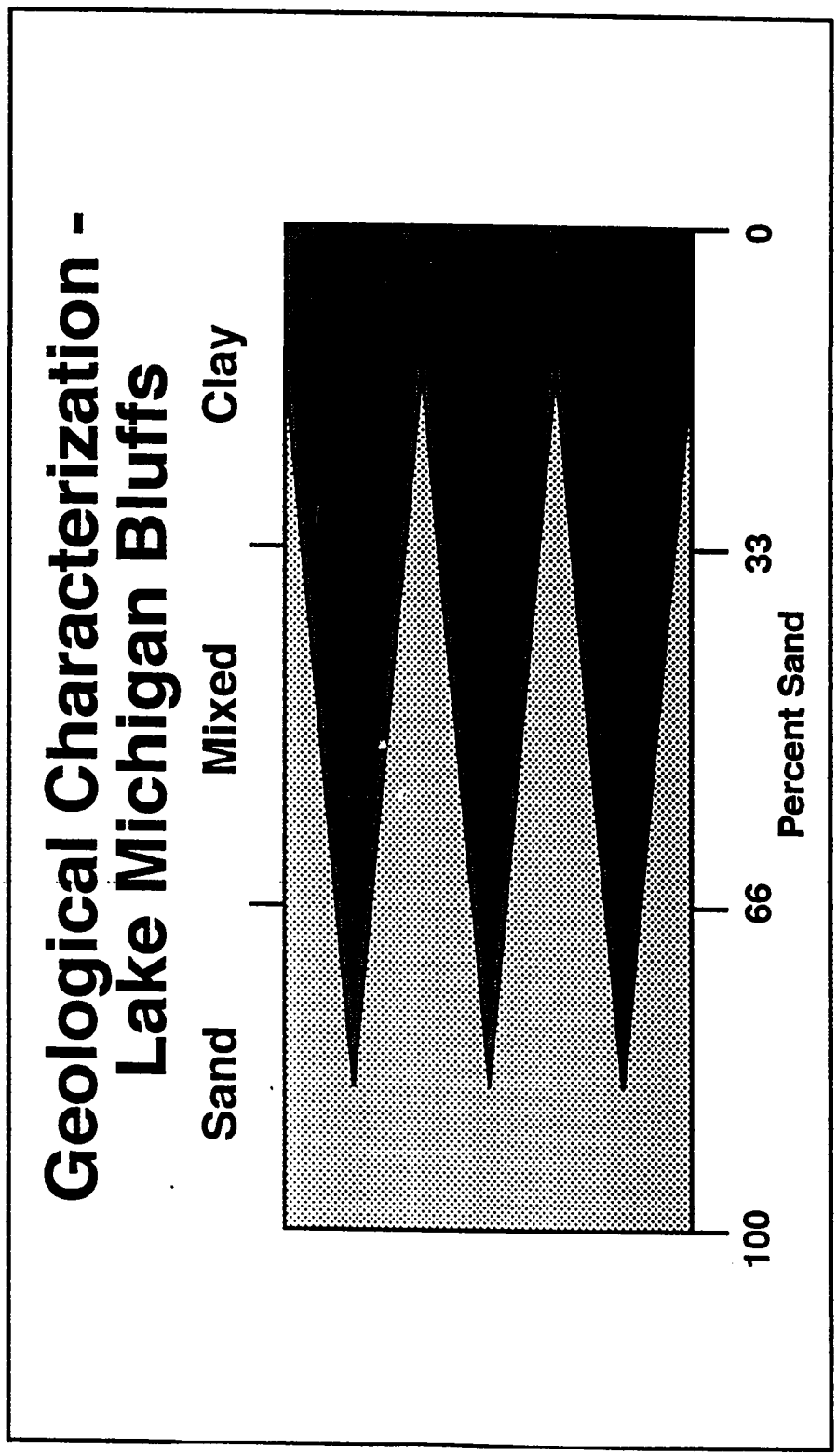

Figure 9. Method for Characterization of Bluff Lithology.

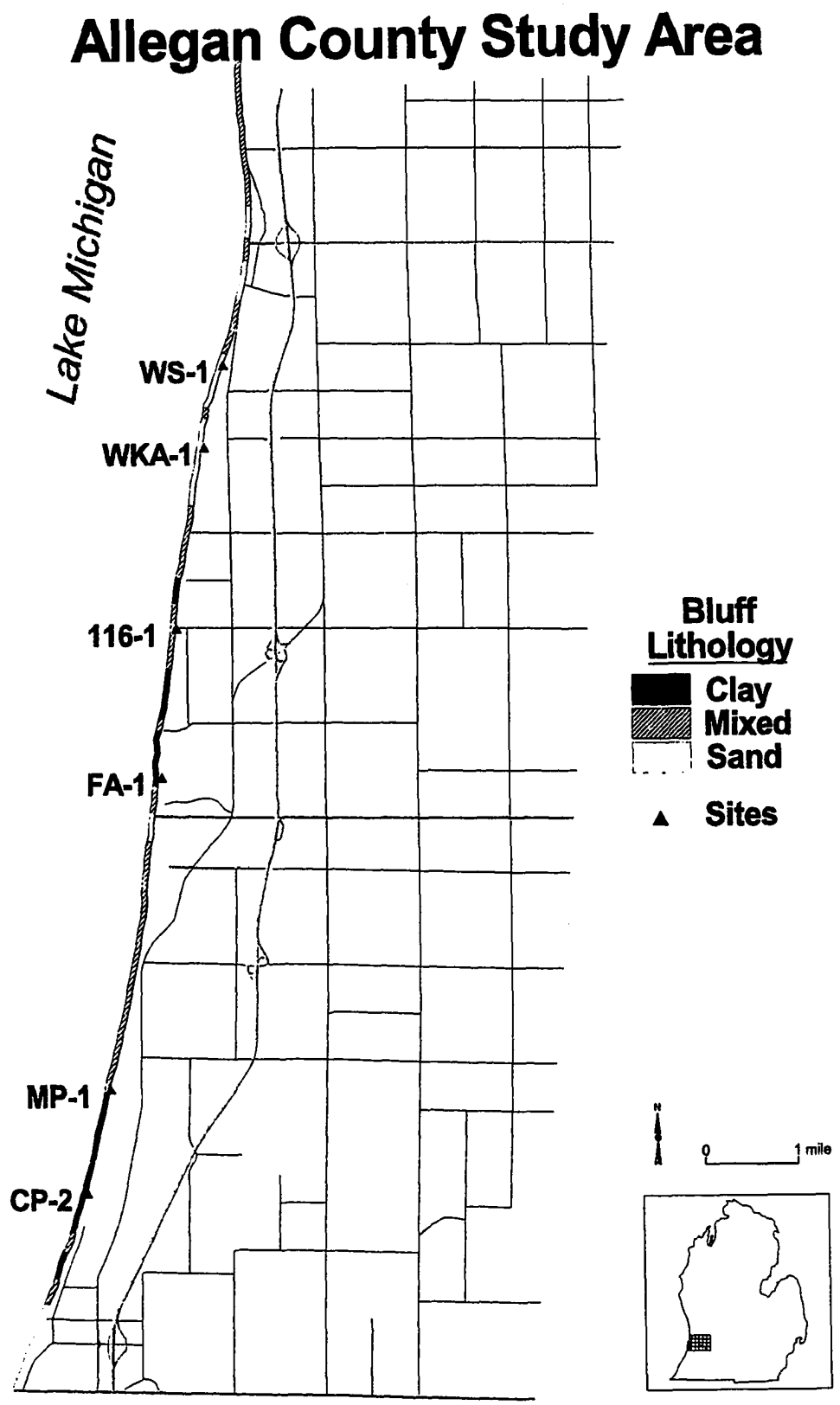

Figure 10. Bluff Lithology Characterization Map with Locations of Monitoring Sites. Further Discussion Provided in Text.

(1) pressure head (elevation of the water column in the well above the point of fluid entry, and (2) elevation head (the distance from the point of fluid entry relative to an arbitrary datum). The arbitrary datum chosen was sea level; for reference, the elevation of Lake Michigan at the time of mapping was approximately 580 feet (175.76 m) above sea level.

Aquifer Systems

It was determined through the interpretation of subsurface geologic data, completion zone data, and hydraulic head data that Pleistocene deposits in the study area comprise three discrete aquifer systems: (1) shallow, (2) intermediate, and (3) deep. To a first approximation, these systems may be portrayed as aquifers coupled with basal aquitards as in the stratigraphic column of Figure 3, although this is probably an oversimplification. Total hydraulic head values were determined for each of the interpreted aquifer systems based upon available well control (Figure 4), and a contour map of total head was generated for each system.

Total Hydraulic Head Contour Maps

The shallow aquifer system (Figure 11) exhibits heads that generally are perched at varying heights above lake level, most likely on top of the Saugatuck till or Ganges till. The head map on this system is not particularly well controlled, because there are only 40 shallow aquifer well records in the study area. However, it was assumed that the topography of the Lake Border Moraine complex exerted a strong control over flow in this aquifer system, so topography was used to guide the contouring of head in the absence of well control.

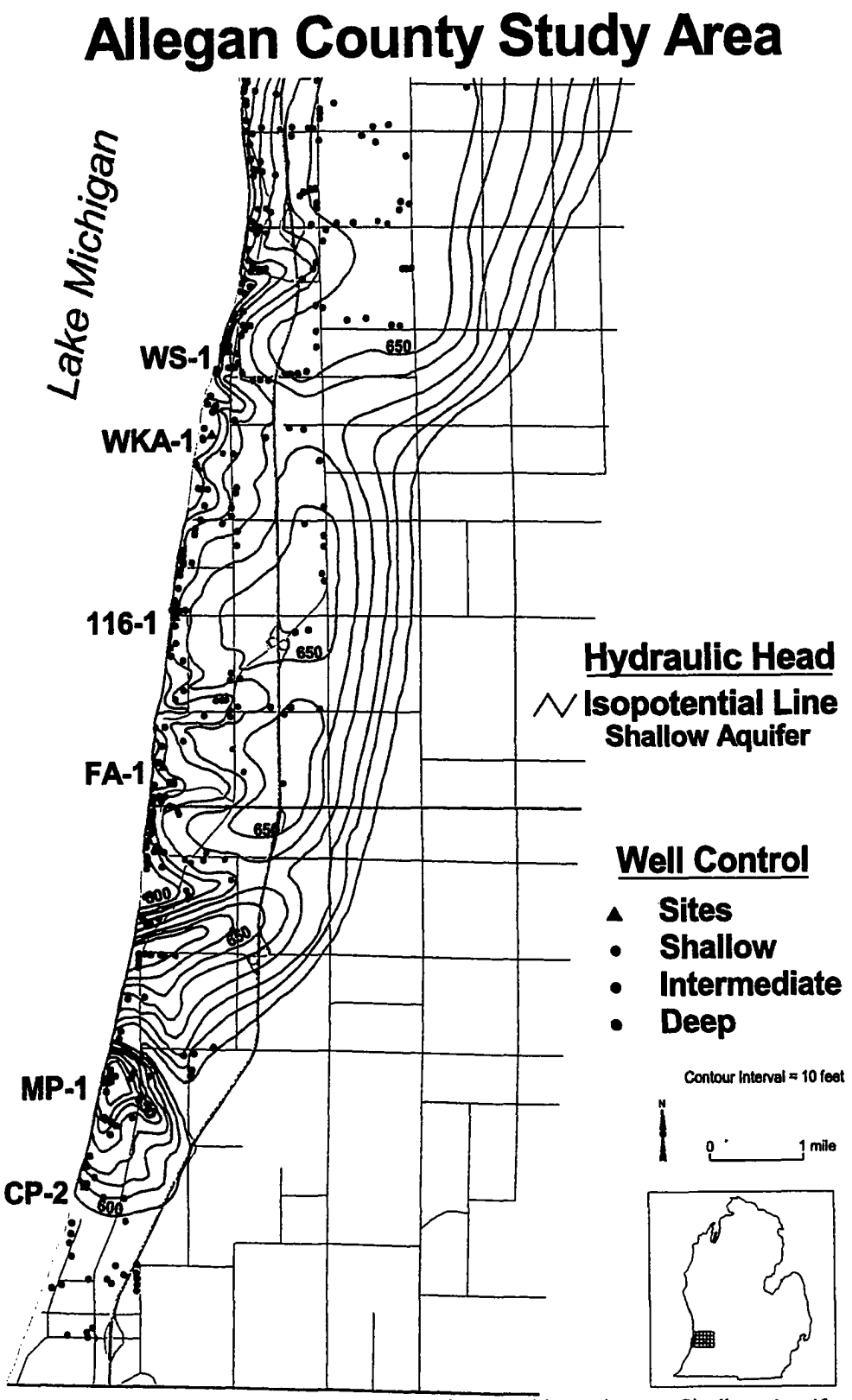

Figure 11. Contour Map of Shallow Aquifer Head based upon Shallow Aquifer Well Control. Includes Shallow Aquifer Data from Monitoring Sites.

The intermediate aquifer system (Figure 12) is the primary aquifer for potable (drinking) water in the central and northern portions of the study area, and as such has the most well control (250 wells). This aquifer also appears to often be in hydraulic communication with Lake Michigan. It is very difficult to say with certainty what position the Ganges Till occupies in this system, in that wells completed both above and below this unit often have the same head. There is sufficient well control in the area to indicate that the topography of the Lake Border Moraine complex exerts some control on flow in this aquifer system.

The deep aquifer system (Figure 13) appears to be discontinuous in the northern portion of the study area, but it is well developed in the southern part of the study area, where it is the main aquifer for potable water. The deep aquifer head map is only moderately well-controlled (75 wells) in the study area. In contrast to the shallow and intermediate aquifers, which are mapped with groundwater divides coincident with the topographic crest of the Lake Border Moraine complex, the deep aquifer exhibits relatively uniform flow from high head in the interior of the study area to lower head near the lakeshore.

Head Characterization

The intermediate aquifer head map was chosen as representative of the head conditions on the bluff for two reasons: (1) it has much more well control than either the shallow or deep aquifers, and (2) a substantial amount of the bluff face is interpreted to contain lithologic units of this aquifer system. However, it is acknowledged that this approach is probably simplistic. Future work may involve subdivision of the bluff face into units correlative with the appropriate aquifer

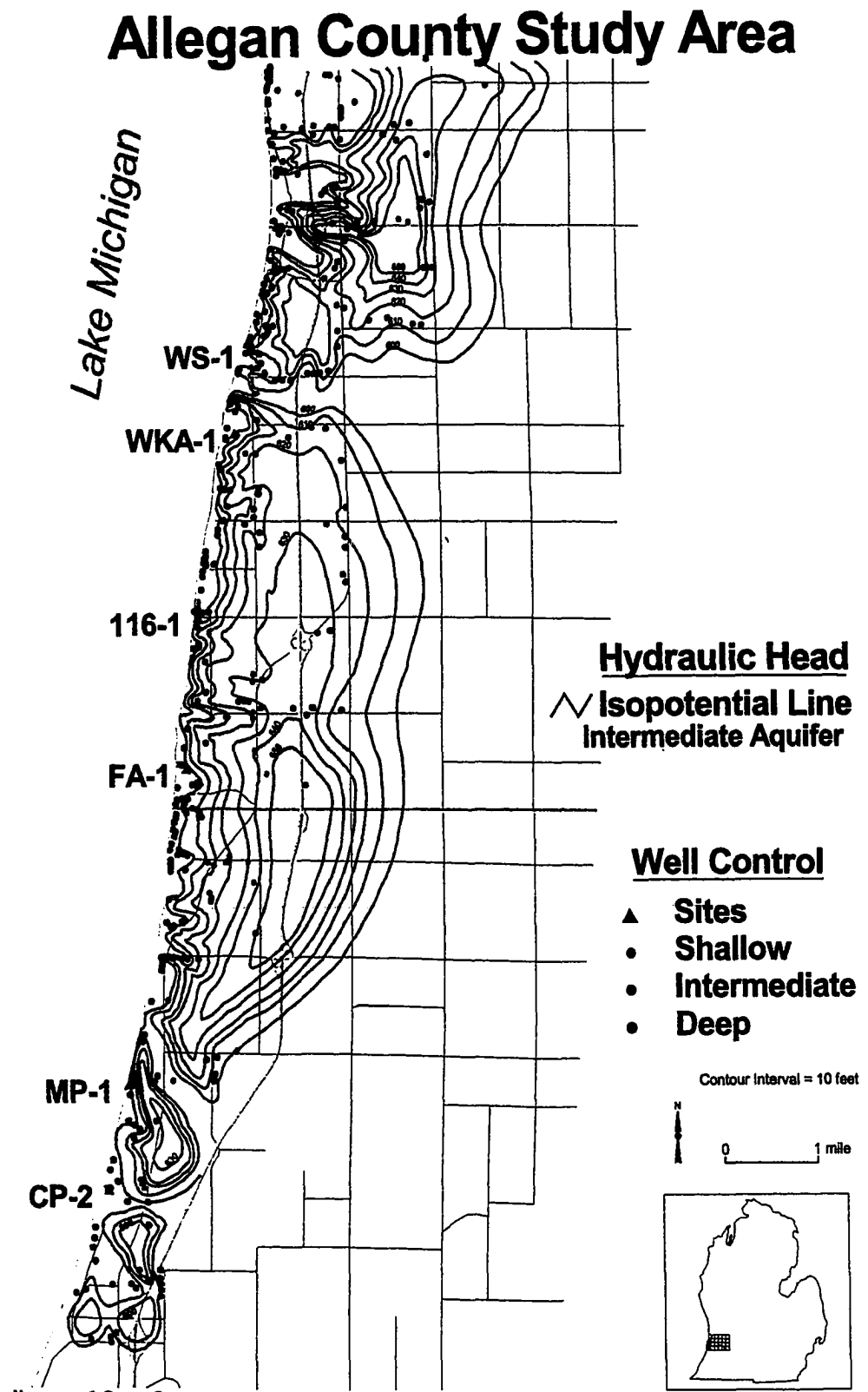

Figure 12. Contour Map of Intermediate Aquifer Head based upon Intermediate Aquifer Well Control. Includes Intermediate Aquifer Data from Monitoring Sites.

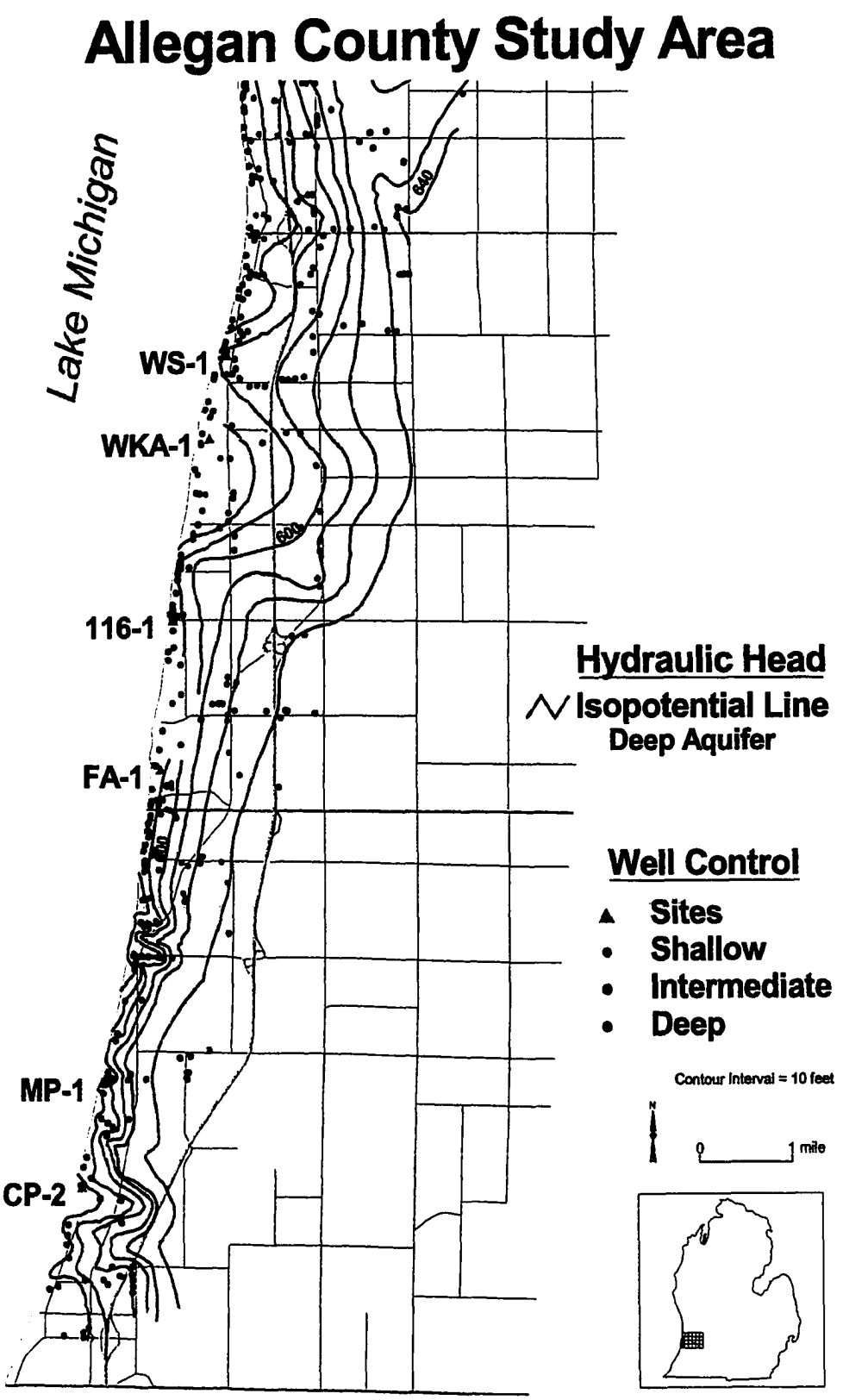

Figure 13. Contour Map of Deep Aquifer Head based upon Deep Aquifer Well Control. Includes Deep Aquifer Data from Monitoring Sites.

system, and then using the head map from that aquifer system for characterization of that portion of the bluff.

No single head value as represented by a contour line was adequate to differentiate high head from low head, though approximate lake level (580 feet; 175.76 m) was used in the absence of mapped trends. Where possible, trends of either high or low head evident from the intermediate aquifer map were projected toward the bluff face in order to determine head conditions on the bluff face. Those segments of the bluff face that intersected trends of high head were characterized with high head cells, whereas those segments of the bluff face that appeared to be on trend with re-entrants or that exhibited lake level values for head were characterized with low head cells. Cell boundaries were digitized into an Arc/Info system at the Western Michigan University GIS Research Center from a 1:24,000 - scale topographic base map to produce a characterization map of bluff hydrology (Figure 14).

Combined Characterization of Bluff Lithology and Hydrology

The Arc/Info GIS system at Western Michigan University's GIS Research Center was used to perform an overlay operation between the geologic and hydrologic characterization maps to produce a combination bluff lithologic/hydrologic characterization map with six different attributes (Figure 15). Following this, plans were developed to field-test the hypothesis that different combinations of lithology (sand, mixed, clay) and hydraulic head (high, low) would fail in different ways and at different rates.

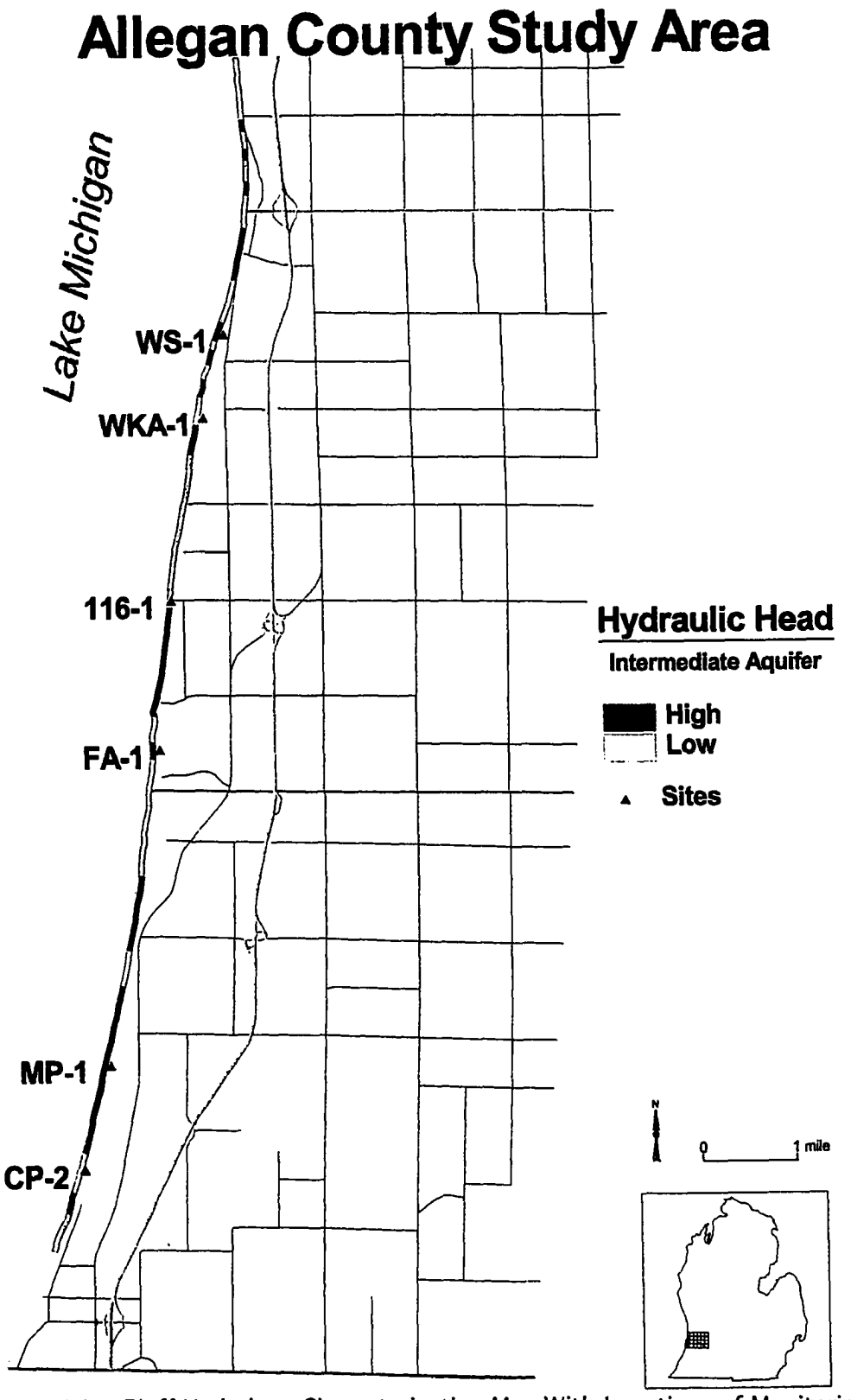

Figure 14. Bluff Hydrology Characterization Map With Locations of Monitoring Sites. See Discussion of Aquifer Head in Text.

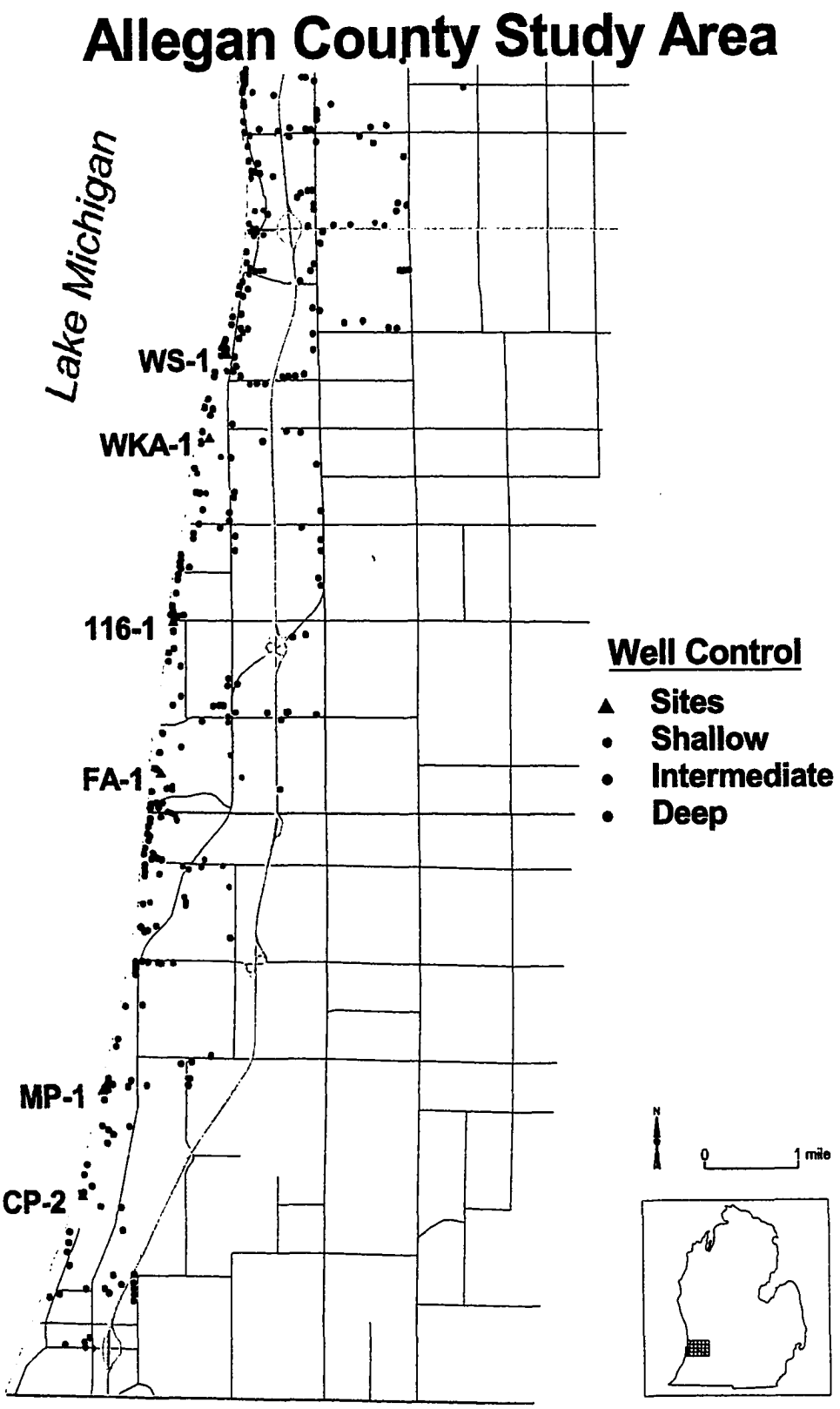

Figure 15. Bluff Lithologic/Hydrologic Characterization Map With Locations of Monitoring Sites. See Discussion of Combined Characterization in Text.

Methods of Acquisition of Field Data

Introduction

Six sites, each one representative of a particular lithologic/hydrologic combination as determined from field observations and the GIS methodology, were selected for long-term field study (Figure 15). Drilling, subsurface sampling, and piezometer installation operations were conducted at each site in July and August, 1996. Undisturbed samples obtained during drilling yielded geotechnical data through laboratory testing conducted in September and October, 1996. Hydraulic head and slope failure monitoring at the sites began in the latter half of 1996. Factors in failure being monitored include: (a) changes in hydraulic head, (b) wave climate, (c) ice protection or damming, (d) atmospheric temperatures, and (e) precipitation (Chase et al., 1997).

Representative Field Sites

Many bluff segments were evaluated during the search for field sites representative of the six lithologic/hydrologic combinations. Technically, there were several good candidates for each of the six sites. However, non-technical issues such as accessibility and level of property development also influenced final site selection.

Real estate values on the Lake Michigan shore have been climbing steadily for years (Raphael and Kureth, 1988), and lakefront property is extremely valuable. Although many bluff owners are interested in the results of shoreline recession research, they are often reluctant to subject their property to field study, especially when drilling operations are involved. Because of potential difficulty securing

access to private property, various sites on public property were evaluated as to their technical merit. Two sites were found to be representative of lithologic/hydrologic conditions as mapped.

One site with public access is 116th Avenue (116), which is mapped as a mixed sand/clay site with low head ("LM"). Another site with public access is the West Side County Park (WS), on trend with the westward extension of 122nd Avenue. It was initially mapped as a sandy site with low head ("LS").

Ultimately, four private sites representative of mapped conditions were also made available for study. Consumers Power (CP), now Consumers Energy, offered their South Haven Conference Center near 104th Avenue for study. It is mapped as a clay site with low head ("LC"). The Miami Park (MP) subdivision, located just south of 107th Avenue, has a mixed bluff lithology with a mapped high head ("HM"). Fabun Road (FA), just south of 114th Avenue, is mapped as a clay site with high head ("HC"). Wau-Ken-A (WKA) is a sandy site that originally was mapped as high head ("HS").

Drilling Procedure

Mateco Drilling, Inc. of Grand Rapids, MI was the primary drilling contractor for this study, because they had prior experience with geotechnical sampling and were reasonable in terms of cost. A large-diameter shallow well (WKA-2) was drilled by Koops Well Drilling of Hamilton, MI, a licensed water well drilling firm, to serve as a shallow piezometer at Wau-Ken-A. The site owner wanted to preserve the option of converting this well to water production at the end of the study period.

Sites were drilled in a general progression from south to north in the late summer of 1996. The initial plan was to drill, sample, and finish three 2-inch

(5.1 cm) diameter open-standpipe piezometers (Casagrande, 1936) in the shallow, intermediate, and deep aquifer systems at each of the six field sites. Hollow-stem augers were used for drilling from the surface to varying depths (generally about 30 feet (9.1 m)). The limiting factor on hollow-stem auger depth was drilling difficulty and/or the risk of losing the hole. On the deep piezometers, the augers were left in the hole as temporary surface casing, then the drilling system was switched to mud rotary and remained that way to total depth (TD).

The first piezometer drilled at each site was the deepest. Sample and wireline log information from that borehole was used to guide the choice of completion zones in the shallow and intermediate piezometers. Plastic (PVC) drop pipe and screens were installed in each piezometer. Screen length varies, but is on the order of 5 feet (1.5 m) to 10 feet (3.0 m) in most piezometers. To facilitate fluid entry, a coarse sand filter pack was placed in the annulus between the screen and the formation over the length of the screen and then extended to variable heights above it. The remainder of the annulus between the drop pipe and formation was grouted to surface or near-surface. On occasion, excess drill cuttings were returned to the annulus near the top of the well.

Sampling Program

Rigorous sample collection during drilling is important for a number of reasons. Samples form the only physical record of the subsurface that is kept by the geologist. Samples also provide a basis for interpretation and calibration of subsurface wireline logs (such as the gamma ray log). In addition, undisturbed samples provide a critical link to engineering models.

Disturbed Samples

Disturbed samples were usually retrieved every 10 feet (3.03 m) during the drilling of each piezometer with a thick-walled "split-spoon" sampler that was driven ahead of the drill bit into native formation by a standard weight falling a preset distance. This standardized procedure allows the "blow count" - the number of blows per distance traveled, usually 0.5 feet (0.15 m) or 1.0 feet (0.30 m) - to be used for the estimation of geotechnical parameters in the absence of more accurate information. Upon retrieval of the sampler, the contents (2 feet; 0.61 m) were removed, examined, and described. For each spoon that was retrieved, lithology representative of the entire sample was preserved in an airtight glass jar.

Undisturbed Samples

Disturbed samples are too disrupted during acquisition to be adequate for geotechnical testing. Undisturbed samples, however, can be used to adequately assess geotechnical parameters if those parameters are not compromised during retrieval, preservation, shipping, or final removal and preparation (Hvorslev, 1949). Geotechnical test results from this study appeared to be of very high quality (V. Torrey, 1996, personal communication) due to care in retrieval and preservation at the field sites and due to careful sample preparation and test execution at WES.

Undisturbed samples were retrieved at the field sites with a thin-walled, 3-inch (7.62 cm) diameter sampler known as a Shelby tube (Hvorslev, 1949; McCarthy, 1993). At the desired sampling point, the Shelby tube was attached to the drill string and hydraulically pressed slowly ahead into native formation for a distance of 2-3 feet (0.61-0.91 m). If the Shelby tube is advanced at a sufficiently slow rate, deformation of the sample during entry into the tube can be limited to a

thin, sheared band of material at the outer circumference of the sample which can be removed subsequently at the laboratory (Hvorslev, 1949). Thus, the undisturbed nature of the sample is essentially preserved.

Immediately upon retrieval at the field site, the ends of the Shelby tube were cleared of debris, and a sufficient amount of hot paraffin wax was poured into the tube to ensure that no water would escape from the sample during shipping. This is important to the accurate determination of parameters such as water content and saturation, unit weight, and pore pressure. Some studies (McManis and Lourie, 1995) suggest that onsite extrusion of undisturbed samples from Shelby tubes with piston-type devices does not adversely affect geotechnical testing results. However, the possibility of sample disturbance due to onsite extrusion was eliminated by transporting the sealed Shelby tubes to WES prior to any sample removal attempts.

Sample and Gamma Ray Wireline Logs

Sample logs were made for each piezometer during drilling. Gamma ray wireline logging was performed on the deepest piezometer at each field site. In general, four different types of glacial or glacio-lacustrine lithologies were encountered during drilling. These are: (1) glacial till (diamicton), gray to brown, usually silty, sandy, and/or pebbly; (2) lacustrine clay, brown, laminated, very fine-grained, sometimes interbedded with silt and/or fine sand; (3) sand, buff to tan, usually fine-medium grained, well-rounded, well-sorted, often laminated, occasionally cross-bedded; and (4) interbedded sand and clay, usually thinly bedded (beds 1/2 " to 2" thick).

Methods of Determination of Index Properties and Geotechnical Parameters

Introduction

Determination of index properties and geotechnical parameters is critical to the development of a through understanding of failure mechanics of soils. Grain size distributions and Atterberg limits were determined for the purpose of soil classification. This information also provided insight concerning potential lithologic/hydrologic controls on slope failure mechanisms (e.g., liquefaction vs. slippage on a failure surface). Two different types of triaxial compression tests and a set of consolidation tests were performed in order to acquire new geotechnical data that was utilized in slope failure modeling. All work was performed under the auspices of the U.S. Army Corps of Engineers (USACE), at its Waterways Experiment Station (WES) Geotechnical Laboratory in Vicksburg, MS. All tests were performed in accordance with standard procedures (USACE, 1986).

Grain Size Distribution Determination

Sieve and hydrometer analyses (USACE, 1986) of 16 samples were performed. A series of wire mesh sieves were used to determine weight percentages of gravel (clast diameter > 5 mm) and sand (5 mm > clast diameter > .075 mm) fractions, while hydrometers were used to determine weight percentages of silt and clay (0.75 mm > clast diameter) fractions.

Atterberg Limit Determination

Atterberg limits (Casagrande, 1948) were determined for the same 16 samples used in grain size distribution determination. Atterberg limit

determination is important not only for soil classification, but also because these limits quantify important behavioral transition points of cohesive soils that are controlled by water content (weight water/weight solids). The liquid limit (LL) of a lithology specifies the water content at which a material changes from plastic to liquid behavior. The plastic limit (PL) of a lithology specifies the water content at which the material changes from a semisolid state to a plastic state. The difference between these two limits is the plasticity index (PI):

$$PI = LL - PL$$

Triaxial Compression Tests

Specimen Preparation

Upon arrival at WES, two 3 inch (7.6 cm) long sample lifts were trimmed off the end of a Shelby tube by cutting the tube laterally with a band saw. The tube pieces were then carefully trimmed away from the sample by use of a thin, taut wire saw. The two cylindrical sample lifts were sliced longitudinally, yielding four semi-cylindrical specimens. A trimming machine set up in the WES "humid room" was used to shape these semi-cylindrical specimens into four 1.35 inch x 3 inch (3.4 cm x 7.6 cm) cylinders.

After trimming, specimen volume was determined with an electronic caliper, and specimen weight was determined with an electronic balance. Each specimen was then placed in an airtight aluminum or stainless steel container. As soon as was practicable, a specimen was jacketed with an impermeable latex membrane, secured between plexiglas end caps, placed in a triaxial testing chamber, and loaded to a

predetermined confining pressure via hydraulic pressure from water surrounding the specimen (Figure 16).

Triaxial Test Types

The triaxial tests performed in this study are designed to replicate different in situ loading conditions and time frames in which soils may be exposed to stresses that could lead to shear failure. Two types of triaxial tests were performed in this study: (1) Unconsolidated-Undrained tests ("UU" or "Q" tests) and (2) Consolidated-Undrained tests ("CU" or "R" tests). A third type of triaxial test, Consolidated-Drained ("CD" or "S" test), is prohibitively long in duration to perform in soils of low hydraulic conductivity such as those present in the study area.

Unconsolidated-Undrained (UU) Test Conditions. As the name implies, these tests are performed under conditions of no consolidation (compaction) and no drainage in the presence of an applied load. UU tests are designed to replicate conditions of rapid stress buildup and no drainage that usually occur in soils with very low hydraulic conductivity. Civil engineers often use UU tests to model short-term stress change situations such as immediately after the end of construction of buildings (McCarthy, 1993) or end of excavation of pits or trenches. These tests can be run quickly, hence the "Q" designation by the USACE, and are relatively inexpensive. Accurate laboratory replication of in situ failure under these conditions requires preservation of initial water content and no sample drainage.

Thirteen sample lithologies were tested, using a total of 43 specimens. Tests were usually performed in groups of three specimens per sample, under different

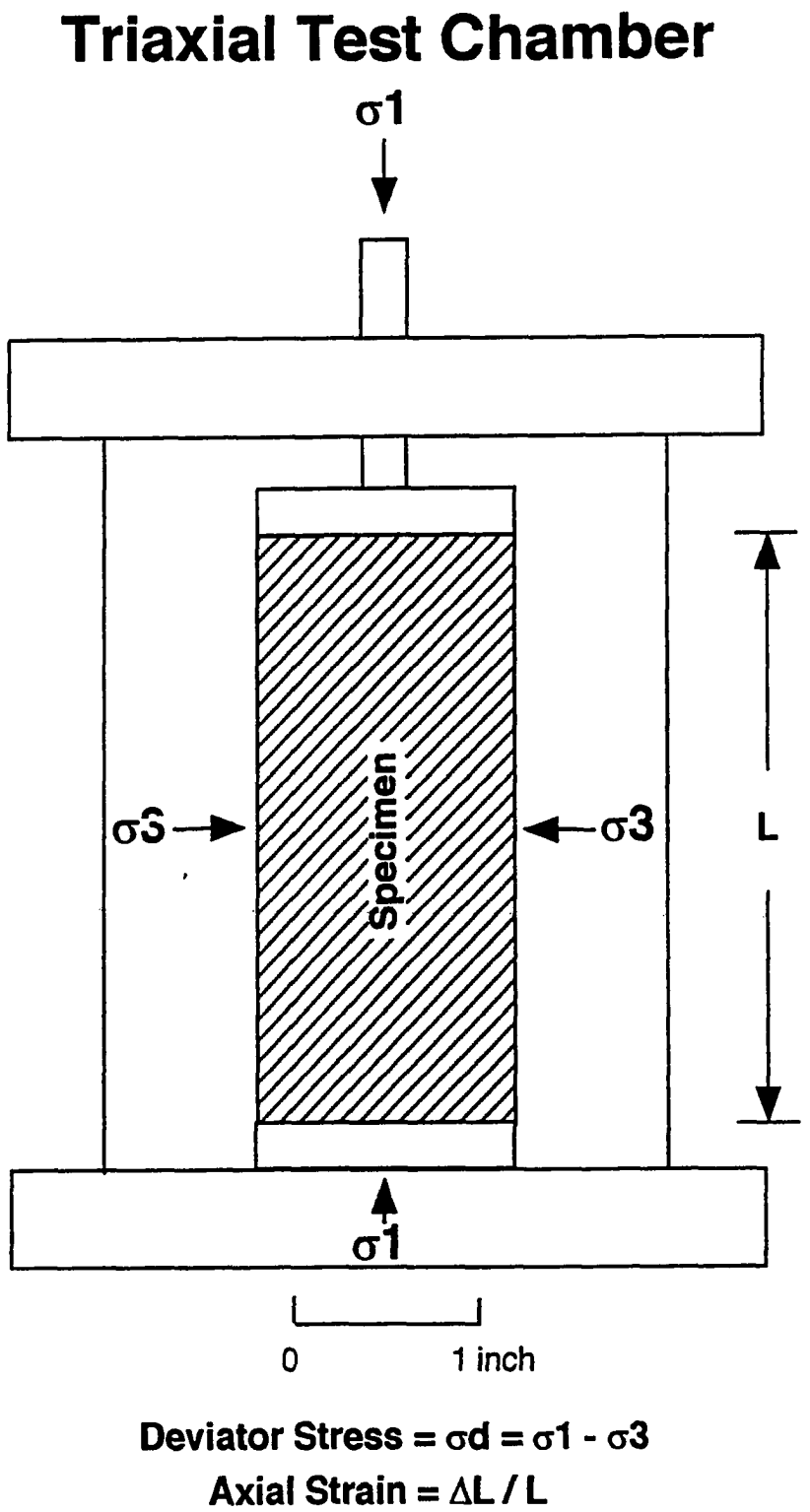

Figure 16. Triaxial Test Chamber (after USACE, 1986).

conditions of confining stress calculated to bracket the original in situ sample stress based upon measured unit weights of overlying stratigraphic units and sample depth. With four sample lithologies, stratigraphic variation in the amount of interbedded silt and sand in lacustrine clay dictated the need for four specimens to be run: two that were more sandy, two that were less sandy. Where possible, all specimens in a test were taken from adjacent sample lifts.

Consolidated-Undrained (CU) Test Conditions. These tests are performed under conditions of varying levels of preconsolidation and no drainage in the presence of an applied load. CU tests are generally used to model intermediate- to long-term conditions following a stress buildup. Under these conditions, groundwater drainage and soil consolidation (which increases shear strength) should be replicated (McCarthy, 1993). CU tests are much more complex and time-consuming to run (days vs minutes) than UU tests, but they provide otherwise unobtainable information about pore pressures in specimens, which may ultimately be critical in failure analysis.

Five samples were selected for CU testing (a total of 15 specimens). Two diamicton samples (from 20 feet; 6.0 m and 55 feet; 16.5 m) and two lacustrine clay samples (from 40 feet; 12.0 m and 80 feet; 24.0 m) were selected. The remaining CU test was performed on specimens from an interbedded sand/clay lithology (from 80 feet; 24.0 m).

A CU test required considerable time for one set of specimens, usually on the order of 36 hours. After preparation, each of three specimens was placed in a triaxial testing apparatus with water lines attached to the end caps. A low confining pressure ($\sigma 3$) was applied to the specimens, and they were the fully saturated as water was fed slowly into the sample through one of the endcaps while air was forced

out the other. After a visual determination that all air had been removed from the specimen, a b-value test (USACE, 1986) was run with the drain lines closed to ensure that saturation was complete:

$$b = \frac{\Delta u}{\Delta \sigma 3}$$

where b = b-value

Δu = change in sample pore pressure

$\Delta \sigma 3$ = change in confining pressure

A b-value close to unity indicates that any increase in confining pressure on the specimen is carried completely by a commensurate increase in pore pressure, which means the soil skeleton is not carrying any incremental increase in stress. This indicates that the sample is fully saturated.

The next step required consolidation of each specimen in the presence of the confining pressure that would be present during shear. As in the UU tests, the goal was to adequately bracket a sample's calculated in situ overburden pressure with three different confining pressures. The endcap drain line remained open during this phase so that pore water could drain and the soil skeletons could consolidate. The rate of consolidation vs. time was graphed, and when the rate leveled off, a specimen was considered to be fully consolidated (USACE,1986). At this point, the drain line was closed, attached to a pressure gauge, and then re-opened for subsequent pore pressure measurement once the test began. Three specimens, consolidated to three different confining pressures, were compressed undrained at very low rates of strain until failure was achieved.

Stress-Strain Curves Generated From Triaxial Compression

Under the appropriate UU or CU conditions, specimens were axially compressed at a constant strain rate (Figure 17a). Deviator stress ($\sigma_d = \sigma_1 - \sigma_3$; axial stress - confining stress), which is a measure of specimen strength, was recorded vs. axial strain (ε, per cent shortening of the specimen) throughout the duration of the test on an IBM 286 computer (Figure 17b). Mechanically, specimen failure occurs at the point where internal shearing develops, manifested as grains and/or particles rolling or sliding past each other. The automated computer software at WES selected the specimen failure point as the peak deviator stress or the deviator stress at 15% strain, whichever was higher.

Mohr Circles and Failure Envelope Construction

A Mohr circle is a graphic device used to represent relationships between normal stress (σ) and shear stress (τ) at specimen failure (Figure 17c). For a single specimen, axial stress (σ_1, derived from the relationship $\sigma_d = \sigma_1 - \sigma_3$) and confining stress ($\sigma_3$) at failure can be plotted on the normal stress axis. These principal stresses exist only in the absence of shear stress (τ=0). The point of maximum shear stress (τ_{max}) on the Mohr circle is one-half the deviator stress ($\sigma_d/2$).

For each undisturbed sample, a set of Mohr circles (one for each specimen) was automatically plotted by computer utilizing the peak stress and strain data recorded during shear. All stress-strain, index property, and Mohr circle data were then printed out on standard USACE (1986) data sheets for each sample. Sets of data sheets were generated for both UU and CU tests. For each sample, a failure envelope derived from a set of Mohr circles was drawn by hand. Total stress (UU test)

Triaxial Testing & Failure Analysis - Procedure

A. Specimen Compression to Failure

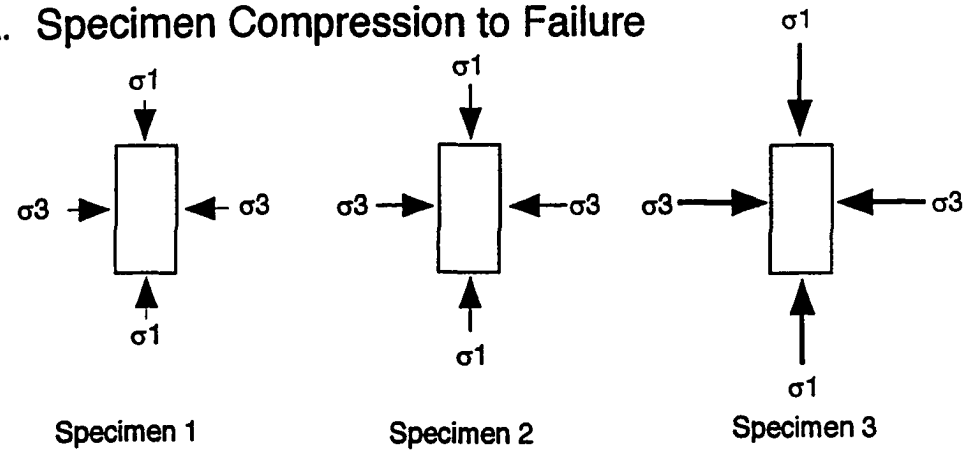

B. Stress - Strain Curve Analysis

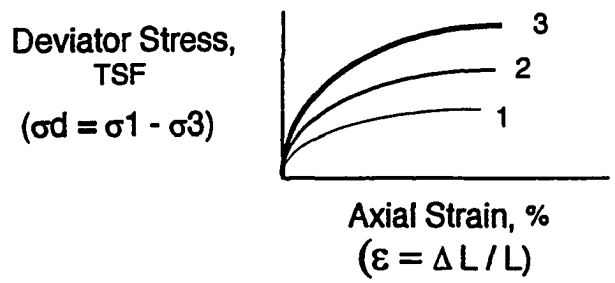

C. Mohr Circle / Failure Envelope Construction & Analysis

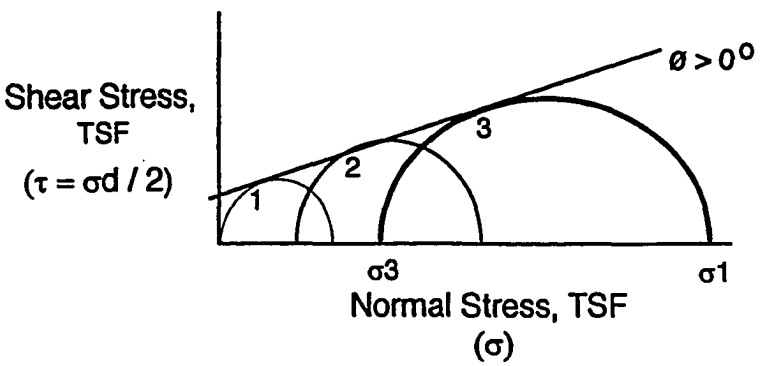

Figure 17. Triaxial Testing and Failure Analysis Procedure.

geotechnical parameters including undrained shear strength (S_U) and cohesion (c), and effective stress (CU test) parameters including effective internal angle of friction (ø') and effective cohesion (c') were then measured from the failure envelopes.

Stress Path Analysis

An alternative or adjunct to Mohr-Coulomb failure envelope construction (USACE, 1993) involves the analysis of specimen stress paths to failure and the construction of a p, q failure envelope (Figure 18). The total stress path to failure in Figure 16 is composed of the series of points (p, q) that trace the evolving stress conditions in one specimen under increasing load throughout the duration of a CU compression test, where:

$$p = \frac{\sigma_1 + \sigma_3}{2}, \quad q = \frac{\sigma_1 - \sigma_3}{2}$$

A series of specimen stress paths to failure form a p, q failure envelope for a given sample. The stress paths of individual specimens as they approach the p, q failure envelope may vary because of their differences in pore pressure, consolidation state, etc. However, once the failure envelope is reached, the specimens tend to track along it. The y-axis intercept (a) and slope (α) of the p, q failure envelope can be related to the more familiar parameters c and ø from a Mohr-Coulomb failure envelope by the following relationships :

$$\tan ø = \sin \alpha$$

$$a = c \cos ø$$

Comparison of Mohr-Coulomb and p,q Failure Envelopes

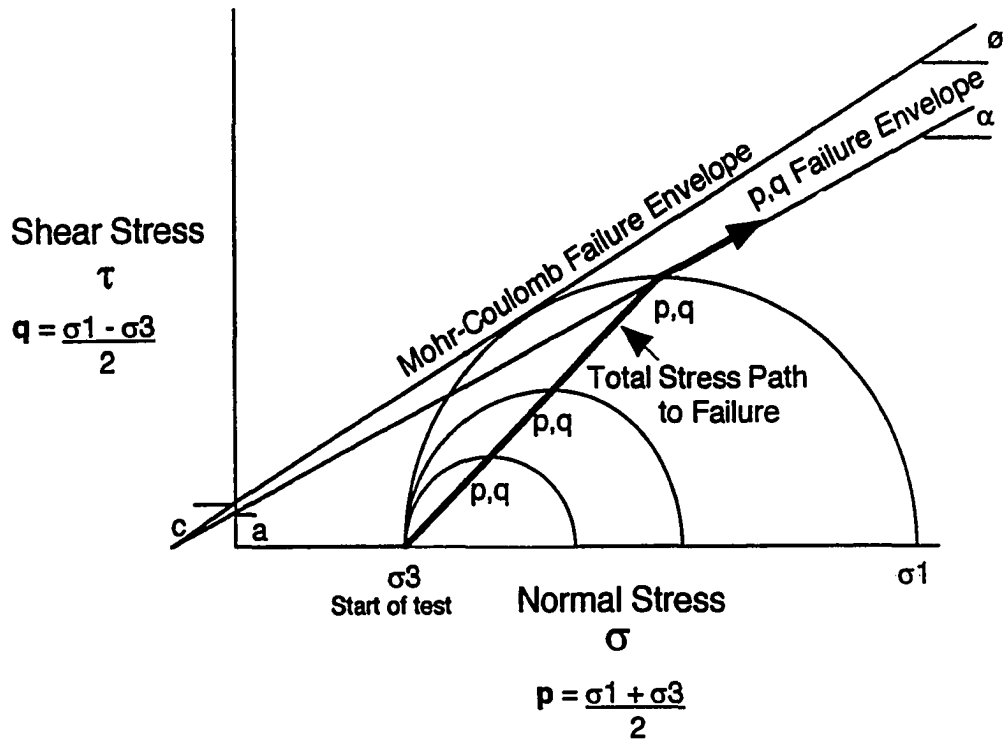

Relationships: $\tan \alpha = \sin \phi$

$a = c \cos \phi$

(after USACE, 1993)

Figure 18. Comparison of Mohr-Coulomb and p,q Failure Envelopes.

Effective stress paths to failure can be determined from total stress paths if pore pressures are known. Therefore, effective stress paths to failure for the five samples tested under CU conditions were able to be generated in this study.

Overconsolidation Ratio (OCR) Determination

Two general types of consolidation states -normal and overconsolidated- are often used to describe the inferred compaction history of cohesive soils (Lambe and Whitman, 1969). However, a broad range of states actually exist (Mayne et al., 1995). A clay's consolidation state is identified by its overconsolidation ratio (OCR):

$$OCR = \frac{\sigma'_{vm}}{\sigma'_{vc}}$$

where σ'_{vm} = maximum vertical effective stress in the past

σ'_{vc} = current vertical effective stress

Normal consolidation describes a state wherein a soil's current in situ compaction state is as dense as it has ever been (OCR ~ 1). Overconsolidation refers to a state wherein a soil's current in situ compaction state is less dense than it was in the past (thus OCR > 1). Consolidation tests (USACE, 1986) were performed on three samples in the study area.

Method of Limit Equilibrium Analysis

Introduction

One bluff failure mechanism that has been observed in the study area involves slippage of materials on a failure surface. Limit equilibrium analysis (also known

as slope stability or factor of safety analysis) provides a framework for the study of the interaction of forces and materials that lead to slippage on a failure surface (Bishop, 1955). The weight (W) of a soil mass can be broken vectorally into two components operating upon a potential failure surface (Figure 19). One vector is a shear force (W sin α) parallel to the failure surface that acts to drive slippage. The other vector is a normal force (W cos α) that acts to resist slippage in conjunction with the soil's internal angle of friction (ø) and cohesion (c), which are measures of a material's internal resistance to shear (Lambe and Whitman, 1969).

The sum of the resisting forces divided by the sum of the driving forces yields the Factor of Safety (FS):

$$FS = \frac{\sum \text{Forces resisting shear failure}}{\sum \text{Forces driving shear failure}}$$

If FS > 1.0, stability on the surface is implied; if FS $\leq$ 1.0, instability is implied. Any incremental loss of stability that lowers the factor of safety beyond FS = 1.0 will lead to immediate failure, which suggests that any calculated FS < 1.0 is theoretically impossible. However, reality is more complicated (or more difficult to model) than this. FS calculations performed on unfailed Great Lakes bluffs sometimes yield FS < 1.0 (Sterrett, 1980).

Factor of Safety Analytical Methods

Factor of Safety analytical methods are all similar in their approach to modeling failure (e.g., Bishop, 1955; Fellenius, 1936; Morgenstern and Price, 1965; Janbu, 1954). The method most intuitively understood and easiest to determine by hand calculation or graphical methods is the Ordinary Method of Slices

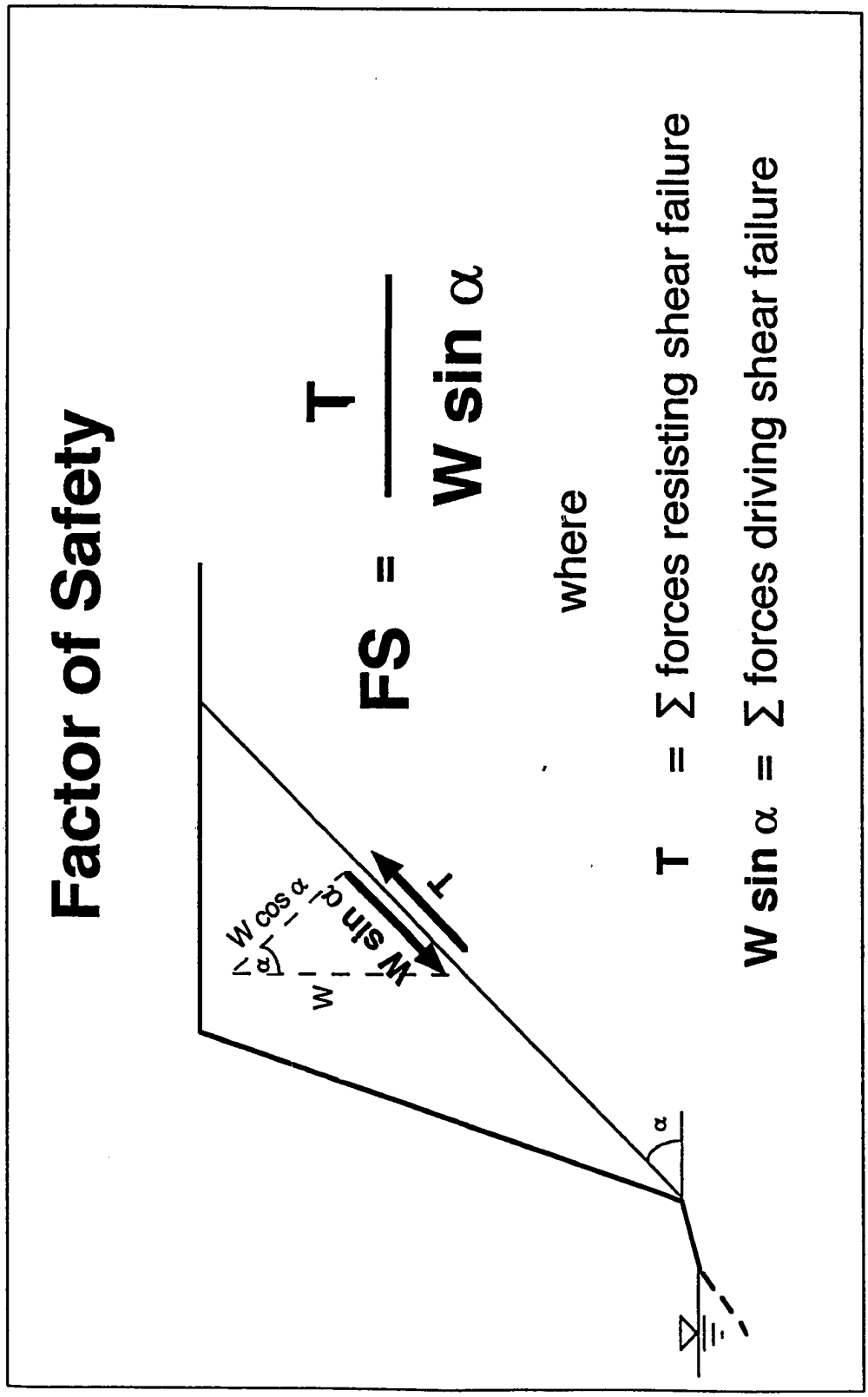

Figure 19. Concept of Factor of Safety Analysis.

(Fellenius, 1936). First, the soil above the potential failure surface is divided into a series of vertical slices of varying width (Figure 20). One factor that dictates the width of a slice is the requirement that the base of the slice on the failure surface comprise only one soil type. This is necessary in order to define a singular value for each material property at the base of each slice. Another factor dictating the width of a slice is the curvature (if any) of the failure surface. More than one slice will be required on a curved failure surface, even in homogeneous material, because the failure surface angle (α) will change.

The forces resisting and causing failure are identified in each slice and summed in order to calculate a Factor of Safety representing the entire system along the defined failure surface:

$$FS = \frac{\sum \text{Forces resisting shear failure}}{\sum \text{Forces driving shear failure}} = \frac{\sum (cl + W \cos \alpha \tan \phi)}{\sum W \sin \alpha} \sim \frac{\text{Shear strength}}{\text{Shear stress}}$$

where W = weight (lb/unit width) of material in slice

l = length (feet) of base of slice along fault plane

α = failure plane angle (degrees)

ϕ = internal angle of friction (degrees) (determined from Mohr envelope)

c = cohesion (lb/ft^2) of material in slice (determined from Mohr envelope)

Total Normal Stress vs Effective Normal Stress

Water is a complicating factor in stability analysis. Water, being a fluid, has zero shear strength, but it can act to strengthen (through negative pore pressure) or weaken (through positive pore pressure) specimens in undrained triaxial tests, the results of which are used in stability analysis. Effective stress

Ordinary Method of Slices

(Schematic) (Felenius, 1936)

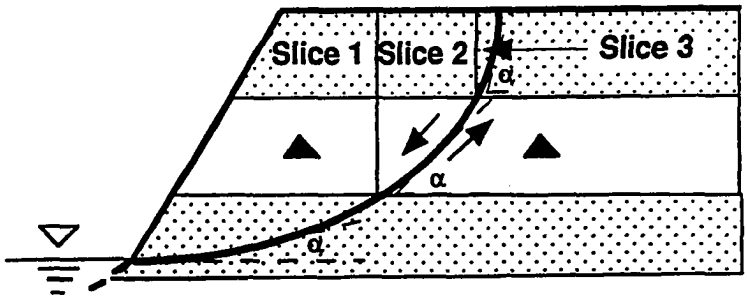

$$FS = \frac{\sum \text{forces resisting failure}}{\sum \text{forces causing failure}}$$

Forces in all slices are summed:

$$FS = \frac{\sum [c'l + (W \cos \alpha - ul) \tan \phi']}{\sum W \sin \alpha}$$

where for each slice:

W = weight of slice
c(') = cohesion (effective)
ø(') = internal friction angle (effective)
l = length of slice base on failure surface
u = pore pressure (when known)
α = average failure surface angle at base of slice

Figure 20. Specific Components In Ordinary Method of Slices for Factor of Safety Analysis.

effects of pore pressure, so that FS calculations reflect only an effective normal stress component, rather than total normal stress.

Effective stress analysis requires modification to both the Mohr failure envelope and Factor of Safety equations. The equation describing the Mohr failure envelope line becomes:

$$\tau' = c' + (\sigma_t - u) \tan \phi$$

or $$\tau' = c' + \sigma' \tan \phi'$$

where τ' = effective shear stress

σ_t = total normal stress

σ' = effective normal stress

u = pore pressure

c' = effective cohesion

ϕ' = effective internal angle of friction

The Factor of Safety equation incorporating effective stress analysis becomes:

$$FS = \frac{\sum \text{Forces resisting shear failure}}{\sum \text{Forces causing shear failure}} \sim \frac{\sum (c'l + (W \cos \alpha - ul) \tan \phi')}{\sum W \sin \alpha}$$

It must be emphasized that there is no universal consensus as to the efficacy of total vs effective stress analysis (Mayne et al., 1995). The only consensus among practicing civil engineers is that local experience with the technique that best imitates reality is the key to predictive success.

Stability Analyses in the Study Area

Initial Factor of Safety analyses were performed by hand calculation for all clay, all sand, and mixed sand/clay bluffs based upon slope geometry measured in the

field and geotechnical parameters measured either during drilling or in the laboratory (Montgomery, 1996 b). The initial analyses were later augmented by computer analysis of the six field sites using UTEXAS3 version 1.120, guided by documentation and user instructions developed by Edris and Wright (1992), as well as support from USACE personnel (Vanadit-Ellis and Edris, 1997, personal communication).

Initial hand calculations were performed on predetermined failure surfaces whose angles were estimated from bluff face geometry, but UTEXAS3 performs an automated search for the most likely failure surface with the lowest Factor of Safety.

Method of Historical Bluff Recession Analysis

Introduction

High resolution airphoto analysis of bluffline recession in the study area was performed at USACE Detroit District offices with state-of-the-art Intergraph GIS hardware and software. This analysis allowed for a detailed comparison of predictions based upon bluff characterization, geotechnical properties, and Factor of Safety analysis with the historic record. Although recession rate data have previously been generated by both the Michigan Department of Natural Resources and the Corps of Engineers, the former data are old (mid-1970s), and the latter data are imprecise (averaged over 1 km lengths). For a more complete treatment of airphoto and remote sensing analysis, consult a reference text such as Avery and Berlin (1985) or Lillesand and Kiefer (1994).

Potential Sources of Error in Shoreline Change Mapping

Anders and Byrnes (1991) distinguish between accuracy and precision when identifying potential errors associated with shoreline change mapping. The types of problems likely to reduce accuracy vary depending on whether maps or air photos are used. With maps, problems with scale, paper stretch, surveying standards, and differences in projection can cause inaccuracy. In the case of air photos, location of the reference high water or bluff line, quality and location of control points, aircraft tilt/pitch and altitude changes, camera distortion, and the media used (negatives vs contact prints) can all cause inaccuracy.

Stafford and Langfelder (1971) suggested that the mean high water line is the best indicator of shoreline position at a given instant in time on the Outer Banks portion of the North Carolina coast. This has been adopted by many later workers (e.g., Anders and Byrnes, 1991; Crowell et al., 1991) for open ocean, sandy coastlines. However, much of the previous work in measuring shoreline change in the Great Lakes, especially in areas with relatively high bluffs, utilizes the blufftop edge (often associated with a significant break in slope) as the reference line (Buckler and Winters, 1983; Seibel, 1972; Powers, 1958; Johnson and Johnston, 1995). The lakeward limit of bluff vegetation has also been used as a reference point by the Michigan Department of Natural Resources in studies dating from the 1970s, especially on older, black and white photos. However, the bluff edge in Allegan County coincides with the lakeward limit of vegetation only in certain cases.

Some studies refer to General Land Office (GLO) records referencing Lake Michigan shoreline position that date back to 1831; these formed the basis for Powers' (1958) estimates of recession rates on Lake Michigan. The 1831 measurements were recorded as distances from section corners to the "meander line"

(Powers, 1958; Buckler and Winters, 1983). Workers who have utilized the 1831 data have implicitly accepted the "meander line" as the edge of the bluff, but this is only an assumption.

Digital Technology and Reduction of Measurement Error

Some of the map and air photo errors that were cited as sources of concern by Anders and Byrnes (1991) have been minimized by recent improvements in technology. In particular, digital technology has reduced the impact of many error sources that were of major concern just a few years ago. For example, a digital map database (MIRIS) is now utilized extensively in Michigan. Although points in this data base are subject to some error because of original digitization procedures from hard copy, earlier problems with scale, paper stretch, and projection are now avoided or eliminated because the data can be manipulated digitally. Digital scanning of aerial photography has also contributed to the error reduction process. Air photos can now be digitally enhanced and/or altered to reduce much of the distortion inherent in hard copy photos. These distortions, such as radial distortion away from the center of the photo and relief distortion due to elevation differences, formerly had to be manipulated with manual devices such as the Zoom Transfer Scope (Leatherman, 1983).

Measurement Error and Measurement Time Frames

Embedded in much of the literature on shoreline change (Leatherman, 1983; Crowell et al., 1991; Stafford and Langfelder, 1971; Anders and Byrnes, 1991) are cautionary statements that coastal change measurement errors come from many sources and that these errors can seriously compromise conclusions about the

magnitude and rate of coastal change. This can be a particularly significant problem on coasts that do not exhibit large amounts of change within the time frame selected for study (Stafford and Langfelder, 1971). When studying shoreline change over a short duration, as in this study, it is of importance to standardize procedures, identify potential sources of error, and utilize the best techniques and equipment possible within the parameters established by time, cost, and equipment availability. This will facilitate reduction of error to a level such that meaningful conclusions can be drawn.

Measurement Time Frames Selected for Study

The first available stereoscopic air photos of Lake Michigan were taken in 1938 by the U.S. Department of Agriculture. They are black and white, 1:20,000-scale (1 inch =1667 feet = 505.1 m) photos that are reasonably detailed when viewed with stereo magnifying glasses. The most recent stereo air photos available for this study were acquired in the spring of 1996 by the USACE. These are high resolution, natural color photos at a scale of 1:6,000 (1 inch = 500 feet = 151.5 m) that allow the accurate location of features such as sidewalk and deck corners to within +/- 0.5 foot (0.15 m) with stereo magnifying glasses.

Since one objective of the study was to measure recession during periods of average (as opposed to high) lake level, 1989 was chosen as the third point in time in which to measure the Allegan County bluffline. Hydrographs indicate that Great Lakes water levels had dropped back from record highs in 1986 to historical averages by 1989. Fortunately, the 1989 photos are of the same high resolution as the 1996 photos.

Areas of Study

Rather than attempt to compile and analyze a recession history for the entire study area, it was decided to study three distinct segments (Northern, Central, and Southern Areas) through detailed airphoto analysis. Each area contains two study sites (West Side County Park and Wau-Ken-A, 116th Avenue and Fabun Road, Miami Park and Consumers Power, respectively from north to south). This limited the amount of memory required for a mosaic and kept computational speed up to an acceptable level. It also facilitated the implementation of procedural changes as they became necessary.

Equipment

State-of-the-art Intergraph PC- and Unix-based hardware equipped with Intergraph ISI-2 software, in addition to a high-quality Umax Mirage D-16L Scanner were utilized at the Detroit District USACE GIS Center. A significant advantage of performing the work at this facility was the amount of memory available. Although compressed file management was used wherever possible, digital color air photos divided into pixels small enough to ensure accuracy and precision require an enormous amount of memory, even in a limited area.

Scanning of Air Photos

The scanning of an air photograph results in a computerized image made up of small squares known as pixels (Lillesand and Kiefer, 1994). Some professionals (T. Bennett, Michigan Department of Natural Resources, 1996, personal communication) indicate that computer images of scanned negatives are of higher resolution and accuracy than those scanned from contact prints. However, time and

budget limitations dictated the use of paper contact prints for scanning in this study. In each of the three study areas, enough contact prints were scanned to ensure good stereoscopic coverage. Typically, this translated to five to seven prints at the 1:6,000 scale and three at the 1:20,000 scale. Optimum scanning resolution was determined to be 400 dots per inch (dpi) for the 1:6,000 scale 1996 and 1989 prints; this scan resolution was also used for the 1:20,000 scale 1938 prints.

Contact Prints and Possible Scanning Interference

A potential side effect of using contact prints instead of negatives was noted in the scanning process. Computerized imaging usually involves tradeoffs between file size and resolution: the finer the pixel size, the better the resolution, but at the expense of a geometric increase in file size and computer memory requirements. However, with the 1989 and 1996 contact prints used in this study, it was visually evident that a scanning resolution of 400 dots per inch (dpi) resulted in better image resolution than either 300 dpi or 600 dpi. This may be attributable to some type of interference phenomenon between computer pixel size and photographic grain of the contact prints that might not have occurred if negatives had been used (D. Gerczak, USACE Detroit District, 1997, personal communication).

Ground Resolution

The ground resolution or pixel size that results from a 400 dpi scan of a 1996 or 1989 1:6,000 - scale (1 inch = 500 feet = 151.5 m) photo is 1.25 feet (0.38 m) on a side. This resolution was deemed to be adequate for the purposes of this study. The 1938 1:20,000 - scale (1" = 1667 feet = 505.1 m) photos were also scanned at a resolution of 400 dpi, but pixel size for these photos was 4.17 feet

on a side because of their larger scale. At the time of scanning, it seemed logical to assume that the 1938 photos were "grainier" than the more recent photos, and thus the study would not benefit from increased scanning resolution. However, as image manipulation and overlay progressed through the study, it became apparent that it would have been much easier to compare and compute sources and amounts of error if the scanning resolution of the 1938 photos had been increased such that the pixel sizes of all three years analyzed would have been the same. Furthermore, judging from the resolution of the 1938 images on the computer screen, it is possible that the 1938 contact prints may be of sufficient quality to warrant higher resolution.

Overlay Operations

Determination of Standard Error

Standard Error (SE) as measured in overlay operations such as registration and rectification on the Intergraph system requires some explanation. Once a common registration or rectification point on two images has been selected by the user, the computer essentially takes the input point from the input image, fits it onto the control image, then returns the input point (now in the same position as the control point) back to the input image and compares its new position to its original position. In the Intergraph system, the difference between the two positions is measured not in units of length such as feet or meters, but rather in pixels. Thus, an SE of 1.0 after an overlay operation means that, on average, the new position of a point on the input image is within one pixel of its old position on the input image. Alternatively viewed, the input point is accurately located to within one pixel of the control point. The computer keeps a running total of the accuracy of the entire image such that the end product is an averaged standard error for the entire image.

Image to Image Registration

Registration and rectification of digital airphoto images are critical steps in the recession analysis process. These operations, in conjunction with bluff edge positional uncertainty, constitute the major sources of error in this analysis. Registration of an input image to a control image was accomplished by: (a) identification of identical features in overlapping portions of the images (e.g., deck or sidewalk corners), then (b) computer "warping" and overlay of the input image upon the control image. A number of computer images (usually four to six) were successively warped to each other to create progressively larger mosaics in each of the three study areas.

Registration Error

Generally, 8-20 common points were adequate for achievement of a low SE of about 1.0 when registering one airphoto computer image to another. Registration of larger, composite image mosaics to each other usually required 30-60 common points to get a good fit of SE ~ 3.0.

Image to Map Rectification

Rectification is a somewhat different operation than registration, although the principles are the same. Rectification is the procedure whereby a non-standardized image (in this case, a photo mosaic) becomes oriented, scaled, and projected in space while distortions are removed to acceptable levels of measurement error. The rectification process creates maps, or in this case, images with the properties of maps.

One - Time Rectification to MIRIS

Rectification to MIRIS at some point in the process was necessary to minimize significant distortion in the photo mosaics. Some professionals argue that the central image sections of modern air photos contain less distortion than maps generated from MIRIS. However, there were several instances in this study where it was observed that some portions of the photomosaics containing well-known features such as paved roads were more than 100 feet (30.3 m) out of position when compared to MIRIS base maps, whose accuracy is no worse than +/- 40 feet (12.1 m) at 1: 24,000 scale according to national map standards (Anders and Byrnes, 1991).

Rectification to MIRIS was thought to be of concern from the standpoint of measurement error, because significant error can be introduced during the rectification process due to positional uncertainty of the control points. For example, the best control points utilized in rectification of images to MIRIS are road intersections, the center points of which on even undistorted photos are uncertain. As a result, a 1996 photomosaic fit to MIRIS was no better than SE = 6, or about +/- 7.5 feet (2.3 m).

However, reduction of rectification error as a component of measurement error was achieved by performing just one rectification to MIRIS with the 1996 mosaic. The rectified 1996 image became ground truth to which the 1989 and 1938 mosaics were subsequently registered. This was possible because the study focused on relative amounts of change from 1938 to 1996. The initial rectification from a 1996 image to MIRIS may have introduced some positional error relative to absolute spatial coordinates, but the only error introduced in the process from this point forward was that involving successive registrations, the SEs of which are much lower than those of rectification operations.

Image Registration to Rectified Image

The 1996 mosaics were rectified to MIRIS, the State of Michigan digital map base developed from 1:24,000 scale U.S.G.S topograhic maps. The 1996 rectified mosaics served as ground truth to which the 1989 mosaics were registered and automatically rectified. In turn, the 1989 rectified mosaics served as the control images to which the 1938 mosaics were registered and automatically rectified.

Successive Image Registration

The mosaic-to-mosaic registration process resulted in more accurate and precise images than would have resulted from individual mosaic rectification to MIRIS. However, a brief explanation may be in order concerning the choice to successively register 1989 mosaics to 1996 mosaics and then 1938 mosaics to 1989 mosaics, rather than to register both 1989 and 1938 mosaics to 1996. The latter option intuitively would seem to result in less error than the successive registration process. There are two major reasons why this choice was made.

First, there were a significantly larger number of common points between the 1989 and 1938 mosaics than there were between 1996 and 1938; this led to increased confidence about the reliability and accuracy of the points. It was evident from the photos that sufficient change had occurred in the years between 1989 and 1996 to result in the loss of a number of points that had been common to the 1938 and 1989 photographs.

Second, even though the SE calculated slightly lower (5 vs. 6) on a direct warp of 1938 to 1996 mosaics as compared to successive registration, careful onscreen comparison demonstrated that successive registration was slightly truer to MIRIS than was the direct 1938 to 1996 registration. Although this result is

somewhat counter-intuitive, it was not the first time during the study that a lower SE had not translated to the best visual fit. Rather, it was found that a large (but not always the biggest) number of reliable, well-spaced, carefully chosen points produced the best balance between visual accuracy and low standard error.

Registration and Measurement Error

The estimated registration error between 1989 and 1996 images is +/- 3.75 feet (1.1 m) and +/- 0.5 foot (0.15 m) measurement error from the photos, for a total of +/- 4.25 feet (1.29 m) when comparing 1989 to 1996 bluff positions. There was one instance, probably due to relief distortion at the base of Fabun Road, where there was observed to be more variance than this; in this case, the edge of a lawn could not be resolved to a difference of less than 6 feet. However, the vast majority of decks, corners of sidewalks, house corners, and other high-resolution control points were generally found to be no more than +/- 1.0 foot (0.30 m) in variance. This is truly extraordinary accuracy and precision.

Because of differing pixel sizes and photo scales, the 1938 to 1989 to 1996 compound error is greater than that of the more recent photos. The compound error involved in registering a 1938 to 1989 mosaic, +/- 12.5 feet (3.8 m), must be added to the +/- 4.25 feet (1.29 m) error from 1989 to 1996 when comparing 1938 bluffline position to that of 1996. In terms of measurement error from the 1938 photos themselves, another +/- 4.2 feet (1.27 m), the size of a pixel, needs to be added to the +/- 16.75 feet (5.08 m) because of the large 1:20,000 scale and resultant "graininess" on the computer image. Total hardware and software error for the period 1938 to 1996 is +/- 20.95 feet (6.35 m).

Long Term vs. Short Term Measurement Error

Stafford and Langfelder (1971) indicate that larger amounts of error can be tolerated in analysis of long-term coastal change than in short-term change, because more change in shoreline position is likely to occur over a longer time frame. Their premise is that large error bars will not overwhelm the changes being measured over the long term, and confidence concerning the validity of these measurements will be preserved.

In this study, larger error bars (+/- ~21 feet; 6.36 m) are being applied over the long term (from 1938 to 1996) than those for the short 1989 to 1996 period. The high accuracy and precision required in order to adequately evaluate bluff edge change over the short time period 1989 to 1996 was maintained (+/- 4.25 feet; 1.29 m) because of the small pixel sizes of the 1989 and 1996 photo images, as well as the high resolution and large scale of the original color photos.

Onscreen Digitizing and Positional Uncertainty of the Bluff Edge

Onscreen digitizing of the bluff edge in the study area was performed utilizing 1996, 1989, and 1938 mosaics as base images. Digitizing was guided with stereo viewing of hardcopy photos. In areas of uncertainty, a conservative estimate of change in bluff edge through time guided interpretation. The importance of stereo viewing as a guide to onscreen digitizing cannot be overemphasized. Without stereo viewing, a general rule of thumb such as the "lakeward extent of vegetation" may have to be used as a fallback position. This method results in accurate bluff edge detection only in very specific circumstances associated with unvegetated slopes, which comprise only 25% - 33% of the bluff in the study area.

The biggest cause of bluff edge positional uncertainty is tree cover. Stereo viewing and estimation of breaks in slope using tree canopy minimize this error, but error is introduced nonetheless. Both the Michigan Department of Natural Resources and the U.S. Army Corps of Engineers now try to acquire photo coverage under "leaf-off" conditions in early spring. However, the 1989 and 1996 photos used in this study were acquired in late spring, and trees had already begun to sprout new growth. Dashed bluff edge lines on the mosaics reflect their positional uncertainty.

Method of Comparison of Historical Recession Data to Bluff Lithology/Hydrology

Large-scale 1:2,400 (one inch = 200 feet = 60.6 m) airphoto mosaics were used to identify historical recession patterns in the three study areas during the periods 1938-1996 and 1989-1996. It is evident from the mosaics that there were only a few areas of the bluff that experienced measurable recession from 1989 to 1996, so no quantitative recession analysis was undertaken for this time period.

For the 1938-1996 study period, manual measurements from the airphoto mosaics led to identification of shoreline segments (recession cells) that range in amounts of recession from nil to as much as one hundred feet (30 m) (Figure 21). Recession cell boundaries were placed in such a manner as to distinguish these shoreline segments from each other. For each recession cell, comparisons were then undertaken between average recession magnitude, type of bluff lithology (sand, mixed, or clay) present, and hydraulic head mapped at the bluff face in each aquifer system in order to determine what, if any, relationships may have existed among lithology, hydrology, and shoreline recession between 1938 and 1996.

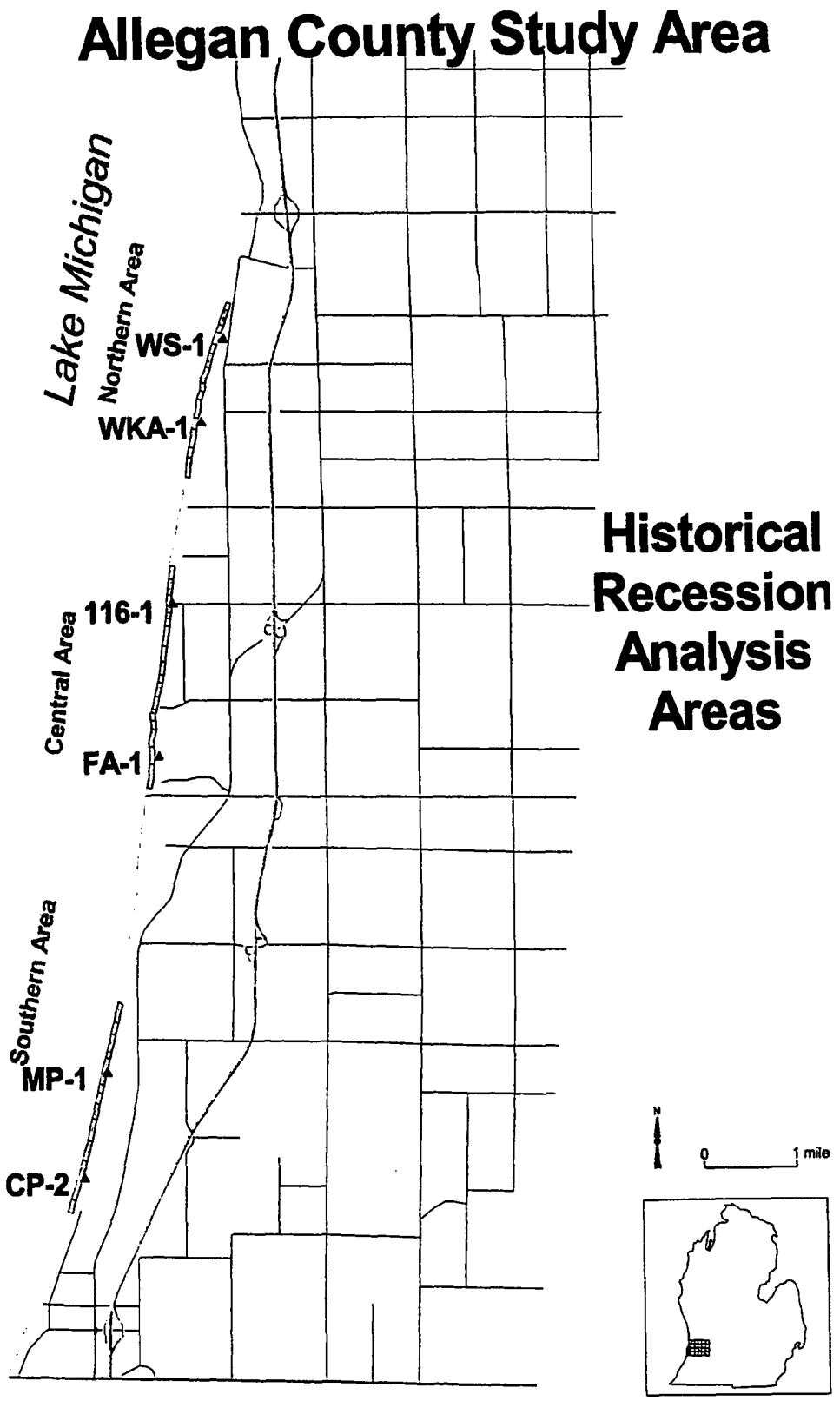

Figure 21. Historical Recession Analysis Areas Showing Locations of Recession Cells.

CHAPTER IV

WORK PRODUCTS AND NEW DATA

Chapter Overview

New work products in the form of bluff characterizations were generated from existing lithologic and hydrologic data through development and implementation of a new GIS-based methodology. New lithologic and hydrologic data were collected from the field through drilling, sampling, and long-term monitoring. New index property and geotechnical data were generated through laboratory measurement and testing, and were then utilized in the generation of limit equilibrium analyses of the field sites. Measurements from new high-resolution airphoto mosaics with superimposed 1938, 1989, and 1996 bluff lines resulted in the generation of a new historical bluff recession data set. Historical recession and lithologic/hydrologic data sets were reformatted into a cell-based GIS format to facilitate comparison and identify patterns.

Bluff Characterization Maps

Three new Lake Michigan bluff characterization maps were generated based upon the GIS-based methodology developed by Montgomery et al. (1996a). These maps were created at the Western Michigan University GIS Research Center.

The lithologic characterization map (Figure 10) consists of cells of either all sand, all clay, or mixed sand and clay lithotypes according to the classification previously developed (Figure 9). Quantitatively, the transition from clay to mixed lithology occurs at 33% sand, and the transition from mixed lithology to sand occurs

at 66% sand. The regional north-south cross section (Figure 6) indicates that the bluff is clay-rich at the southern end of the study area, and sand-rich at the northern end. Mixed sand/clay cells represent transition zones between the all-sand and all-clay end members.

The hydrologic characterization map (Figure 14) consists of cells of either high head or low head, based upon the intermediate aquifer total head contour map. Cells characterized with high head at the bluff face are associated with mapped trends of high head that branch off the groundwater divide coincident with the crest of the Lake Border Moraine complex. Cells characterized with high head occur in areas near Miami Park (MP), Fabun Road (FA), and the West Side County Park (WS), among others. The mapped groundwater divide in the proximity of Miami Park in the southern part of the study area may exert a particularly strong influence on groundwater flow at that site.

The combined characterization map (Figure 15) was created by a GIS overlay operation in Arc/Info utilizing the lithologic and hydrologic characterization maps. This map consists of cells of six different types : (1) sand lithology, high head ("HS"); (2) sand lithology, low head ("LS"); (3) mixed lithology, high head ("HM"); (4) mixed lithology, low head ("LM"); (5) clay lithology, high head ("HC"); (6) clay lithology, low head ("LC"). The combined characterization map, in conjunction with the surface work of Chase (1990; 1996, personal communication) and field traverses by the author, provided the basis for selection of six field sites for further data acquisition, each site representative of one lithologic/hydrologic combination.

Lithologic and Hydrologic Field Data Presentation

Introduction

Three piezometers were drilled at each of six field sites save Wau-Ken-A (WKA), where only two piezometers were drilled. Disturbed samples were collected from all piezometers, usually every 10 feet (3.0 m). Undisturbed samples were acquired where possible at each site. A gamma ray log was run in the deepest piezometer at each site (Appendix A); log depths for lithologic descriptions are relative to and below ground level. Piezometer water levels were monitored weekly or bi-weekly during the first year of study, and monthly thereafter.

Consumers Power (CP)

Stratigraphy

The uppermost 10 feet (3.4 m) (Figure 22) of bluff is brown, clayey diamicton. Predominant lithology below this is gray, silty to pebbly diamicton, except for sands that were logged at 32 to 38 feet (9.8 to 11.6 m), 65 to 70 feet (19.8 to 21.3 m), and 108 to at least 140 feet (32.9 to 42.0 m), which was total depth.

Gamma ray radioactivity is moderately high at this site, reflecting the predominant bluff composition of silty diamicton. Zones of low radioactivity, thought to be associated with sand, were logged from 32 to 38 feet (9.6 to 11.4 m), 66 to 70 feet (19.8 to 21.0 m), and 98 to 140 feet (29.4 to 42.0 m). The gamma ray log records higher radioactivity in fine-grained clay (e.g., 85 to 90 feet; 25.5 to 27.0 m) than in diamicton (e.g., 20 to 22 feet; 6.0 to 6.6 m), reflecting the greater sand and silt content present in the diamicton. Gamma ray signature was used for general

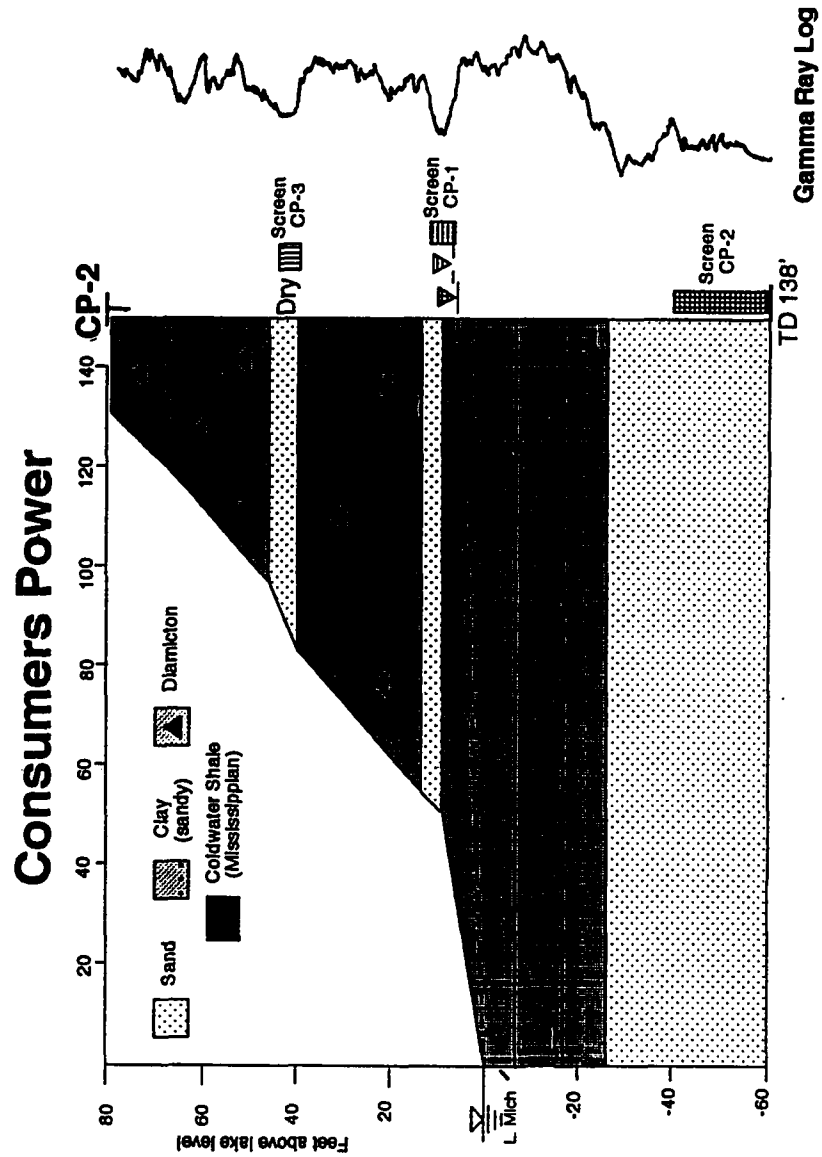

Figure 22. Consumers Power (CP) Bluff Profile. Includes Screened Intervals and Static Water Levels From Piezometers. Gamma Ray Log From CP-2.

subsurface identification in conjunction with sample control throughout the study area. It was particularly useful in interpretation and correlation when samples were either of poor quality or non-existent.

Hydrogeology

Piezometers were drilled to 40 feet, 12.1 m (CP-3); 70 feet, 21.1 m (CP-1); and 138 feet, 41.8 m (CP-2) (Figure 23). CP-3 was intended for completion in an apparent shallow sand at 32 to 38 feet (screen depth 35 to 40 feet; 10.5 to 12.0 m), but this piezometer has never had any water enter its well bore . CP-3 may be inadequately developed, but there are no telltale signs of this such as excess bentonite or mud. CP-1 was completed in an apparent sand at 65 to 70 feet (screen depth 66 to 71 feet; 19.8 to 21.3 m), but water is only intermittently recorded here, and never rises more than an inch (2.5 cm) or so above the bottom of the screen. Slight amounts of mud found on the tip of the electronic water level indicator suggest that CP-1 may have been inadequately developed. CP-2 was completed in a deep, thick sand below 98 feet (29.4 m) (screen depth 128 to 138 feet; 38.4 to 41.4 m). This sand exhibits a head value consistently 6 to 7 feet (1.8 to 2.1 m) above lake level .

Miami Park

Stratigraphy

The upper bluff (Figure 24) is composed primarily of gray, silty diamicton except for sands that were logged from 0 to 5 feet (0 to 1.5 m) and 15 to 20 feet (4.5 to 6.0 m) depth. The middle bluff consists of brown, fine-grained laminated clay from 32 to 45 feet (9.6 to 13.5 m) , then sand from 45 to 52 feet (13.5 to

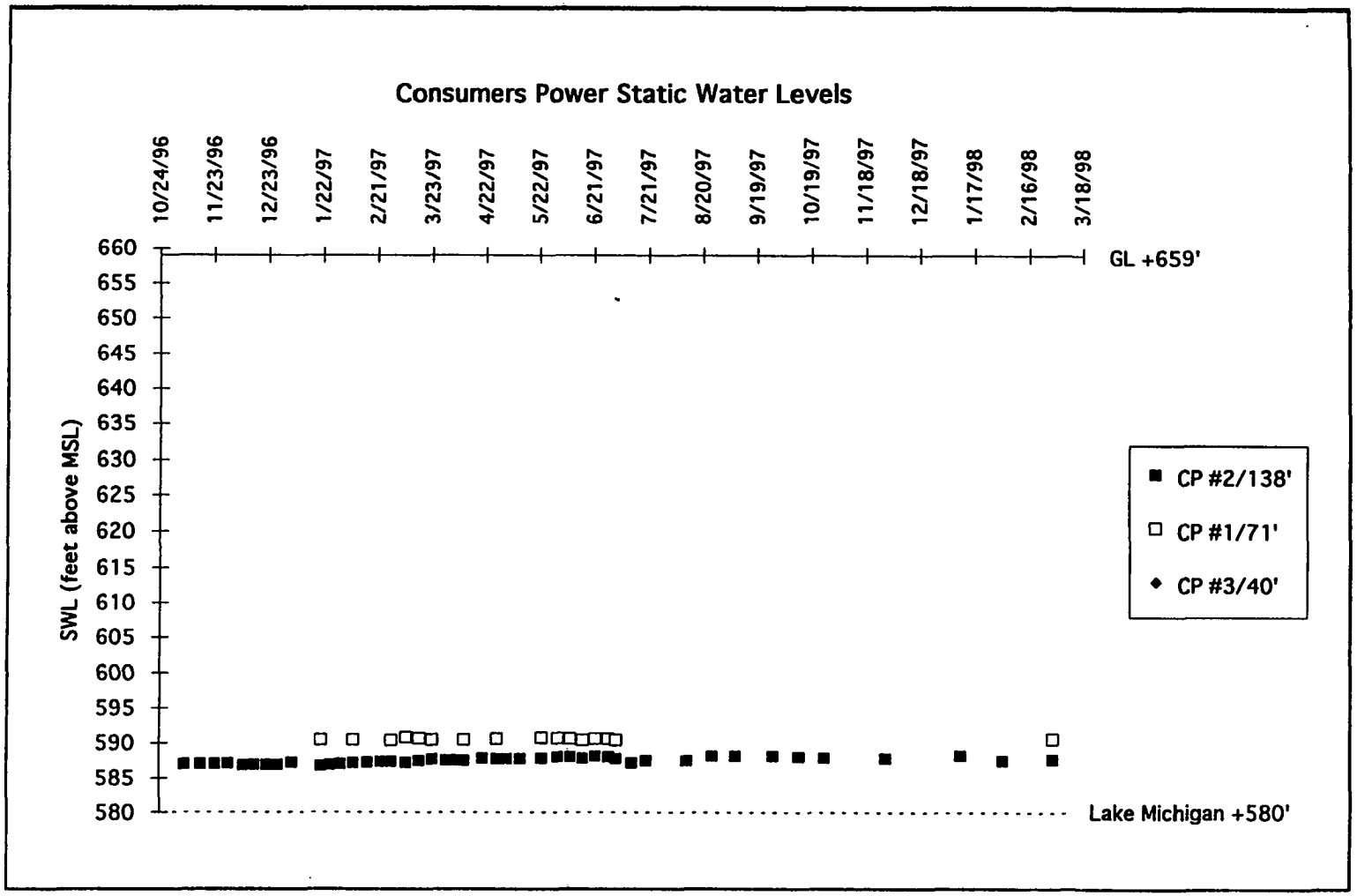

Figure 23. Consumers Power (CP) Static Water Levels.

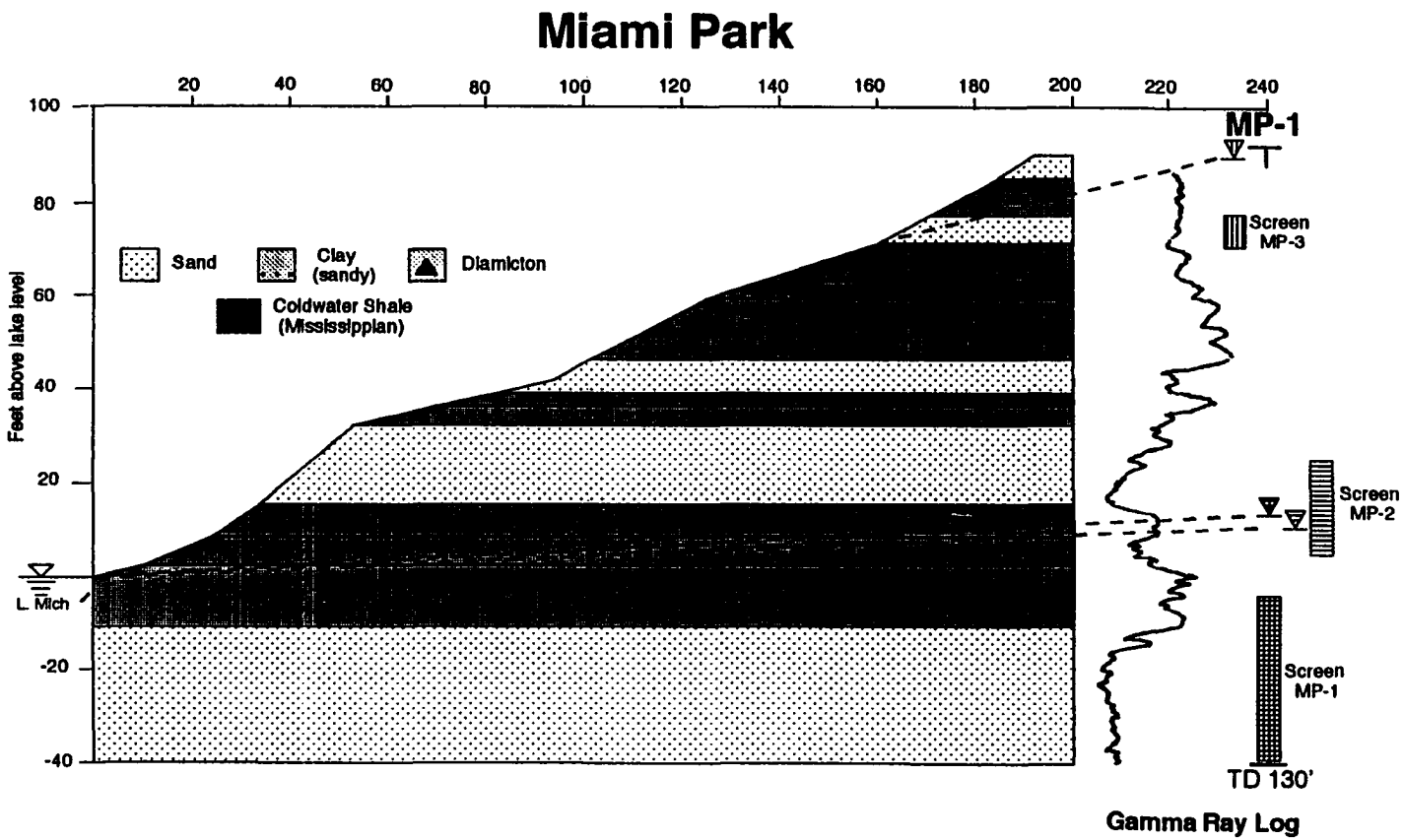

Figure 24. Miami Park (MP) Bluff Profile. Includes Screened Intervals and Static Water Levels From Piezometers. Gamma Ray Log From MP-1.

15.6 m), sand interbedded with fine-grained brown clay from 52 to 60 feet (15.6 to 18.0 m), and cross-bedded sand from 60 to 76 feet (18.0 to 22.8 m). Underlying this is brown, fine-grained laminated clay from 76 to 82 feet (22.8 to 24.6 m), followed by sand interbedded with fine-grained brown clay from 82 to 89 feet (24.6 to 26.7 m), fine-grained laminated clay from 89 to 102 feet (26.7 to 30.6 m), and buff colored, fine- to medium-grained sand from 102 to at least 140 feet (30.6 to 42.0 m), which was total depth.

Cast iron augers acting as surface casing to a depth of 36 feet (10.9 m) in MP-1 appear to have caused a baseline curve shift of the gamma ray curve to the left, by shielding the gamma ray detector from the formation. It is thus difficult to determine lithology based upon quantitative response or to compare quantitative log values to other sites, because everything shielded by the augers appears less clay-rich than it is in reality. To help compensate, the portion of the gamma ray curve above 36 feet was manually shifted to the right about 400 units. Below the base of the augers, more quantitative comparisons are possible. Two low-radioactivity sections associated with sand are present. They occur above (67 to 77 feet ; 20.1 to 23.1 m) and below (102 to 140 feet; 30.6 to 42.0 m) a highly radioactive section associated with laminated, fine-grained clay from 89 to 102 feet (26.7 to 30.6 m).

Hydrogeology

Piezometers were drilled to 20 feet, 6.1 m (MP-3); 85 feet, 25.8 m (MP-2); and 130 feet, 39.4 m (MP-1) (Figure 25). MP-3 was completed in a shallow sand from 15 to 20 feet (screen depth 15 to 20 feet; 4.5 to 6.0 m). It has exhibited very high head during the course of monitoring, at times reaching within one foot (0.30 m) of the surface. MP-2 was completed in a sand from 60 to 76 feet and

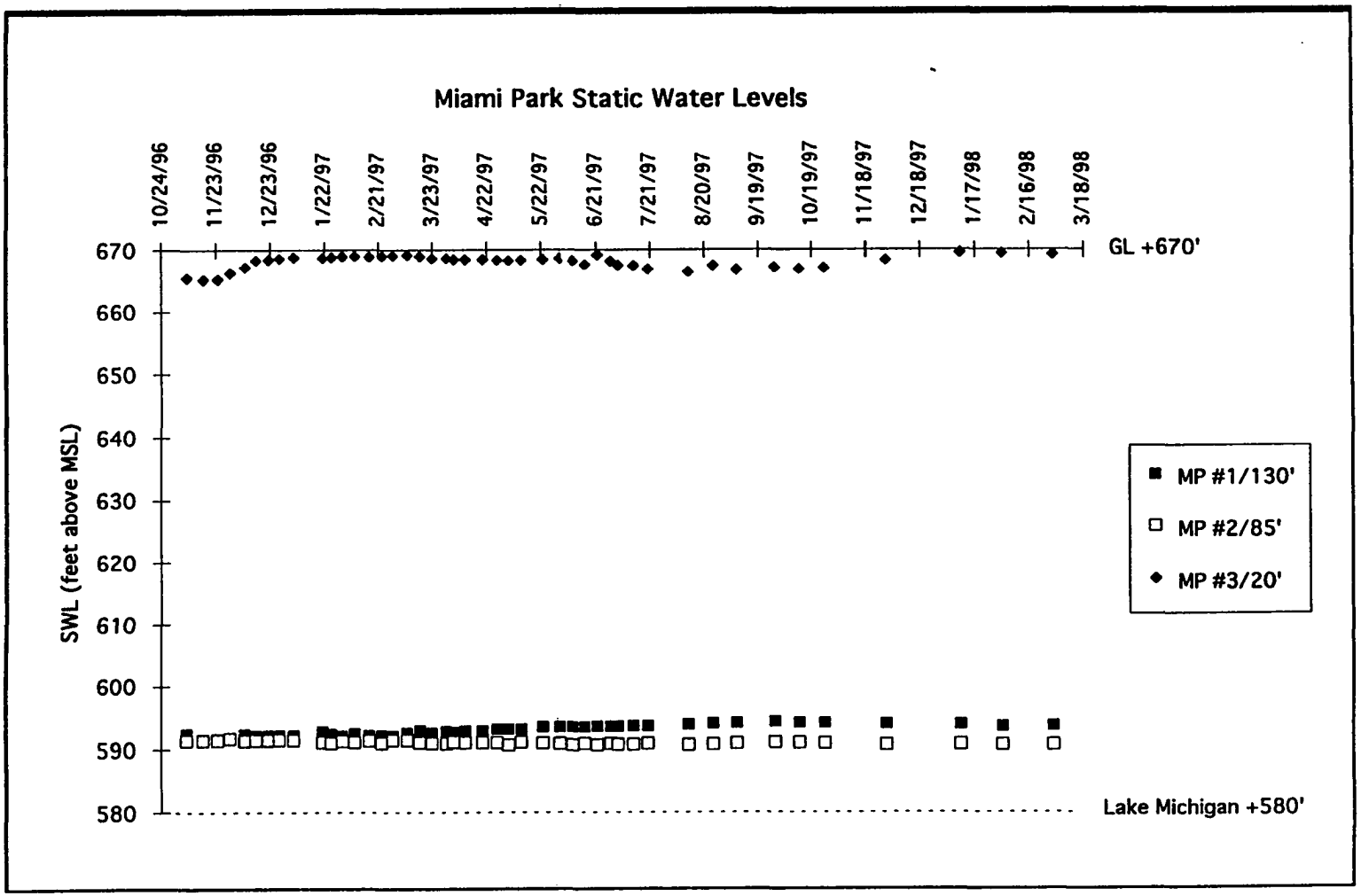

Figure 25. Miami Park (MP) Static Water Levels.

interbedded sand and clay from 82 to 89 feet (screen depth 65 to 85 feet (19.5 to25.5 m). MP-2 exhibits head that is consistently 9 to 10 feet (2.7 to 3.0 m) above lake level. MP-1 was completed in the deepest sand (screen depth 100 to 130 feet (30.0 to 39.0 m). MP-1 has consistently exhibited head values on the order of 12 to 13 feet (3.6 to 3.9 m) higher than lake level.

Fabun Road

Stratigraphy

The bluff (Figure 26) is composed primarily of gray, silty diamicton except for a midbluff sand logged from 20 to 25 feet (6.0 to 7.5 m) depth. Underlying the gray diamicton is sand (or very sandy till) from 45 to 50 feet (13.5 to 15.0 m), followed by possible sand interbedded with fine-grained brown clay from 50 to 55 feet (15.0 to 16.5 m), a thick sand section from 55 to 77 feet (16.5 to 23.1 m), fine-grained brown clay from 77 to 98 feet (23.1 to 29.4 m), and gray, pebbly clay diamicton from 98 to 112 feet (29.4 to 33.6 m).

Perhaps due to shielding by augers in FA-1 to a depth of 34 feet (10.2 m), the gamma ray log is not particularly diagnostic of sands in the shallow section. An interpreted sand from 20 to 23 feet (6.0 to 6.9 m) depth was sampled by Shelby tube FA-1 #1 and found to be a sandy, pebbly till instead. However, a low-radioactivity section associated with sand is present below lake level, and a highly radioactive section associated with fine-grained, laminated clay is present below the sand. Below the highly radioactive section, intermediate radioactivity is associated with pebbly diamicton to total depth.

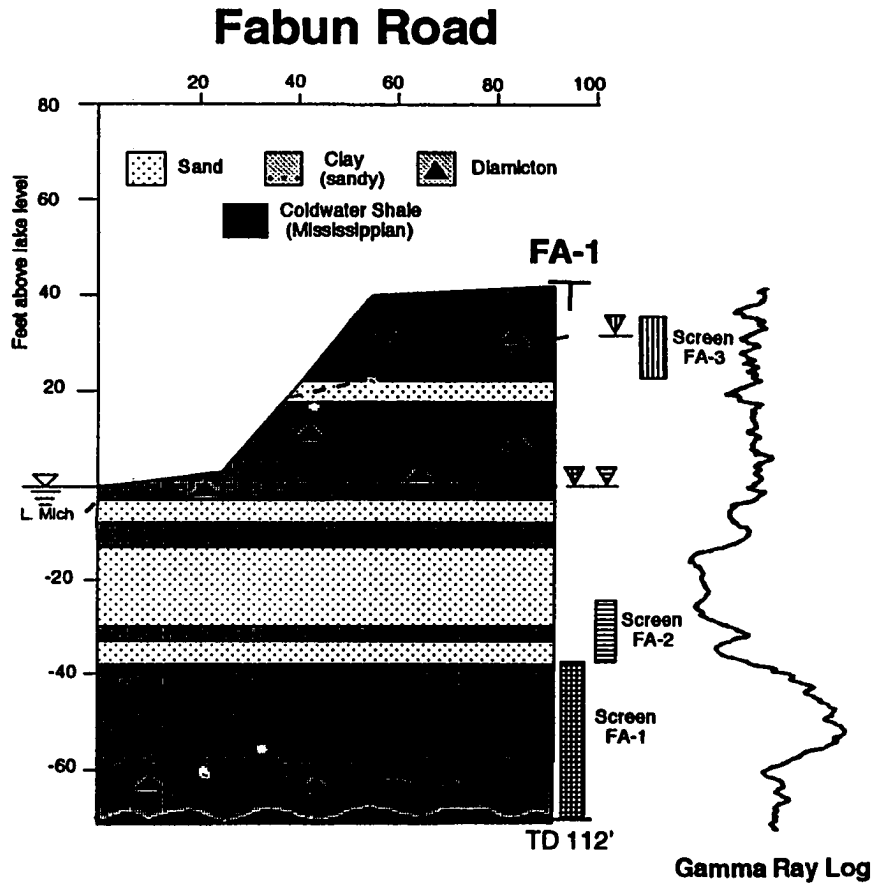

Figure 26. Fabun Road (FA) Bluff Profile. Includes Screened Intervals and Static Water Levels From Piezometers. Gamma Ray Log From FA-1.

Hydrogeology

Piezometers were drilled to 17 feet, 5.1 m (FA-3); 81 feet, 24.3 m (FA-2); and 112 feet, 33.6 m (FA-1) (Figure 27). FA-3 was intended to be completed in shallow diamicton (screen depth 7-17 feet; 2.1 to 5.1 m), but the base of the screen may be in communication with the top of the perched midbluff sand from 20 to 25 feet (6.0 to 7.5 m). This piezometer exhibits varying head 30 to 34 feet (9.0 to 10.2 m) above lake level that is associated with seasonal variations. FA-2 was completed in the sand from 55 to 77 feet (16.5 to 23.1 m) (screen depth 66 to 81 feet; 19.8 to 24.3 m). This piezometer exhibits head consistent with lake level. FA-1 was originally intended to be completed in a deep diamicton at TD (screen depth 102 to 112 feet; 30.6 to 33.6 m), but heavy mud in the annulus kept sand pack in suspension, and eventually the top of the filter pack rose to 80 feet below surface. Unfortunately, this is the approximate base of the sand completed in FA-2, so hydraulic connection between the two zones may have been inadvertently established. Water levels in FA-1 and FA-2 are consistently within 0.10 to 0.30 feet (3.0 to 9.0 cm) of each other, and have not fluctuated over time to the degree seen in the perched shallow aquifer penetrated by FA-3.

116th Avenue

Stratigraphy

The bluff (Figure 28) is composed primarily of gray, silty diamicton except for a possible midbluff sand at about 20 feet (6.0 m) depth and another sand logged from 33 to 41 feet (9.9 to 12.3 m). Grey diamicton is present from 41 to 67 feet (12.3 20.1 to m) depth, followed by sand from 57 to 68 feet (17.1 to 20.4 m),

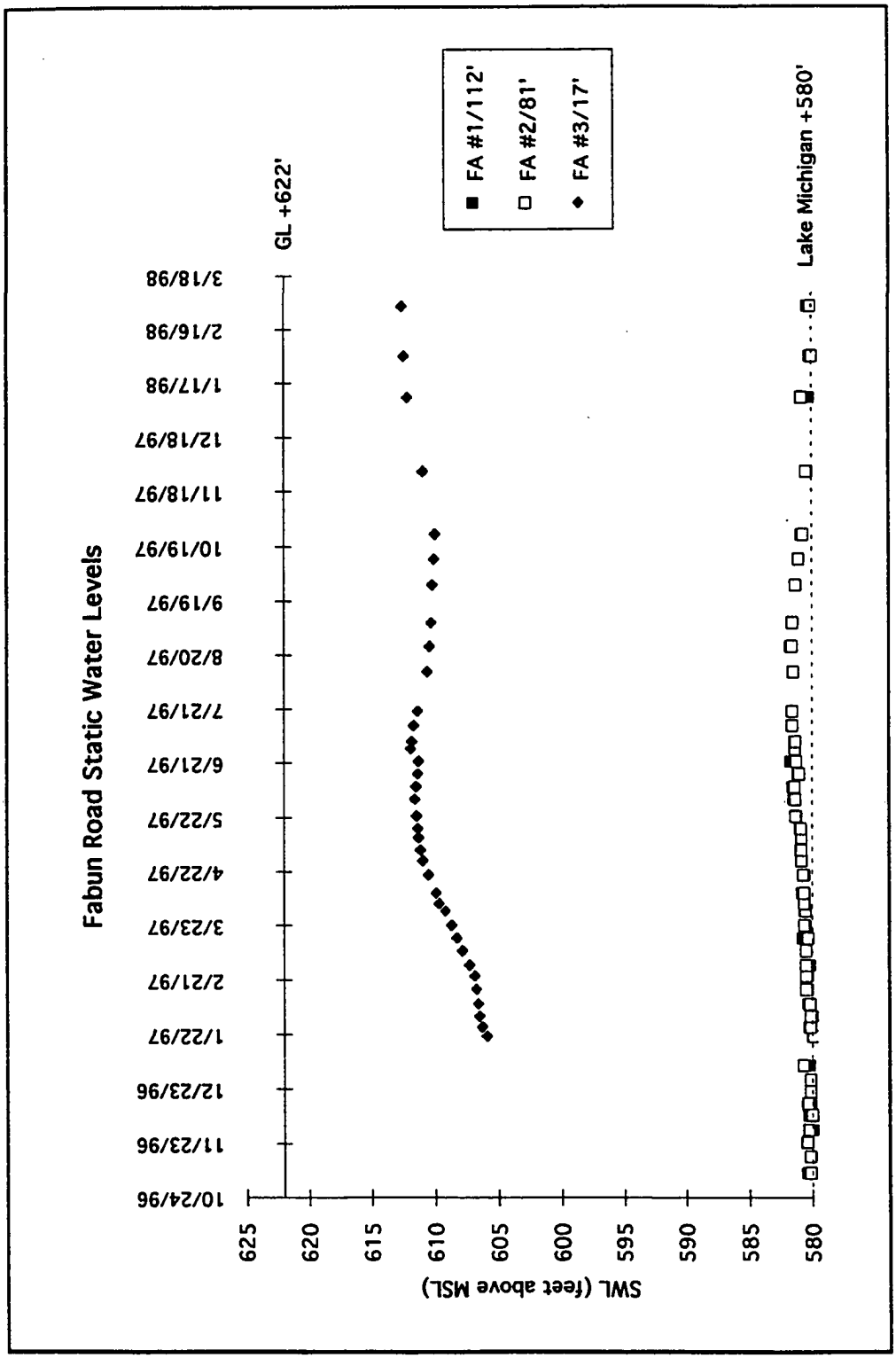

Figure 27. Fabun Road (FA) Static Water Levels.

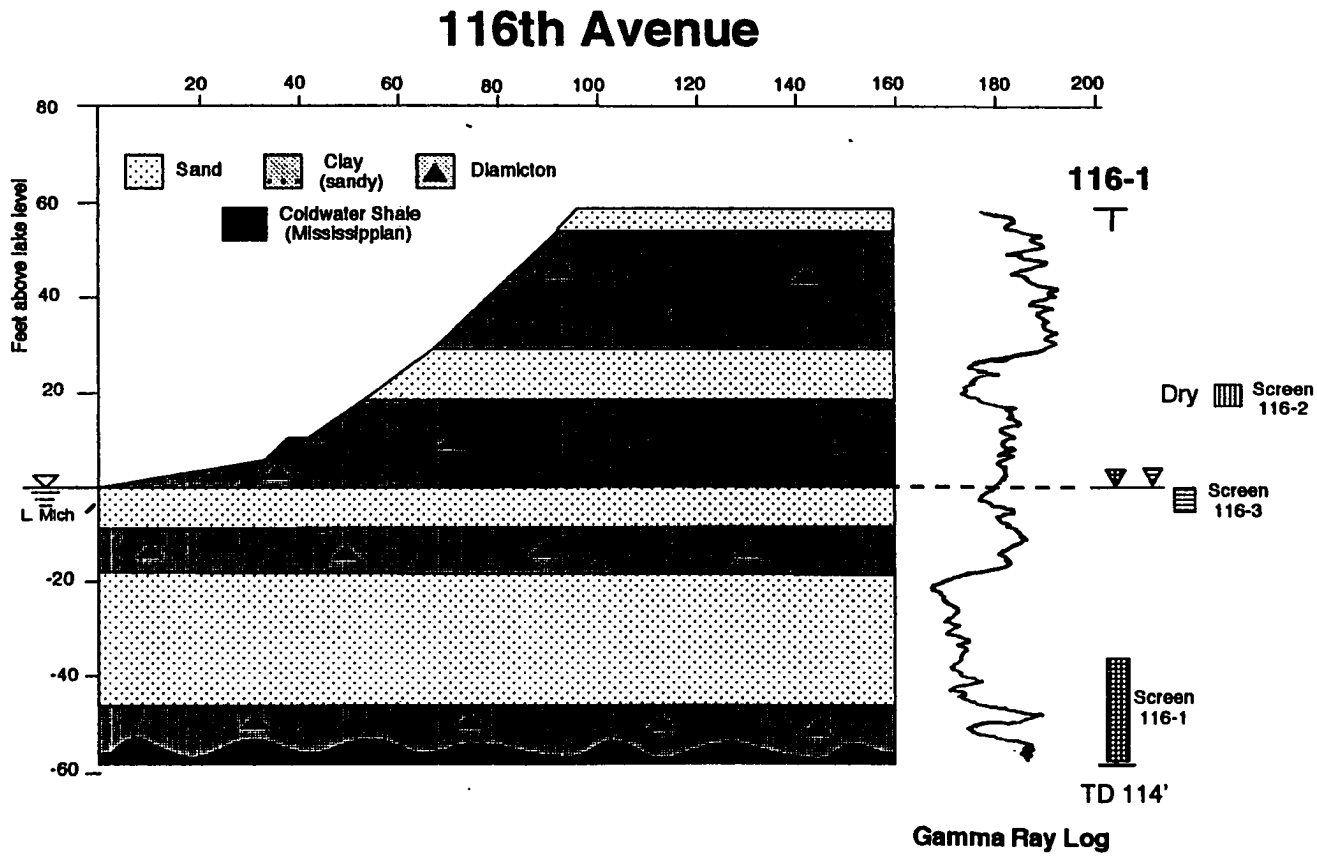

Figure 28. 116th Avenue (116) Bluff Profile. Includes Screened Intervals and Static Water Levels From Piezometers. Gamma Ray Log From 116-1.

interbedded sand and clay from 68 to 77 feet (20.4 to 23.1 m), and sand from 77 to 104 feet (23.1 to 31.2 m). Gray, pebbly, clay diamicton from 104 to 114 feet (31.2 to 34.2 m; TD) depth was logged from inconclusive samples and a very slow drill rate. Refusal to further drilling or sampling was encountered at 114 feet.

Augers in 116-1 to a depth of 16 feet (4.8 m) compromise lithologic interpretation of the shallow section. A low radioactivity zone, apparently sandy, was identified from 33 to 41 feet (9.9 to 12.3 m), but the shallow piezometer has yielded no water from this zone. Perhaps the gamma ray identified a sandy till rather than a sand. It is difficult to project this zone to the face of the bluff because of vegetative cover. Zones of low radioactivity can be correlated with sands present below lake level. High radioactivity at the base of the hole suggests the possible presence of clay-rich lithologies from 104 to 107 feet (31.2 to 32.1 m) and 110 to 114 feet (33.0 to 34.2 m).

Hydrogeology

Piezometers were drilled to 42 feet, 12.6 m (116-2); 64 feet, 19.2 m (116-3); and 114 feet, 34.2 m (116-1) (Figure 29). 116-2 was intended to be completed in the apparent sand from 33 to 41 feet (9.9 to 12.3 m) (screen depth 33 to 42 feet, 9.9 to 12.6 m). Sample recovery was poor in this interval, and the piezometer has never yielded any water from this zone. There are no signs of plugging or inadequate development. 116-3 is completed in an intermediate sand section logged from 57 to 68 feet (17.1 to 20.4 m) (screen depth 55 to 64 feet; 16.5 to 19.2 m). The gamma ray log indicates that the completed zone is not particularly sandy, but this zone caused a good drilling break (increased penetration rate) during drilling, and there was fine sand in the split spoon samples. Head in

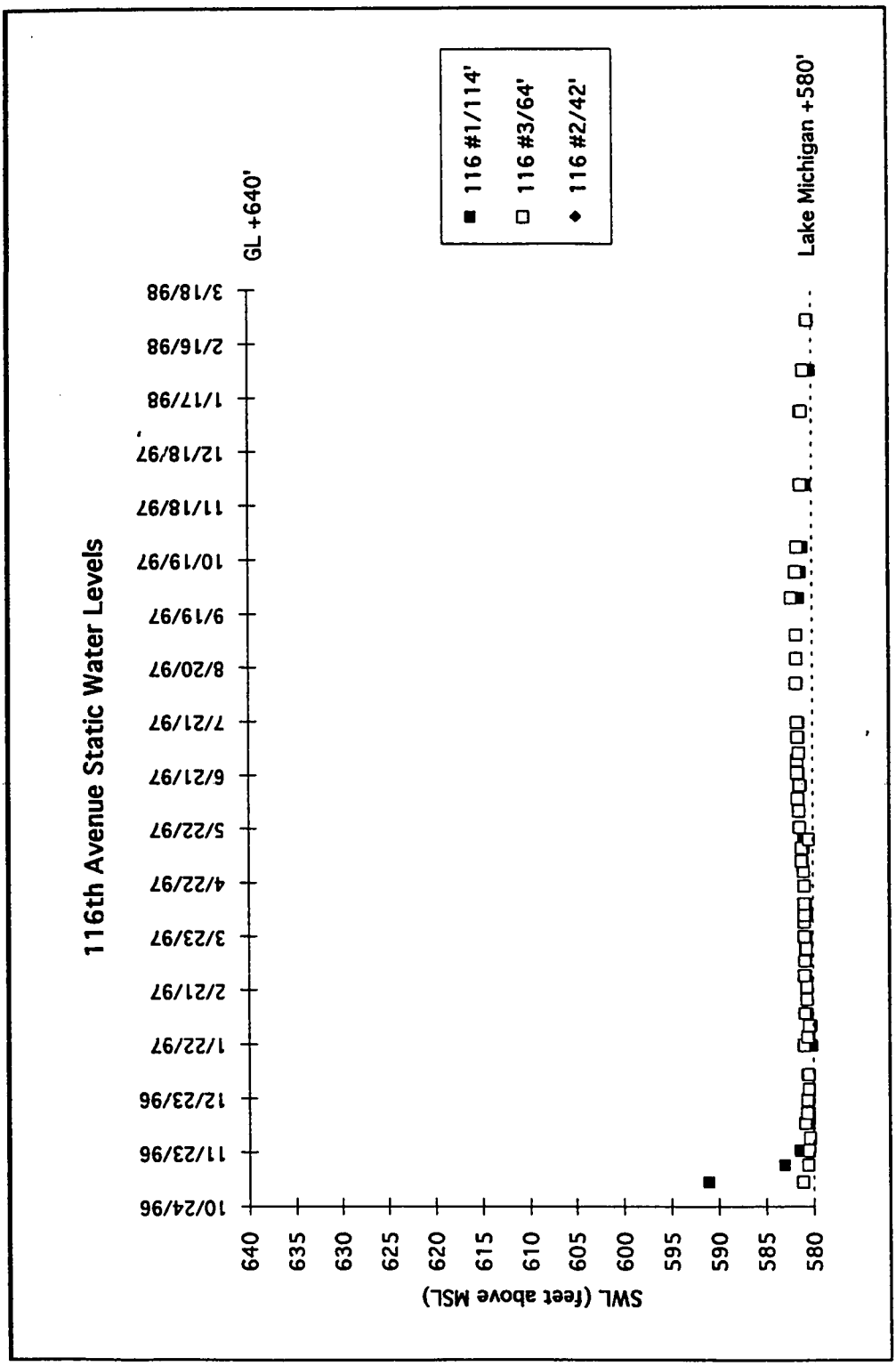

Figure 29. 116th Avenue (116) Static Water Levels.

116-3 is usually slightly (0.5 to 1.5 feet; 15.0 to 45.0 cm) above lake level. 116-1 is completed in an interval that encompasses both a possible deep till and the lower portion of the sand from 77 to 104 feet (23.1 to 31.2 m) (screen depth 94 to 114 feet; 28.2 to 34.2 m). The head in 116-1 reflects lake level, and is slightly (0.2 to 0.9 feet; 6.0 to 27.0 cm) lower than the head in 116-3 on a consistent basis.

Wau-Ken-A

Stratigraphy

The bluff (Figure 30) is composed of buff to light brown, medium- to coarse-grained sand from the surface to 42 feet (12.6 m) depth. Below the sand, purple-grey, silty diamicton is present from 42 to 59 feet (12.6 to 17.7 m), although two thin fine-grained clay zones may be present in this interval as well, from 49 to 51 feet (14.7 to 15.3 m) and from 57 to 59 feet (17.1 to 17.7 m). Buff to light gray, very fine-grained sand and silt is present from 59 to 77 feet (17.7 to 23.1 m), directly overlying Mississippian Coldwater Shale that was drilled from 77 to 98 feet (23.1 to 29.4 m; TD). The Coldwater Shale is dark grey to black, foliated, and pebbly at its top. The upper portion of this interval was originally described as diamicton from samples because of the foliations and pebbles present.

Augers in WKA-1 to a depth of 42 feet (12.6 m) compromise quantitative interpretation of this portion of the gamma ray log, but it is clearly associated with a massive sand section as determined from good sample retrieval. Below this, zones of intermediate to high radioactivity may indicate the presence of differing lithologies in the interval from 41 to 59 feet (12.3 to 17.7 m). Thin, highly radioactive zones are present from 49 to 51 feet (14.7 to 15.3 m) and from 57 to 59 feet (17.1 to

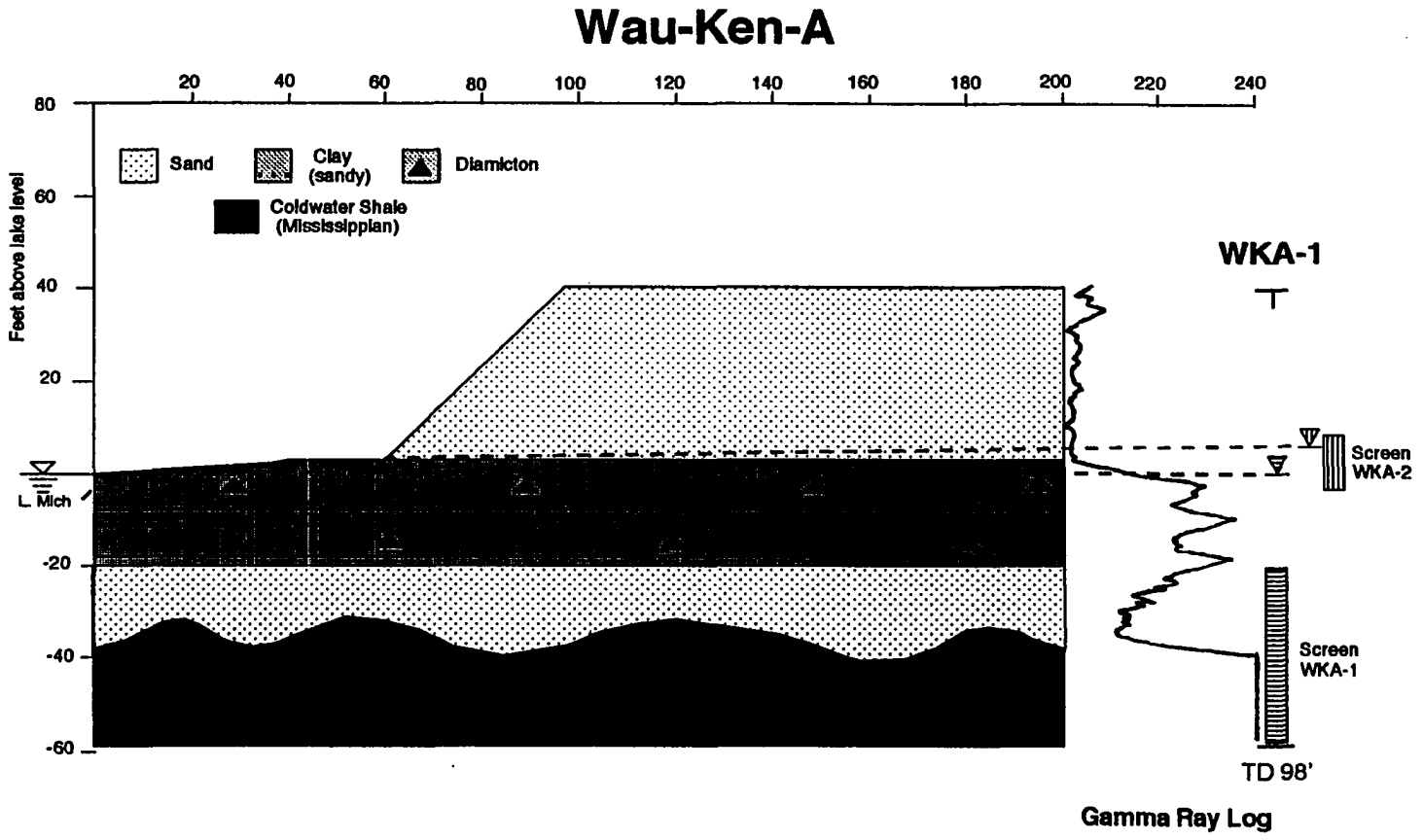

Figure 30. Wau-Ken-A (WKA) Bluff Profile. Includes Screened Intervals and Static Water Levels From Piezometers. Gamma Ray Log From WKA-1.

17.7 m); the lithology of the latter zone is fine-grained clay as confirmed by a split-spoon sample. Drilling rate suggests that the zone of intermediate gamma ray response from 51 to 57 feet (15.3 to 17.1 m) may be associated with diamicton. Below a zone of low radioactivity associated with a sand from 59 to 77 feet (17.7 to 23.1 m), the gamma ray curve goes abruptly off scale. This response is caused by the highly radioactive Mississippian Coldwater Shale.

Hydrogeology

Piezometers were drilled to 43 feet, 12.9 m (WKA-2) and 98 feet, 29.4 m (WKA-1) (Figure 31). WKA-2 was completed in the shallow, massive sand section (screen depth 31 to 43 feet). Water levels in this sand are consistently 5 to 6 feet (1.5 to 1.8 m) above lake level, and reflect a perched water table above the purple-grey diamicton at the base of the bluff. WKA-1 was completed in the deeper sand section logged from 59 to 77 feet (17.7 to 23.1 m) (screen depth from 60 to 98 feet; 18.0 to 29.4 m). Water level in this sand consistently reflects lake level.

West Side County Park (WS)

Stratigraphy

The bluff (Figure 32) is composed of buff to tan, fine- to medium-grained sand from the surface to 70 feet (21.0 m) depth, with the exception of a possible diamicton at 15 to 18 feet (4.5 to 5.4 m). Below this, sand with wood fragments is present from 70 to 84 feet (21.0 to 25.2 m), followed by a possible diamicton from 84 to 98 feet (25.2 to 29.4 m). Medium- to coarse-grained sand with wood fragments is present from 98 to 116 feet (29.4 to 34.8 m). Silt and fine sand,

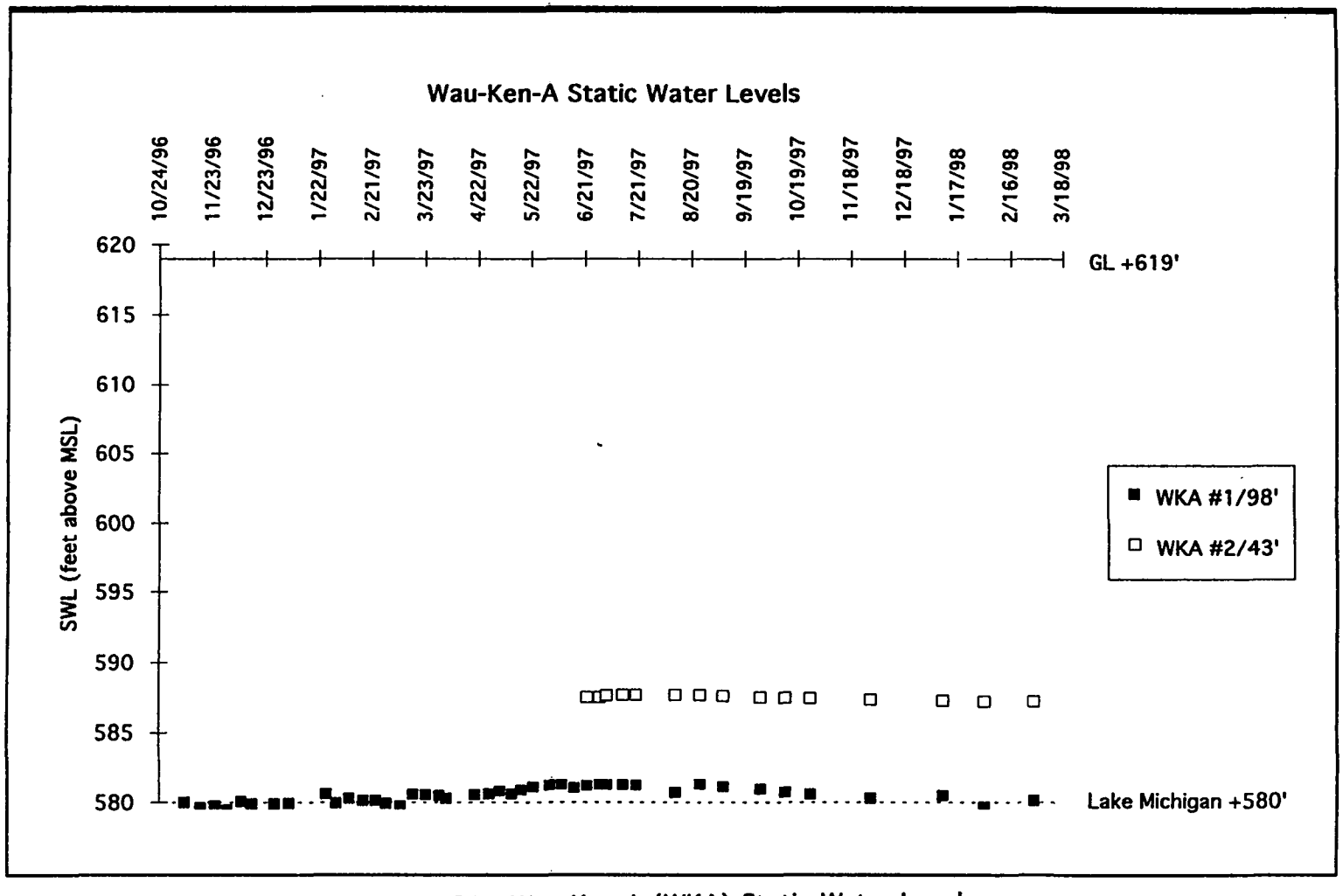

Figure 31. Wau-Ken-A (WKA) Static Water Levels.

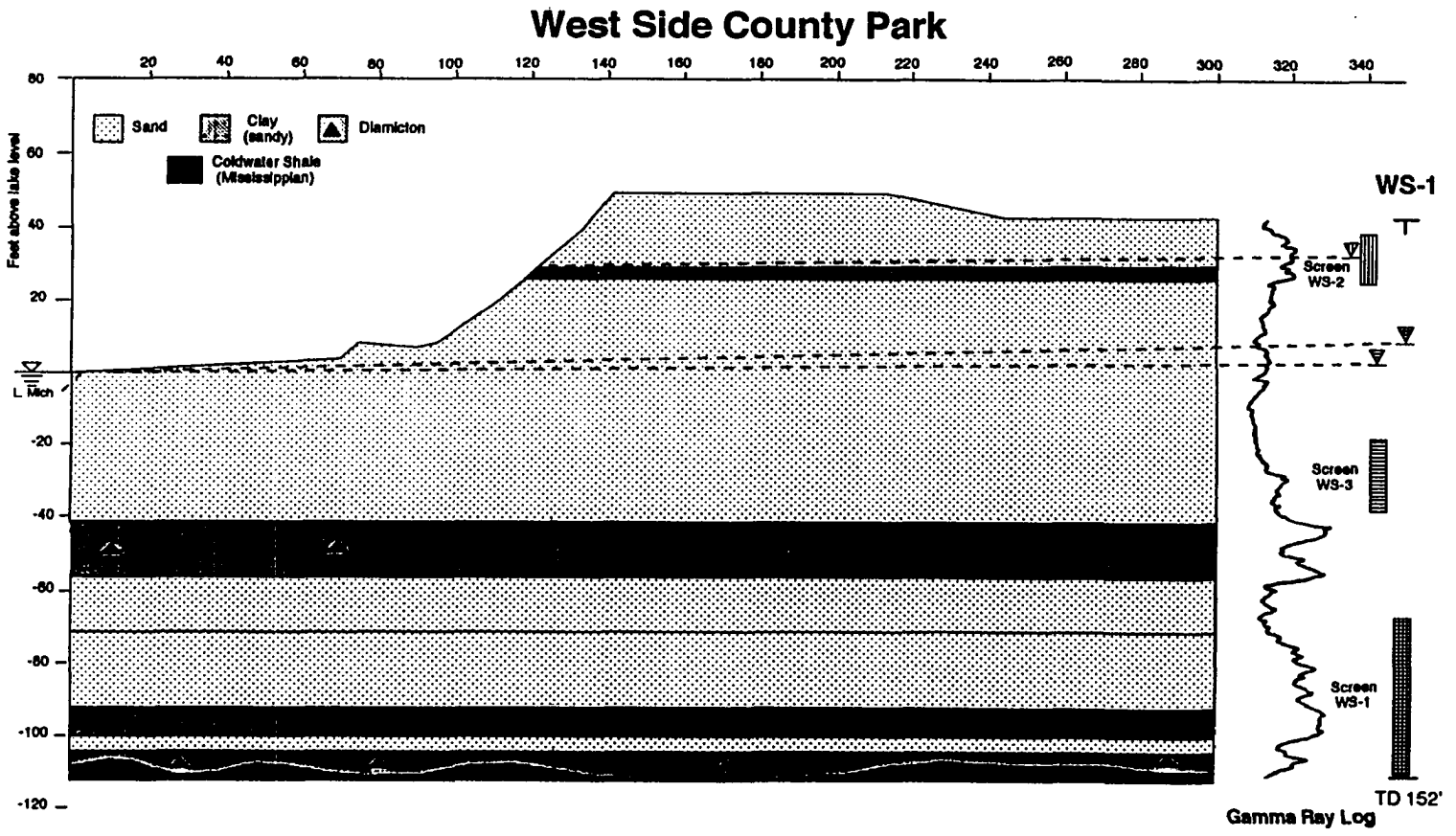

Figure 32. West Side Co. Park (WS) Bluff Profile. Includes Screened Intervals and Static Water Levels From Piezometers. Gamma Ray Log From WS-1.

possibly interbedded with clay, is present from 116 to 141 feet (34.8 to 42.3 m). Medium- to coarse-grained sand is present from 142 to 146 feet (42.6 to 43.8 m), followed by a possible pebbly diamicton present from 146 to 152 feet (43.8 to 45.6 m; TD). Refusal to further drilling was encountered at 152 feet (45.6 m).

Low radioactivity associated with sand characterizes the gama ray response of the entire section, with the exception of higher radioactivity from 5 to 20 feet (1.5 to 6.0 m), 84 to 87 feet (25.2 to 26.1 m), 94 to 98 feet (28.2 to 29.4 m), 116 to 142 feet (34.8 to 42.6 m), and 146 to 152 feet (43.8 to 45.6 m). Poor sample recovery in many of the more highly radioactive zones makes lithologic identification difficult, but the zones from 84 to 87 feet (25.2 to 26.1 m), 94 to 98 feet (28.2 to 29.4 m), and 133 to 142 feet (39.9 to 42.6 m) may be associated with fine-grained clay.

Hydrogeology

Piezometers were drilled to 18 feet, 5.4 m (WS-2); 80 feet, 24.0 m (WS-3); and 152 feet, 45.6 m (WS-1) (Figure 33). WS-2 was completed in the shallowest sand at the site (screen depth 8 to 18 feet; 2.4 to 5.4 m). Water levels from this zone range from 36 to 39 feet (10.8 to 11.7 m) above lake level, and strongly suggest the presence of a perched water table, although no seeps are readily apparent on the face of the bluff. WS-3 was completed near the base of a massive sand sequence (screen depth 60 to 80 feet; 18.0 to 24.0 m). Head in this sand reflects lake level. WS-1 was completed in the sand extending from 98 to 116 feet (29.4 to 34.8 m) through the lowermost sand from 142 to 146 feet (42.6 to 43.8 m) (screen depth 100 to 152 feet; 30.0 to 45.6 m). Head in this combined interval is consistently 9 to 10 feet (2.7 to 3.0 m) above lake level.

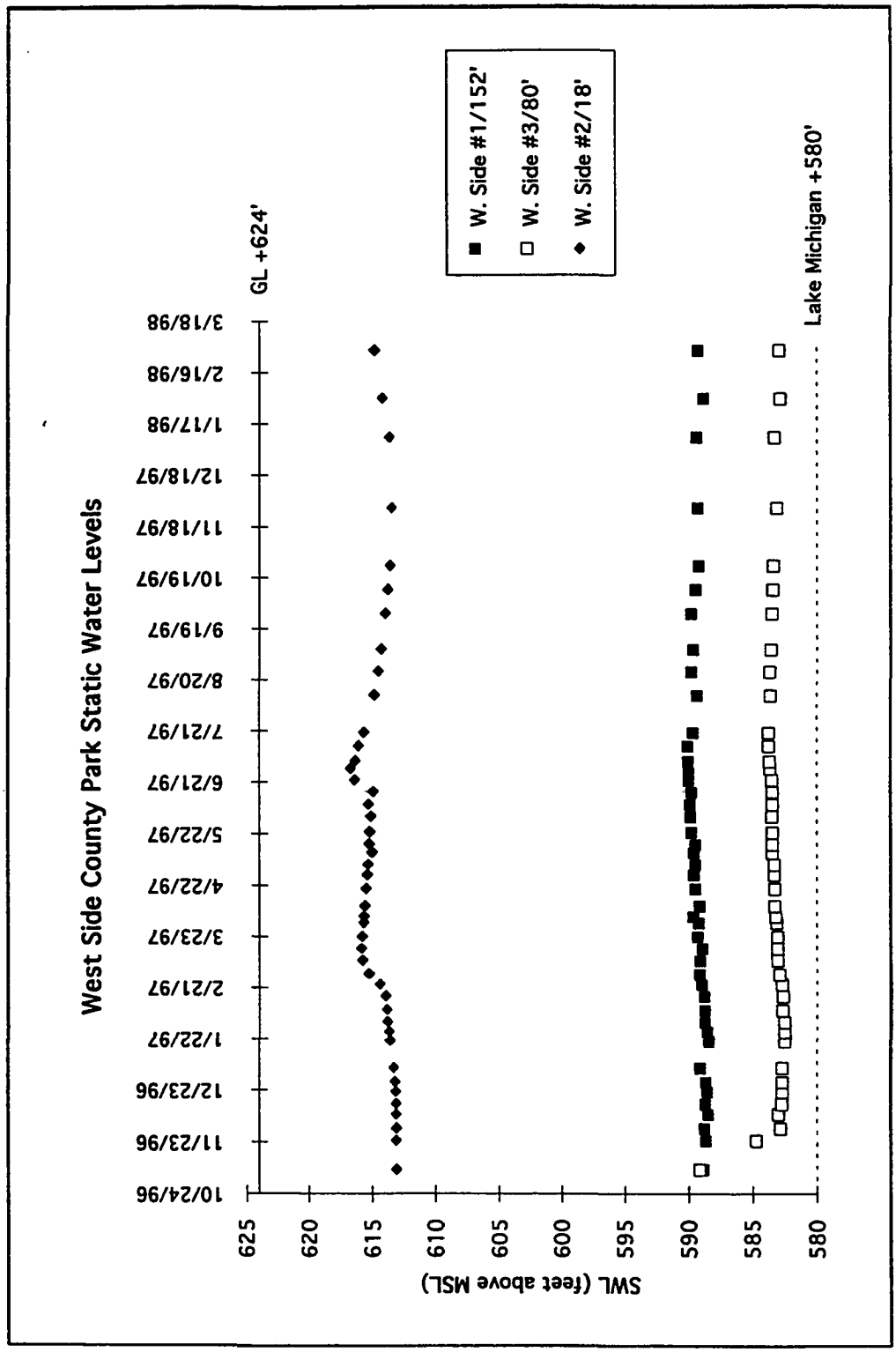

Figure 33. West Side County Park (WS) Static Water Levels.

Lithologic and Geotechnical Laboratory Data Presentation

Introduction

Lithologic and geotechnical data new to the study area (and West Michigan in general) were generated at the WES Geotechnical Laboratory from up to 16 sample sets. Trimmings from triaxial test specimens were utilized in the generation of grain size distribution and Atterberg limits data sets. Measurements performed on the triaxial test specimens produced a variety of index property data. Triaxial compression testing under both UU and CU conditions produced two new data sets. Overconsolidation ratio (OCR) testing also produced a new data set.

Grain Size Distributions, Atterberg Limits, and Soil Classification

Grain size distributions were determined from sieve and hydrometer analyses (Appendix B). Grain size distribution by weight percent is shown in Table 2. Gravel and significant percentages of sand (25 to 42% by weight) are found in samples CP-2 #1, #2, #3; MP-1 #1, FA-1 #1, and 116-1 #1; these are classified as diamicton. Samples CP-2 #4A, 4B; MP-1 #3B, and WKA-1 #1 contain from 3.6 to 12% sand; these are classified as clayey silt or silty clay. Samples CP-2 #5A, #5B and MP-1 #2, #3A, #4, #5 contain 0.9 to 3.7% sand; these are classified as clay or clay with traces of sand.

Atterberg limits (liquid limit, plastic limit, and plasticity index) data (Appendix B) are summarized in Table 2. A standard plasticity chart (USACE, 1986) (Figure 34) shows the relationships between liquid limit, plasticity index, and soil classification according to the Unified Soil Classification System (U.S.C.S.; Wagner, 1957). Liquid limits and plasticity indices of laminated clay samples MP-

Table 2

Summary of Grain Size Distributions, Atterberg Limits, and Index Properties of Undisturbed Samples in the Study Area

Sample	Depth,ft below GL	Lithology	Size (Wt%)			Attbrg Limits			USCS	Index Properties (source: UU data)					Comments
	(ft above MSL)		Gvl	Sand	Fines	LL	PL	PI	Class	Dns Dry	Wtr Cnt	Dns Wet	Wtr Sat	Vd Ratio	
										(lb/cu ft)	(%)	(lb/cu ft)	(%)		
CP-2 #1	8-10 (651-649)	Dmct,brn, clayey	3.1	27.5	69.4	20	13	7	CL	113.6	15.1	130.8	84.5	0.484	Unsaturated
CP-2 #2	18-20 (641-639)	Dmct,gry,silty	1.8	25.1	73.2	24	15	9	CL	124.6	12.7	140.4	96.9	0.353	OC
CP-2 #3	53-55 (606-604)	Dmct,gry,silty	4.6	33.8	61.7	25	14	11	CL	124.3	12.6	140.0	95.7	0.357	OC
CP-2 #4A	81-82 (578-576)	Silt, clayey	0.0	3.6	96.4	18	15	3	ML	107.6	17.2	126.1	78.9	0.381	NC; vd ratio from spec #4
CP-2 #4B	81-82 (578-576)	Clay, silty	0.0	2.5	97.5	21	14	7	CL	114.5	17.7	134.8	99.8	0.473	
CP-2 #5A	99-100 (560-559)	Clay,brn,lam	0.0	3.7	96.3	39	15	24	CL	106.0	21.7	129.0	98.4	0.591	NC
CP-2 #5B	99-100 (560-559)	Clay,tr sand	0.0	3.0	97.0	35	17	18	CL	100.3	24.3	124.7	96.0	0.682	
MP-1 #1	20-22 (650-648)	Dmct,gry,silty	3.4	32.6	64.0	24	14	10	CL	126.0	12.9	142.3	97.5	0.337	OC
MP-1 #2	40-42 (630-628)	Clay, tr sand	0.0	4.1	95.9	41	19	22	CL	101.3	24.9	126.5	99.8	0.664	NC
MP-1 #3A	60-62 (610-608)	Clay,brn,lam	0.0	0.9	99.1	40	17	23	CL	100.1	25.5	125.6	99.2	0.686	
MP-1 #3B	60-62 (610-608)	Silt, clayey	0.0	11.9	88.1	18	16	2	ML	102.4	19.6	122.5	82.2	0.648	Unsat, sand affects Att lims
MP-1 #4	80-82 (590-588)	Clay,brn,lam	0.0	0.5	99.5	48	18	30	CL	97.9	27.0	124.3	100.0	0.722	NC
MP-1 #4R	80-82 (590-588)	Clay/sand													
MP-1 #5	95-97 (575-573)	Clay,brn,tr sand	0.0	0.9	99.1	42	17	25	CL	99.7	24.9	124.5	97.4	0.691	NC
FA-1 #1	21-22 (601-600)	Dmct,gry,gravelly	26.1	41.7	32.2	16	10	6	SM	131.9	8.3	142.8	80.6	0.279	Unsat
116 #1	18-20 (622-620)	Dmct,brn, clayey	1.1	24.7	74.2	30	14	16	CL	117.3	13.9	133.6	85.8	0.441	clay clasts control strgth ?
WKA-1 #1	63-65 (556-558)	Clay, silty	0.0	5.2	94.8	26	14	12	CL	112.7	18.7	133.8	98.3	0.498	
															WWM 2/98

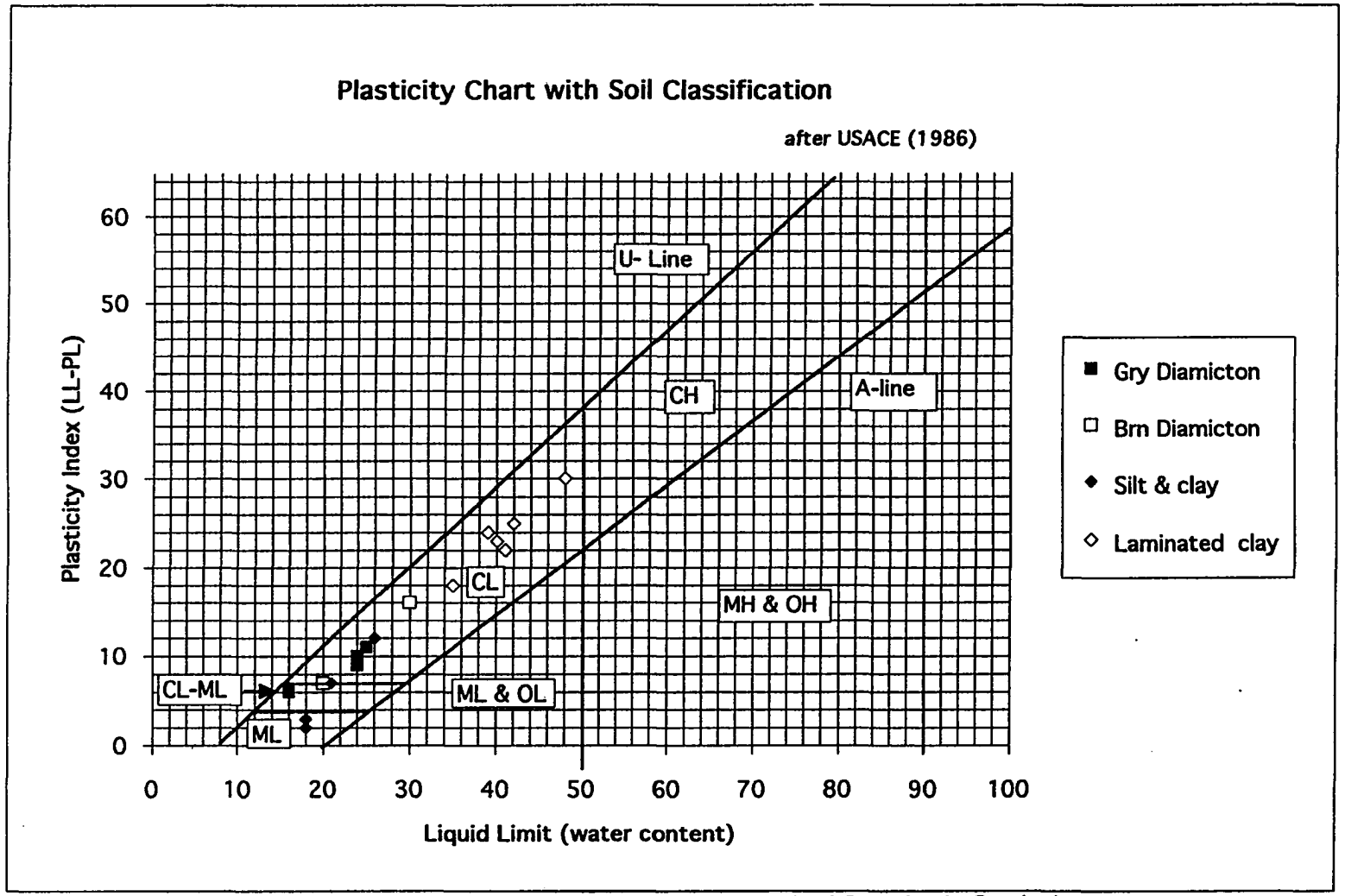

Figure 34. U.S.C.S. Soil Classification of Undisturbed Samples in Study Area. See Discussion of Soil Classification in Text for Definitions.

1 #3A, #4, #5, and CP-2 #5 are high. These samples are classified as lean clay (CL), but they border on high-plasticity fat clay (CH). Diamicton samples 116-1 #1; CP-2 #1, #2 #3; MP-1 #1; and samples CP-2 #4B and WKA-1 #1 exhibit intermediate plasticity. These samples are lean clay (CL) bordering on silty clay (CL-ML). The remaining samples all have low liquid limits and plasticity indices. Diamicton sample FA-1 #1 is classified as a silty sand (SM) due to its high sand/gravel content, and clayey silt samples CP-2 #4A and MP-2 #3B are classified as silt (ML).

Index Properties

Water Content

Lowest water contents (8.3 to 19.6% by weight) are present in diamicton samples CP-2 #1, #2, #3; MP-1 #1; FA-1 #1; 116-1 #1; and in clayey silt / silty clay samples CP-2 #4A&B, MP-1 #3B, and WKA-1 #1. Highest water contents (21.7 to 25.5%) are present in laminated clay samples CP-2 #5; MP-1 #2, #3, #4, #5.

Dry Density

Diamicton samples (CP-2 #2, #3; MP-1 #1; FA-1 #1) are the most dense (124.6 to 131.9 lbs/ft^3). These are followed by diamicton samples (116-1 #1; CP-2 #1), silt and silty clay (WKA-1 #1; CP-2 #4A) that weigh 112.7 to 117.3 lbs/ft^3. The least dense samples are laminated clay (CP-2 #5; MP-1 #2, #4, #5) that weigh from 97.9 to 106 lbs/ft^3.

Water Saturation

Laminated clay samples CP-2 #4B, #5A, #5B; MP-1 #2, #3A, #4, #5 and silty clay sample WKA-1 #1 exhibit very high water saturations (96 to 100% S_W). High saturations are also present in diamicton samples CP-2 #2, #3; and MP-1 #1 (96.9 to 97.5% S_W). Lesser saturations are present in diamicton samples 116-1 #1 and FA-1 #1, and clayey silt samples CP-2 #4A and MP-1 #3B (78.9 to 85.8% S_W).

Void Ratio

Silty grey diamicton samples (CP-2 #2, #3; MP-1 #1; FA-1 #1) and silt sample CP-2 #4A all exhibit low void ratios (0.279 to 0.381). Brown diamicton samples (116-1 #1; CP-2 #1) and silty clay samples WKA-1 #1 and CP-2 #4B exhibit intermediate void ratios (0.473 to 0.498). Laminated clay samples CP-2 #5; MP-1 #2, #3A, #4, #5 and clayey silt sample MP-1 #3B all exhibit high void ratios (0.591 to 0.722).

Triaxial Test Data Sets

Data derived from UU testing consist of stress-strain curves and total stress Mohr circles. Data derived from CU testing include stress-strain curves, total stress Mohr circles, pore pressure data, effective stress Mohr circles, and stress path data.

Stress-Strain Curves

UU Curves. Two types of stress-strain curve shape are evident in UU test results (Figure 35): peak deviator stress > residual stress, and peak deviator stress = residual stress. Silty, grey diamicton samples CP-2 #2, #3; MP-1 #1 tend to exhibit the former shape. Brown diamicton samples 116-1 #1 and CP-2 #1; clayey silt/silty clay samples MP-1 #3B and WKA-1 #1; and laminated clay samples CP-2 #4, #5; MP-1 #2, #3A, #4, #5 tend to exhibit the latter shape.

CU Curves. In general, only one type of stress-strain shape is evident in CU curves (Figure 35): peak deviator stress = residual stress. Silty, grey diamicton samples MP-1 #1 and CP-2 #3; laminated clay samples MP-1 #2 and MP-1 #4/5, and silty clay sample MP-1 #4R all exhibit this shape.

Failure Envelopes and Geotechnical Properties

UU-derived Failure Envelopes

UU stress-strain data (Appendix C) were used to generate total stress Mohr circles. Interpretation of Mohr circle data was required in order to construct an undrained total stress envelope for each sample (Figure 36). In situ vertical normal stress for each sample was determined by multiplying the weight of overburden (in lbs/ft^3) times the depth of burial (in feet). In theory, only one effective undrained shear strength value (Figure 37a) can be obtained from a set of UU specimens trimmed from one sample (Lambe and Whitman, 1969; Torrey, 1997, personal communication.). In actuality, however, interpretation of the Mohr circle data indicates that some increase in shear strength with increasing confining

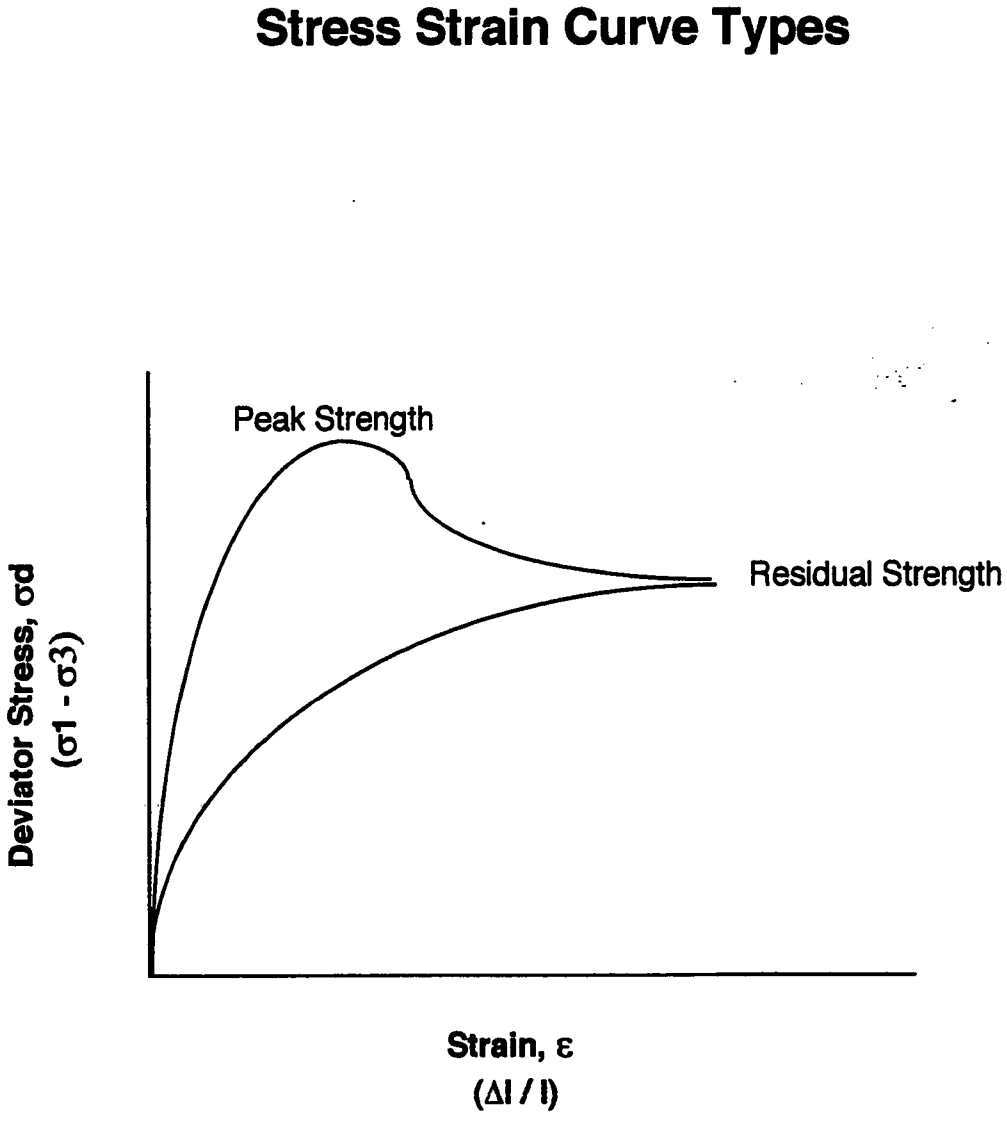

Figure 35. Two Idealized Types of Stress-Strain Curves Produced From Undisturbed Samples in the Study Area. See Discussion of Stress-Strain Curves in Text.

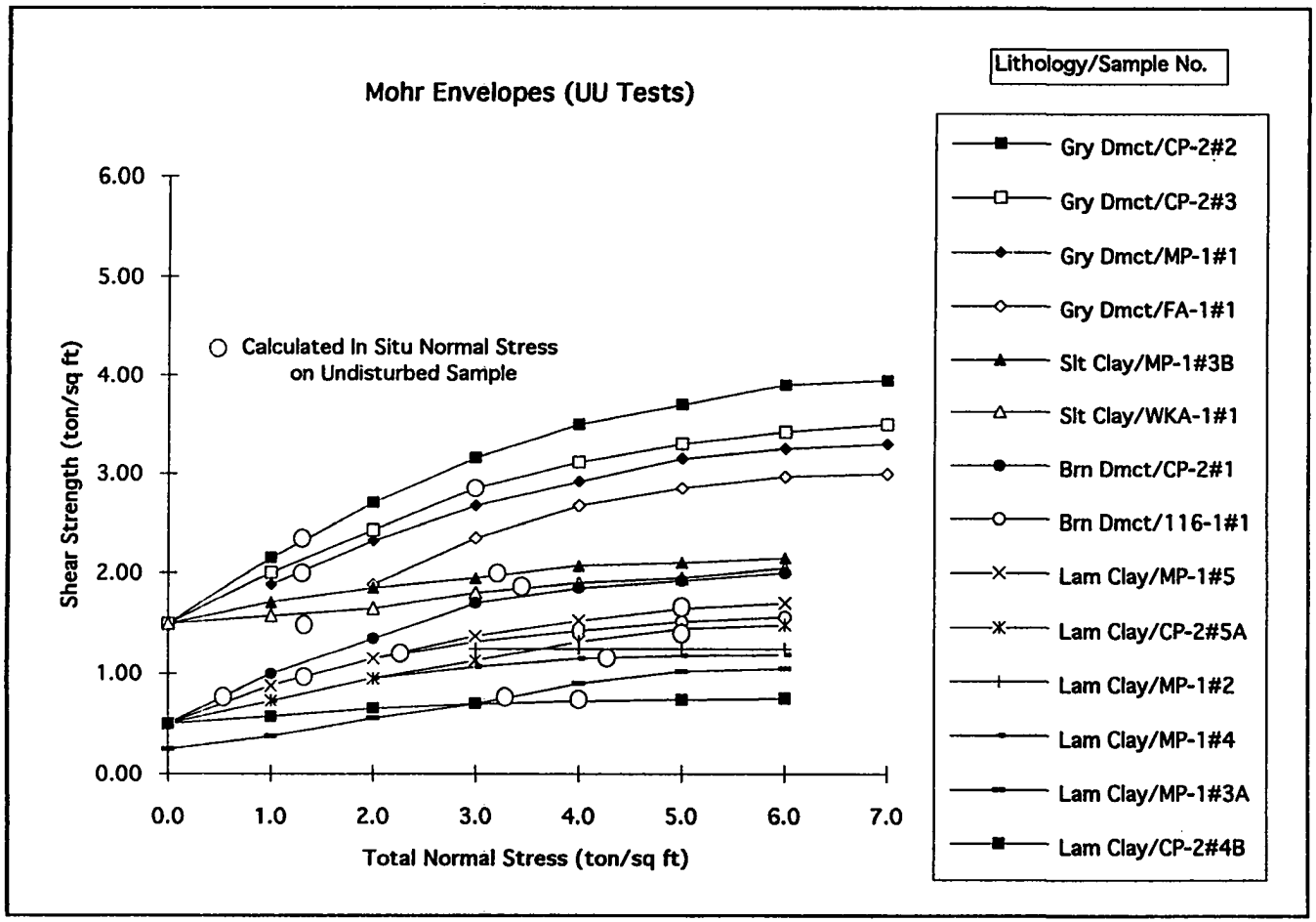

Figure 36. Non-Linear Mohr Failure Envelopes Generated From UU Tests Performed upon Undisturbed Samples in the Study Area. Calculated In Situ Vertical Stress on Sample Shown on Envelope. See Discussion of UU-derived Failure Envelopes in Text.

Failure Envelope Types

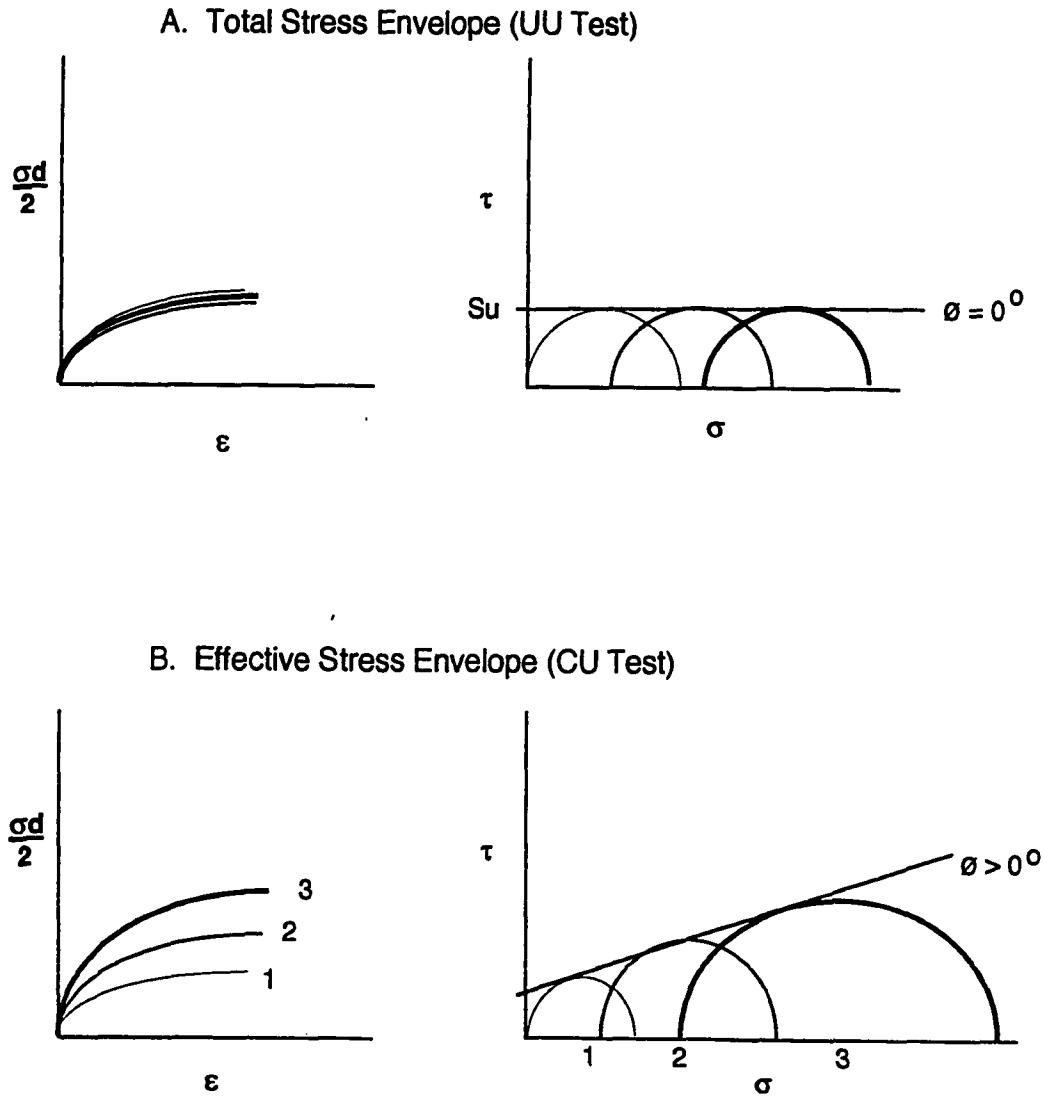

Figure 37. Idealized Mohr Failure Envelopes Generated In Total (UU) and Effective (CU) Stress Testing Environments.

stress occurred over the initial portions of many of the UU-derived failure envelopes. As a result, two sets of shear strength values are presented in Table 2: (1) in situ shear strength at the calculated normal stress due to overburden for that sample, and (2) the maximum undrained shear strength value (S_u) obtained at $\phi=0^o$.

CU-derived Failure Envelopes

CU stress-strain data (Appendix D) were used to generate both total and effective stress Mohr circles, although generation of effective stress data is the primary goal of CU testing. Preconsolidation procedure ensures that sample shear strength increases with depth; thus $\phi > 0^o$ for both total and effective stress envelopes (Figure 34b) generated under CU conditions. Laminated clay samples MP-1 #2 and #4/5 both exhibit an effective friction angle (ϕ') of 20 °; grey diamicton samples CP-2 #3 and MP-1 #1 exhibit an effective friction angle of 28 to 29 °; and silt/clay sample MP-1 #4R also exhibits an effective friction angle of 28 to 29 ° (Table 3). No effective cohesion (c') intercepts were measured from any of the five CU effective stress failure envelopes. Effective cohesion intercepts are often assumed to be zero in practice, because they are small and are thought to contribute negligibly to effective shear strength (Lambe and Whitman, 1969; McCarthy, 1993; Torrey, 1997, personal communication).

Overconsolidation Ratios and Consolidation State

Overconsolidation ratios (OCRs) were generated for three samples in the study area (Appendix E). The OCR for grey, silty diamicton from MP-1 #1 (20 feet; 6.1 m) was determined to be ~12; that for fine-grained laminated clay from

Table 3

Summary of Total Stress and Effective Stress Data for Undisturbed Samples in the Study Area

Sample	Depth,ft below GL	Lithology	Depth			UU (total stress) data				CU (effec stress) data		Comments
	(ft above MSL)		feet	Dev strs (TSF)		In situ strs	Cohesion	In situ strgth	Su	Cohesion	Eff Frc Ang	
				Peak	Resid	(TSF)	c (TSF)	(TSF)	(TSF)	c' (TSF)	ø' (deg)	
CP-2 #1	8-10 (651-649)	Dmct,brn, clayey	10		4.0	0.50	0.50	0.75	2.00			
CP-2 #2	18-20 (641-639)	Dmct,gry,silty	20	8.0	7.0	1.25	1.50	2.30	4.00			
CP-2 #3	53-55 (606-604)	Dmct,gry,silty	55	8.0	7.0	3.00	1.50	2.77	3.55	0	29	CU test #2
CP-2 #4B	81-82 (578-576)	Clay, silty	80		1.5	4.00	0.50	0.75	0.75			
CP-2 #5A	99-100 (560-559)	Clay,brn,lam	100		3.0	5.00	0.50	1.45	1.50			
MP-1 #1	20-22 (650-648)	Dmct,gry,silty	20	6.0	5.0	1.25	1.50	2.05	3.30	0	28	CU test #1
MP-1 #2	40-42 (630-628)	Clay, tr sand	40		3.0	2.25	1.25	1.25	1.25	0	20	CU test #5
MP-1 #3A	60-62 (610-608)	Clay,brn,lam	60		2.0	3.25	0.25	0.75	1.10			
MP-1 #3B	60-62 (610-608)	Silt, clayey	60		4.0	3.25	1.50	2.00	2.20			diff in Att limits due to sand
MP-1 #4	80-82 (590-588)	Clay,brn,lam	80		3.0	4.25	0.50	1.18	1.20	0	20	CU test #3 on MP-1/#4&5
MP-1 #4R	80-82 (590-588)	Clay/sand	80							0	29	CU test #4 on sd/clay lith
MP-1 #5	95-97 (575-573)	Clay,brn,tr sand	95		3.5	5.00	0.50	1.65	1.70			
FA-1 #1	21-22 (601-600)	Dmct,gry,gravelly	20		6.0	1.25	0.50	1.40	3.00			till very sandy, gravelly
116 #1	18-20 (622-620)	Dmct,brn, clayey	20		3.0	1.25	0.50	0.95	1.50			clay clasts control strgth ?
WKA-1 #1	63-65 (556-558)	Clay, silty	65		4.0	3.50	1.50	1.85	2.00			WWM 2/98

Note: See Discussion of Failure Envelopes and Geotechnical Properties in Text.

MP-1 #2 (40 feet; 12.2 m) was determined to be ~ 4, and that for fine-grained laminated clay from MP-1#4 (80 feet; 24.4 m) was determined to be 1.25. For comparison, OCRs from 1 to 32 have been reported by Edil and Mickelson (1995) in Wisconsin. In theory, any OCR > 1 indicates overconsolidation, but in practice an OCR ~ 4 is often used as a demarcation point between over- and normal consolidation (Mayne et al., 1995).

Input Data for Limit Equilibrium Analyses of the Field Sites

Introduction

Results from geotechnical testing provided the input parameters necessary to perform limit equilibrium (Factor of Safety) analyses at each of the six field sites in the study area. Two different sets of analyses were performed, one by hand and the other by computer.

Initial Hand Calculation of Factor of Safety

Preliminary Factor of Safety (FS) hand calculations were performed early in the study using the simplified Bishop method (Bishop, 1955). The calculations were based upon linear failure envelopes, and they were performed upon predetermined failure surfaces modeled after bluff face geometry observed in the field. These initial calculations suggested that sandy bluffs in the study area are the least stable (FS~1.0), mixed sand/clay bluffs tend to be more stable (FS = 1.0 to 1.5), and clay bluffs appear to be most stable (FS~1.5) (Montgomery et al., 1996a).

Computer Calculation of Factor of Safety

UTEXAS3 (Edris and Wright, 1992) is capable of performing automated searches for the failure surface with the lowest Factor of Safety on a bluff, as well as FS calculations for predetermined surfaces. The input data required to perform Factor of Safety modeling with UTEXAS3 are summarized in Table 4. Study area lithology can be grouped into four general material types: (1) sand, (2) laminated clay, (3) silty clay/brown diamicton, and (4) grey diamicton. Each of these material types was assigned a set of material properties that reflect either total or effective stress conditions. UTEXAS3 has the option to utilize a non-linear failure envelope to characterize how a material's shear strength changes with depth. Total stress data (Figure 34) suggest that many of the study area samples can be characterized by this type of envelope. Representative non-linear failure envelopes for grey diamicton (CP-2 #3), silty clay/brown diamicton (WKA-1 #1), and laminated clay (MP-1 #4) were input into UTEXAS3 and utilized for the total stress Factor of Safety runs. Later runs incorporated linear effective stress envelopes and field-derived piezometric data.

Airphoto Mosaics

Airphoto mosaics covering selected portions of the study area (Northern, Central, and Southern Areas; Figure 1) were produced at the Detroit District headquarters of the USACE using 1938, 1989, and 1996 airphoto mosaic bases (Appendix F). Each airphoto study area includes two field sites: West Side County Park and Wau-Ken-A are in the Northern Area, 116th Avenue and Fabun Road are in the Central Area, and Miami Park and Consumers Power are in the Southern Area.

Table 4

Summary of Geotechnical Data Utilized as Input Into UTEXAS3 Computer Program for Slope Stability Analysis

Input Data for UTEXAS3							
			Total Stress Parameters			Effective Stress Parameters	
Material Type	Material Lithology	Dry Density (lb/cu ft)	ø (deg)	c (lb/cu ft)	Su avg (lb/cu ft)	ø' (deg)	c' (lb/cu ft)
1	Sand	130	34-43	0	0	34-43	0
2	Lam Clay	100	0	1000	2000	20	0
3	Silty Clay/Brn Dmct	110	0	3000	4000	28	0
4	Grey Dmct	125	0	3000	7000	28	0
Note:	"Non-linear shear strength envelope option" was used in UTEXAS3 for total stress modeling to provide a						
	realistic assessment of changing Su with depth as suggested by Mohr envelopes from UU tests.						
	The representative strength envelopes used in UTEXAS3 for three cohesive material types are as follows:						
Nonlinear Strength Envelope Data							
Normal Stress		Shear Strength (lb/sq ft)					
(lb/sq ft)	Type 2 Lam Clay	Type 3 Slt Cly/Bn Dmct	Type 4 Grey Dmct				
0	1000	3000	3000				
2000	1450	3150	4000				
4000	1900	3300	4850				
6000	2150	3600	5700				
8000	2300	3800	6250				
10000	2350	3900	6600				
12000	2400	4000	6850				
	(MP-1 #4)	(WKA-1 #1)	(CP-2 #3)				
							WWM 3-98

Superimposed upon the photo bases are individual lines representing the 1938, 1989, and 1996 bluff lines determined from stereoscopic viewing of air photographs. Solid lines reflect confidence in the mapped position of the bluff edge, while dashed lines reflect positional uncertainty.

Bluff Recession and Lithologic/Hydrologic Characterization Data

Data on bluff lithology, mapped head in each of three aquifer systems at the bluff face, and the amount of 1938-1996 bluff recession measured from the airphoto mosaics are provided in Table 5. Recession cells (Figure 21) that were delineated according to average amount of 1938-1996 recession are listed in order from north to south for each of the three airphoto study areas; locations of the six field sites within cells are also provided. The shallow, intermediate, and deep aquifer head values listed in each cell represent the average head value for that particular cell as determined from the hydraulic head contour maps. Bluff height, feet of sand, and feet of clay for each cell were measured from the regional north - south cross section, and checked against the field profiles of Chase (1990; 1996, personal communication). Percent sand computed for each cell is shown adjacent to the initial, qualitative lithologic/hydrologic characterization of that cell. In only four cases was it necessary to revise the initial qualitative characterization to maintain consistency with the characterization according to percent sand.

Table 5

Summary of Data on Bluff Lithology, Hydraulic Head, and 1938-1996 Bluff Recession for Each Recession Cell in the Northern, Central, and Southern Historical Recession Analysis Areas

Factor of Safety - Summary of Calculations from UTEXAS3								
Site	**Run**	**Stress Conds**	**Factor of Safety**	**Failure Position**	**Comments**			
Consumers Power	cpnlt	Total	Indeterminate		Indeterminate results due to strong diamicton?			
	cpep	Effective	0.57	Shallow, lower bluff	Thin slice of lower bluff			
Miami Park	mpnlt	Total	2.29	Entire bluff	Failure surface subparallel to current bluff face			
	mpep	Effective	0.53	Shallow, lower bluff	Failure surface mapped by Chase et al. (1997)			
Fabun Road	fanlt	Total	6.09	Entire bluff				
	faep	Effective	0.43	Shallow, md/upr bluff	Position of failure surface coincident with recession observed in field			
116th Avenue	116nlt	Total	1.81	Entire bluff	Failure surface subparallel to current bluff face			
	116ep	Effective	0.37	Shallow, middle bluff	Position of failure surface coincident with recession observed in field			
Wau-Ken-A	wkatep	Effective & Total	0.91	Shallow, middle bluff	Position of failure surface coincident with recession observed in field			
W. Side Co. Park	wstep	Effective & Total	1.49	Entire bluff	Failure surface subparallel to current bluff face			
								WWM 3-98

CHAPTER V

DISCUSSION AND INTERPRETATION OF WORK PRODUCTS AND NEW DATA

Chapter Overview

Discussions and interpretations of the various work products and new data generated as part of this study follow. Topics covered include: (a) adequacy of GIS-based lithologic and hydrologic bluff characterizations as evaluated with field data collected through drilling, sampling, and groundwater monitoring; (b) significance of Atterberg limits and index properties of materials as controlling factors on shear strength and mechanical behavior; (c) significance of results of stress-strain, Mohr failure envelope, and stress path analysis; (d) input assumptions and results of limit equilibrium analyses performed for each of the six field sites; (e) analysis of spatial patterns of bluff recession and comparison to lithologic/hydrologic bluff characterizations and computed Factors of Safety.

Field Data Interpretation and Evaluation of Bluff Characterizations

Consumers Power (CP)

Interpretation and Correlation of Units

Shelby tube recoveries and geotechnical test results indicate that both weak, brown, clayey diamicton and strong, gray, pebbly diamicton are present on the bluff here. Shallow- and intermediate-depth piezometers are essentially dry; only a deep sand below lake level is water-bearing year-round. This deep sand is interpreted to

be the deep aquifer based upon correlations with well control further to the north. A Geochron Laboratories radiocarbon date of 32,680 +/- 500 years BP has been determined from wood fragments recovered from this deep sand. The date places this sand as part of a depositional system slightly younger than the Glenn Shores till (Monaghan and Larson, 1986).

Adequacy of Characterization

This site was characterized as clay with low head (LC). Site lithology is almost entirely clay diamicton above lake level, and surface seepage is nil. Shallow and intermediate aquifer equivalents, both above lake level, are interpreted to be present here based upon subsurface control, but they yield little or no water in the piezometers. The only significant amount of water here is in the deep aquifer, which is below lake level. The head in the aquifer is consistently 6 to 7 feet (1.8 to 2.1 m) above lake level, which is quite high and implies confined aquifer conditions. It is hypothesized that poor hydraulic conductivity between the deep aquifer and the bluff face at this site does not allow the high head from the deep aquifer to transmit an upward hydraulic seepage pressure to the face of the bluff. It appears that the predrill characterization of the bluff at Consumers Power as clay with low head (LC) was adequate, at least for the portion of the bluff situated at and above lake level.

Miami Park (MP)

Interpretation and Correlation of Units

The upper bluff consists of diamicton and shallow sand interpreted to be part of a perched shallow aquifer system. The middle and lower bluff here is significantly different than Consumers Power, in that it is predominantly interbedded sand and

fine-grained clay rather than diamicton. This sand and clay section is interpreted to be the intermediate aquifer system. Below this section is more fine-grained clay underlain by a deep sand. Both gamma ray signature and lithologic correlations strongly suggest that the fine-grained clay and deep sand section here is equivalent to that at Consumers Power approximately 1.5 miles (2.4 km) to the south. Field observations (Chase et al., 1997) suggest that diamicton is present at or near lake level, but it was not readily observed during drilling.

Adequacy of Characterization

This site was characterized as mixed sand/clay with high head (HM). Site lithology as determined from well control consists of upper bluff sand and diamicton, middle bluff sand and lacustrine clay, and more lacustrine clay and sand present below lake level. High head is exhibited in all aquifers: shallow, intermediate, and deep. The head data are suggestive of discharge conditions that could exist between the deep and intermediate aquifers at this site. This has significance with respect to slope stability, because an upwardly-directed seepage gradient from the deep aquifer toward the intermediate aquifer could contribute to bluff instability where the intermediate aquifer outcrops on the bluff face. The predrill site characterization of the bluff at Miami Park as mixed sand/clay with high head (HM) was correct .

Fabun Road (FA)

Interpretation and Correlation of Units

The bluff here is predominantly gray, sandy diamicton with a thin midbluff sand interpreted to be part of a perched shallow aquifer system. The diamicton is significantly sandier here than it is to the south at either Consumers Power or

Miami Park. Below the bluff face lies a sand interpreted to be the intermediate aquifer by correlation with nearby wells. This is underlain by a thick, brown, fine-grained clay interpreted to be the same lacustrine clay that overlies the deep aquifer at both Miami Park and Consumers Power. This interpretation is supported by radiocarbon age dates of wood fragments recovered in sand immediately above this clay here (30,870 +3,930/-2,630 years B.P.) and immediately below the clay at Consumers Power (32,680 +/- 500 years B.P.), which tightly bracket the time of deposition of this clay.

Directly beneath this fine-grained clay, a dark grey, pebbly diamicton (Glenn Shores till?) is found in lieu of the deep sand that is present at Miami Park and Consumers Power. It is reasonable to interpret that the deep aquifer sand (which is slightly younger than the Glenn Shores till) has pinched out somewhere between here and Miami Park about 3 miles (4.8 km) to the south, and the fine-grained laminated clay directly overlies Glenn Shores till here at Fabun Road.

Adequacy of Characterization

This site was characterized as clay with a high head (HC). Site lithology above lake level consists primarily sandy diamicton bluff, with a 5 foot (1.5 m) thick shallow aquifer sand. High head in this shallow sand reflects a perched condition, while intermediate aquifer head reflects lake level. It is unlikely that a deep aquifer is present.

In conjunction with the shallow midbluff sand, the very high sand and gravel content of diamicton here (noted during drilling and confirmed by laboratory measurements at WES) could produce high hydraulic conductivity at Fabun Road, and would explain the often wet appearance of the bluff face at this site. Increased

hydraulic conductivity due to increased sand content in a Wisconsin diamicton (New Berlin till) has recently been reported by Edil and Mickelson (1995). The New Berlin till itself has been interpreted, based upon x-ray diffraction patterns (Monaghan, 1990), to be equivalent to the Ganges till. The properties of the sampled Fabun Road diamicton (FA-1 #1) in terms of strength, silt/sand content, and color, appear to be consistent with a Ganges till classification. The predrill site characterization of the bluff at Fabun Road as clay with a high head (HC) was correct, at least for the section above lake level.

116th Avenue (116)

Interpretation and Correlation of Units

Although both 116th Avenue and Miami Park are characterized as mixed sand/clay bluffs, the mixed lithology at 116th Avenue is somewhat different than that at Miami Park. Here, the clay fraction of the bluff appears to be composed primarily of diamicton, while at Miami Park a significant portion of the clay is in fine-grained lacustrine beds as well as diamicton. Geotechnical and lithologic properties of undisturbed sample 116-1 #1 recovered from 18 to 20 feet (5.4 to 6.0 m) indicate that the upper portion of this bluff is relatively weak, brown, clayey diamicton, whereas the lower diamicton is pebbly and grey.

It is unclear from subsurface well control how much sand is interbedded with diamicton here, although field observations (Chase, 1997, personal communication) indicated an upper mid-bluff sand is present. Piezometer results suggest no water-bearing sand is present at a mid-bluff elevation, but the gamma ray log suggests sand is present. Also, there is field evidence of upper- and mid-bluff seepage associated with a shallow aquifer system along this stretch of shoreline.

Lithologic control and the gamma ray log signature of lower stratigraphy here strongly suggest that the sand section present below lake level is correlative with the intermediate aquifer system identified about 1.25 miles (2.0 km) to the south at Fabun Road. Beneath the interpreted intermediate aquifer may be a thin, laminated, brown clay possibly equivalent to the thicker clay section present to the south. Beneath this laminated clay, samples and drilling rate suggest that a thin diamicton (interpreted to be a sliver of Glenn Shores till) overlies the Mississippian Coldwater Shale. The Coldwater is hypothesized to be the cause of refusal to further penetration by the drill bit.

Adequacy of Characterization

This site was characterized as mixed with a low head (LM). Field evidence at and near this site suggest the presence of mixed sand and clay lithologies and a seeping shallow aquifer system that exhibits high head. Piezometer results are somewhat equivocal. Measured water levels in upper and lower portions of the interpreted intermediate aquifer system suggest the presence of low head. Recharge (as opposed to discharge) conditions are suggested by the head data; the upper portion of the intermediate aquifer penetrated in 116-3 appears to recharging into the deeper portion of this aquifer penetrated in 116-1, evidently through limited vertical hydraulic communication via the interbedded sand/clay zone present from 68 to 77 feet (20.4 to 23.1 m). Perhaps the most appropriate characterization of the bluff here would involve segmentation into upper and lower units: the upper bluff is of a mixed lithology with high head, whereas the lower bluff is mixed lithology with low head. This would suggest that the predrill characterization of the

bluff at 116th Avenue as mixed lithology with low head (LM) was at least partially correct.

Wau-Ken-A (WKA)

Interpretation and Correlation of Units

The stratigraphic section is markedly more sand-rich at Wau-Ken-A than the four sites further to the south. Almost the entire bluff face above lake level here is interpreted to be shallow aquifer sand, save the basal portion of the bluff, which is hard, purple-grey, silty diamicton interpreted to be Ganges till. This section also contains two thin zones interpreted to be laminated lacustrine clay. Below the clay and diamicton lies a thick sand interpreted to be the intermediate aquifer, which in turn is resting directly on Coldwater Shale in lieu of the diamicton interpreted as Glenn Shores till. The interpreted Glenn Shores till apparently pinches out somewhere between here and 116th Avenue, about 2 miles (3.2 km) to the south.

Adequacy of Characterization

This site was initially characterized as sand with a high head (HS), because of mapping of well control and the presence of seeps at the base of the bluff. The site is extremely sandy, except for the diamicton and interpreted lacustrine clay present at and below lake level. The shallow aquifer is perched above lake level here, but the intermediate aquifer consistently reflects lake level. In general, the piezometer and well data suggest that a sand with low head (LS) characterization may be more appropriate for Wau-Ken-A than the original sand with high head characterization. The accompanying bluff characterization maps have been modified to reflect a low head characterization.

West Side County Park (WS)

Interpretation and Correlation of Units

Despite its extremely sandy character, there are several different aquifer systems present at the West Side County Park, with at least three distinct heads. The shallowest piezometer is interpreted to reflect a perched aquifer within the shallow aquifer system, while the intermediate completion at the base of the massive sand may represent another level of the shallow aquifer system. Below this is a section interpreted to consist of diamicton (Ganges till?) and fine-grained clay. The sand immediately below this potential confining layer correlates as the intermediate aquifer to Wau-Ken-A about 1.5 miles (2.4 km) to the south. There appears to be a thin sand just above the Coldwater Shale, the correlation of which is problematic; it could be a basal portion of the intermediate aquifer or a thin section of deep aquifer. As at Wau-Ken-A, no diamicton that could be correlated as Glenn Shores till is interpreted to be present above the Coldwater Shale at TD.

Adequacy of Characterization

This site was initially characterized as sand with low head (LS). The site was very sandy, but both shallow head and deep head were higher than anticipated, perhaps due to perching and confining conditions, respectively. As at Miami Park, the head data are suggestive of discharge conditions, in that the deepest piezometer consistently exhibits head ~6 feet (1.8 m) higher than that of the intermediate piezometer. Subsequent re-interpretation of field and well data suggested that the head values here are more consistent with a high head characterization (HS) rather

than one of low head. The accompanying bluff characterization maps have been modified to reflect this interpretation.

Atterberg Limits and Index Properties in Relation to Undrained Shear Strength

Introduction

Relationships between Atterberg limits, grain size distributions, index properties, and undrained shear strength are presented, and the implications of these relationships are discussed. These relationships provide a basis for lithologic and mechanical classification, and they provide insight concerning key factors that may control specimen failure.

Atterburg Limits, Grain Size Distribution, and Soil Classification

U.S.C.S. soil classifications as determined from Atterberg limits and grain size distribution analysis indicate that the samples in the study area are relatively uniform compositionally (Figure 34). They can be classified as either clay (CL), silty clay/clayey silt (CL-ML), or silt (ML), with the exception of the FA-1 #1 pebbly diamicton, which is classified as a silty sand (SM). This may reflect a similar provenance for the diamicton and laminated clay.

Index Property Comparisons to Percent Sand and Gravel

Differences that exist in index properties are reflected in Atterberg limits and are related to lithology. One example of this is an observed inverse relationship between the amount of sand and gravel in a sample and its liquid limit (Figure 38). Laminated clay samples tend to have high liquid limits and low percent sand, while diamicton samples tend to have low liquid limits and high percent sand. Clayey

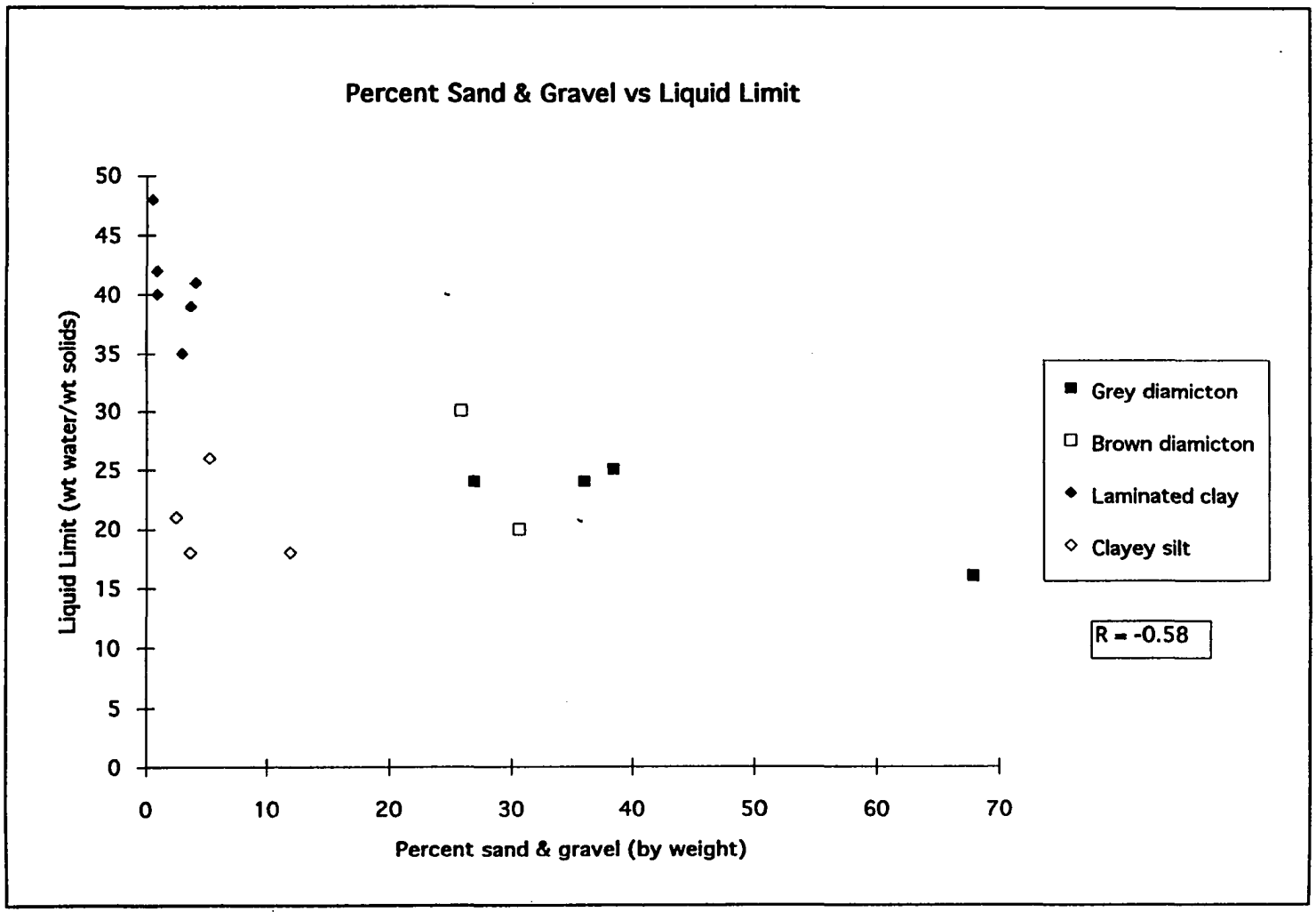

Figure 38. Relationship Between Sand & Gravel Content and Liquid Limit of Undisturbed Samples.

silt/silty clay samples appear to be an exception, in that they exhibit both low sand content and low liquid limits.

A low liquid limit indicates that a material cannot hold a large amount of water without crossing over the threshold from plastic to liquid behavior. Of particular interest are the low liquid limits of diamictons measured in the lab. The low liquid limits provide a credible explanation for the pronounced fluidized behavior observed to occur in bluff diamicton when subjected to increased water seepage and runoff during spring thaws. Low liquid limits measured in clayey silt could also have a significant destabilizing effect on bluffs composed of mixed lithologies, such as the bluff at Miami Park.

An inverse relationship also exists between sand and gravel content and water content (Figure 39). Laminated clay samples with low sand content show significantly higher (up to 25.5%) water content than the sandier diamicton samples, whose water contents are as low as 8.3%. This is because materials with significant amounts of clay tend to have higher porosity than more sand-rich granular materials, and are thus able to hold more water per unit volume.

Dry density (unit weight) appears to reflect sand and gravel content (Figure 40). The lightest samples are laminated clays with low sand content and dry densities on the order of 100 lb/ft^3 (15.7 kN/m^3), whereas sandy/gravelly diamicton samples weigh 125 to 132 lb/ft^3 (19.6 to 20.7 kN/m^3). Grey diamictons, which contain clasts of Paleozoic and Precambrian rocks, are the heaviest samples recovered in the study area.

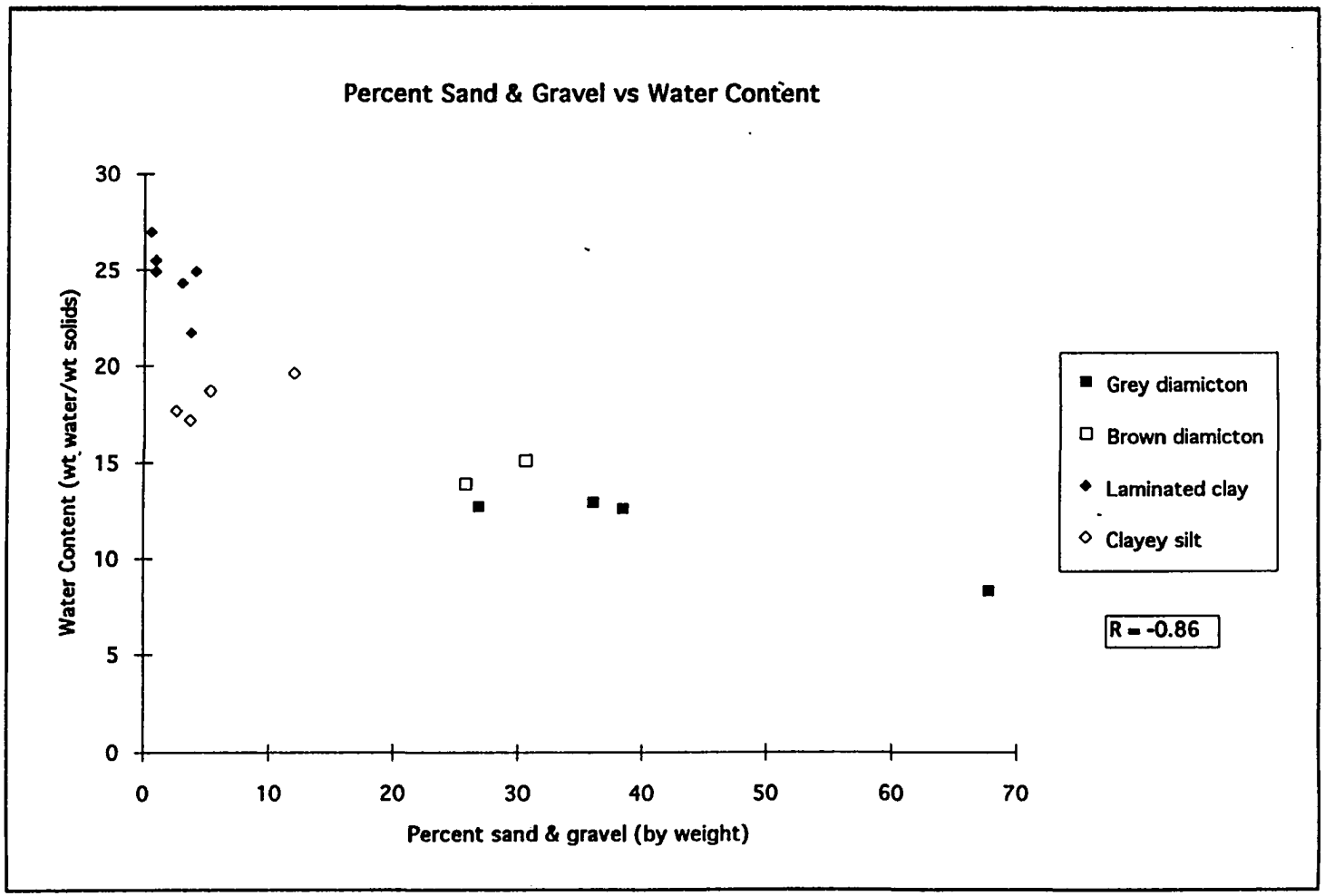

Figure 39. Relationship Between Sand & Gravel Content and Water Content of Undisturbed Samples.

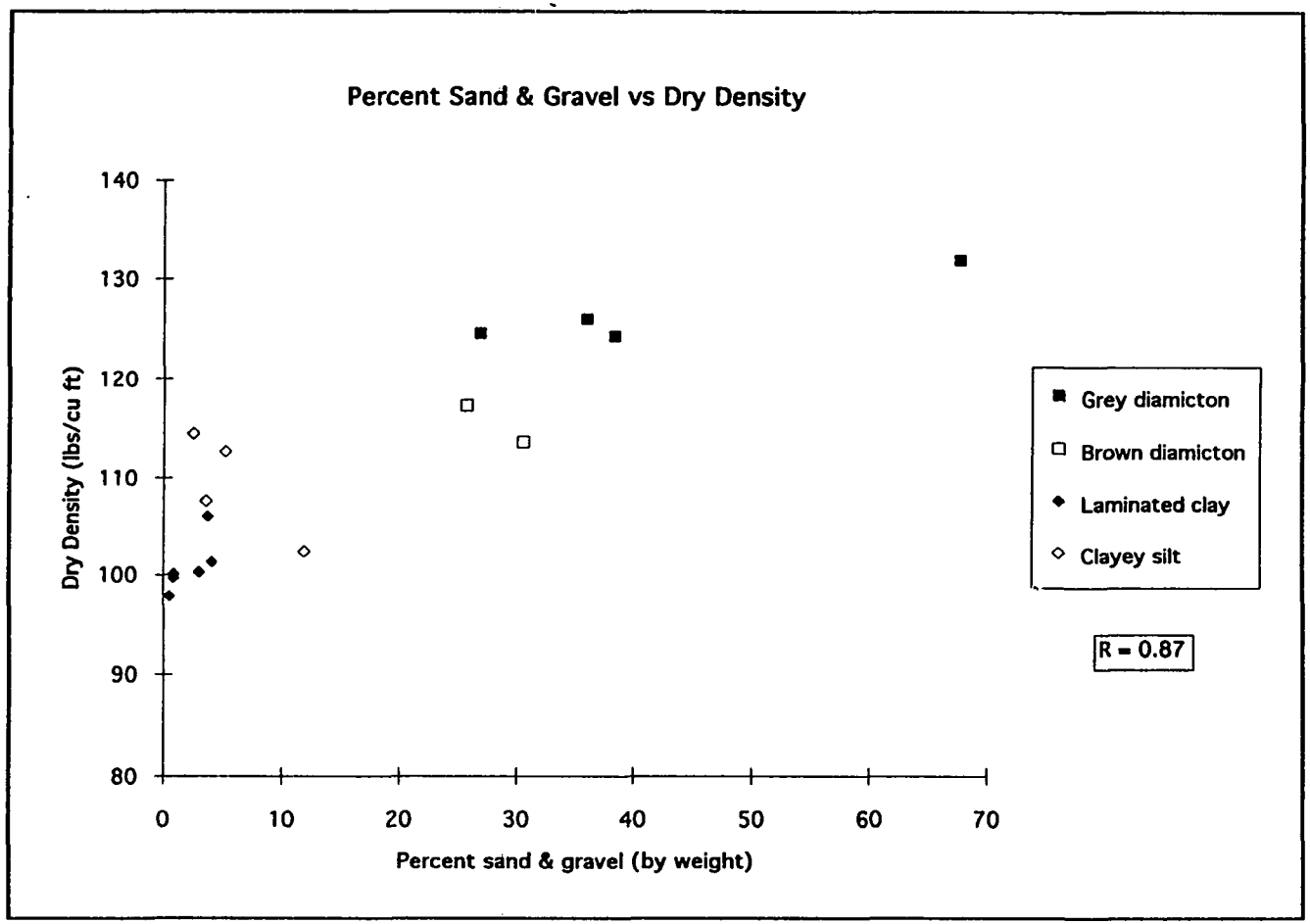

Figure 40. Relationship Between Sand & Gravel Content and Dry Density of Undisturbed Samples.

Index Property Comparisons to Percent Silt and Clay

Water saturation (S_W), in general, increases with silt and clay content (Figure 41). Exceptions to this relationship are found in two silty clay/clayey silt samples (CP-2 #4A and MP-1 #3B) that exhibit low S_W but high silt and clay content.

Void ratio also increases with silt and clay content (Figure 42). There is a large amount of void space present between the clay platelets in laminated clay samples, but the void ratio in several samples drops somewhat when silt-sized grains are introduced. The presence of low-porosity clasts of Paleozoic and Precambrian rocks may also serve to reduce the void ratios of the grey diamicton samples as compared to the brown diamicton samples. Brown diamicton samples with slightly higher void ratios tend to contain clasts of brown, laminated clay, which is a lithology known to exhibit a high void ratio.

Undrained Shear Strength - Ranges and Groups

Index properties and Atterberg limits (Figure 34) suggest that a lithologic classification continuum exists in the study area, ranging from silt (ML) through clayey silt/silty clay (ML-CL) to laminated clay (CL) which borders on fat clay (CH). Mohr envelopes derived from UU triaxial tests (Figure 36) suggest that undrained shear strength (S_u) continuums exist as well, but within at least two, and possibly three, groups. The strongest group consists of grey, silty, pebbly diamicton (S_u ~ 3.0 to 4.0 tons/ft^2; 287.3 to 383.0 kN/m^2). The second group can possibly be further subdivided into two groups: silty clay and brown diamicton share similar undrained shear strength (S_u ~ 1.5 to 2.0 tons/ft^2; 143.6 to 191.5 kN/m^2), while

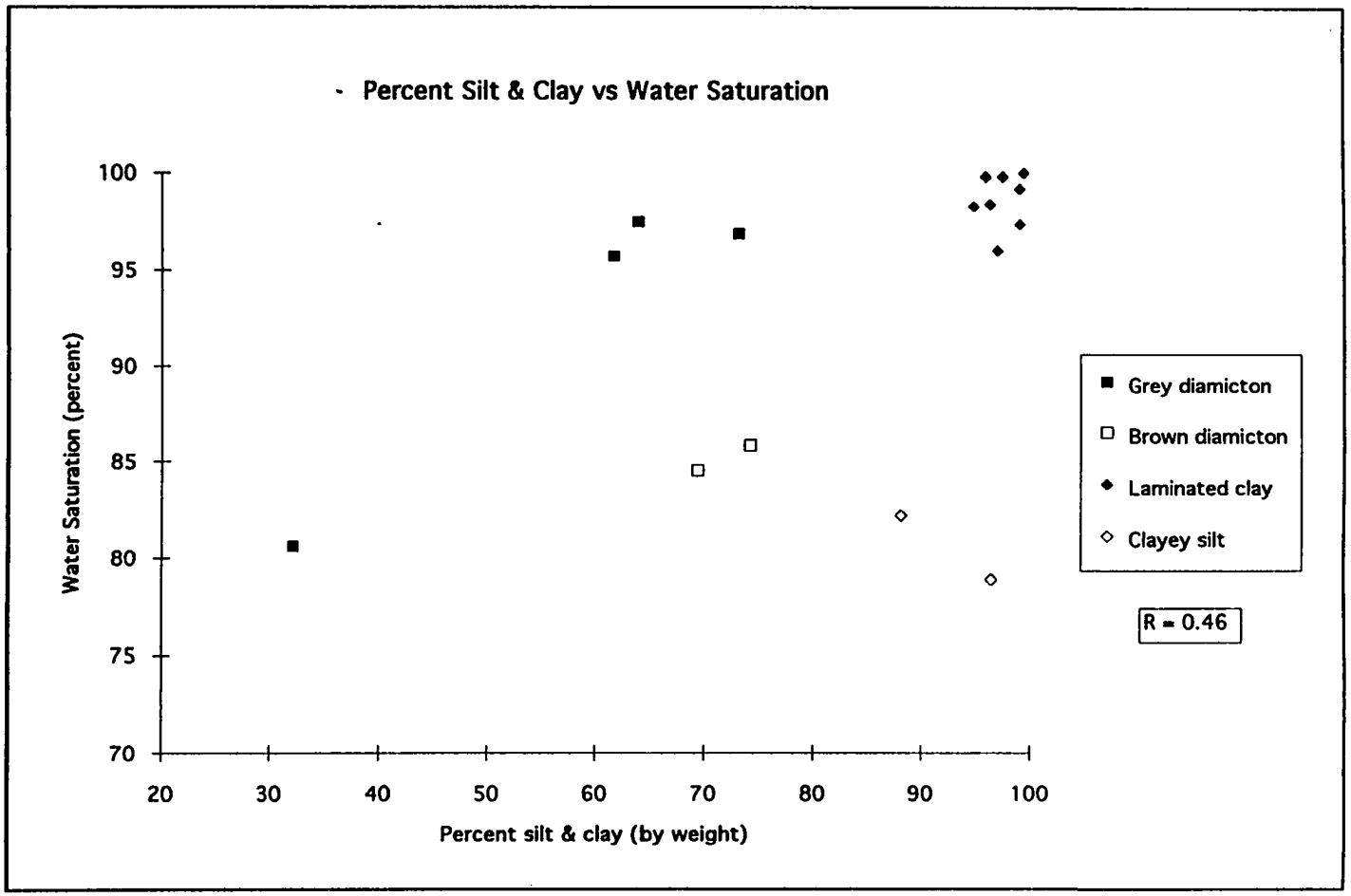

Figure 41. Relationship Between Silt & Clay Content and Water Saturation of Undisturbed Samples.

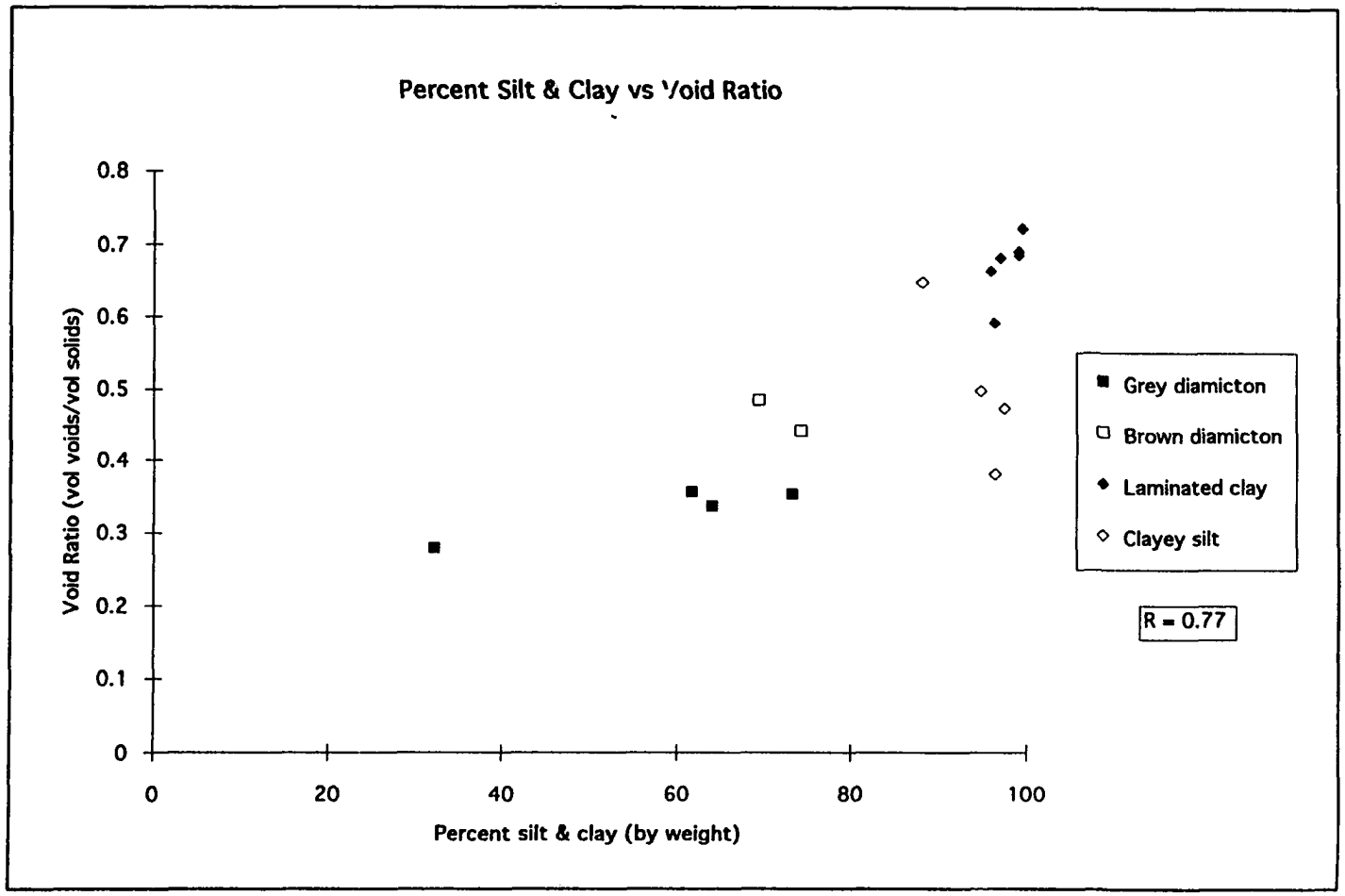

Figure 42. Relationship Between Silt & Clay Content and Void Ratio of Undisturbed Samples.

laminated clay is somewhat weaker (S_u ~ 0.5 to 1.5 tons/ft^2; 47.9 to 143.6 kN/m^2).

Index Property Comparisons to Undrained Shear Strength

Comparison of undrained shear strength (S_u) to a variety of index properties provides valuable insight as to possible factors controlling shear failure. In general, there is a good correlation between increasing percent sand and gravel and increasing S_u (Figure 43), although the brown diamicton is quite weak given its sand and gravel content.

Increasing void ratio correlates with decreasing S_u (Figure 44). Since increasing void ratio has also been shown to correlate with increased silt/clay content (Figure 42), a reasonable inference that shear strength decreases as clay content increases can be drawn.

Increasing water content also correlates with decreasing shear strength (Figure 45). Since increasing water content has been shown to correlate with decreasing sand and gravel content (Figure 39), these data also suggest that shear strength decreases as clay content increases.

Increasing dry density correlates with increasing shear strength (Figure 46). Increased dry density is also associated with increased sand and gravel content (Figure 40). Two distinct populations of data are clearly evident in Figure 46: a grouping that comprises brown till, silty clay, and laminated clay is lighter as well as weaker than grey till.

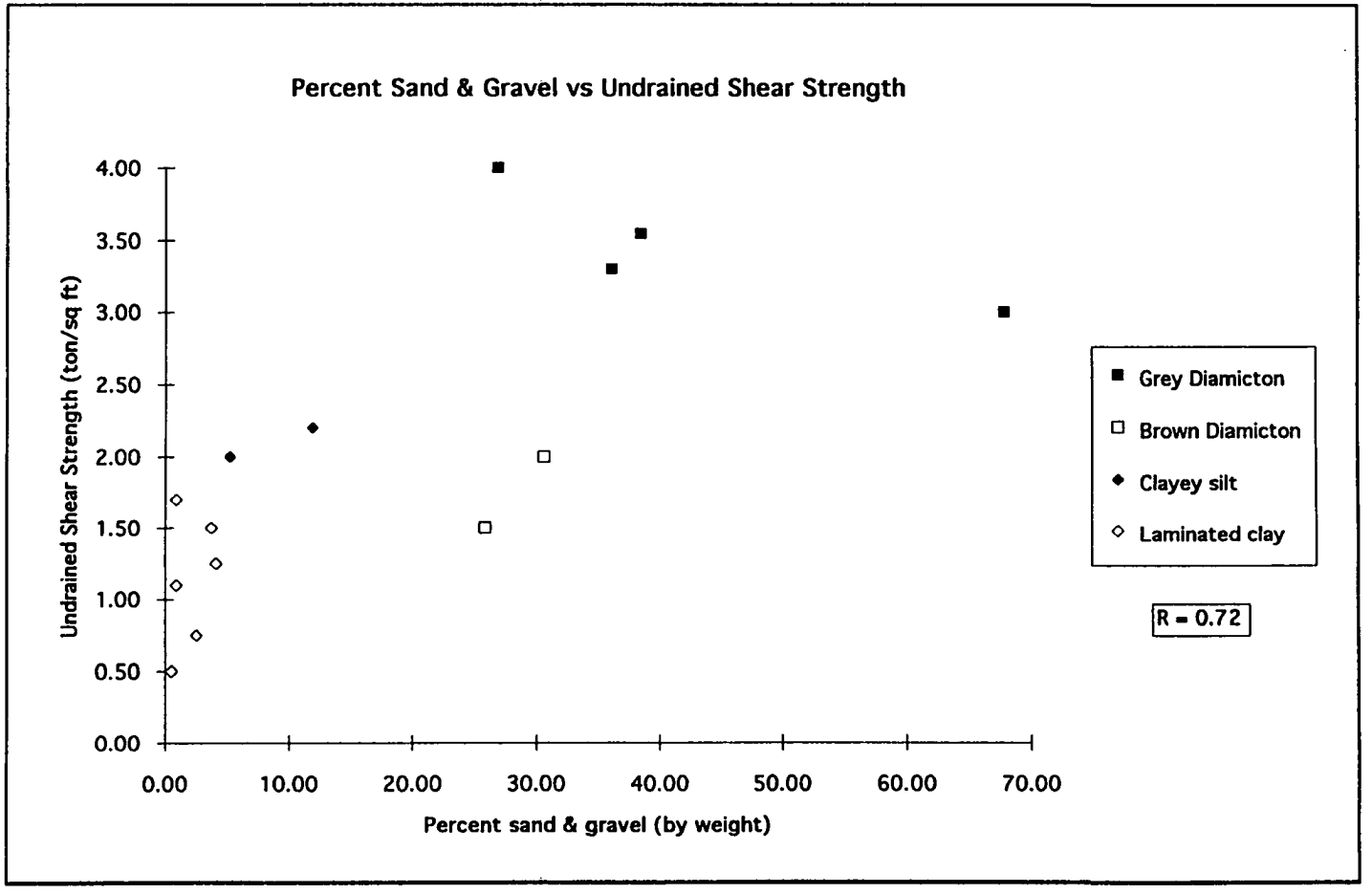

Figure 43. Relationship Between Sand & Gravel Content and Undrained Shear Strength of Undisturbed Samples.

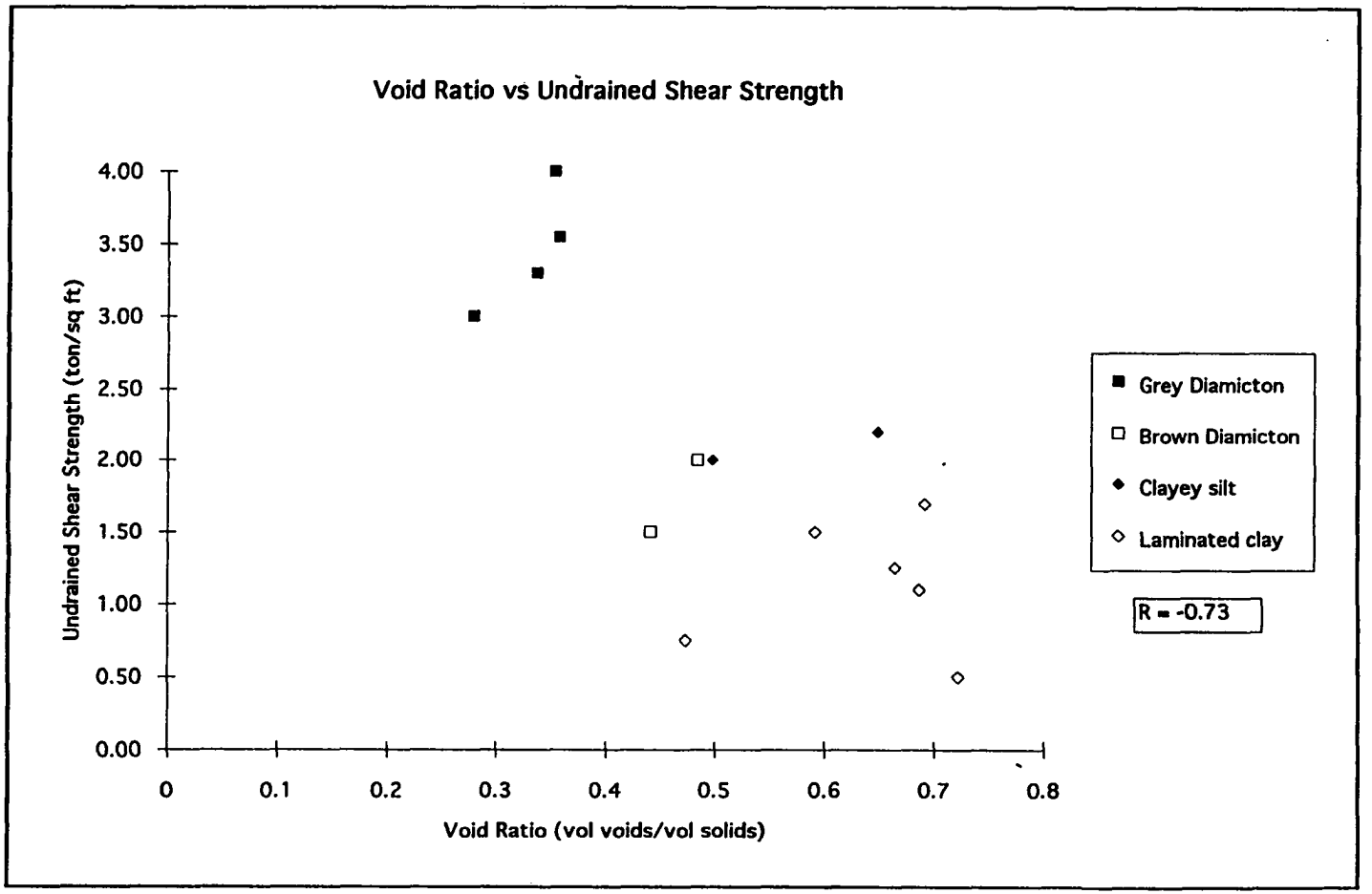

Figure 44. Relationship Between Void Ratio and Undrained Shear Strength of Undisturbed Samples.

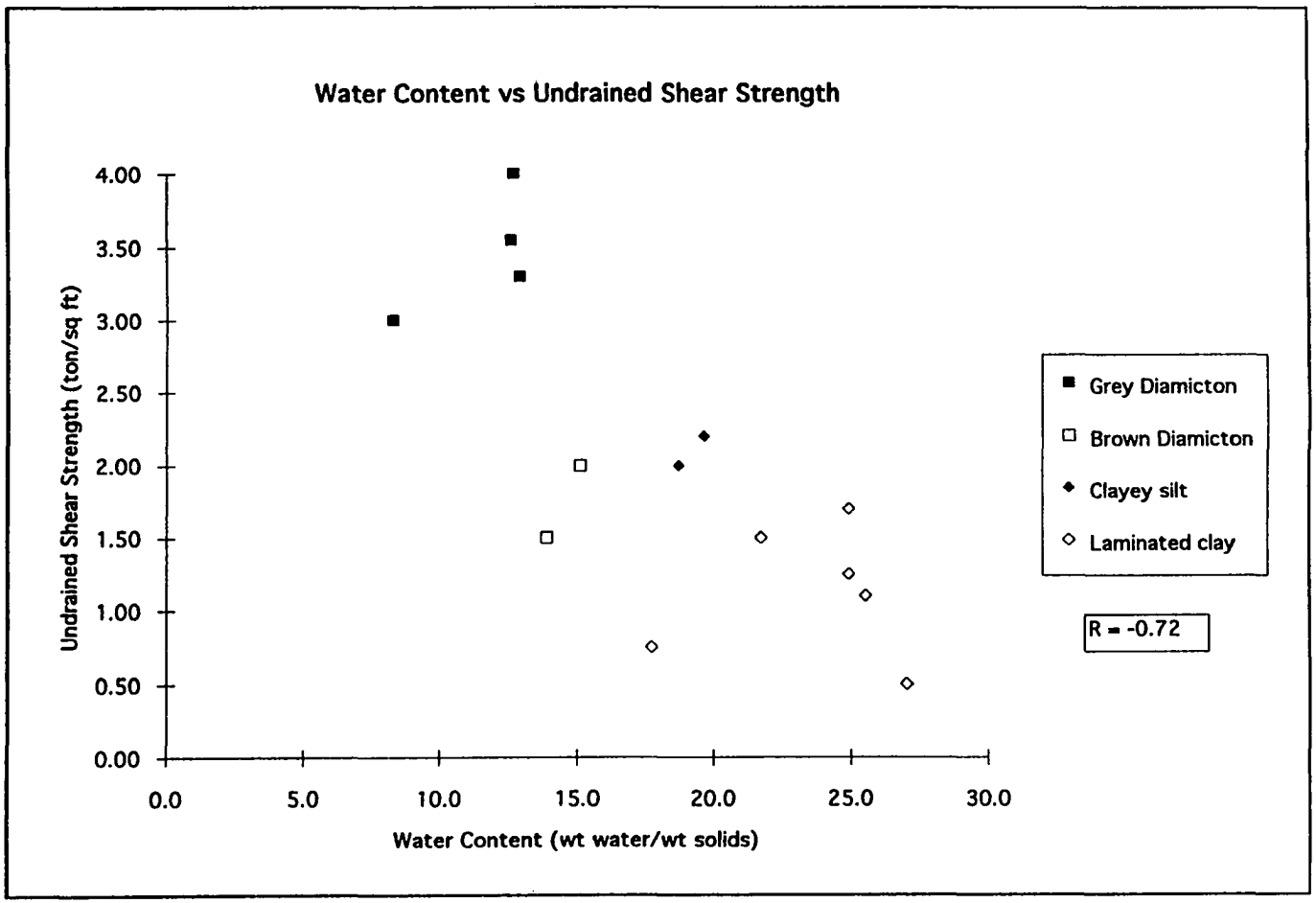

Figure 45. Relationship Between Water Content and Undrained Shear Strength of Undisturbed Samples.

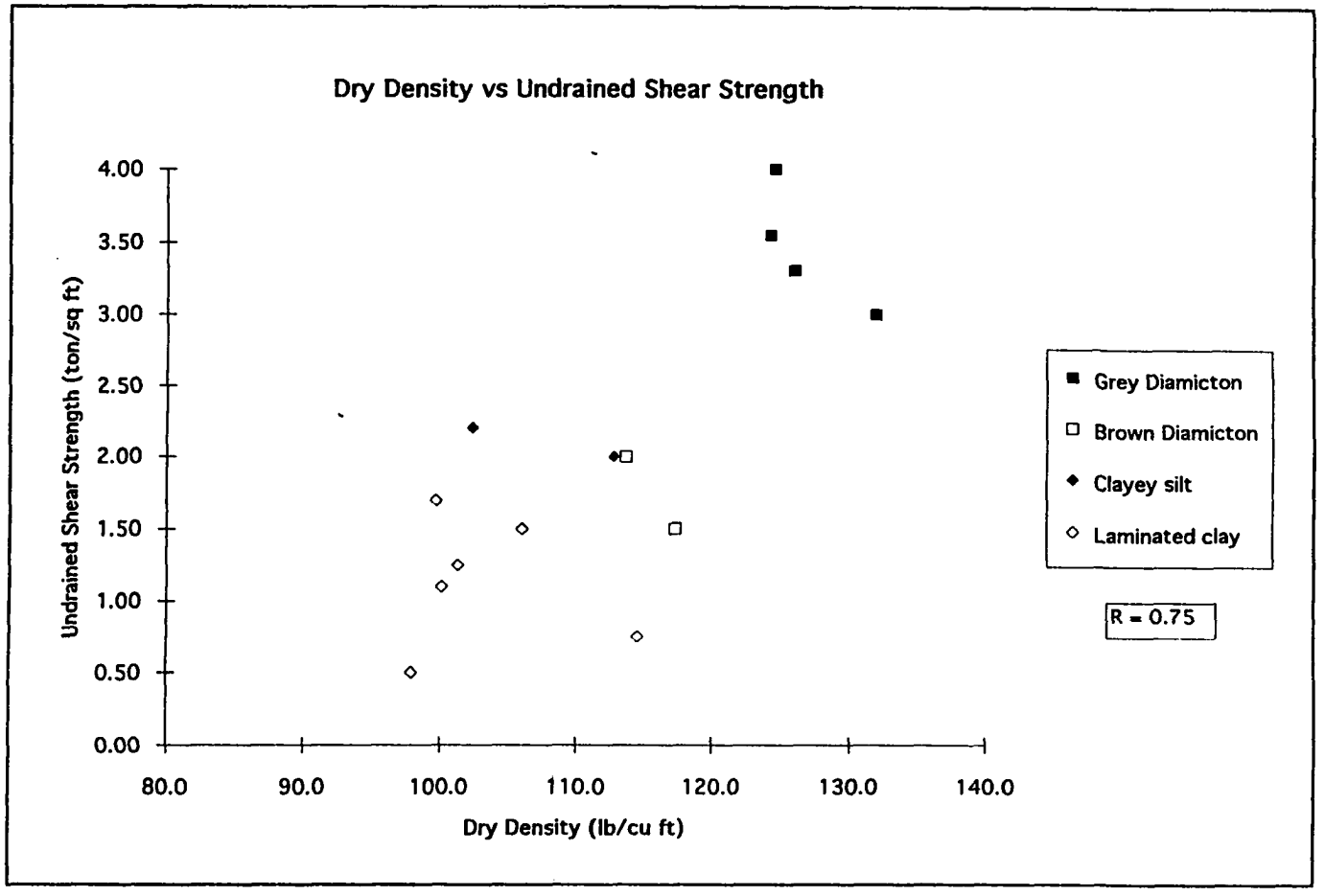

Figure 46. Relationship Between Dry Density and Undrained Shear Strength of Undisturbed Samples.

Proposed Litho-Mechanical Groups

Grey Diamicton

Grey diamicton is the stronger of the two diamictons in the study area. It is represented by samples CP-2 #2 and #3, MP-1#1, and FA-1#1. These diamicton samples have high sand and gravel content, they are heavy, and they exhibit low void ratios and water content as compared to other lithotypes.

Brown Diamicton and Silty Clay/Clayey Silt

Brown diamicton samples CP-2 #1 and 116-1 and silty clay samples MP-1 #3B and WKA-1 #1 exhibit less strength than grey diamicton, but as a group are stronger than laminated clay. These samples in general exhibit intermediate void ratios, water content, and dry density as compared to grey diamicton and laminated clay end members.

Laminated Clay

Laminated clay samples as a group are very weak. Low strength is likely due to lack of sand, high void ratio, and high water content. For example, the amount of sand available to act as a frictional strength component is generally on the order of just 1 to 4.1 percent by weight.

Summary

Index property correlation with undrained shear strength suggests that at least two litho-mechanical groups of cohesive material can be identified in the study area. One group consists of dense, silty, pebbly, grey diamicton. Another group

consists of less dense, silt- and sand-poor, very fine-grained, laminated clay. A third, intermediate litho-mechanical group may also be present, composed of thinly interbedded silt and sand as well as brown diamicton containing clasts of laminated brown clay. The presence of laminated clay clasts in the brown diamicton could explain why this diamicton acts mechanically more like laminated clay than the grey diamicton, which is both sandier than the brown diamicton and contains many more clasts of Paleozoic and Precambrian rocks.

A non-cohesive litho-mechanical group composed of sand can also be identified in the study area. However, sand's non-cohesive nature often precludes procurement of undisturbed samples from the subsurface as well as the ability to perform triaxial tests (Torrey, 1997, personal communication). Rare exceptions to this occur when interbedded clays hold sands in Shelby tubes during sample retrieval and removal, and when they bracket sands in triaxial test specimens. The few interbedded sand/clay samples triaxially tested in this study suggest that sand content dramatically increases shear strength, consistent with Figure 43. In the absence of triaxial test data, information gained from blow count analysis (McCarthy, 1993) and through measurement of sand angles of repose on bluff faces such as those at Wau-Ken-A and the West Side County Park was utilized when internal angle of friction data was required. These angles vary from 34° to 43° (Table 4).

Discussion and Interpretation of Geotechnical Test Results

Introduction

Stress-strain data, Mohr failure envelopes, and stress paths to failure are interpreted in the context of total and effective stress analysis, normal vs.

overconsolidated clay behavior, and lithology. The nature of overconsolidation in the study area and its possible significance is also reviewed.

Stress-Strain Curve Shape

Measurement of a specimen's stress-strain behavior yields critical numerical data such as percent strain and axial/confining stress at failure, but interpretation of a specimen's internal deformation history prior to failure through stress-strain curve shape analysis also provides valuable information about soil properties (Lambe and Whitman, 1969). A brief review of the stress-strain behavior of cohesionless soil provides a framework for analysis of the behavior of cohesive soil specimens tested in this study.

Cohesionless Soil Stress-Strain Behavior

The key factors that control stress-strain behavior in cohesionless soils are the size and shape of particles and the initial density (degree of compaction) of the specimen (Lambe and Whitman, 1969). Initial density, measured by the specimen void ratio e (volume of voids/volume of solids), can itself be responsible for two different types of behavior under identical loading conditions.

Loose Sand. In a loose sand specimen, initial axial loading at the beginning of a triaxial compression test causes compaction and an attendant decrease in void ratio (e) to begin to occur immediately(Figure 47b). As compression progresses, further compaction causes an increase in specimen strength (its ability to carry an axial load), so the specimen stress-strain curve rises (Figure 47a.) as the void ratio of the specimen decreases (Figure 47b.). Ultimately, however, the specimen reaches its compaction limit and critical void ratio. Further axial loading produces specimen

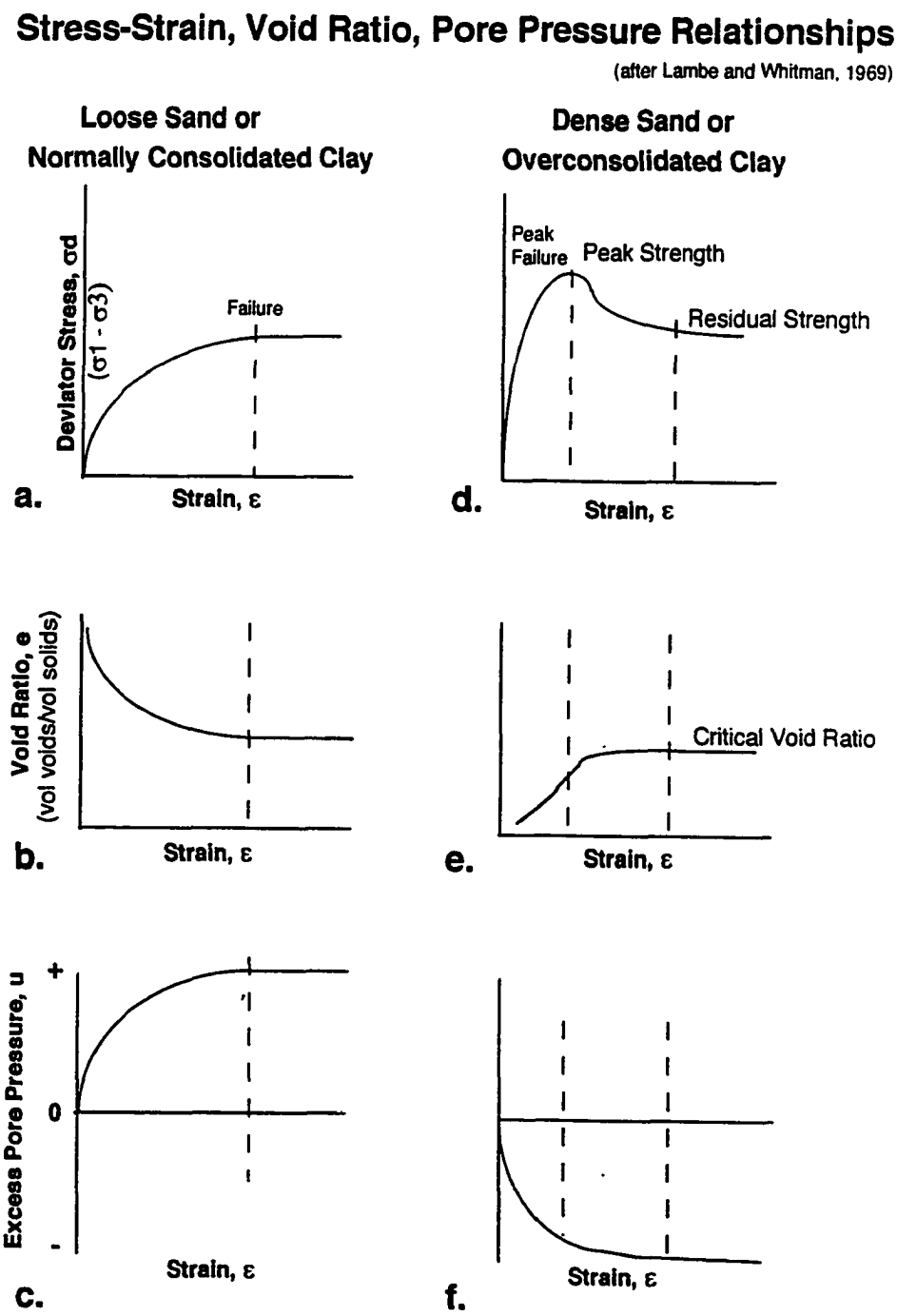

Figure 47. Idealized Stress-Strain, Void Ratio, and Pore Pressure Relationships for Different Specimen Lithotypes.

failure at this critical void ratio, because grains must roll, slide, or otherwise shear past each other to accommodate any further strain. One-half the deviator stress ($\sigma_d/2$) at this point on the stress-strain curve (Figure 47 a.) is defined as the specimen's ultimate or residual shear strength (USACE, 1986).

Dense Sand. A dense sand specimen (Figure 47 d.) begins a triaxial compression test with its grains already compacted and its void ratio low. Since the specimen is already compacted and prepared to carry a high axial load, it exhibits a much higher rate of strength increase under initial load than a loose sand. It also exhibits a higher peak strength at failure than a loose sand. In contrast to the decreasing void ratio that occurs in a loose sand under load, the void ratio in a dense sand must increase under load, because grains must move out of their densely-compacted state in order to slide, roll, and shear past each other (Taylor,1948). The initially differing strengths of dense and loose sand specimens ultimately converge to one residual strength at the critical (equilibrium) void ratio for the material (Figure 47 e.), because grain size and shape are identical in the specimens.

Cohesive Soil Stress-Strain Behavior

In general, particle size/shape and initial compaction state control cohesionless soil behavior under load, whereas clay mineralogy, water content, and consolidation history control cohesive soil behavior under load (McCarthy, 1993). For example, the increased compaction state of an overconsolidated soil may cause higher interparticle frictional resistance or different particle/water surface tension behavior than in normally consolidated soil. The consolidation states (normal and overconsolidated) of cohesive soil are somewhat analogous to the compaction states (loose and dense) of cohesionless soil. However, unlike well-

drained cohesionless soil, cohesive soil behavior is complicated by the presence of water during undrained stress. Pore pressure can act to either weaken or strengthen a specimen during undrained loading, and the consolidation state of the specimen has a major influence on which type of undrained behavior occurs.

Normally Consolidated Cohesive Soil. In the case of a fully (almost 100%) saturated, normally consolidated clay specimen under undrained load, decreasing void space during compression causes excess positive pressure to be generated in trapped pore water (Figure 47 c.). This excess pore pressure acts to force the soil skeleton apart, making it relatively easy to induce shear failure at low loads. Although binding of clay particles may occur prior to shear, it is generally thought (Lambe and Whitman, 1969; McCarthy, 1993) that the generally low resistance of clay to shear is due to the fact that the relatively flat faces and asperites (contact points) of clay minerals do not generate significant interparticle resistance. In fact, clays with low measured friction angles (such as the laminated clays in the study area) are referred to as "supersmooth" (Lambe and Whitman, 1969, p. 67).

Overconsolidated Cohesive Soil. Much like a dense sand, the void ratio of an overconsolidated cohesive specimen tends to increase (Figure 47 e.) when it is loaded, because the densely-packed (overconsolidated) clay particles must move apart in order to shear past each other. Under undrained conditions, the pore water present in an overconsolidated specimen tends to generate a negative excess pressure (an induced vacuum) which serves to increase the strength of the specimen (Figure 47 f.). As a result, failure in an undrained, overconsolidated clay requires a higher axial load than in an otherwise similar undrained, normally consolidated clay. As in cohesionless soil, otherwise similar normal and overconsolidated clays will ultimately converge toward one residual strength and void ratio.

Stress-Strain Curve Types - Discussion and Interpretation

Stress-strain curves generated from UU tests (Appendix C) indicate that both overconsolidated and normally consolidated samples are present in the study area. In general terms, silty grey diamicton samples (CP-2 #2, #3; MP-1 #1) tend to exhibit high strength and overconsolidated behavior. Brown, clayey diamicton samples (CP-2 #1, 116-1 #1), silty clay/clayey silt samples (MP-1 #3B and WKA-1 #1), and fine-grained laminated clay samples (CP-2 #4, #5; MP-1 #2, #3A, #4, #5) tend to exhibit low strength and normally consolidated clay behavior. Overconsolidation is also interpreted to be responsible for low void ratios measured in the grey diamicton.

The stress-strain curves generated from CU tests (Appendix D) indicate that, for the most part, preconsolidated specimens exhibit normally consolidated or only slightly overconsolidated behavior. This is to be expected because of the nature of CU test procedure. Since a specimen's OCR is defined as $\sigma'_{v\ max}$ / $\sigma'_{v\ current}$, consolidation to progressively higher $\sigma'_{v\ current}$ during the consolidation phase of a CU test reduces a specimen's OCR, which lessens a specimen's tendency to exhibit overconsolidated behavior.

Mohr Circles and Failure Envelopes - Discussion and Interpretation

UU and CU test data may to a large degree reflect the different triaxial stress environments (total vs. effective) in which they are produced. Therefore, any interpretation of these test results must be made with consideration of the testing environments themselves, and how they may or may not reflect in situ conditions. There is no unified consensus as to the efficacy or reliability of one testing method

over the other (Mayne et al., 1995) without the benefit of local knowledge and practical experience.

Total vs Effective Stress

Terzaghi (1936) was the first to articulate the principle of effective stress. The effective stress principle can be described in two parts (Lambe and Whitman, 1969, p. 241): (1) *effective stress equals total stress minus pore pressure*; (2) effective stress controls certain aspects of soil behavior, notably compression and strength.

By way of illustration, Figure 48 a. represents a saturated soil sample under confining pressure in a cylinder. There is a tight-fitting piston on the top that can be used to compress the sample, and a valve at the base to allow water to drain. Initially, there is a light drained load on the water-filled sample, and the total axial normal stress (σ_t) applied by the piston is carried by both the skeletal structure of the sample (effective stress, σ') and by pore water (neutral stress, u). The relationship is:

$$\sigma_t = \sigma' + u$$

where σ_t = total normal stress
σ' = effective normal stress
u = neutral stress or pore water pressure

If the drain is closed and the sample is loaded, as in the case of "b-value" tests run during CU consolidation, the neutral stress carries all the total stress ($\sigma_t = u$) and $\sigma' = 0$.

If the valve in the sample chamber is opened, water will be allowed to drain under load, and the sample will compress to a point where all the load of the piston

Total vs Effective Stress Concept

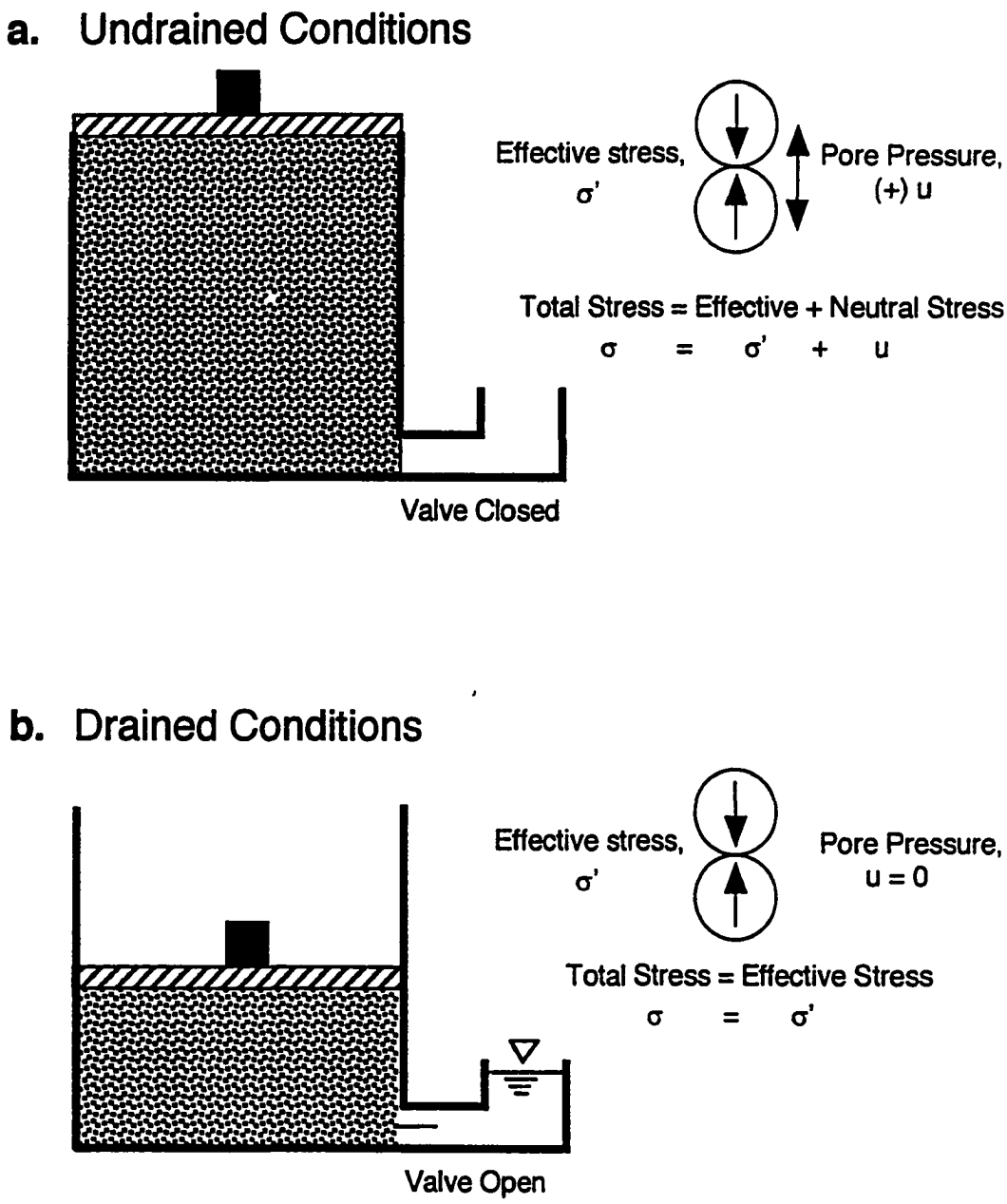

Figure 48. Illustration of Relationships Among Total, Neutral, and Effective Stresses in a Specimen Under Undrained and Drained Conditions.

will be carried by the soil's skeletal structure (Figure 48 b.). In this drained case, $\sigma_t = \sigma'$ and $u = 0$. A drained (effective) strength condition can be determined with undrained CU tests by measuring pore pressure during loading and then removing it from the total stress measurements recorded during the test.

UU-derived Mohr Circles, Failure Envelopes, and ø = 0° Behavior

UU test results reflect undrained, total stress conditions. UU tests are conducted under conditions of increasing confining stress, but any increase in confining stress applied to a saturated specimen is borne completely by a commensurate increase in specimen pore pressure. This is the principle behind the "b-value" test used to determine full specimen saturation during CU testing. Under these conditions (Figure 49), any increase in confining pressure ($\sigma 3b = \sigma 3a + u$) will simply shift a Mohr circle to the right along the x-axis by an amount u, with no change in the height of the circle. The height does not change because the pore pressure terms cancel out in the calculation of shear strength:

$$\tau' = \frac{\sigma 1' - \sigma 3'}{2} = \frac{(\sigma 1 - u) - (\sigma 3 - u)}{2} = \frac{\sigma 1 - u - \sigma 3 + u}{2} = \frac{\sigma 1 - \sigma 3}{2} = \tau$$

where τ' = effective shear strength
τ = total shear strength

The Mohr failure envelope generated from laterally shifting circles of identical height exhibits what is known as ø = 0° behavior, because the envelope has a slope of 0°. Theoretically, the y-intercept (S_u) of this envelope represents the effective shear strength (τ') present in the specimen at its particular in situ confining pressure.

ø = 0° Behavior (Undrained Shear)

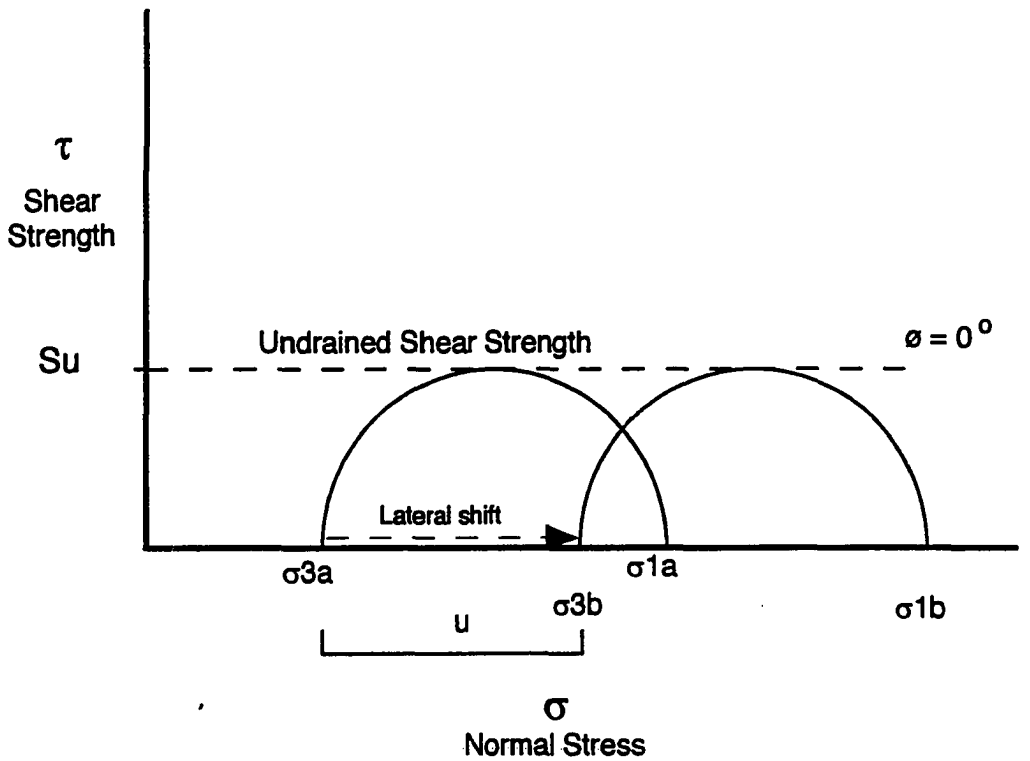

$$\sigma = \sigma' + u ;$$
$$\sigma' = \sigma - u$$

$$\tau = \tau' = \frac{(\sigma 1 - u) - (\sigma 3 - u)}{2}$$
$$= \frac{\sigma 1' - \sigma 3'}{2} = \text{Effective Shear Strength}$$
$$= \frac{\sigma 1 - \sigma 3}{2} = \text{Total Shear Strength}$$

Figure 49. Idealized ø = 0° Mohr Failure Envelope of a Saturated Specimen Sheared Under Undrained Conditions.

Both the weak laminated clays and the diamicton samples from the study area tend to exhibit $\phi = 0^{o}$ behavior under undrained test conditions (Figure 36). The laminated clays achieve this state at very low normal stresses, which suggests that they may not gain much strength with increased confining pressure (depth of burial) when fully saturated. The diamicton samples, however, show a tendency to gain considerable shear strength with increasing confining pressure prior to attaining a $\phi = 0^{o}$ state. This diamicton behavior may be explained by a lack of full saturation or overconsolidation relative to confining stress.

When subjected to compression initially, the soil skeleton of an unsaturated specimen can compress and gain some shear strength before the void space becomes fully saturated (Figure 50). However, when the pore space becomes fully saturated, the skeleton can no longer collapse and gain further strength. At this point, the sample's effective strength is reached, and $\phi = 0^{o}$ behavior is exhibited throughout the remainder of the test. A good example of this behavior was exhibited by unsaturated sample FA-1 #1 (Appendix C).

Overconsolidation of saturated glacial diamicton may also result in undrained failure envelopes that initially rise with increasing normal stress. Overconsolidated clays tend to expand in volume as they tend toward a critical void ratio, which leads to vacuum conditions, negative pore pressure, and increased shear strength. If several undrained overconsolidated specimens are sheared and produce progressively higher peak strength at failure, the resulting failure envelope could rise before it ultimately flattened out. This behavior was observed in saturated diamicton samples CP-2 #2, #3; and MP-1 #1 under undrained shear (Appendix C).

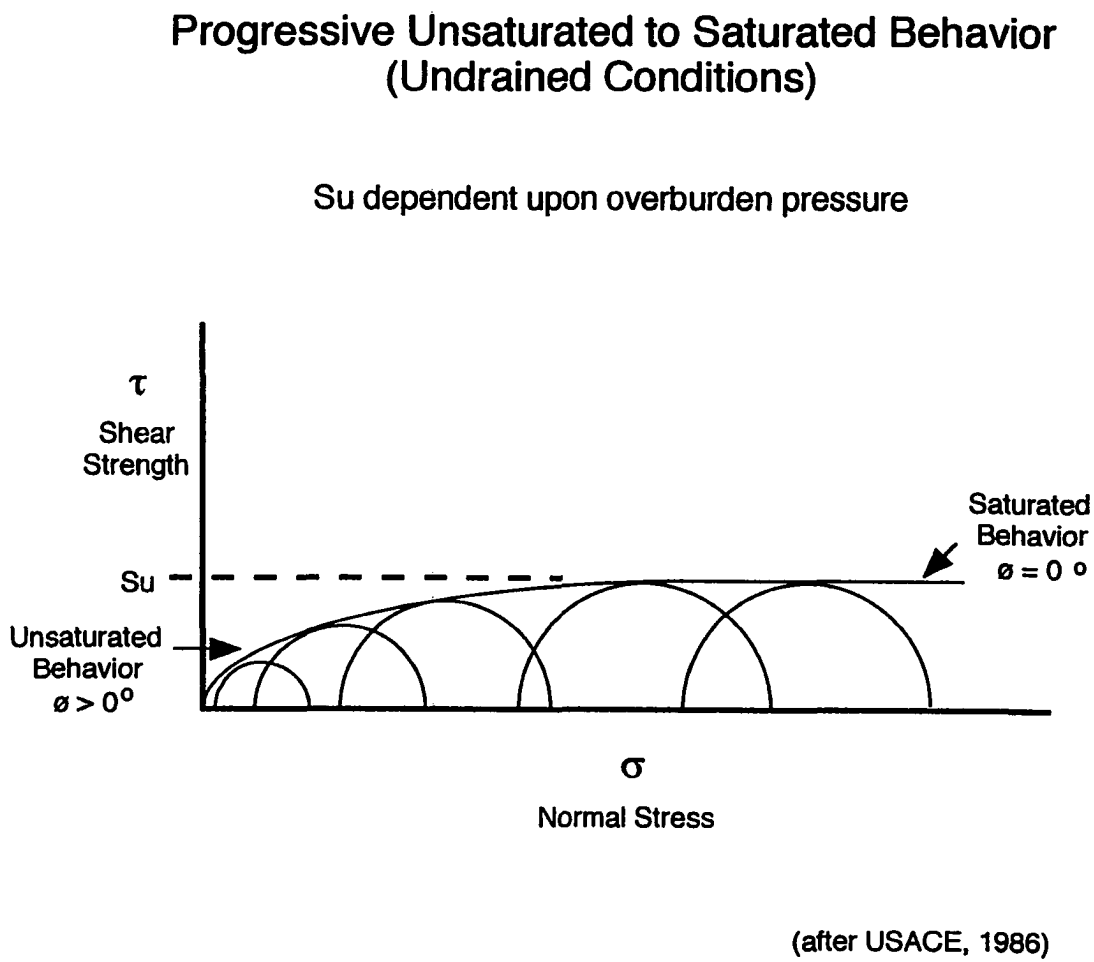

Figure 50. Idealized Mohr Failure Envelope Produced by Specimen Progression From Unsaturated to Saturated State Under Undrained Shear.

CU-derived Mohr Circles, Failure Envelopes, and ø > 0º Behavior

CU testing procedure prescribes that specimens be consolidated to progressively higher effective stresses prior to shear. As a result, the total stress Mohr circles and failure envelopes constructed with CU test data reflect this preconsolidation to higher effective stresses, and failure envelopes constructed with these data show $\phi > 0^{o}$ (Figure 51). The induced pore pressure (u) measured during CU testing allows effective stress (σ') Mohr circles to be generated from undrained stress-strain data (σ_t) because $\sigma' = \sigma_t - u$.

Negative pore pressure measured in diamicton samples MP-1 #1 and CP-2 #3 (Figure 52) is consistent with the interpretation that they are overconsolidated, as initially suggested by the UU data. In contrast, positive (or very slightly negative) pore pressure measured in predominantly fine-grained clay samples MP-1 #2 and MP-1 #4/5 (Figure 53) is s consistent with an interpretation that these are normally consolidated to very slightly overconsolidated . The other CU test sample (MP-1 #4 E1, D1, D2), an interbedded sand/clay lithology, exhibited a combination of both behaviors (Figure 54). The sandy sample, E-1, exhibited a dense sand character with very negative pore pressure, while clay-rich samples D-1 and D-2 exhibited slightly positive pore pressure similar to that seen in the other laminated clay samples.

CU Stress Paths to Failure - Discussion and Interpretation

Pore pressure measurements taken during CU tests provide the data required to determine effective stress paths to failure. In general terms, a specimen will follow one of three stress paths to failure (Figure 55), depending on its consolidation and drainage states (Lambe and Whitman, 1969). In the drained case,

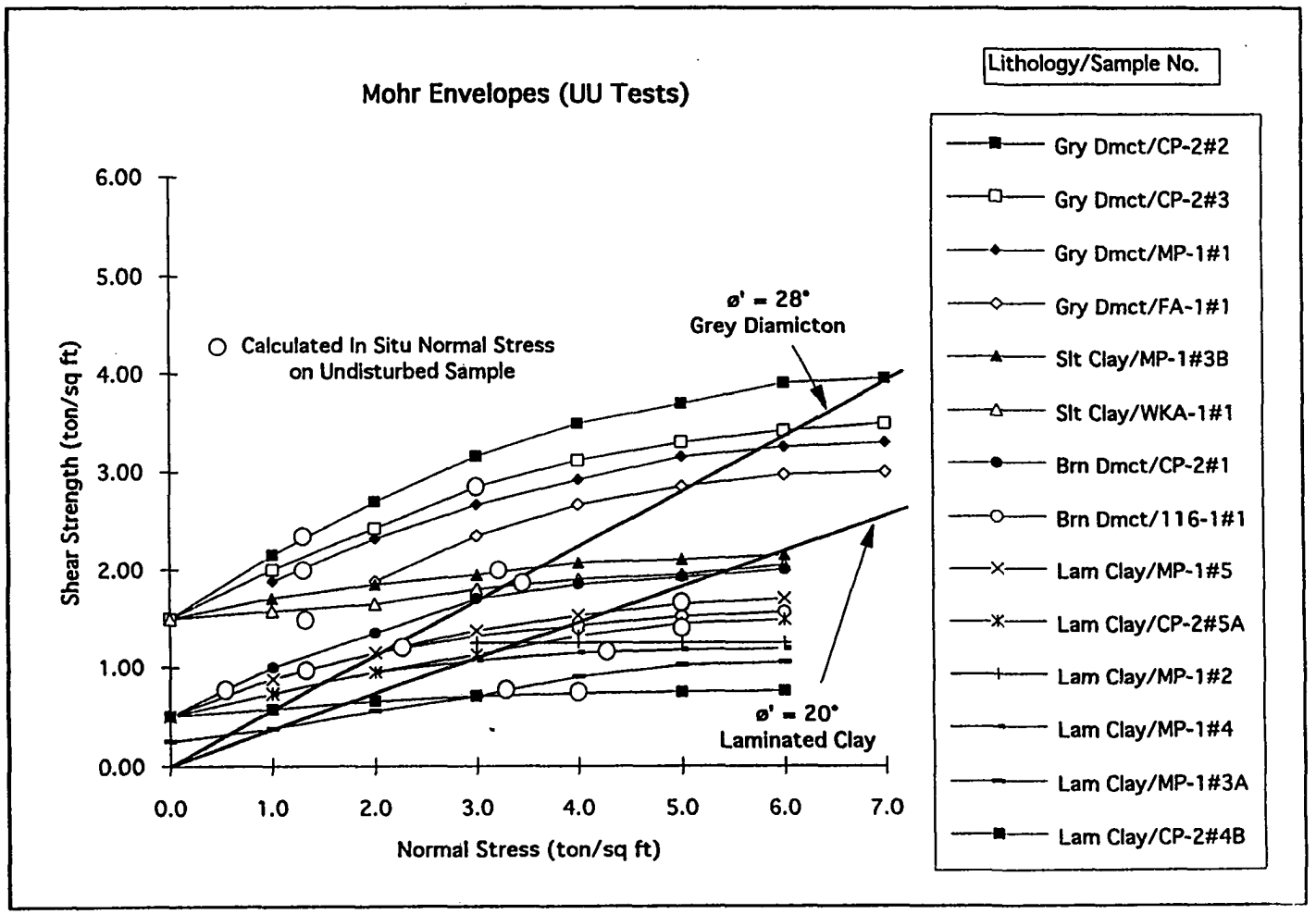

Figure 51. Relationships Between Undrained, Non-Linear, Total Stress Failure Envelopes and Linear, Effective Stress Failure Envelopes of Undisturbed Samples.

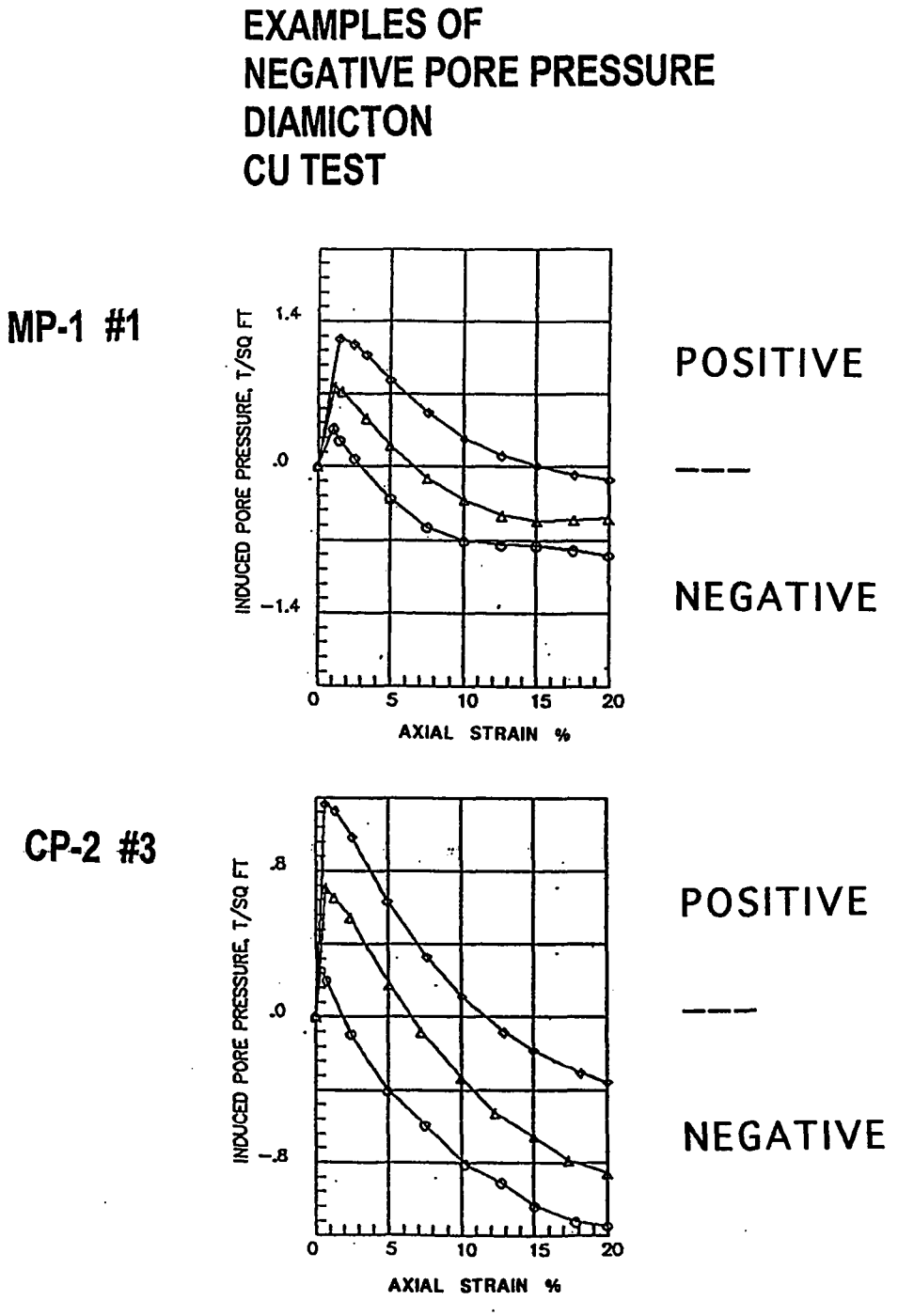

Figure 52. Examples of Negative Pore Pressure in Overconsolidated Grey Diamicton Recorded During CU Testing.

EXAMPLE OF POSITIVE PORE PRESSURE LACUSTRINE CLAY

CU TEST

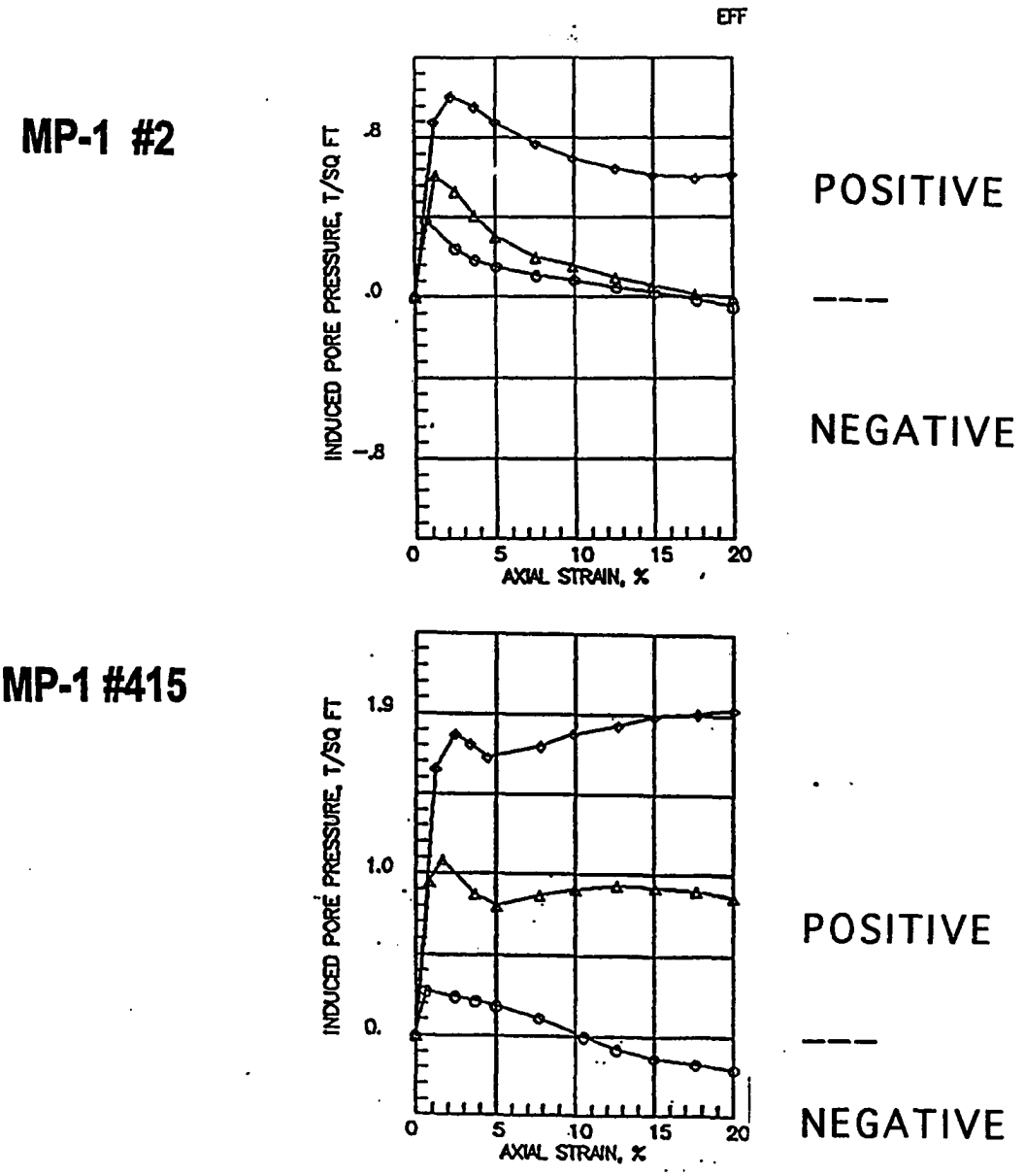

Figure 53. Examples of Positive Pore Pressure in Normally Consolidated Brown Laminated Clay Recorded During CU Testing.

DIFFERENCES IN PORE PRESSURE RESPONSE

SAND-RICH VS CLAY-RICH

MP-1 # 4

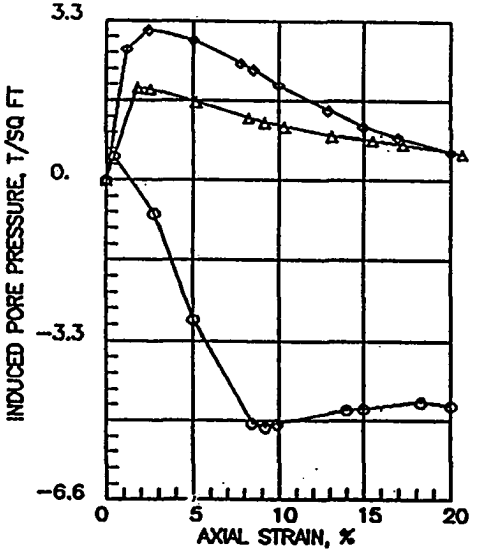

POSITIVE U
CLAY RICH SPECIMENS

NEGATIVE U
SAND-RICH SPECIMEN

Figure 54. Examples of Differences in Pore Pressure Response Caused by Differences in Lithology (Sand vs. Clay).

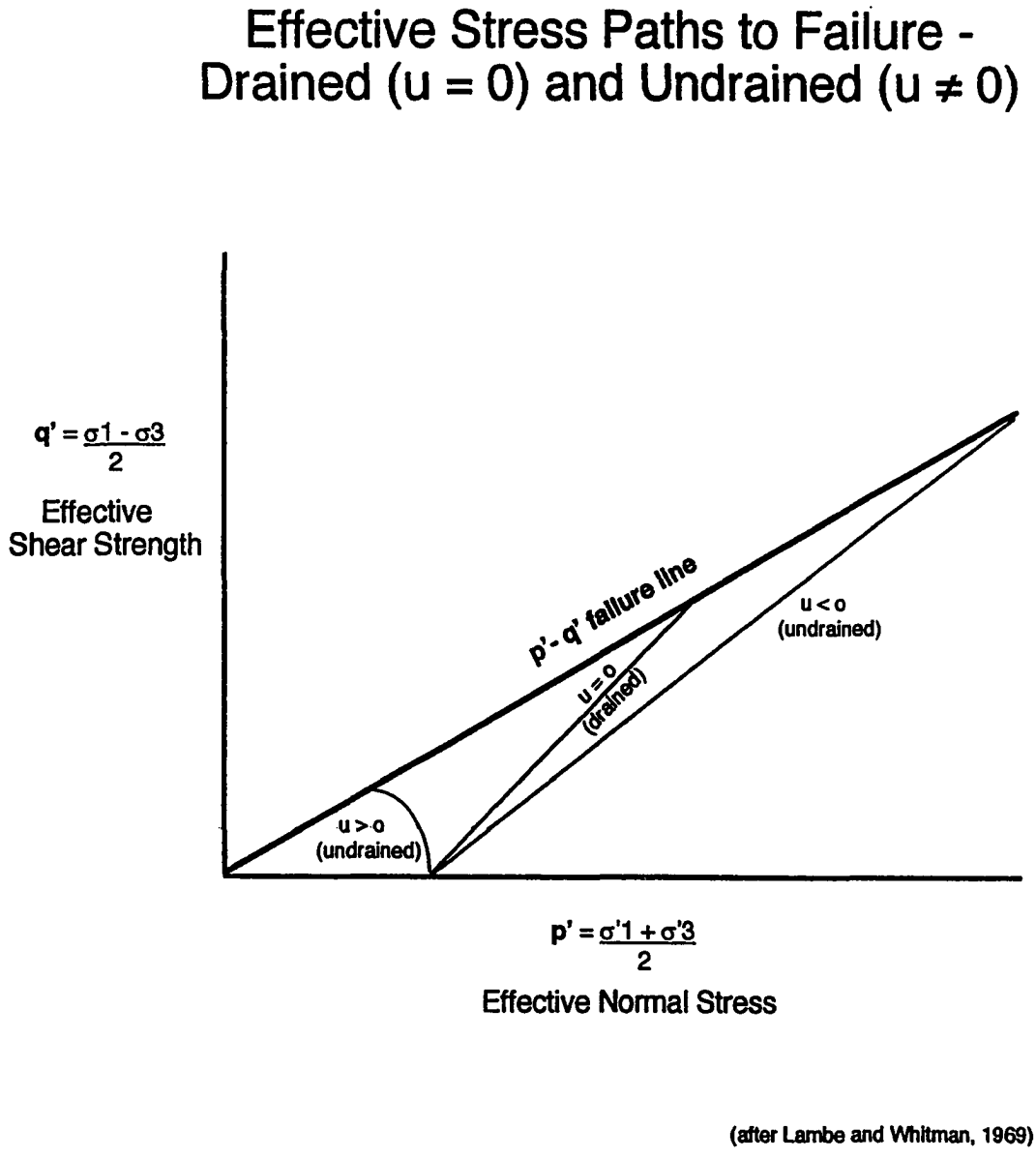

Figure 55. Idealized Specimen Stress Paths to Failure Under Drained and Undrained Conditions.

where u = 0, total and effective normal stress are the same throughout a test, and the specimen will follow a path to failure that is 45° from the horizontal in either a p - q or p' - q' coordinate system (USACE, 1993).

Effective stress in an undrained, normally consolidated clay specimen (Figure 56 a.) typically decreases (deviates to the left of the u = 0 line) as the specimen approaches failure. Since all of the applied load in a saturated, normally consolidated, undrained specimen is carried by increasing pore pressure, subtraction of increasing positive pore pressure (+u) from measured total stress (σ_t) at various points along the failure path yields decreasing effective stress (σ'). Laminated clay specimens from samples MP-1 #2 and MP-1 #4/5 tended to exhibit this type of failure path during CU testing (Appendix D).

In contrast, effective stress in undrained, overconsolidated clays typically increases (Figure 56 b.) as the specimen approaches failure. Total stress in the specimen due to increasing applied load rises as in the prior case, but negative pore pressure (-u) acts to cause the effective stress (σ') to be even greater than the total stress (σ_t). Grey diamicton specimens from samples MP-1 #1 and CP-2 #3 tended to exhibit this type of path to failure during CU testing (Appendix D).

Lambe & Whitman (1969) suggest that soils tend to have rather unique p-q-w (normal stress-shear stress-water content) relationships. It is revealing to overlay the p' - q' failure lines from the CU tests (Figure 57). The failure lines from the grey diamicton samples are virtually identical. The laminated clay failure lines indicate that these specimens have slightly less effective shear strength than the grey diamicton, but the lines are very similar to each other and to the grey diamciton. It is possible that p-q-w analysis might be a useful tool in the regional correlation of glacial units throughout the Midwest, in addition to other more traditional laboratory correlation techniques such as grain size distribution and

Total vs Effective Undrained Stress Paths

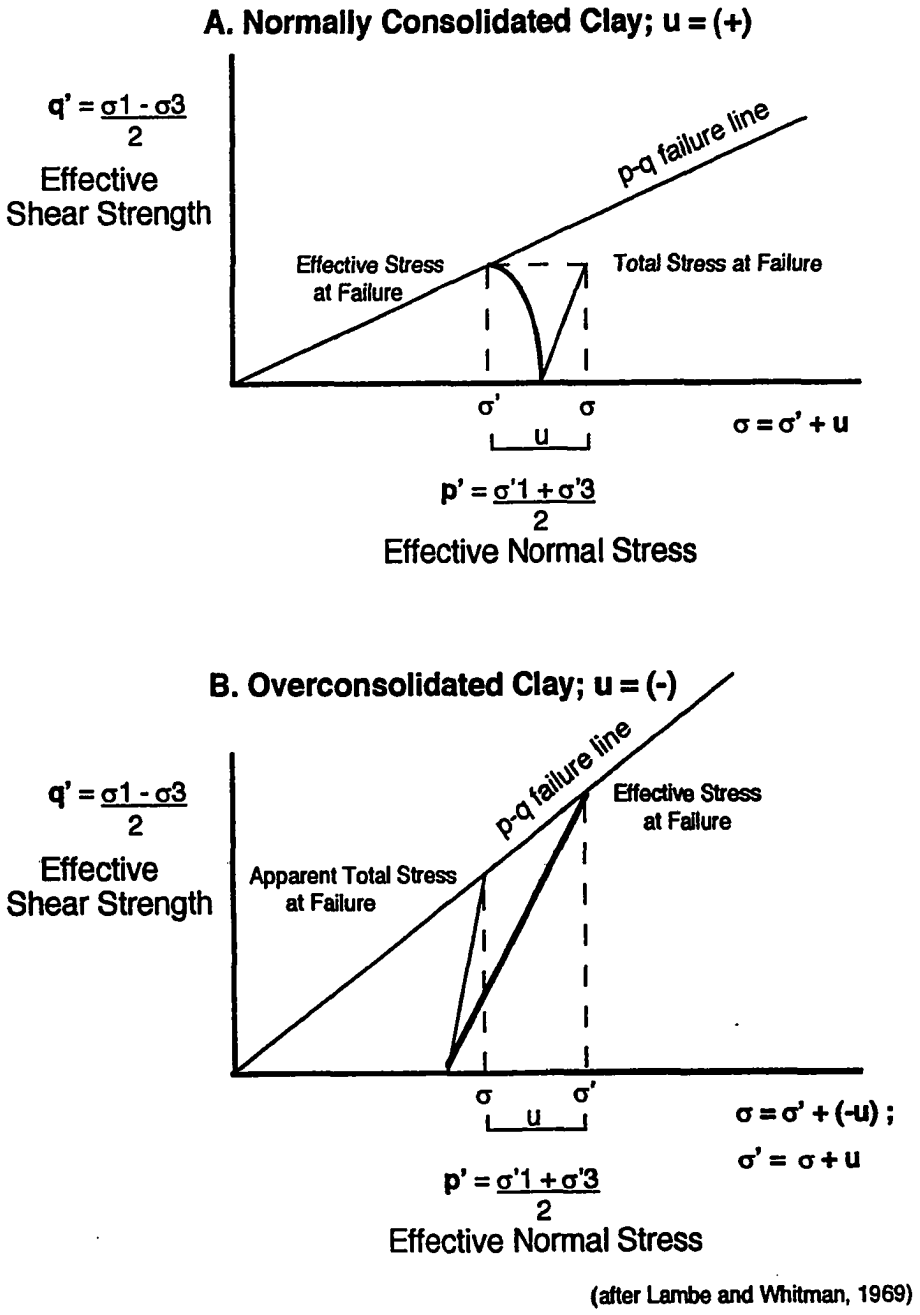

Figure 56. Idealized Illustration of Differences in Stress Paths to Failure Due to Differences in Consolidation State and Pore Pressure.

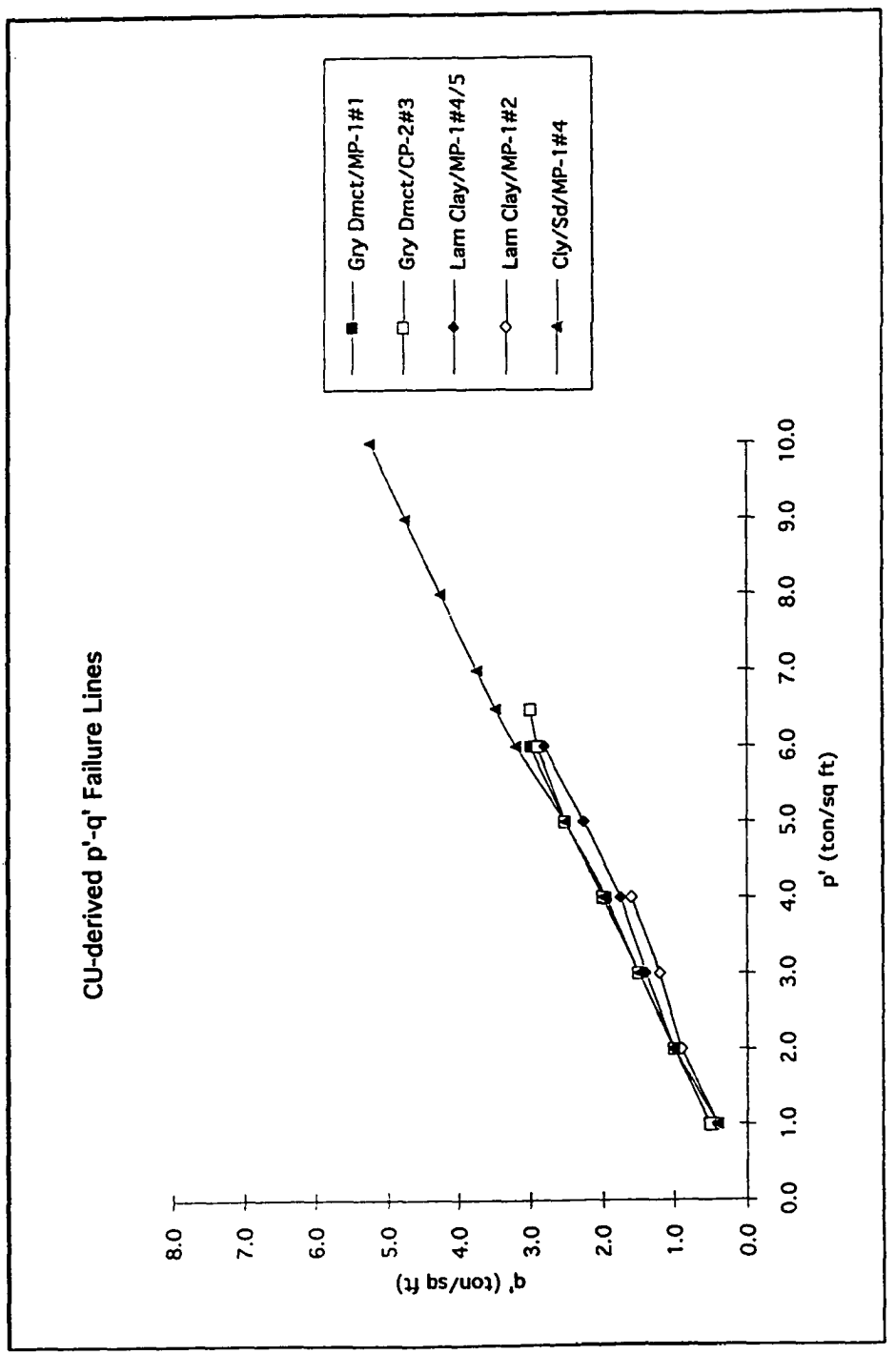

Figure 57. p' - q' Failure Envelopes Derived From Stress Path Data Generated Through CU Testing.

Atterberg limits (Edil and Mickelson, 1995; Muldoon et al., 1988) and x-ray diffraction (Monaghan and Larson, 1986).

Overconsolidation Ratios - Discussion and Significance

Further consolidation testing of more samples is required prior to making conclusive judgments concerning the level of overconsolidation of glacial materials in the study area. However, the consolidation data generated and analyzed thus far are consistent with stress-strain data that suggest that the silty, grey diamicton is significantly more overconsolidated (OCR ~12) than the lacustrine clays (OCR 1 to 4).

Similar trends in OCR decrease with depth have been reported by Edil and Mickelson (1995) in Wisconsin, although their reported OCR range is larger (from 1 to 32) than that measured in the study area (from 1 to 12). In their view, the most tenable hypothesis to explain decreasing OCR with depth is that permafrost conditions could have inhibited pore water drainage from materials at depth, thereby preventing them from consolidating to an equilibrium condition with overburden pressure. Deposits nearer the surface would have been more likely to be able to drain and thereby consolidate under the weight of the ice.

Limit Equilibrium Analyses of the Field Sites - Results and Discussion

Total Stress Analysis

Results of computerized UTEXAS3 Factor of Safety (FS) analysis (Table 6; Figure 58) performed under total stress conditions (non-linear total stress Mohr envelopes and no pore pressure data) portray the same general FS progression that

Table 6

Summary of Factor of Safety Calculations and Output From UTEXAS3

Site/Reach	38-96	Shallow Aq Hd			Intmed Aq Hd			Deep Aq Hd							Initial	Poss
	Recess	Sand	Mxd	Clay	Sand	Mxd	Clay	Sand	Mxd	Clay	Bluff Ht	Ft Sand	Ft Clay	% Sand	Classif	Classif
N1	20		605			585			580		53	30	23	0.57	LM	
N2	30		606			585			585		52	20	32	0.38	LM	
N3 (WS)	30	608			586			588			49	40	9	0.82	HS	
N4	20	602			586			587			45	30	15	0.67	HS	
N5	5	593			582			585			43	41	2	0.95	LS	
N6	50	595			588						44	32	12	0.73	HS	
N7	15	585			581						30	22	8	0.73	LS	
N8	40		598			592					32	20	12	0.63	HS	HM
N9	5	587			585						42	38	4	0.90	HS	
N10	15	584			580						42	36	6	0.86	LS	
N11 (WKA)	15	586			581						40	37	3	0.93	LS	
N12	20	594			582						40	30	10	0.75	HS	
N13	10	590			585						45	30	15	0.67	HS	
N14	15	588									45	35	10	0.78	LS	
C1	20			621			580			587	55	13	42	0.24	LM	LC
C2	40		622			580			586		55	22	33	0.40	LM	
C3 (116)	70		626			580			585		55	21	34	0.38	LM	
C4	60		628			583			584		60	21	39	0.35	LM	
C5	85		630			590					65	35	30	0.54	HM	
C6	60		631			585					65	37	28	0.57	HM	
C7	35			627			585				70	19	51	0.27	LM	LC
C8	20			622			585				65	20	45	0.31	LC	
C9	10			615			586				62	10	52	0.16	HC	
C10	35			618			588				55	8	47	0.15	LC	
C11	50		621			594					45	17	28	0.38	HC	HM
C12 (114)	15			620			595				45	4	41	0.09	HC	
C13	50			620			595				45	12	33	0.27	HC	
C14	35			614			583				50	4	46	0.08	LC	
C15	30			608			580				45	1	44	0.02	LC	
C16 (FA)	40			611			582				45	11	34	0.24	HC	
C17	40		605			579			584		55	25	30	0.45	LM	
S1	100		620			590			590		72	42	30	0.58	HM	
S2	75		600			600			600		75	46	29	0.61	HM	
S3	75		650			600			600		90	41	49	0.46	HM	
S4	30		665			597			595		95	36	59	0.38	HM	
S5 (MP)	80		667			592			595		85	40	45	0.47	HM	
S6	30						585			592	90	24	66	0.27	HC	
S7	15						582			582	85	23	62	0.27	LC	
S8	25						582			582	85	28	57	0.33	LC	
S9	15						585			585	90	20	70	0.22	HC	
S10	20						587			587	95	21	69	0.22	HC	
S11	30			620			584			584	80	21	69	0.26	HC	
S12 (CP)	30			605			581			581	80	20	60	0.25	LC	WWM
S13	20			600			585			585	85	5	80	0.06	LC	Feb-98

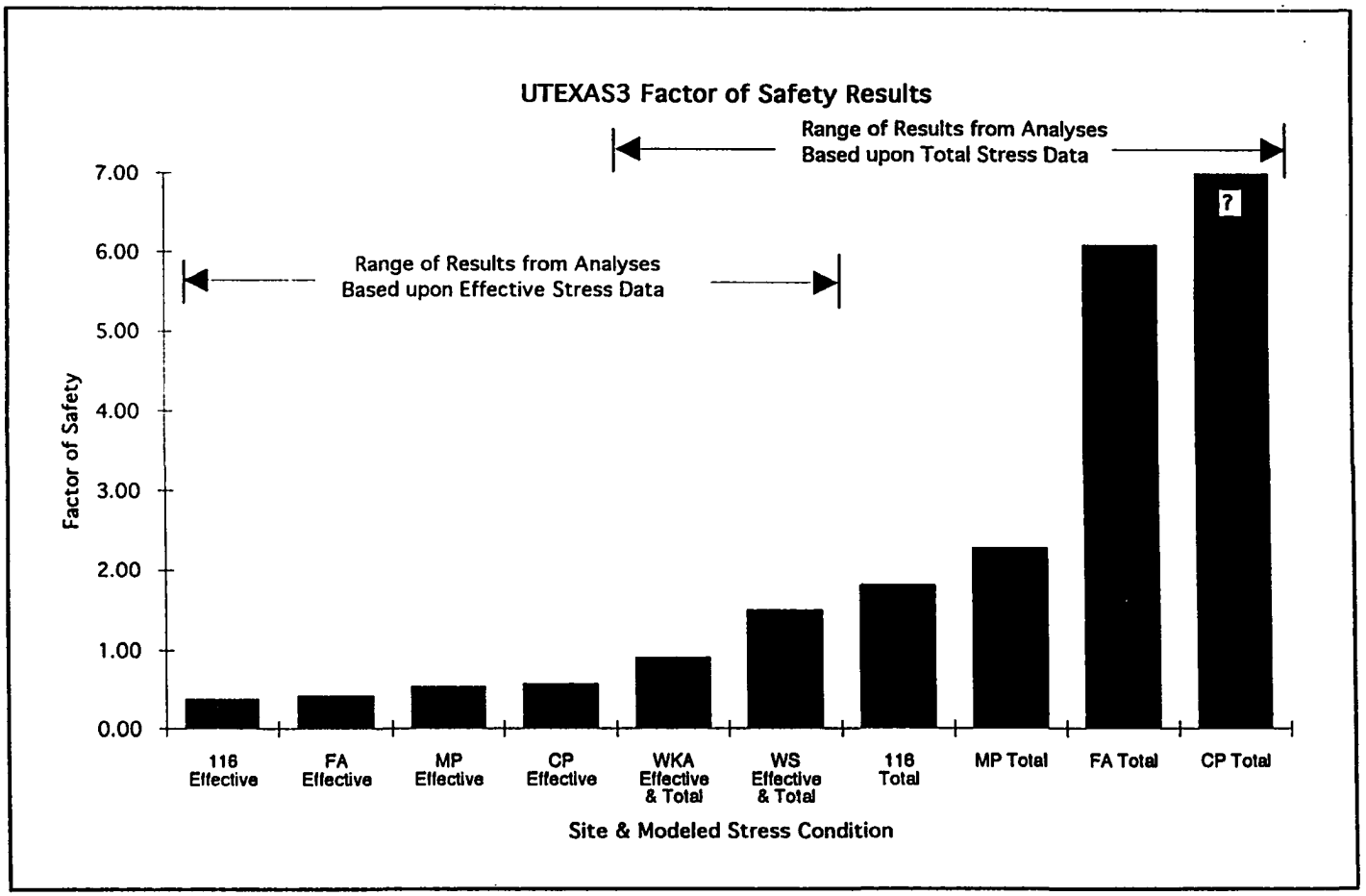

Figure 58. Factors of Safety Calculated at Six Field Sites with UTEXAS3. Results from Analyses Utilizing Total Stress and Effective Stress Data.

was observed from initial hand calculations (FS sand < FS mixed < FS clay), but the magnitudes of the Factors of Safety are larger in the UTEXAS3 analyses. This may be due in large part to the fact that higher shear strength values at shallow depths are produced from non-linear envelopes (Figure 36) than those produced from the linear failure envelopes used for input into the initial hand calculations. These higher shear strengths increase the numerator in the FS equation.

Effective Stress Analysis

It has been suggested (V. Torrey, 1998, personal communication) that what have been described in this study as effective stress (or effective stress-based) Factor of Safety analyses might be more aptly described as long-term stability analyses that incorporate steady state seepage and reflect drained conditions. This is because the term "effectve stress analysis", in a modern context employed by practicing civil engineers, implies that effective stress paths to failure are used in Factor of Safety analysis rather than effective stress Mohr-Coulomb (CU) failure envelopes. However, the UTEXAS3 user's manual (Edris and Wright, 1992) indicates that input parameters required for effective stress analysis in UTEXAS3 are c', ø', and pore pressure data. The UTEXAS3 manual states that c' and ø' should be determined from effective stress (CU or R) envelopes, which were generated for diamicton, clay , and silty/sandy clay in this study. Piezometric data are also available for pore pressure input because of the ongoing groundwater monitoring effort in the field. Therefore, because UTEXAS3 input data requirements for effective stress analysis were met in this study, the terms "effective stress analysis" or "effective stress-based analysis" will continue to be employed in the

remainder of the discussion of Factor of Safety analyses, the suggestions of Torrey (1998, personal communication) notwithstanding.

When effective stress (CU-derived) linear failure envelopes (Figure 51) are substituted for non-linear total stress envelopes in UTEXAS3, the Factors of Safety drop significantly (Figure 58). This is probably because both the linearity of effective stress envelopes and the lack of measured effective cohesion intercepts result in reductions in material shear strength at shallow burial depths. Furthermore, the FS progression is reversed from that calculated under total stress conditions: sand-prone sites now appear most stable, while clay-rich and mixed sand/clay sites appear less stable. The fact that pore pressure neither boosts (under total stress analysis) nor reduces (under effective stress analysis) the apparent Factor of Safety at the well-drained sandy sites (WS and WKA) explains why these two sites are on the weak end of the total stress FS spectrum, yet on the strong end of the effective stress spectrum.

Predicted Failure (UTEXAS3) vs Observed Failure at the Field Sites

Table 6 summarizes the more salient observations from the series of ten UTEXAS3 computer analyses that form the basis of this data set. The sandy sites with the highest Factors of Safety show field conditions consistent with UTEXAS3 predictions: West Side County Park (WS) is predicted to be stable (FS=1.49), with the least stable surface predicted to be sub-parallel to the current bluff face (Figure 59), while Wau-Ken-A is predicted to be slightly unstable (FS=0.91) along a shallow slip surface on the middle bluff face (Figure 60). What little instability has been observed at Wau-Ken-A is mid-bluff and is consistent with UTEXAS3 output.

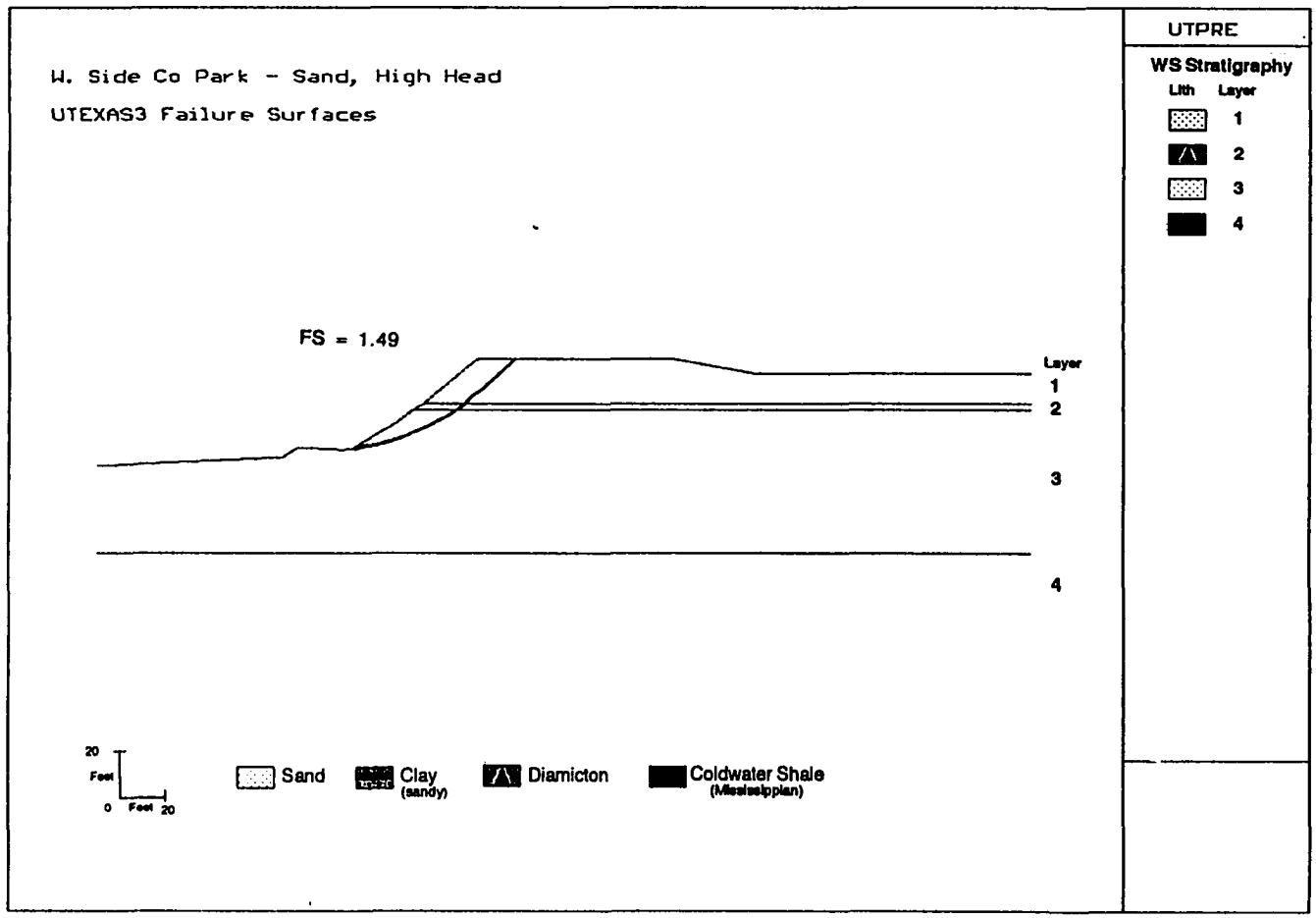

Figure 59. Bluff Profile at West Side County Park Showing Position of Most Conservative Failure Surface (Lowest Factor of Safety) Calculated by UTEXAS3. Total Stress and Effective Stress Conditions Yield Same Result.

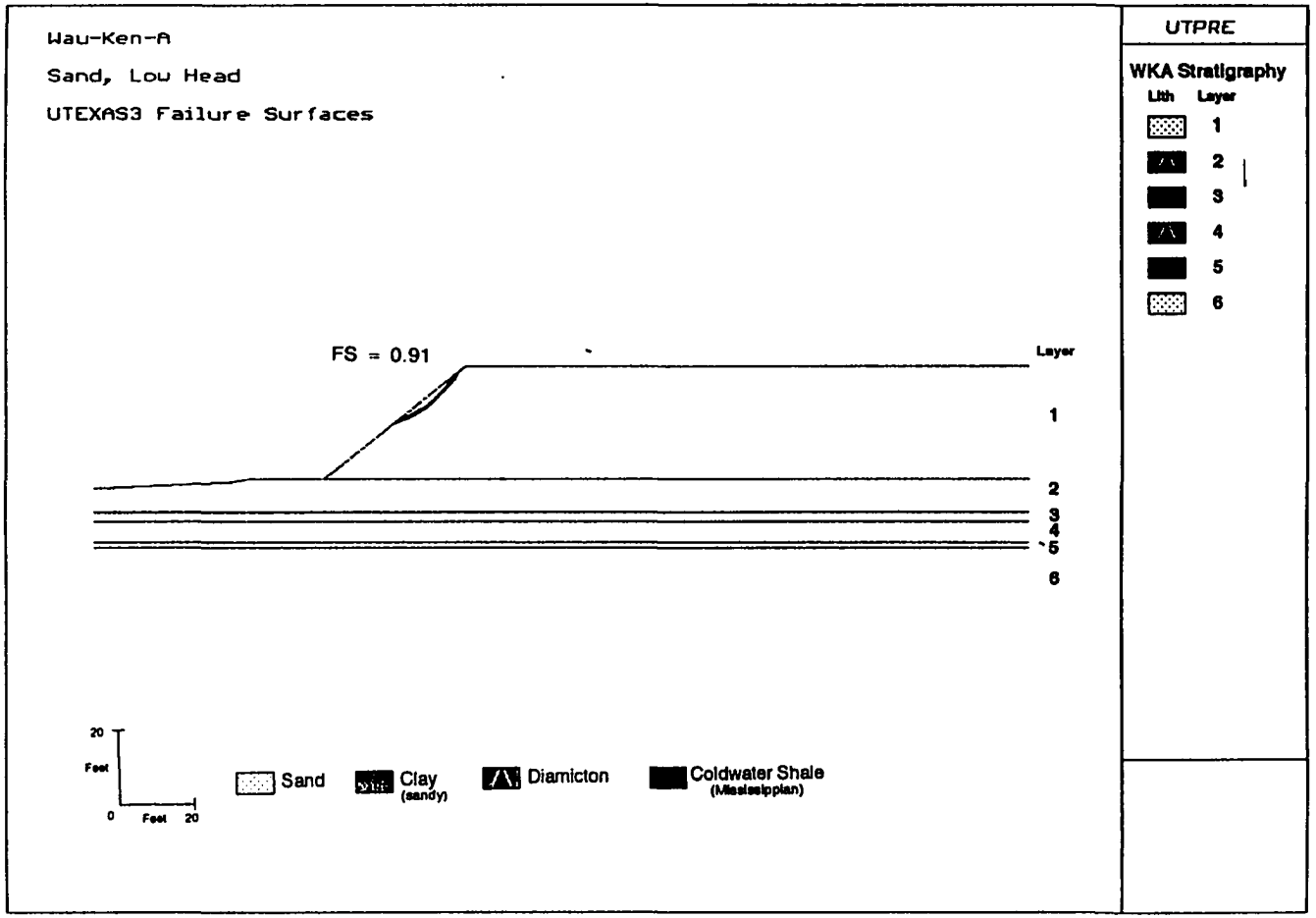

Figure 60. Bluff Profile at Wau-Ken-A Showing Position of Most Conservative Failure Surface (Lowest Factor of Safety) Calculated by UTEXAS3. Total Stress and Effective Stress Conditions Yield Same Result.

116th Avenue is modeled as stable (FS=1.81) under total stress conditions, with a potential failure surface sub-parallel to the current bluff face (Figure 61). This site is predicted to be unstable (FS=0.37) under effective stress conditions along a shallow slip surface located mid-bluff. The predicted slip surface is more or less coincident with the position of maximum recession observed in the field during the course of study.

Fabun Road is modeled as very stable under total stress conditions (FS=6.09), with a potential failure surface that extends inland at a lower angle than that of the current bluff face (Figure 62). Under effective stress conditions, the site is predicted to be unstable (FS=0.43) along a shallow slip surface located mid-bluff. As at 116th Avenue, the predicted slip surface is reasonably coincident with the position of maximum recession observed during the study period.

Miami Park is modeled as stable (FS=2.29) under total stress conditions, with a potential failure surface sub-parallel to the present bluff face (Figure 63). Under effective stress conditions, the site is predicted to be unstable (FS=0.53) along a shallow slip circle near the bluff toe. The position of this predicted slip surface is very close to one mapped by Chase et al. (1997) based upon detailed monitoring.

Consumers Power is extremely stable under total stress conditions; stability was such that UTEXAS3 was not able to generate a potential failure surface. Under effective stress conditions, the site is predicted to be unstable (FS=0.57; Figure 64) along a shallow slip circle on the lower bluff face. This position is somewhat coincident with topple failures observed in the field, but these failures appear to be fracture-controlled, not slip circle-controlled.

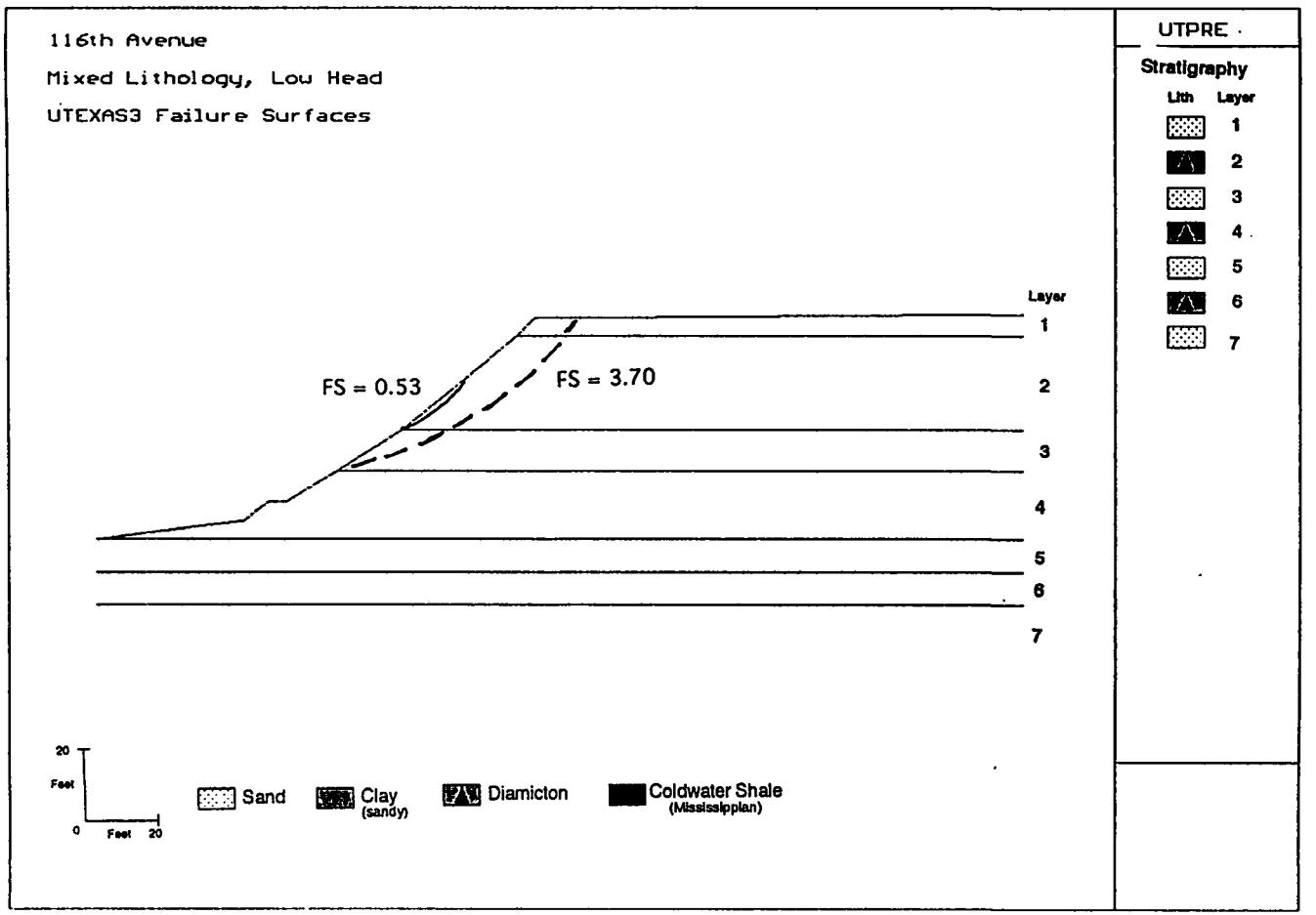

Figure 61. Bluff Profile at 116th Avenue Showing Positions of Most Conservative Failure Surfaces (Lowest Factors of Safety) Calculated by UTEXAS3 for Total Stress and Effective Stress Conditions.

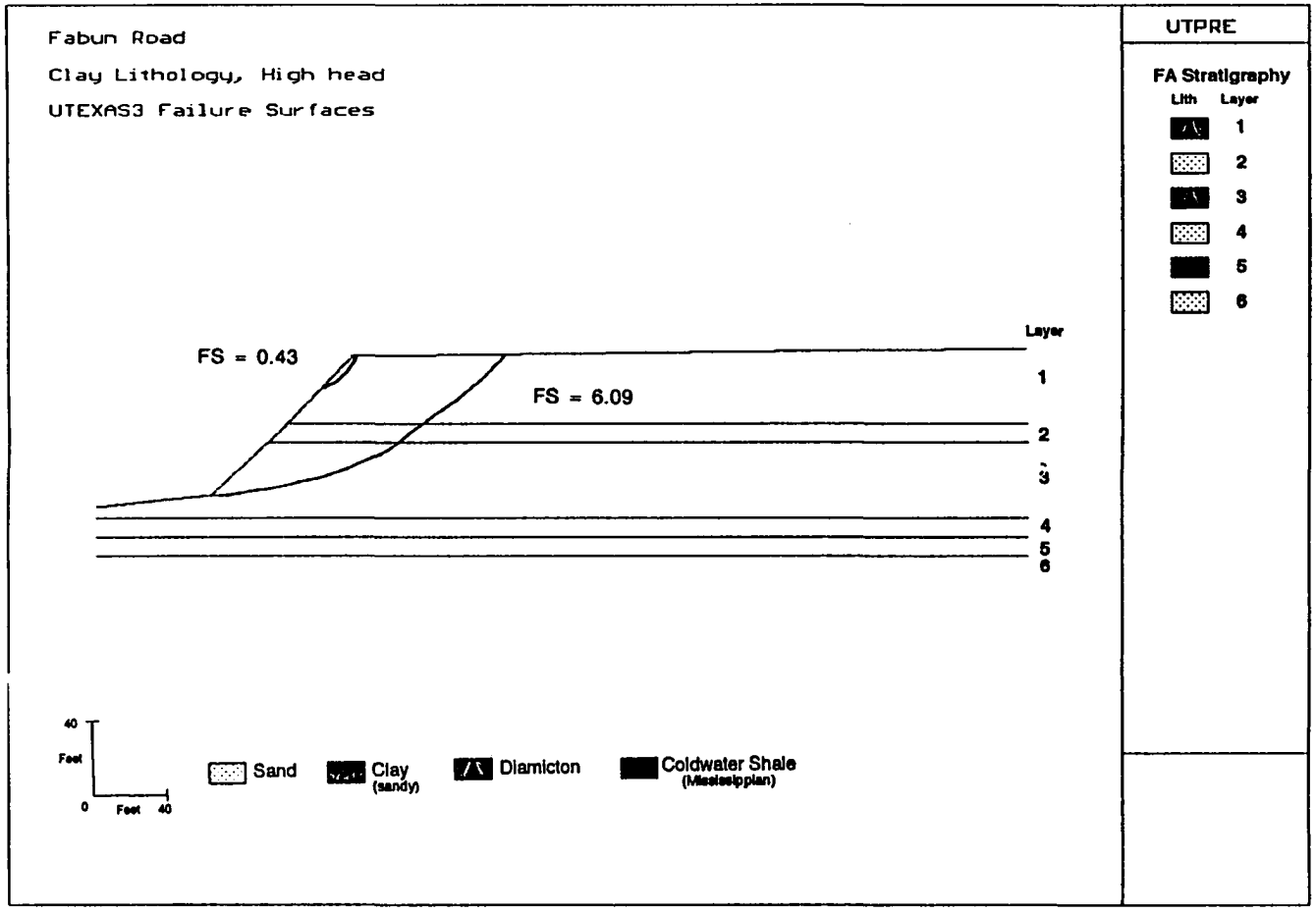

Figure 62. Bluff Profile at Fabun Road Showing Positions of Most Conservative Failure Surfaces (Lowest Factors of Safety) Calculated by UTEXAS3 for Total Stress and Effective Stress Conditions.

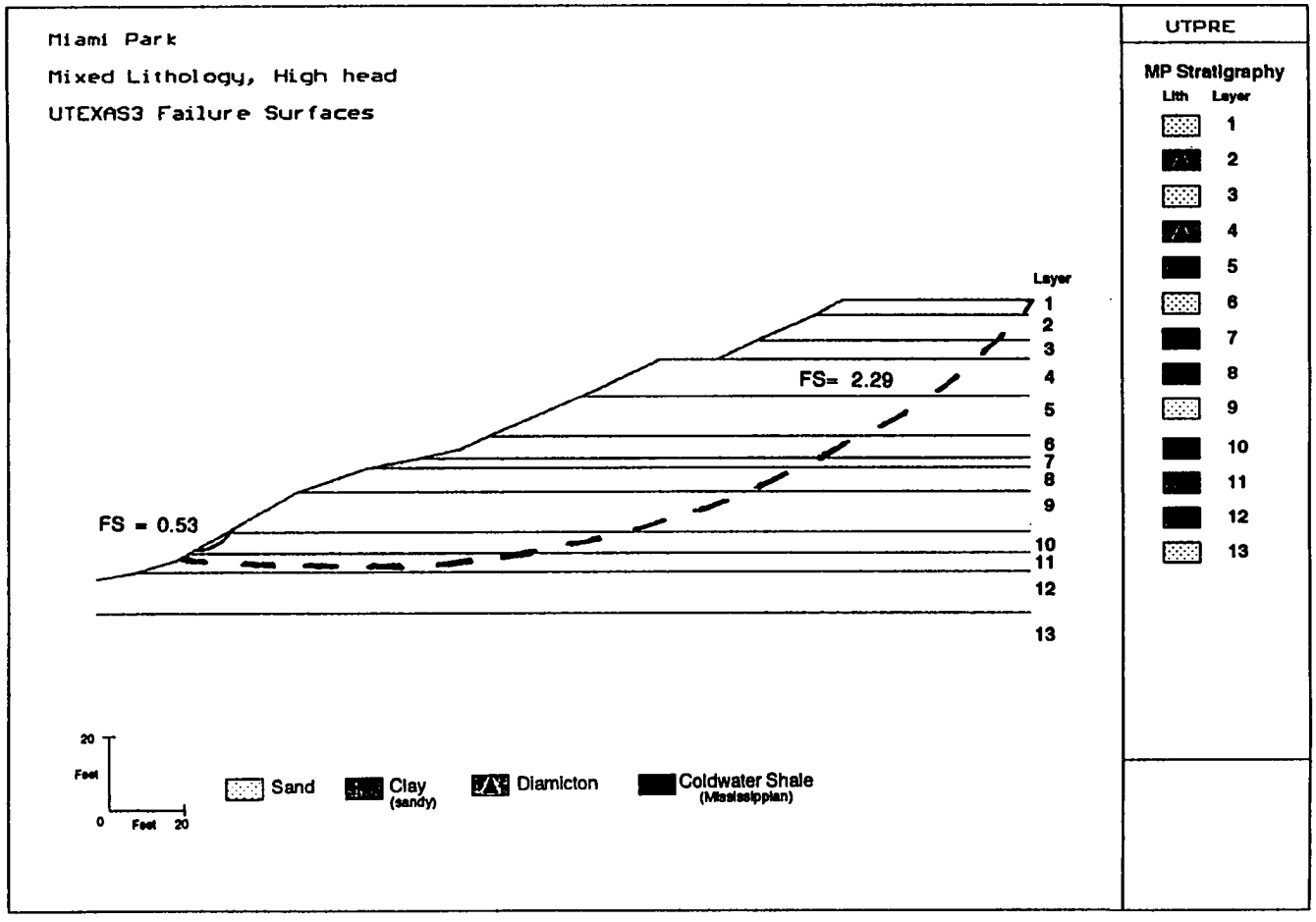

Figure 63. Bluff Profile at Miami Park Showing Positions of Most Conservative Failure Surfaces (Lowest Factors of Safety) Calculated by UTEXAS3 for Total Stress and Effective Stress Conditions.

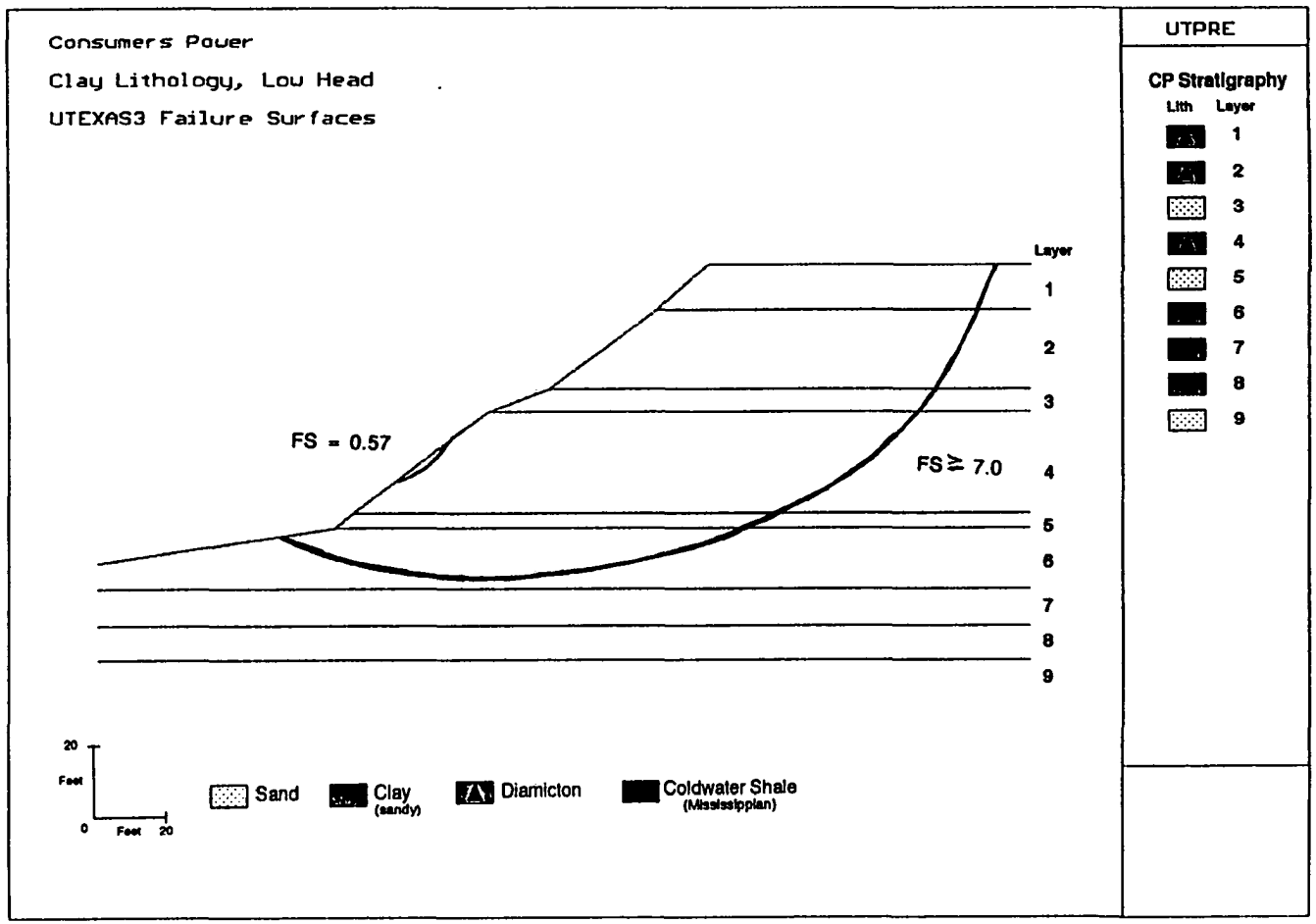

Figure 64. Bluff Profile at Consumers Power Showing Positions of Most Conservative Failure Surfaces (Lowest Factors of Safety) Calculated by UTEXAS3 for Total Stress and Effective Stress Conditions.

Comparison of Historical Recession and Bluff Characterization Data

There is a positive correlation between bluff lithology and 1938 to 1996 recession (Figure 65) in terms of percent sand. Cells characterized as mixed lithology (66% > sand > 33%) exhibited higher recession than those of either clay or sand. There is also a tendency toward slightly higher recession in clay lithology than sand lithology.

Figure 66 shows relationships between bluff lithology, intermediate aquifer hydraulic head, and 1938 to 1996 recession. Sand cells with low and high head (LS and HS, respectively) as well as clay with low head (LC) showed the least amount of recession. As a group, clay cells with high head (HC) tended to show slightly more recession than the LS, HS, or LC cells. Mixed cells with low head (LM) tended to exhibit slightly higher amounts of recession than HC cells, and cells characterized as mixed with high head (HM) exhibited the highest amounts of 1938 to 1996 recession in the study area.

Bluff Characterization, Limit Equilibrium Analysis, and Bluff Recession - Discussion and Interpretation

Integration of lithologic/hydrologic data, geotechnical data, field monitoring data, historical recession data, and results of limit equilibrium analysis form a coherent, internally consistent basis from which to analyze patterns and draw conclusions concerning Lake Michigan shoreline recession. Effective stress-based Factor of Safety analysis, lithologic bluff characterization in terms of percent sand, historical recession data, and field monitoring data all suggest that sandy sections (sand > 66%) of the Lake Michigan shore (e.g., West Side County Park and Wau-Ken-A) are less prone to recession than those segments with greater clay content. These sections of shoreline provide good drainage of groundwater and exhibit bluff

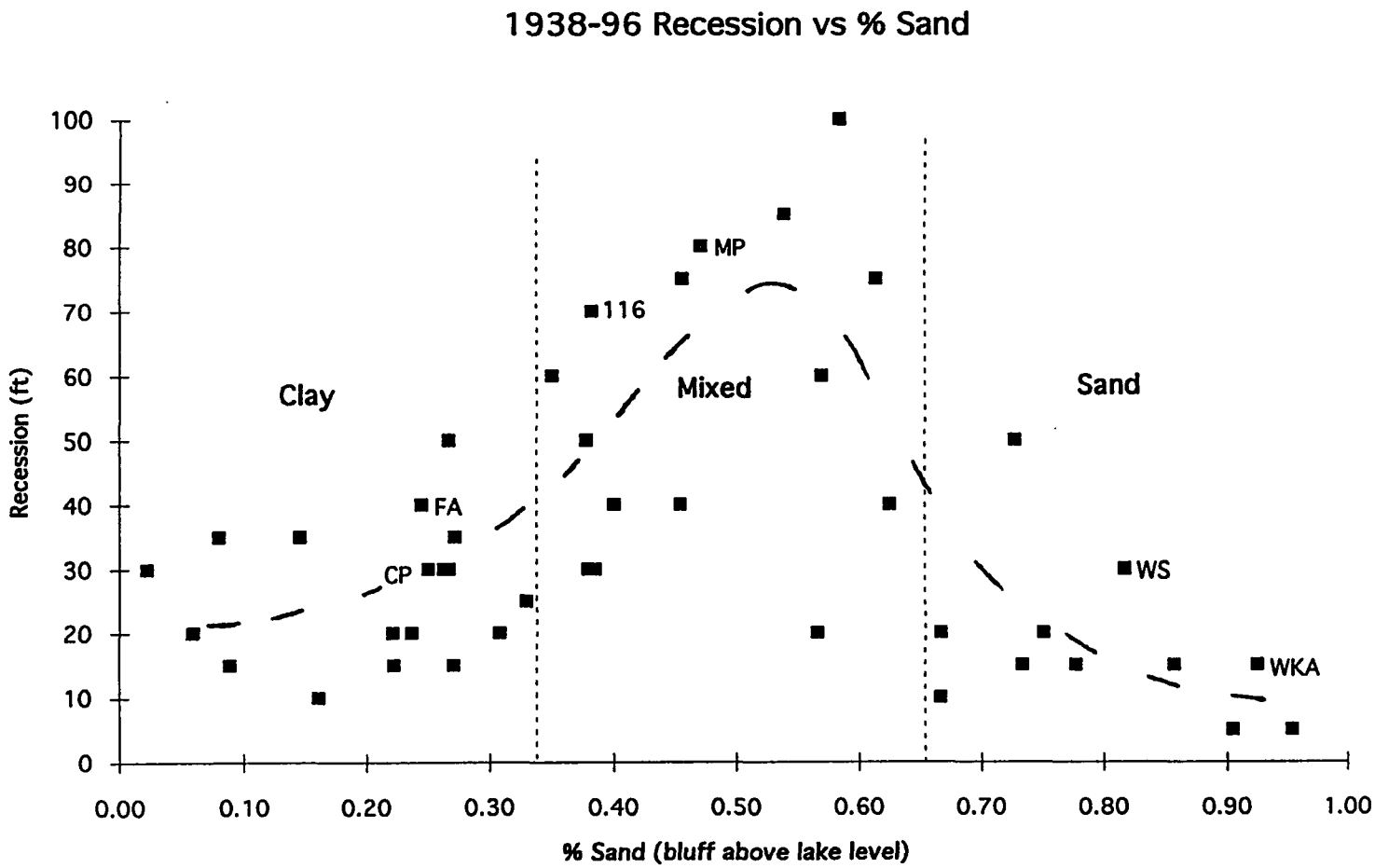

Figure 65. Relationship Between Bluff Lithology (by Percent Sand) and Measured 1938-1996 Bluff Recession in Historical Recession Analysis Areas.

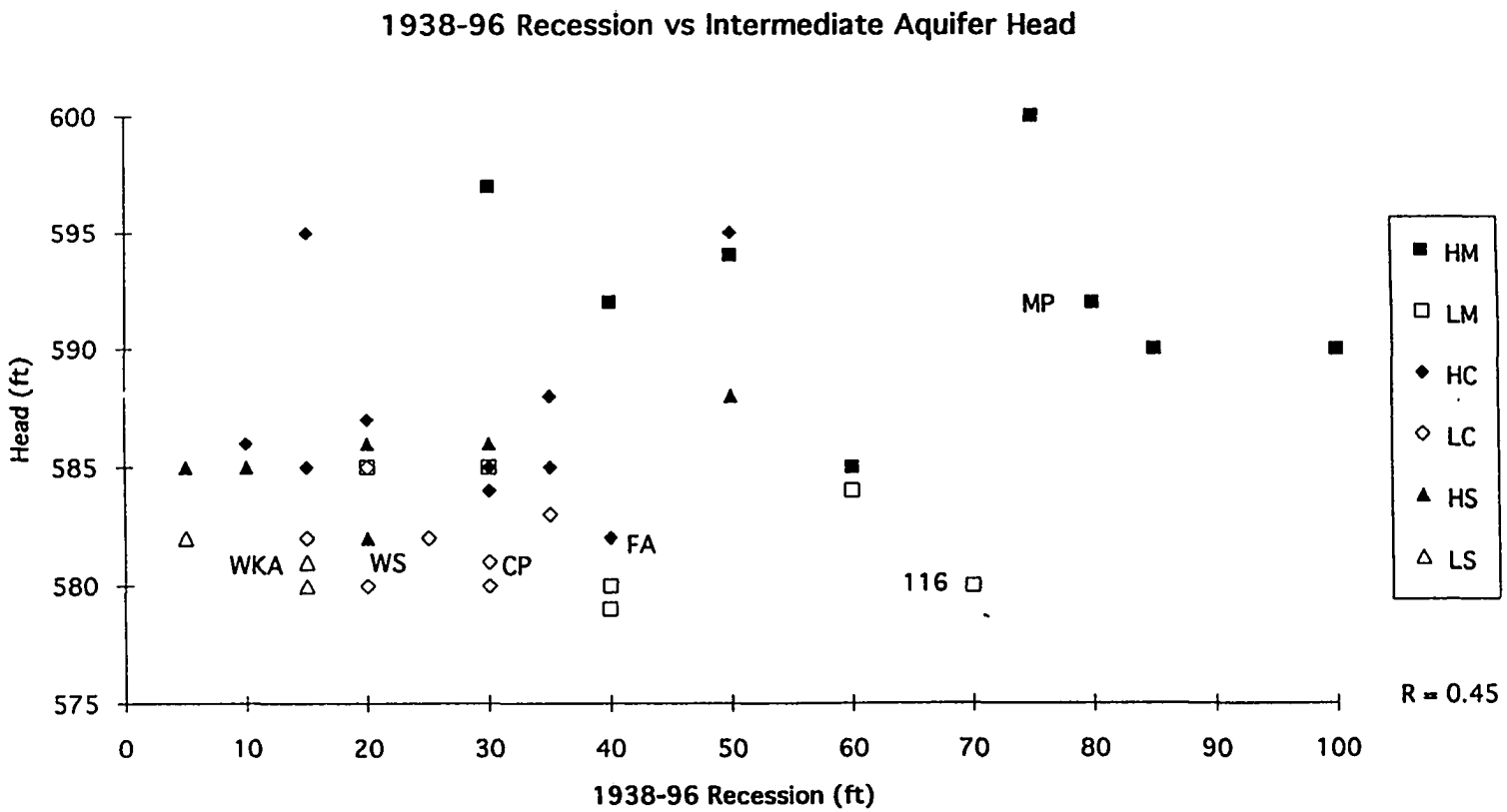

Figure 66. Relationship Between Bluff Hydrology (by Intermediate Aquifer Head) and Measured 1938-1996 Bluff Recession in Historical Recession Analysis Areas.

profiles that yield calculated Factors of Safety that are higher than either predominantly clay or mixed lithology bluffs. The fact that these sections are well-drained means that total stress equals effective stress, and so either type of analysis yields the same result (Figure 58).

Clay-rich bluffs (sand < 33%) appear to exhibit slightly more recession historically than sandy sections. Clay-rich segments have been found to exhibit both high groundwater head (Fabun Road) and low groundwater head (Consumers Power). Both these sites exhibit low Factors of Safety on shallow slip circles computed with effective stress-based data, but the in situ stress conditions at drier sites such as Consumers Power may be better represented by total stress parameters for overconsolidated diamicton. Edil and Vallejo (1977) found that overconsolidated Lake Michigan bluffs they studied in Wisconsin were better modeled by effective stress analysis, because groundwater seepage over the long term caused pore pressure in diamicton to become positive and thus act to destabilize the bluff. This is entirely plausible at a site such as Fabun Road, where a significant groundwater head can be documented. However, for a relatively dry bluff, such as that at Consumers Power, it is equally plausible that groundwater head is not acting to destabilize the bluff with positive pore pressure, and that strong diamicton is present in situ. In this case, total stress-based FS analysis may be a more valid modeling approach than effective stress-based FS analysis.

Mixed sand/clay bluffs (33% < sand < 66%) exhibit the highest amounts of historical recession in the study area. They characteristically have groundwater head that ranges from moderately low (116th Avenue) to very high (Miami Park). Both 116th Avenue and Miami Park exhibit low factors of safety on shallow slip circles computed with effective stress data. At 116th Avenue, the modeled mid-bluff failure surface is reasonably coincident with the portion of the bluff that has

exhibited the most recession during the study period. At Miami Park, there is coincidence between the modeled failure surface at the bluff toe and one identified by Chase et al. (1997) through detailed monitoring. Through either a "search" mode or by single surface analysis, UTEXAS3 calculated Factors of Safety less than one for this surface, which has exhibited slippage since the early stages of the monitoring period. In mixed sand/clay lithologies with some evidence of groundwater head, it appears that effective stress-based FS analysis more adequately reflects the historical record than does total stress-based FS analysis.

Idealized geometric relationships are presented in Figure 67 that are consistent with bluff lithologic/hydrologic characterization, field monitoring, Factor of Safety analysis, and the historical recession record. In the case of essentially all sand bluffs Figure 67a), it is suggested that groundwater moves vertically downward inland of the bluff face, so there is little destabilizing hydraulic head gradient at the face of the bluff, save for the occasional perched aquifer. In the case of primarily clay bluffs (Figure 67b), it is suggested that groundwater is for the most part diverted laterally in a shore-parallel, north-south direction inland of the bluff face. Whatever groundwater reaches the bluff face may destabilize it, especially if composed of overconsolidated diamicton that will weaken in the presence of positive pore pressure.

Mixed sand/clay bluffs (Figure 67c) present a set of conditions that could result in greater instability due to the presence of groundwater than in either sand-dominated or clay-dominated bluffs. Sands with high hydraulic conductivity allow water to move to the bluff face, but the presence of interbedded clay has been observed to cause multiple zones of perching in this lithotype. In addition to the sapping of sand, perched water can act to destabilize the bluff through the addition of weight on the bluff face, which can act to increase the driving force to failure.

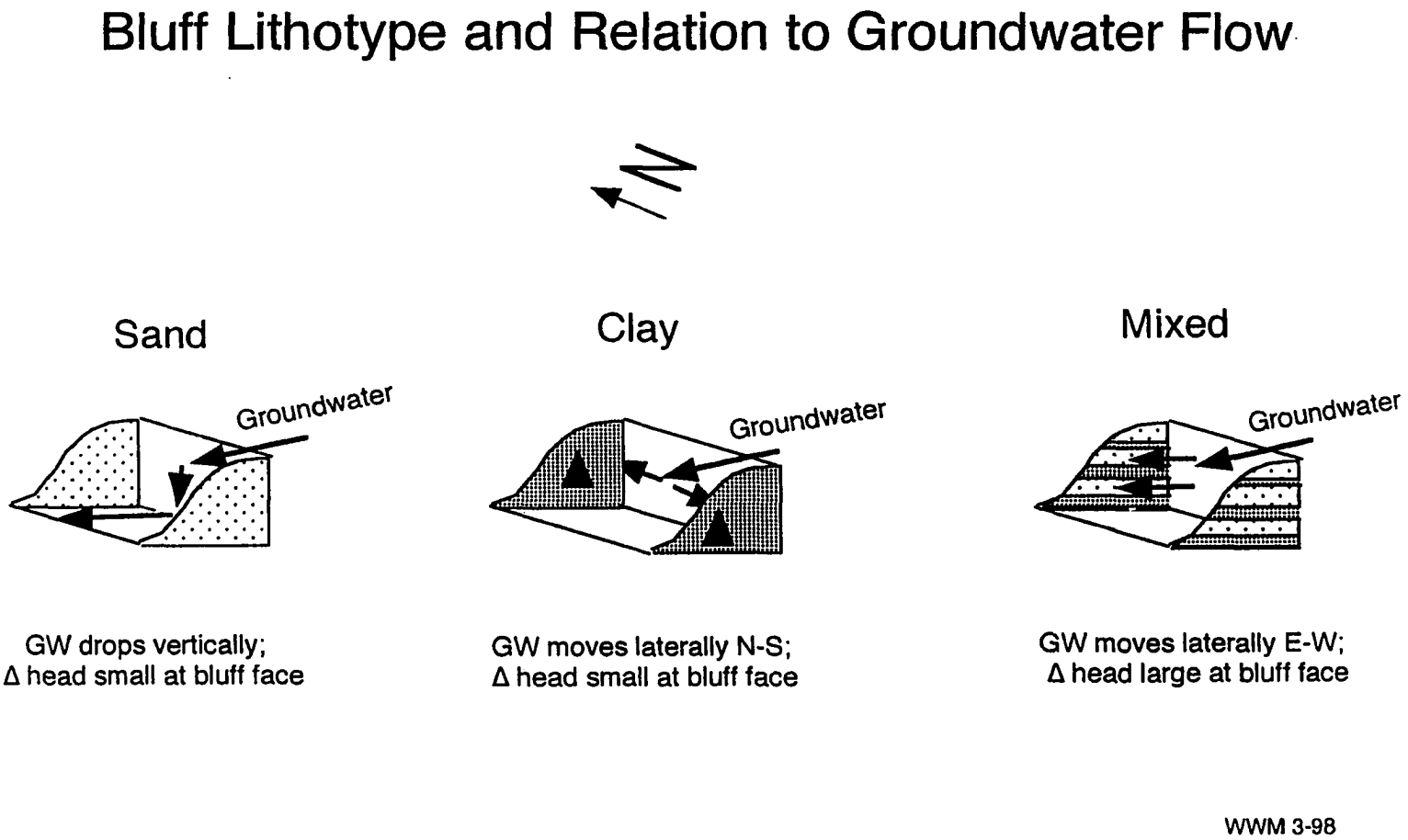

Figure 67. Conceptual Lithologic/Hydrologic Models for Three Bluff Types in the Study Area.

Positive pore pressure, which has been observed in the field just north of MiamiPark and has been documented in Miami Park undrained clay specimens, can cause a reduction in effective stress that reduces the resisting force to failure. These factors could create very unstable conditions and a recession-prone bluff.

CHAPTER VI

CONCLUSIONS

Analysis of data and work products generated as part of this study allow a number of conclusions to be drawn in several areas of study.

GIS-Based Bluff Characterization

Field mapping coupled with subsurface water well control provides data of sufficient quality and quantity to adequately characterize bluff lithology and hydrology in the study area. Bluff characterization maps generated using a GIS-based cell format were field-tested at six sites. At all six sites, subsurface sampling verified the predrill lithologic characterizations (sand, clay or mixed sand/clay). At four sites, groundwater monitoring verified, either fully or partially, predrill hydrologic characterization of head as either high or low. At two sandy sites, predrill head characterizations were reversed based upon monitoring results.

Lithologic and Geotechnical Controls on Mechanical Behavior of Bluff Materials

Comparison of Atterberg limits and index properties with each other and with undrained shear strength yields important insight concerning mechanical behavior of bluff materials. Important factors controlling shear strength include sand and gravel content, void ratio, water content, and dry density. Silty, pebbly, grey diamicton exhibits high undrained shear strength, clayey brown diamicton and silty laminated clay exhibit intermediate undrained shear strength, and brown laminated clay exhibits low undrained shear strength.

Consolidation state and pore pressure also combine to control shear strength under undrained shear. Normally consolidated, laminated clay develops destabilizing positive pore pressure under conditions of undrained shear, while negative pore pressure can actually serve to strengthen overconsolidated diamicton under these conditions. Triaxial testing coupled with pore pressure measurements allow for determination of linear, effective stress envelopes for both clay and diamicton *lithotypes. Laminated clay effective stress envelopes exhibit* $\phi = 20^{o}$, while diamicton effective stress envelopes exhibit $\phi = 28\text{-}29^{o}$. Both sets of envelopes exhibit zero cohesion intercepts.

Factor of Safety Analyses

Results of both total stress-based and effective stress-based Factor of Safety analysis - the latter representative of long-term, drained stability and steady state seepage (Torrey, 1998, personal communication) - provide insight as to conditions that may exist in the subsurface at the six field sites. Sandy, non-cohesive sites (West Side County Park and Wau-Ken-A) exhibit drained conditions, thus total stress equals effective stress in terms of input to Factor of Safety analysis. The sandy sites appear to be either more or less prone to recession than the other four sites, which are cohesive in nature, depending on whether total stress data or effective stress data are input into Factor of Safety analyses at these sites.

Factors of Safety at cohesive sites composed of mixed sand/clay bluffs (116th Avenue and Miami Park) and predominantly clay bluffs (Fabun Road and Consumers Power) are calculated to be higher than Factors of Safety of sandy bluffs when cohesive material property data is taken from non-linear, total stress Mohr failure envelopes. However, the calculated Factors of Safety of cohesive bluffs are lower

than those of sandy bluffs when linear, effective stress envelopes and field-derived piezometric data are the source of cohesive material property input data.

Historical Bluff Recession and Relation to Bluff Lithology/Hydrology

Comparison of historical bluff recession patterns with bluff characterization maps yields important insight as to possible factors in recession. There is good historical evidence to suggest that lithology is an important control in recession. Mixed sand/clay bluffs have receded considerably more than either all-clay or all-sand bluffs over the long term (1938-1996). Furthermore, this is the only lithotype that showed measurable recession over the short term (1989 to 1996).

The influence of hydraulic head on bluff recession is not as clear as the influence of lithology, especially in all-sand or all-clay bluffs. However, there appears to be a correlation, at least in mixed sand/clay bluffs, between higher rates of long-term recession and higher hydraulic head mapped at the bluff face.

Comparison of Historical Bluff Recession, Factor of Safety Analyses, and Bluff Characterization

Comparison of results from different avenues of study provides confirmation of the potential value of the proposed bluff characterization methodology in the prediction of shoreline recession. Factor of Safety analysis and historical recession analysis both suggest that mixed sand/clay bluffs are particularly prone to recession, especially in conjunction with high hydraulic head. Factor of Safety analysis that incorporates effective stress data (c', ø') and piezometric data may be most appropriate in this case, based on results of both historical analysis and recent field monitoring.

Clay bluffs with high hydraulic head also appear to be most appropriately modeled with effective stress-based Factor of Safety analysis. Researchers studying overconsolidated diamicton in both Canada and Wisconsin suggest that groundwater infiltration over time can cause a reduction in in situ effective stress (and therefore a reduction of the Factor of Safety) in this lithotype. Clay bluffs with low head may recede at lower rates than clay with high head. This appears to be the case at the present time at the dry clay site (Consumers Power), where the primary failure mechanism is fracture-controlled topple. In relatively dry diamicton, total stress-based FS analysis that utilizes non-linear Mohr total stress envelopes, and produces significantly higher Factors of Safety than effective stress-based FS analysis, may be most appropriate for predicting recession.

Sand bluffs over the long term appear to be slightly less prone to recession than clay bluffs, and significantly less recession-prone than mixed sand/clay bluffs. When considering the range of results from the total stress-based FS analyses performed on various lithotypes in this study, the Factors of Safety of sandy bluffs are on the low end of the spectrum, thereby suggesting they may be more prone to recession than cohesive bluffs. This conclusion is consistent with what can be surmised from the older historical literature in the Great Lakes. However, when considering the range of results from effective stress-based FS analyses performed in this study, the Factors of Safety of sandy bluffs are on the high end of the spectrum, thereby suggesting that they are less recession-prone than cohesive bluffs. This finding is consistent with more recent literature in the Great Lakes.

Appendix A

Gamma Ray and Sample Logs From Deepest Piezometer at Each Field Site

FABUN ROAD

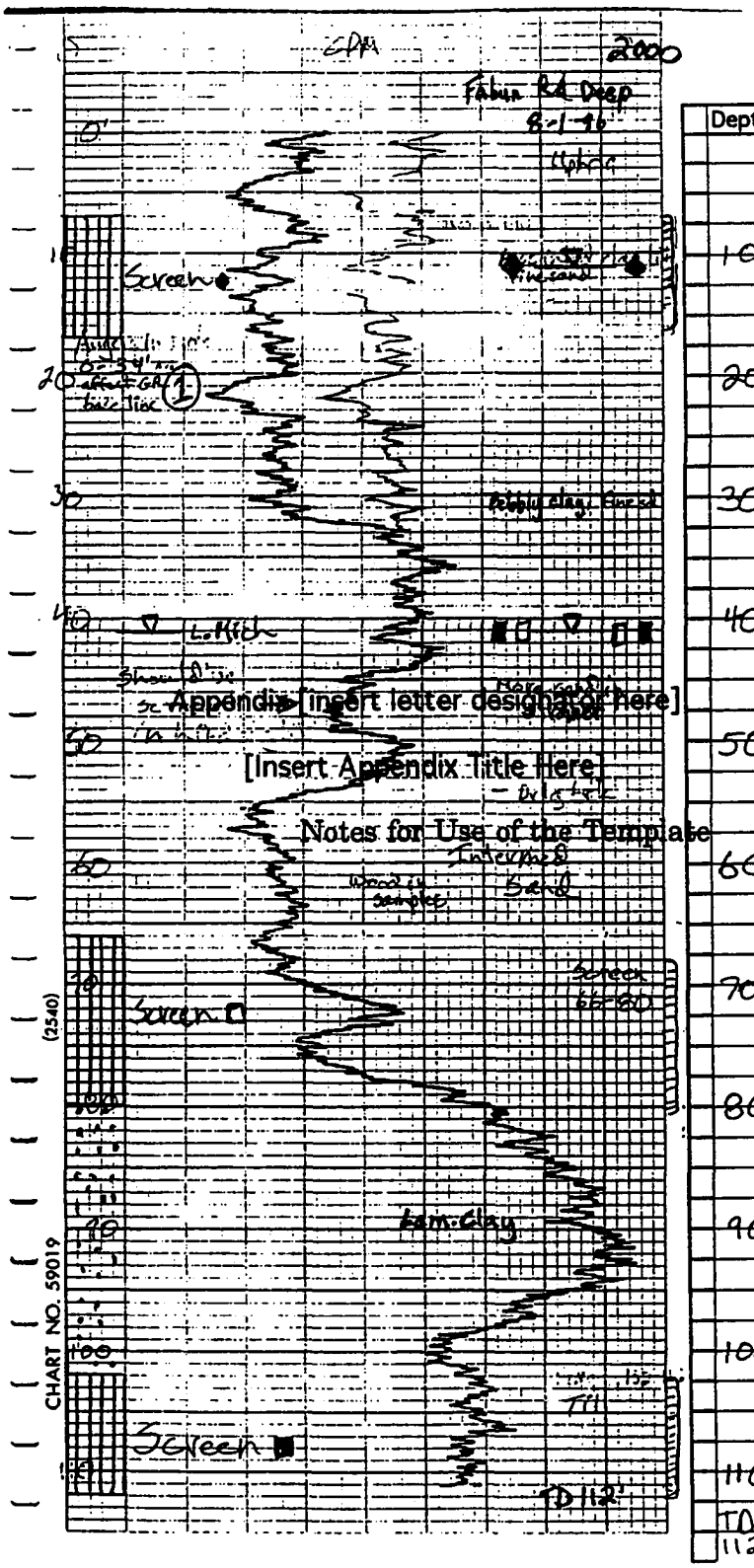

FA-1

Depth	Lith	Description
		Diamicton; grey, silty
10		
		Diamicton; A/A
20		Diamicton; very sandy
		Diamicton; grey, silty, pebbly
30		
40		Diamicton A/A
		Sand; brown, med-grained
50		Clay; brown, fine-grained
		Sand; brown, fine-to medium-grained
60		Wood fragments; red-brown
70		Clay; brown, laminated(?)
		Sand; brown, fine-med grained
80		Clay; brown, laminated, very fine grained
90		Clay; brown A/A
100		Diamicton; grey, sandy, pebbly, hard
110		
TD 112'		

CONSUMERS POWER

CP - 2

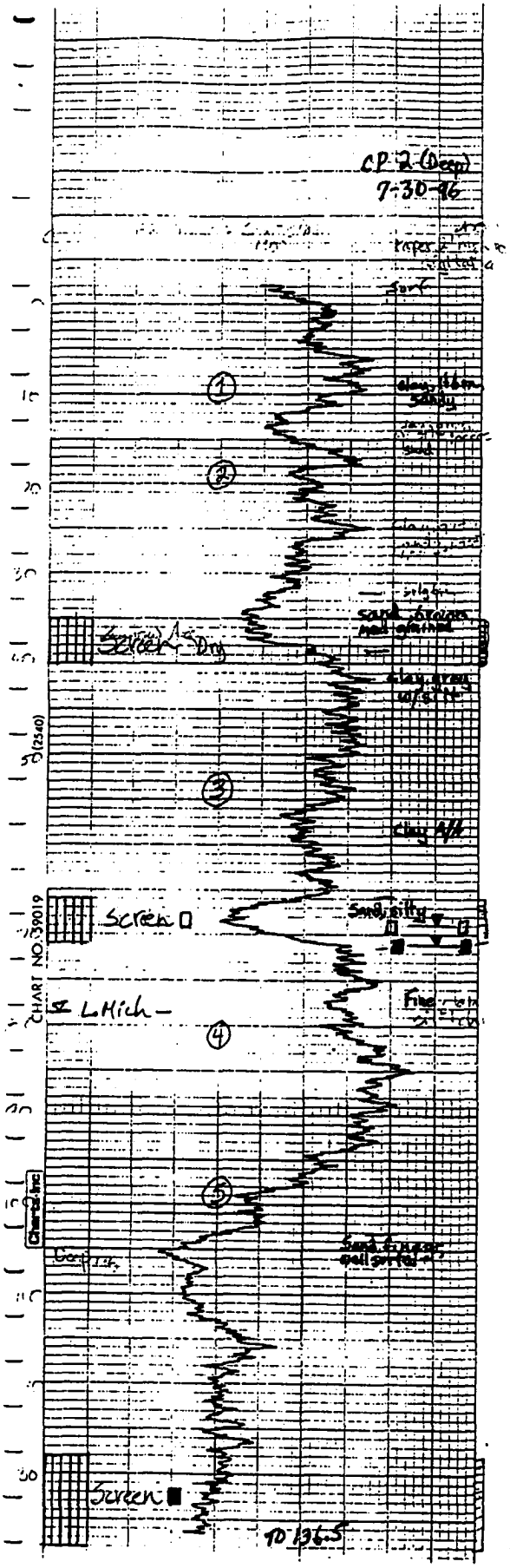

Depth	Lith	Description
		Diamicton; brown, sandy
10		
		Diamicton; grey, silty, Hard
20		
		Diamicton A/A
30		
		Sand; brown, med grained
40		Diamicton; grey, silty, pebbly
50		
		Diamicton A/A
60		
		Sand; brown, med grained
70		Clay; brown, lam, interbedded w/silt; buff, sand; buff
80		
		Clay; brown, laminated, very fine grained
90		
		Clay; brown, interbedded with silt; buff
100		
		Sand; buff-brown, fine-grained occasional fragments of wood, red-brown
110		
120		
130		

TD 138

MIAMI PARK

MP - 1

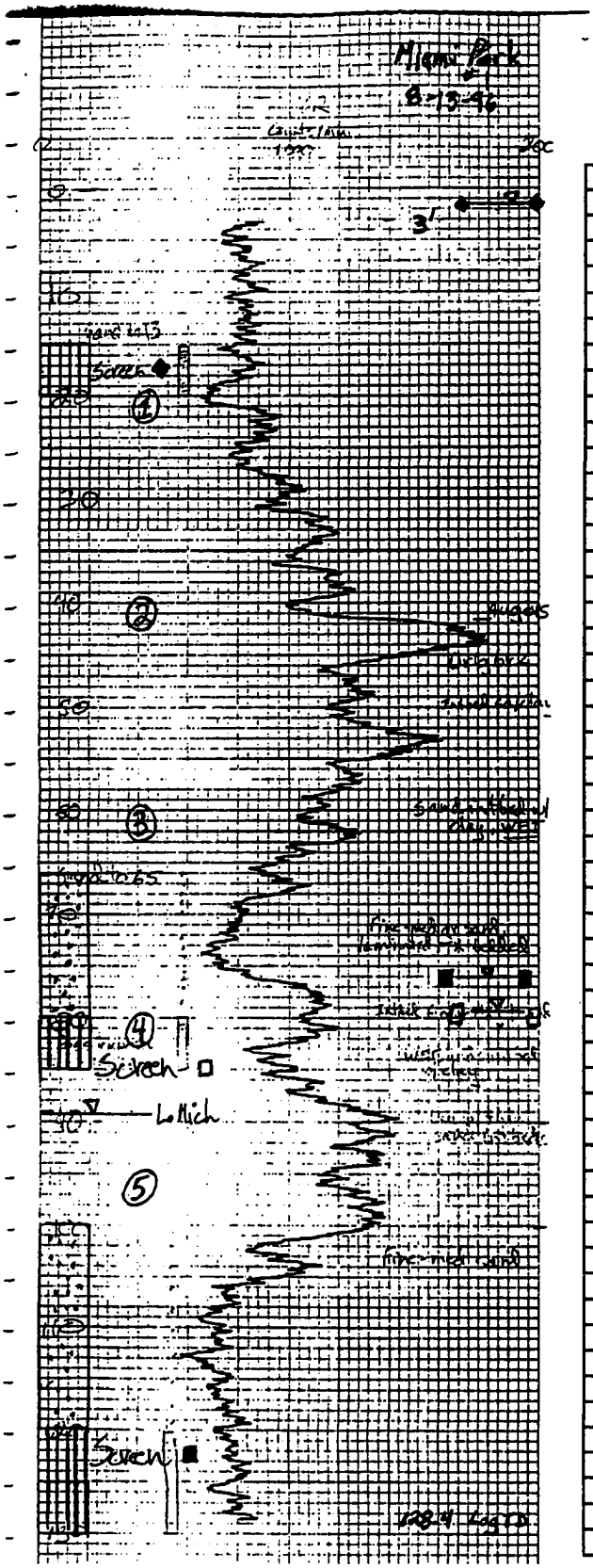

Depth	Lith	Description
		Top soil, surface sand
		Diamicton; grey, silty
10		
		Sand; brown, medium grained
20		
		Diamicton; grey, silty
30		
		Clay; brown, laminated, fine-grained
40		Clay; grey-green, very fine-grained; interbed w/ Sand
		Sand; buff-brown, fine-med grained
50		
		Clay; brown, lam
		Sand; buff, interbed w/ clay, brown
60		
		Sand; buff, fine-med gr, cross-bedded
70		
		Clay; brown, v fine gr, laminated
80		
		Sand; brown, fine-grained interbed w/ clay, fine-grained
90		
		Clay; brown, laminated, interbedded w/ sand; fine grained
100		
		Sand; buff-brown, fine-medium grained
110		
120		Sand; buff, fine-gr A/A
130		

TD 136

116TH AVENUE

116-1

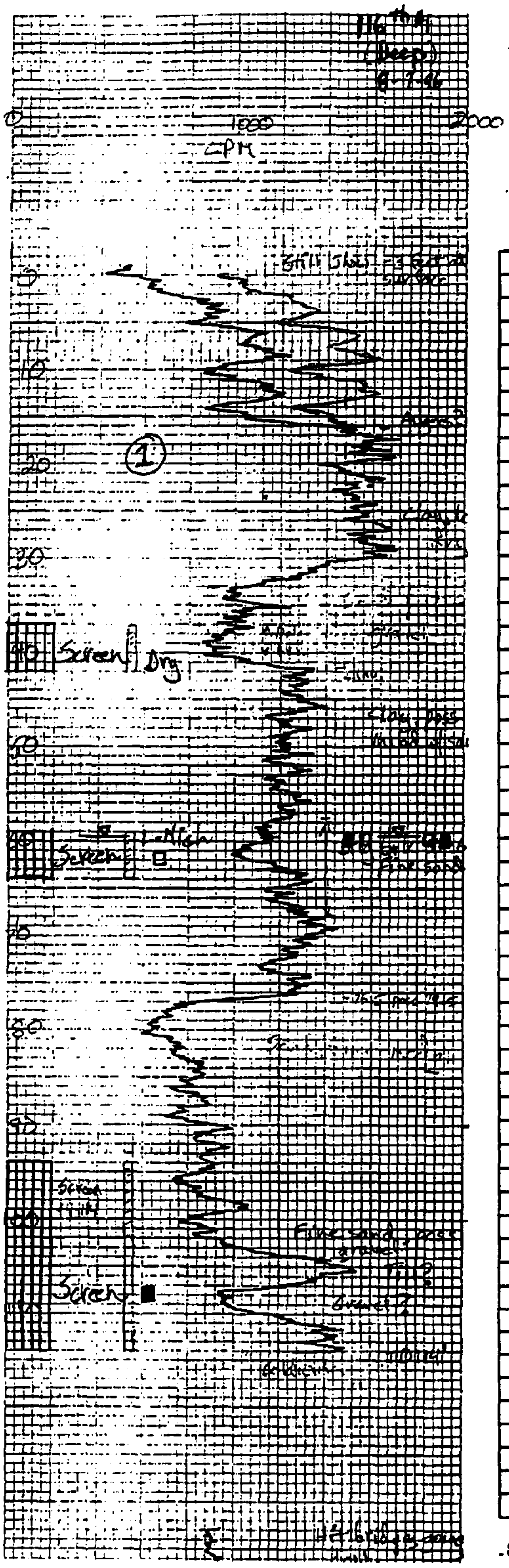

Depth	Lith	Description
		Sand; orange, clayey
10		Diamicton; brown, pebbly, clasts of laminated clay
20		
		Diamicton; A/A
30		
		Sand; brown, med-grained
40		
		Diamicton; grey, silty
50		
60		Sand; brown, med grained
70		Diamicton (?); interbedded w/ sand; fine grained
80		Sand; brown, med grained
90		Sand A/A
100		
		Diamicton; grey, pebbly
110		
TD 114'	?	Shale(?)

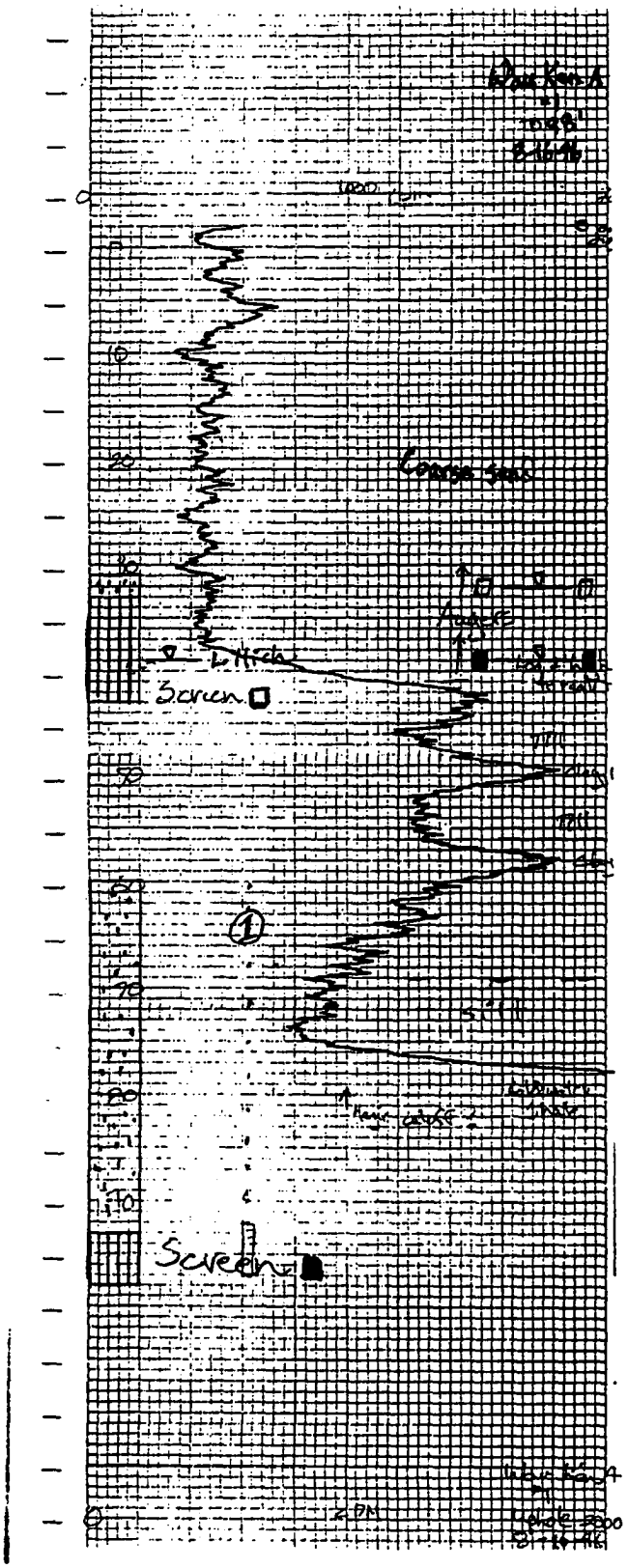

WAU - KEN - A

WKA - 1

Depth	Lith	Description
		Sand; orange, dry
10		Sand; buff - lt. grey, moist, abundant heavy minerals
20		
30		Sand; buff - lt. brown, coarse - grained
		Sand saturated @ 37'
40		Gravel; abund. pebbles
		Diamicton; purple-grey, sandy, very hard
50		~~Clay(?); brown, laminated~~
		Diamicton; grey, hard
60		Clay(?); brown, laminated
		Silt; lt grey, interbedded w/ clay; brown, laminated
70		Silt; lt grey, interbedded w/ some clay; brown, laminated
80		Shale; black, foliated, pebbly
90		Shale; black, fissile
TD98		

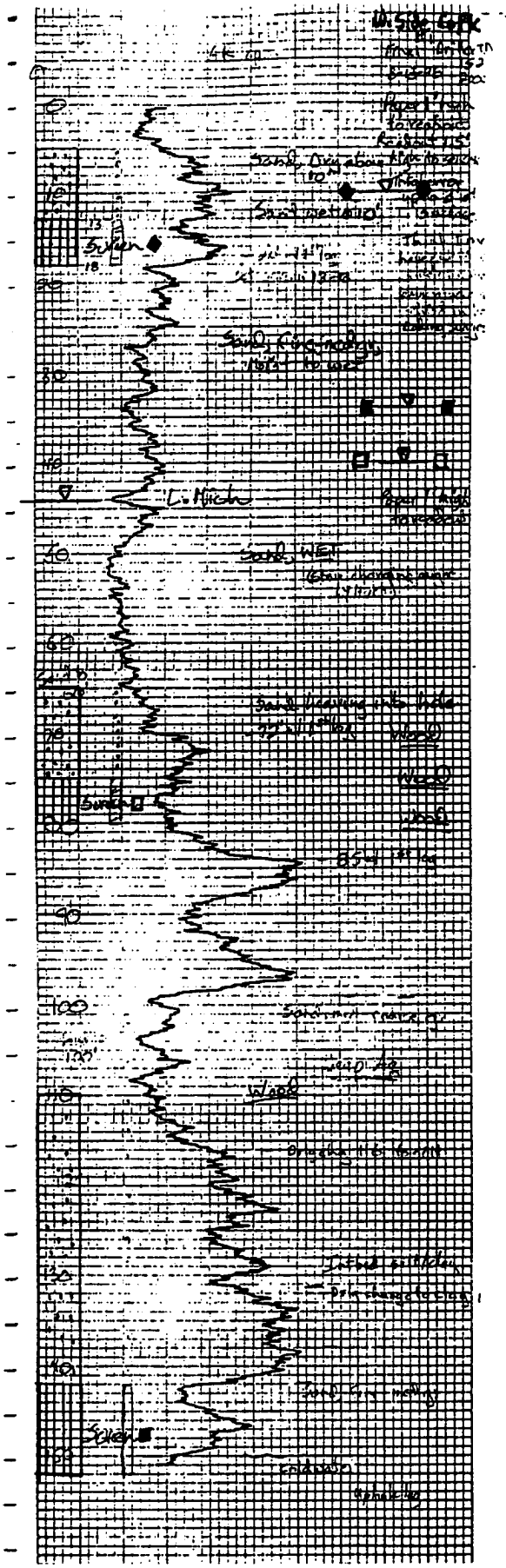

WEST SIDE COUNTY PARK

190

Depth	Lith	Description
		Sand; brown
10		
		Diamicton; grey, silty
20		Sand; buff, fine to medium grained
30		
40		Sand A/A
50		Sand; A/A, very wet
60		
70		Sand; brown, containing wood fragments, interbed w/ clay; pebbly
80		Sand; clr - buff, fine-med grained, well-rounded, well-sorted
		Clay(?); fine grained
90		Diamicton(?); hard drilling; rig bouncing; poss. gravel
		Clay(?); fine grained
100		Sand; buff, med-coarse grained
110		Gravel (?); pebbly, interbedded w/ sand; containing wood fragments
		Silt; buff, sandy
120		Silt; poss interbedded w/ clay
130		Sand; silty, clayey
		Clay; fine-grained, laminated
140		
		Sand; buff, med-grained, well-rounded, well-sorted
150		Diamicton (?), pebbly, very hard drilling
		Shale (?)
	?	

Appendix B

Grain Size Distribution and Atterberg Limits Data From Undisturbed Samples

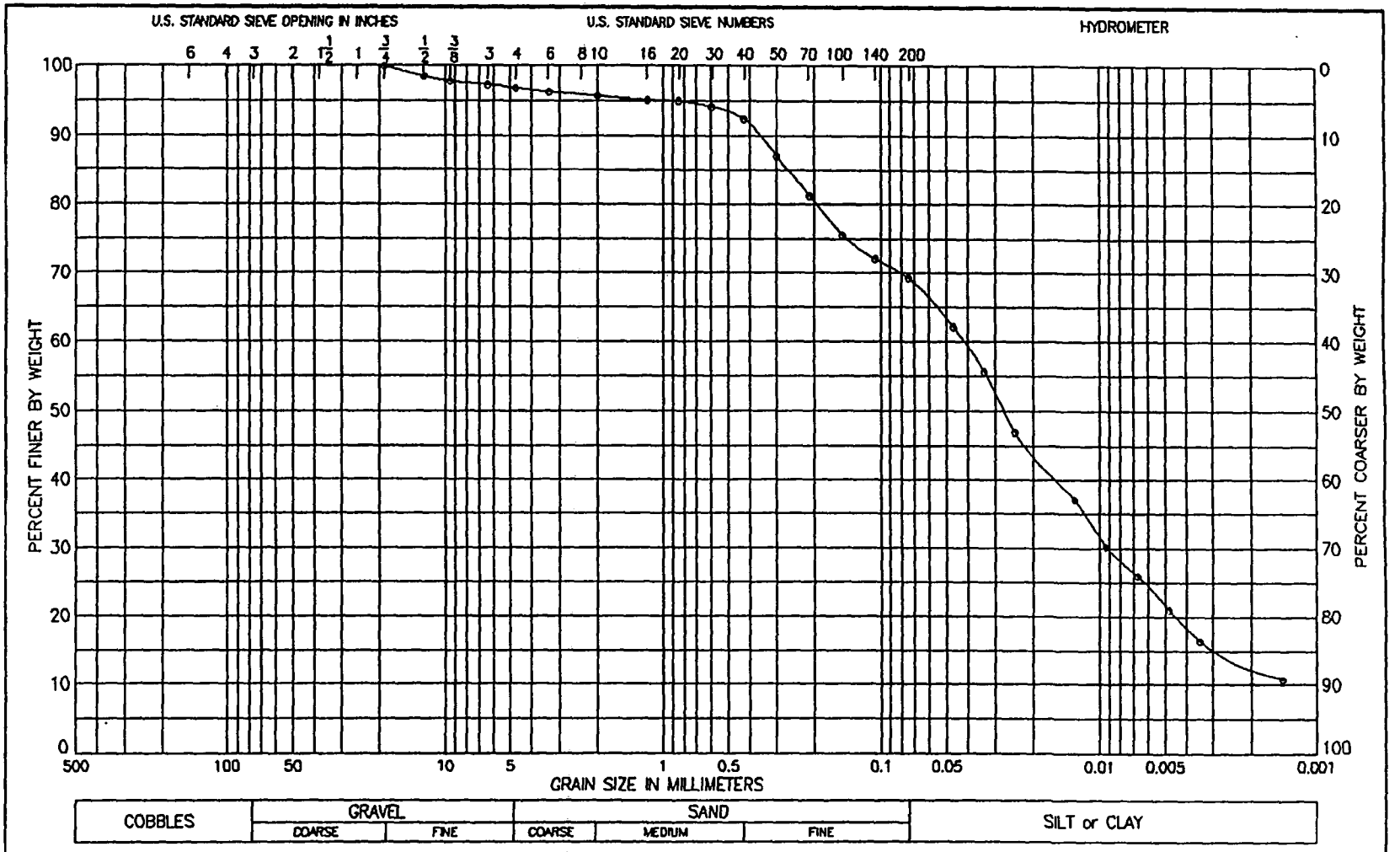

LL	PL	PI	GS	NAT W,%	ORG,%
20	13	7	2.69 EST		

CLASSIFICATION
SANDY SILTY CLAY (CL), BROWN; TRACE OF GRAVEL

GRADATION CURVE | LABORATORY USAE WES – STF/GL

PROJECT USARO/WMU

BORING NO. CP-2 SAMPLE NO. 1

DEPTH/ELEV 8-10 DATE 02 OCT 96

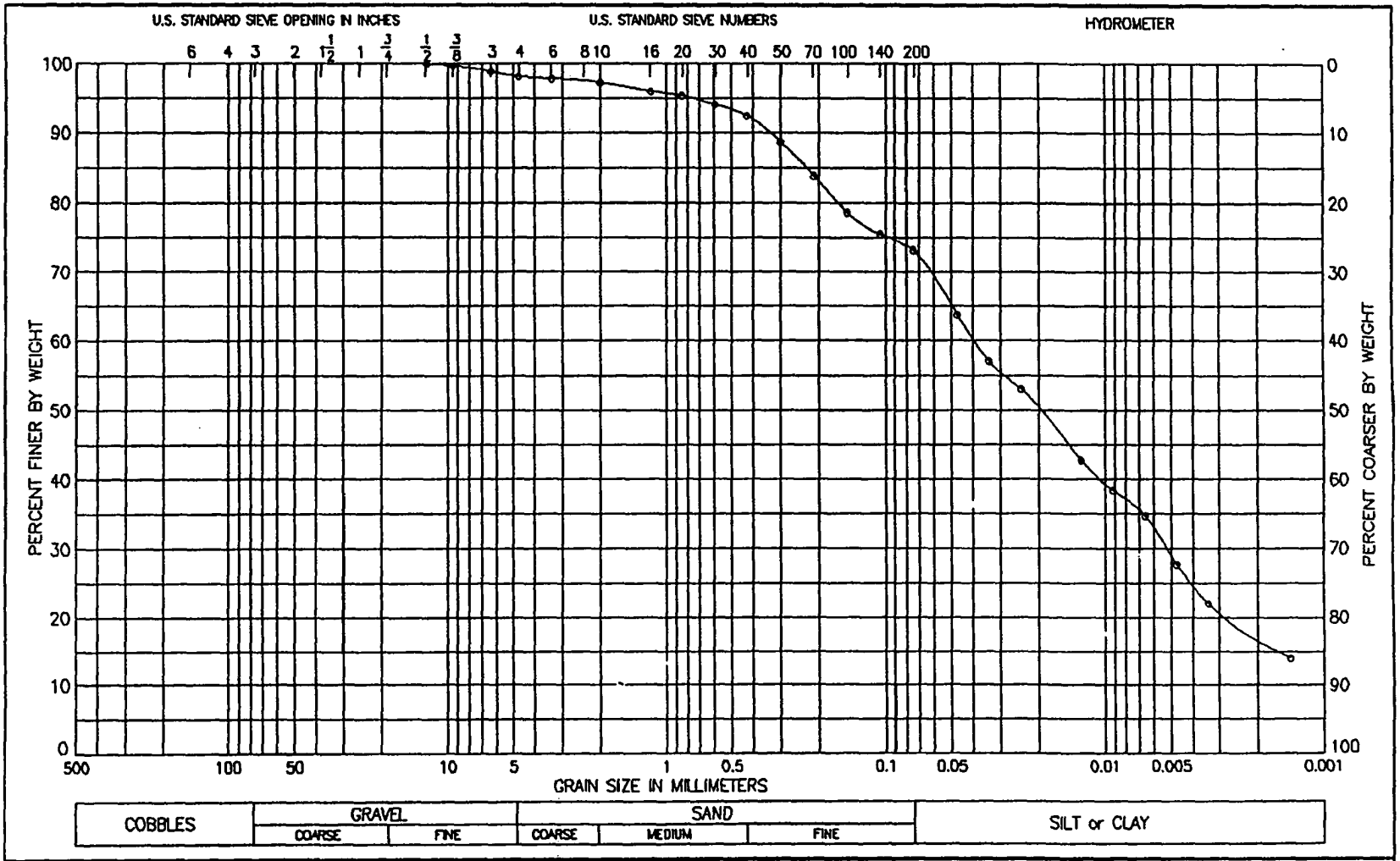

LL	PL	PI	GS	NAT W,%	ORG,%
24	15	9	2.70 EST		

CLASSIFICATION
SANDY CLAY (CL), GRAY

GRADATION CURVE | LABORATORY USAE WES – STF/GL

PROJECT USARO/WMU

BORING NO. CP-2 SAMPLE NO. 2

DEPTH/ELEV 18-20 DATE 02 OCT 96

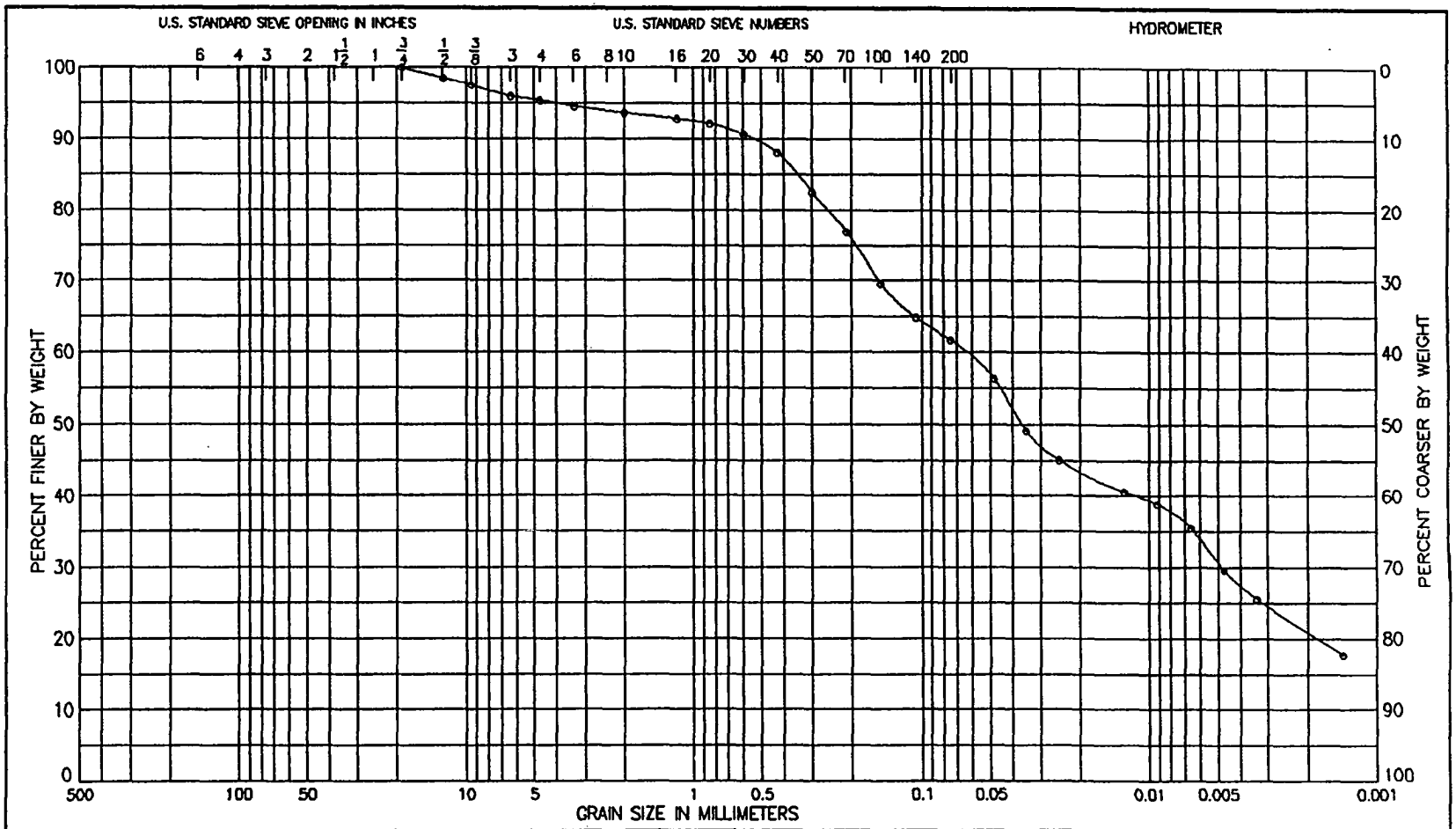

LL	PL	PI	GS	NAT W,%	ORG,%
25	14	11	2.70 EST		

CLASSIFICATION
SANDY CLAY (CL), GRAY; TRACE OF GRAVEL

GRADATION CURVE | LABORATORY USAE WES – STF/GL

PROJECT USARO/WMU

BORING NO. CP-2 SAMPLE NO. 3

DEPTH/ELEV 53-55 DATE 03 OCT 96

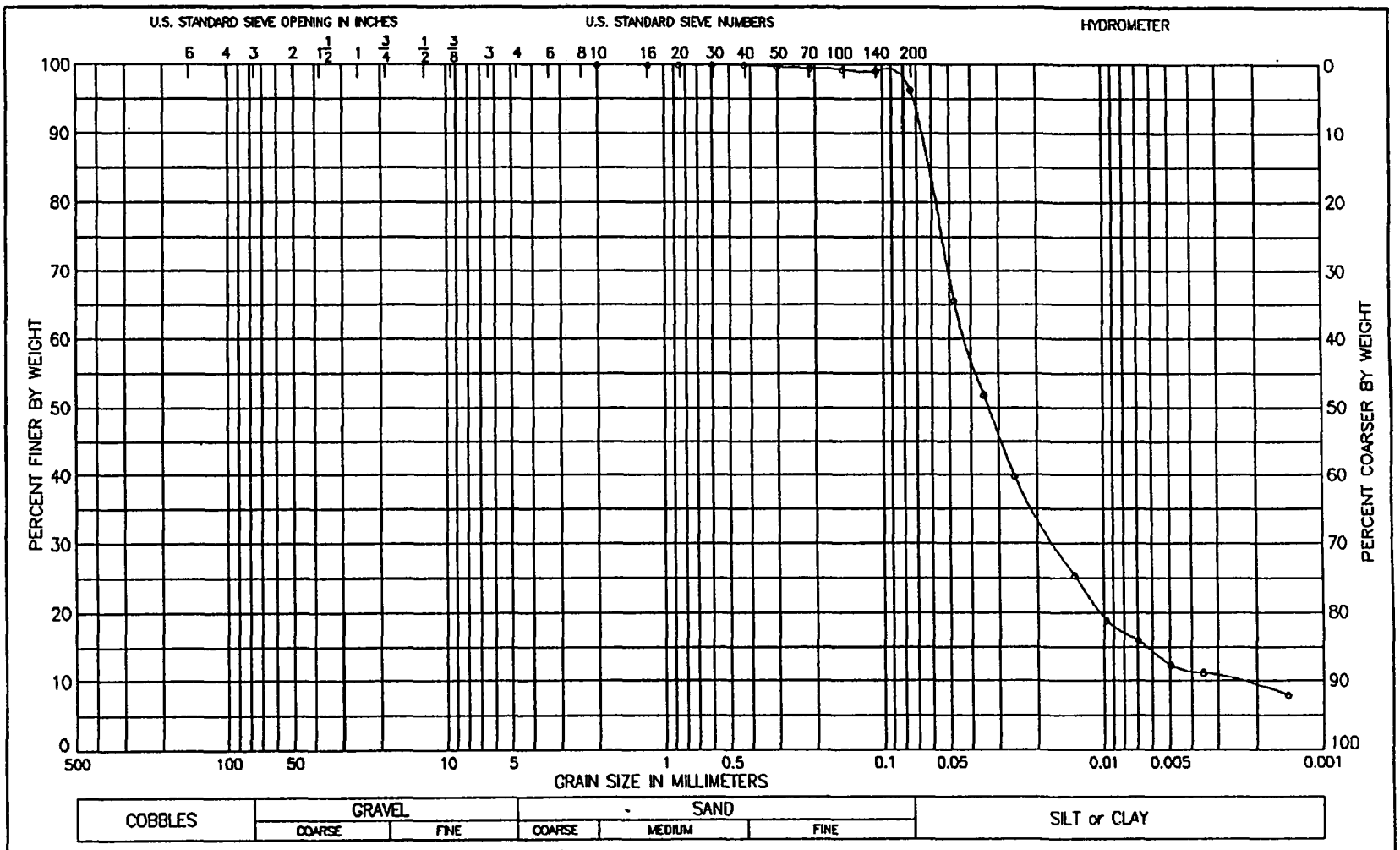

LL	PL	PI	GS	NAT W,%	ORG,%
18	15	3	2.68 EST		

CLASSIFICATION
CLAYEY SILT (ML), BROWN; TRACE OF SAND

GRADATION CURVE | LABORATORY USAE WES – STF/GL

PROJECT USARO/WMU

BORING NO. CP-2 SAMPLE NO. 4A

DEPTH/ELEV 81.75-82.0 DATE 02 OCT 96

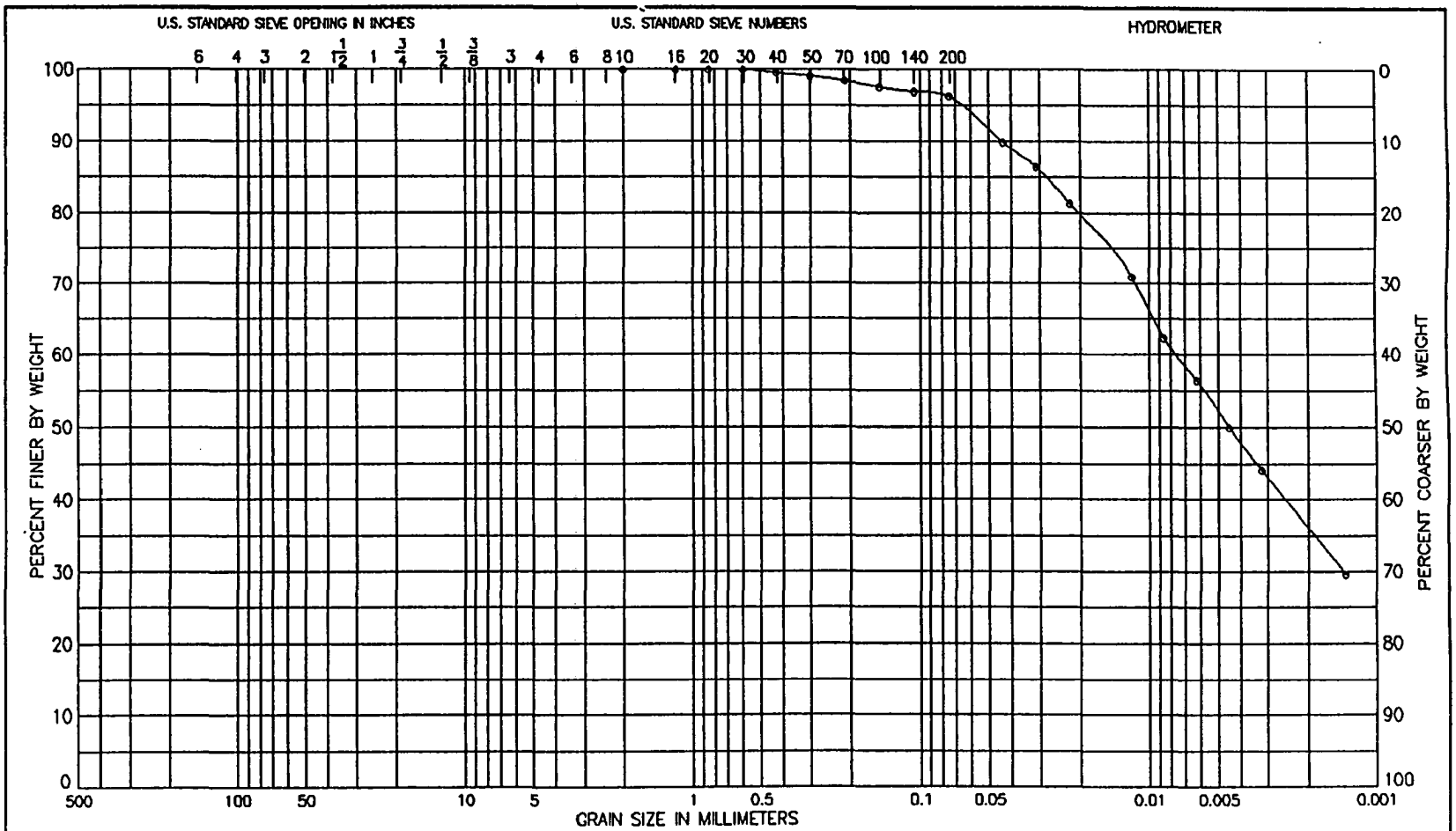

LL	PL	PI	GS	NAT W,%	ORG,%
39	15	24	2.70 EST		

CLASSIFICATION
CLAY (CL), BROWN; TRACE OF SAND

GRADATION CURVE | LABORATORY USAE WES – STF/GL

PROJECT USARO/WMU

BORING NO. CP-2 SAMPLE NO. 5A

DEPTH/ELEV 99.75-100 DATE 02 OCT 96

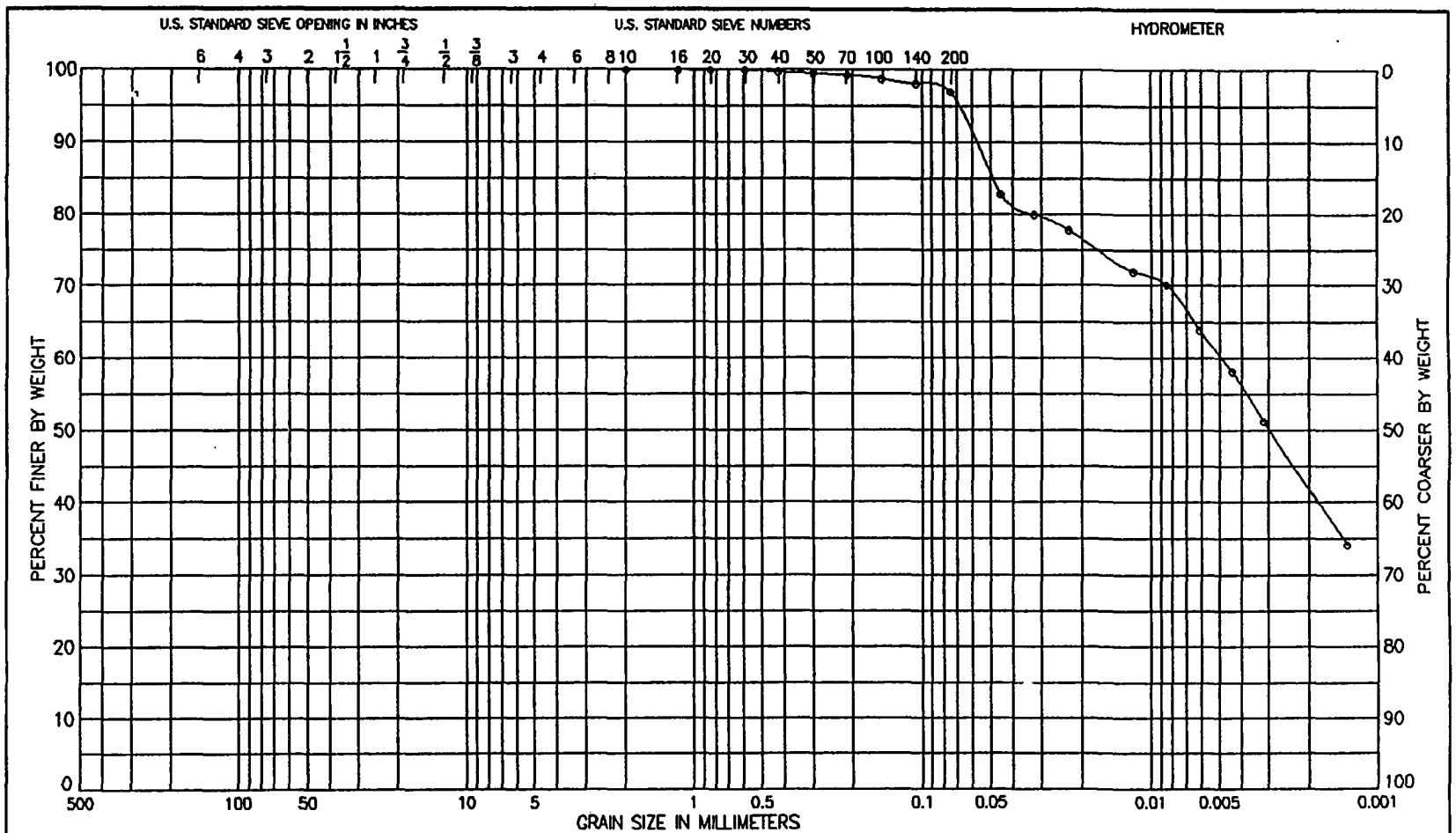

LL	PL	PI	GS	NAT W,%	ORG,%
35	17	18	2.70 EST		

CLASSIFICATION
CLAY (CL), BROWN

GRADATION CURVE | LABORATORY USAE WES – STF/GL

PROJECT USARO/WMU

BORING NO. CP-2 SAMPLE NO. 5B

DEPTH/ELEV 99.5-99.75 DATE 02 OCT 96

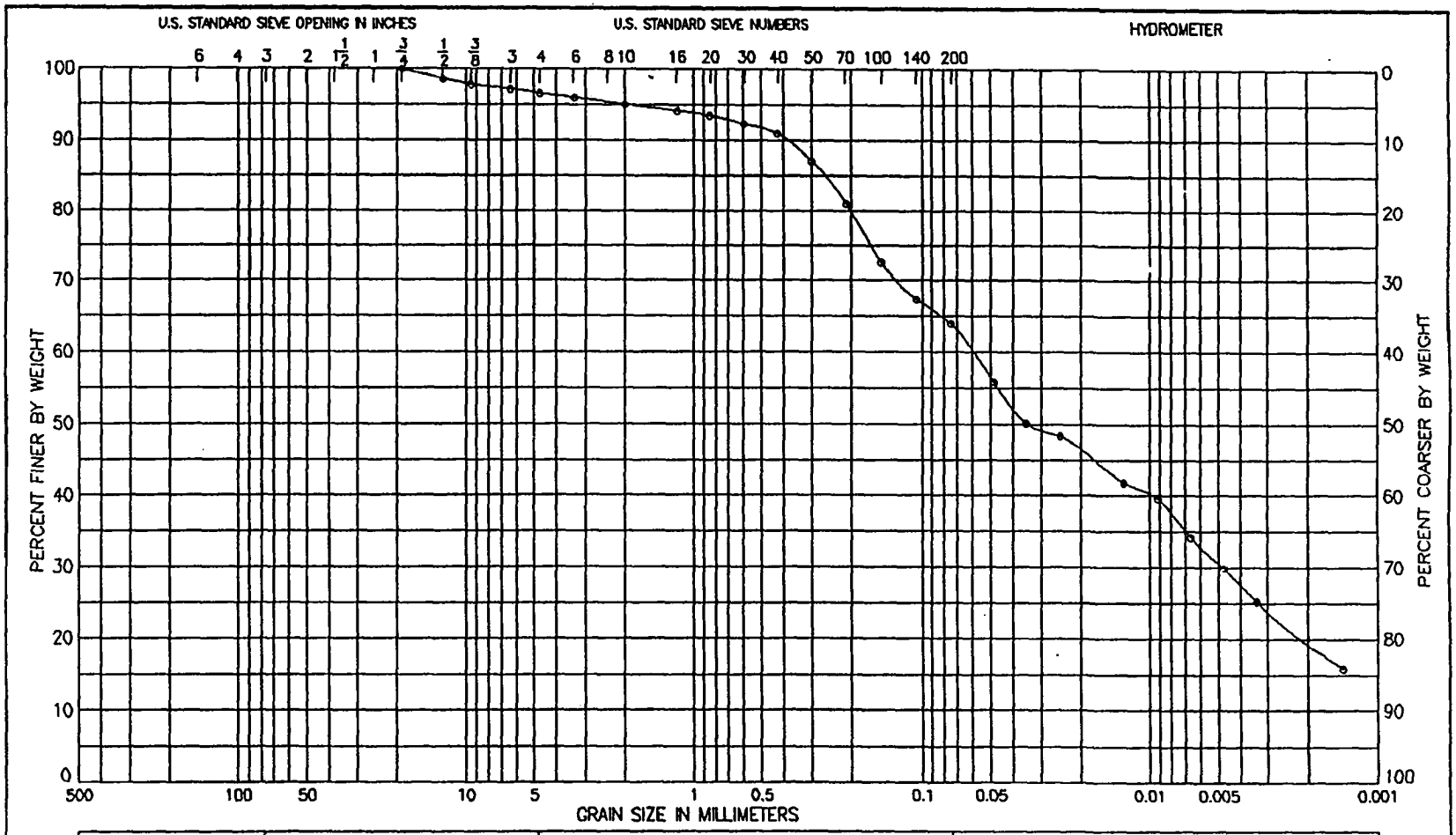

LL	PL	PI	GS	NAT W,%	ORG,%
24	14	10	2.70 EST		

CLASSIFICATION
SANDY CLAY (CL), GRAY; TRACE OF GRAVEL

GRADATION CURVE | LABORATORY USAE WES – STF/GL

PROJECT USARO/WMU

BORING NO. MP–1 SAMPLE NO. 1

DEPTH/ELEV 20–22 DATE 02 OCT 96

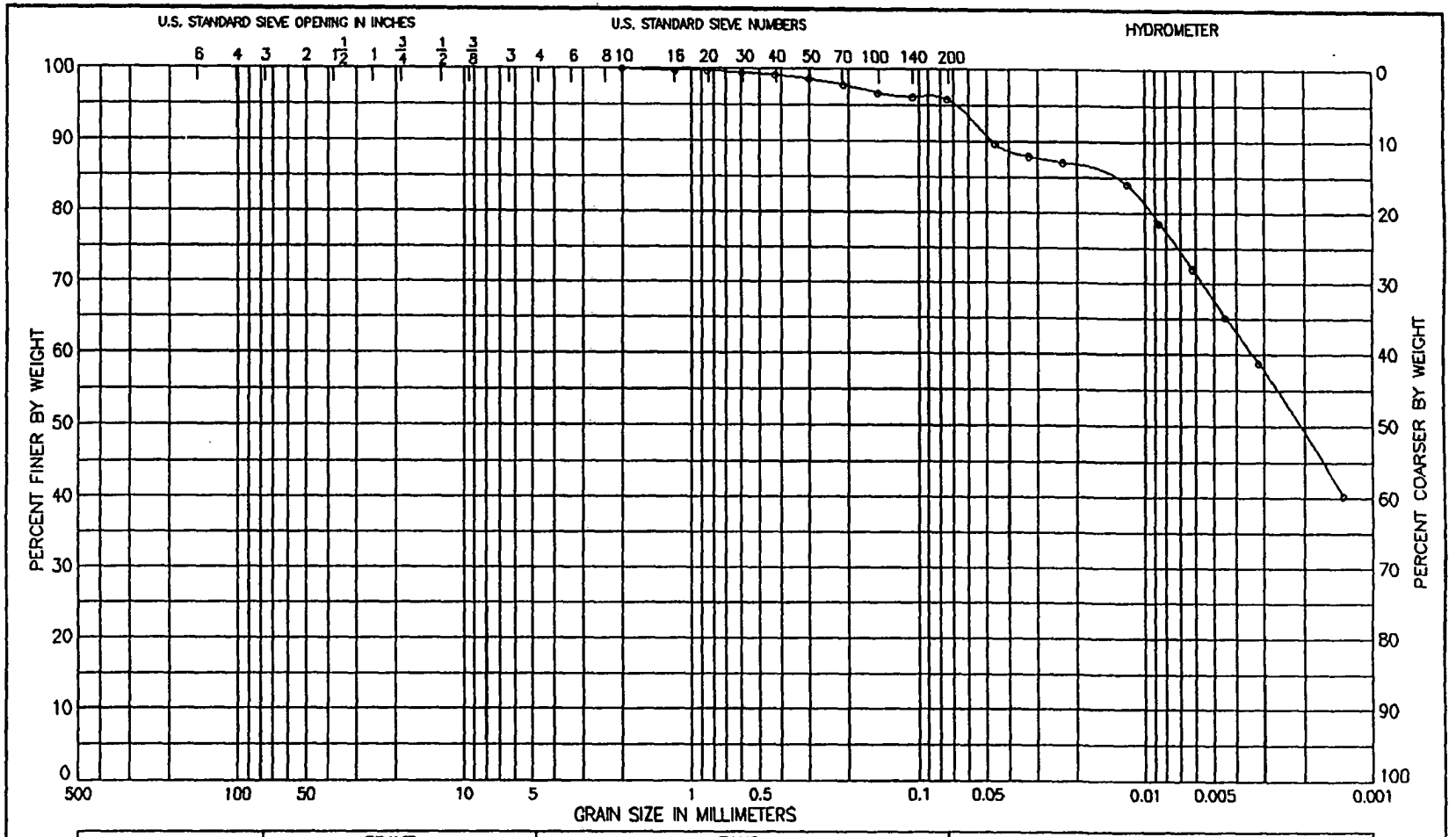

LL	PL	PI	GS	NAT W,%	ORG,%
41	19	22	2.70 EST		

CLASSIFICATION
CLAY (CL), BROWN; TRACE OF SAND

GRADATION CURVE | LABORATORY USAE WES – STF/GL

PROJECT USARO/WMU

BORING NO. MP-1 SAMPLE NO. 2

DEPTH/ELEV 40-42 DATE 02 OCT 96

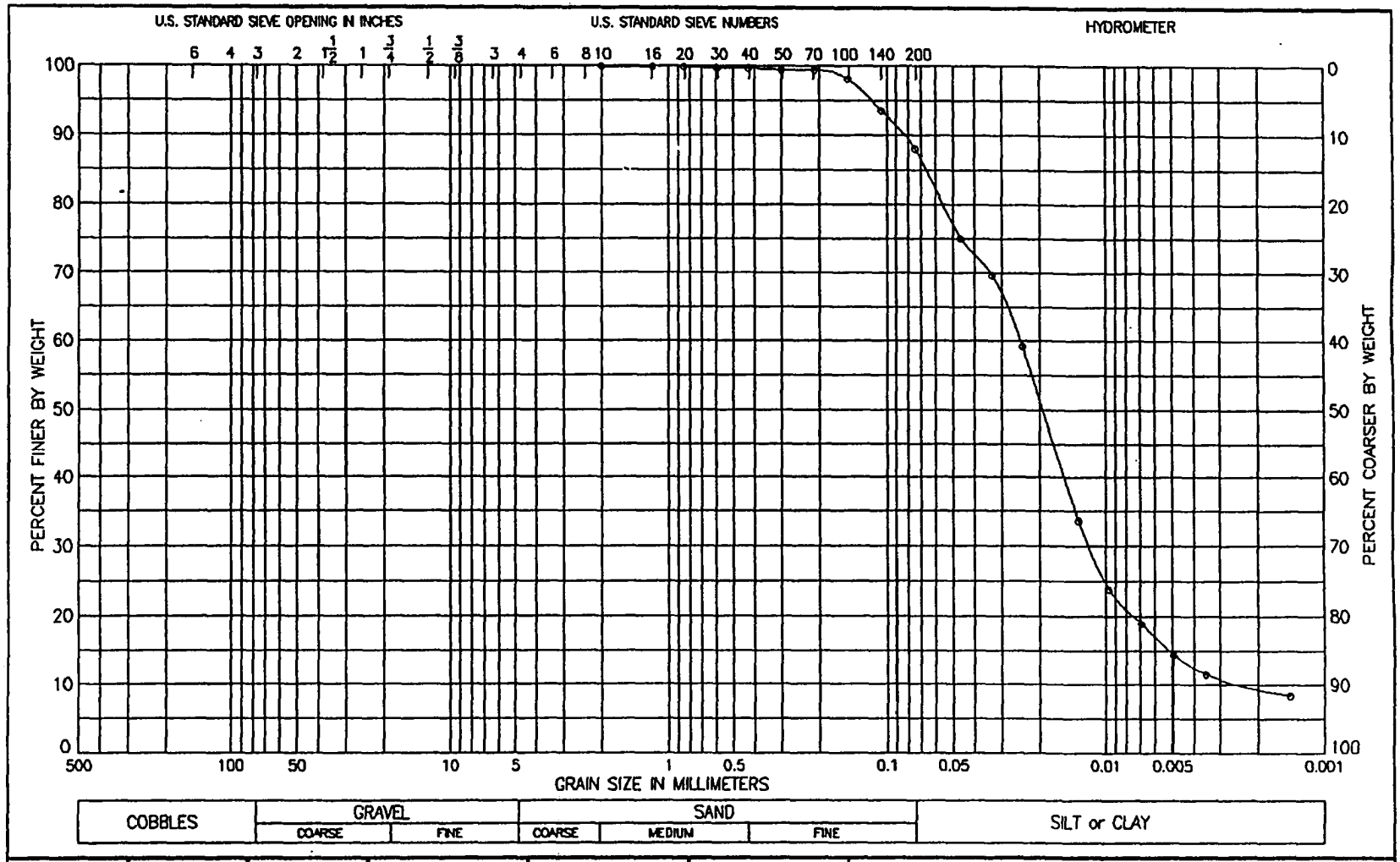

LL	PL	PI	GS	NAT W,%	ORG,%
18	16	2	2.68 EST		

CLASSIFICATION
SILT (ML), BROWN; WITH SAND

GRADATION CURVE | LABORATORY USAE WES – STF/GL

PROJECT USARO/WMU

BORING NO. MP-1 SAMPLE NO. 3B

DEPTH/ELEV 61.33-61.66 DATE 02 OCT 96

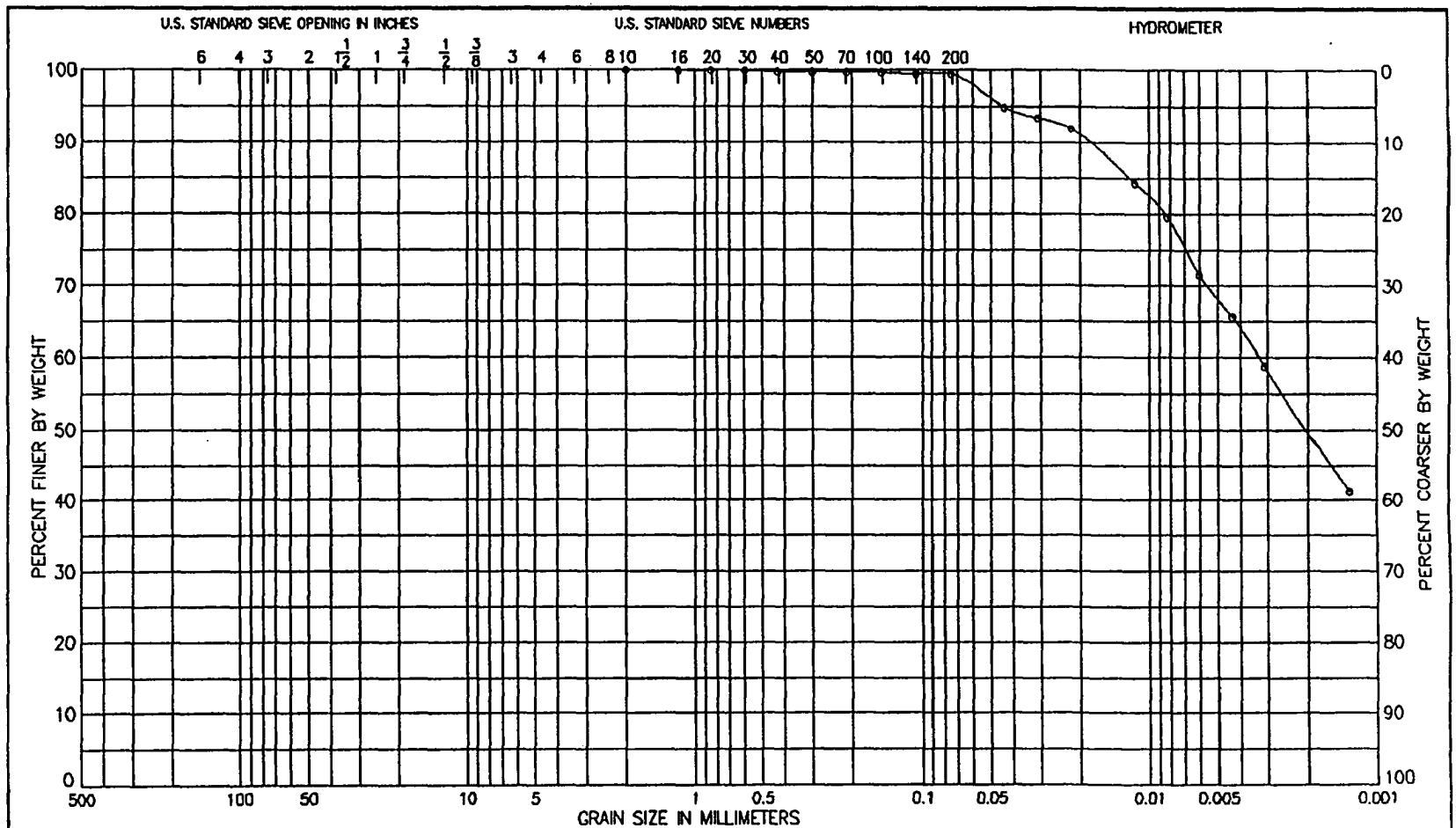

LL	PL	PI	GS	NAT W,%	ORG,%
48	18	30	2.70 EST		

CLASSIFICATION
CLAY (CL), BROWN

GRADATION CURVE | LABORATORY USAE WES – STF/GL

PROJECT USARO/WMU

BORING NO. MP-1 SAMPLE NO. 4

DEPTH/ELEV 80-82 DATE 02 OCT 96

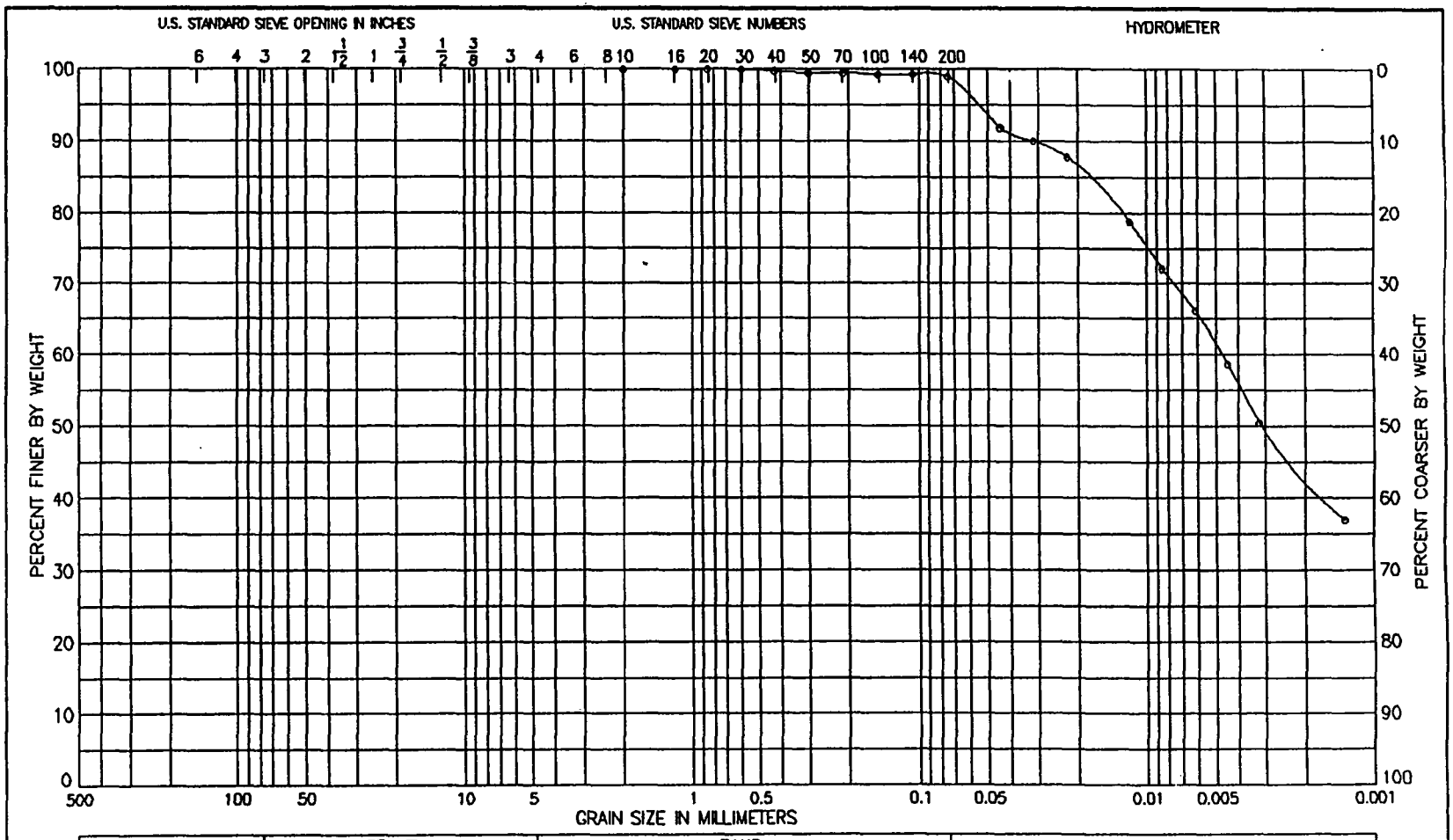

LL	PL	PI	GS	NAT W,%	ORG,%
42	17	25	2.70 EST		

CLASSIFICATION
CLAY (CL), BROWN

GRADATION CURVE

LABORATORY USAE WES – STF/GL

PROJECT USARO/WMU

BORING NO. MP–1 SAMPLE NO. 5

DEPTH/ELEV 95–97 DATE 02 OCT 96

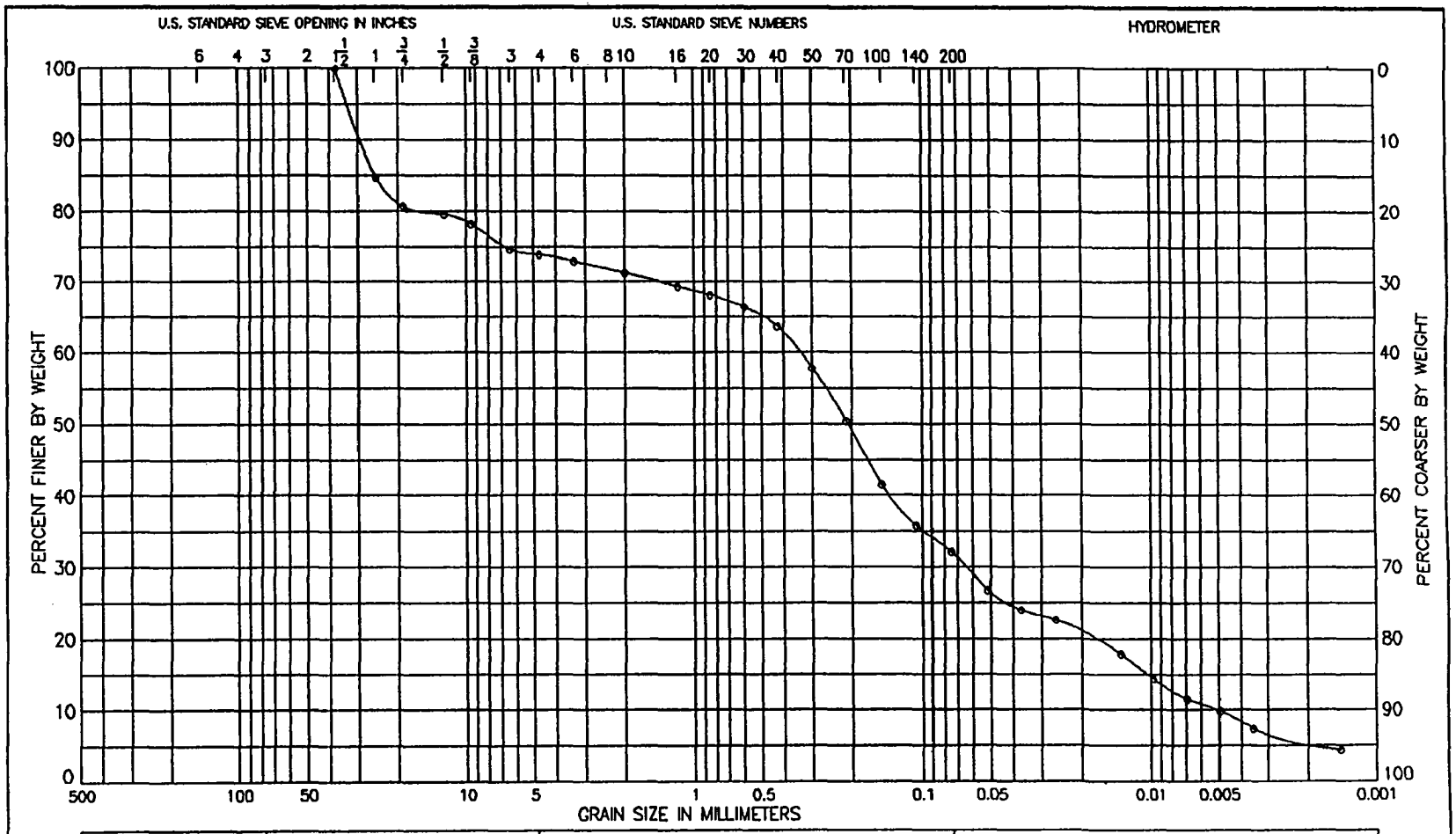

LL	PL	PI	GS	NAT W,%	ORG,%
16	10	6	2.69 EST		

CLASSIFICATION
GRAVELLY CLAYEY SILTY SAND (SM-SC), GRAY

GRADATION CURVE | LABORATORY USAE WES - STF/GL

PROJECT USARO/WMU

BORING NO. FA-1 SAMPLE NO. 1

DEPTH/ELEV 21-22 DATE 02 OCT 96

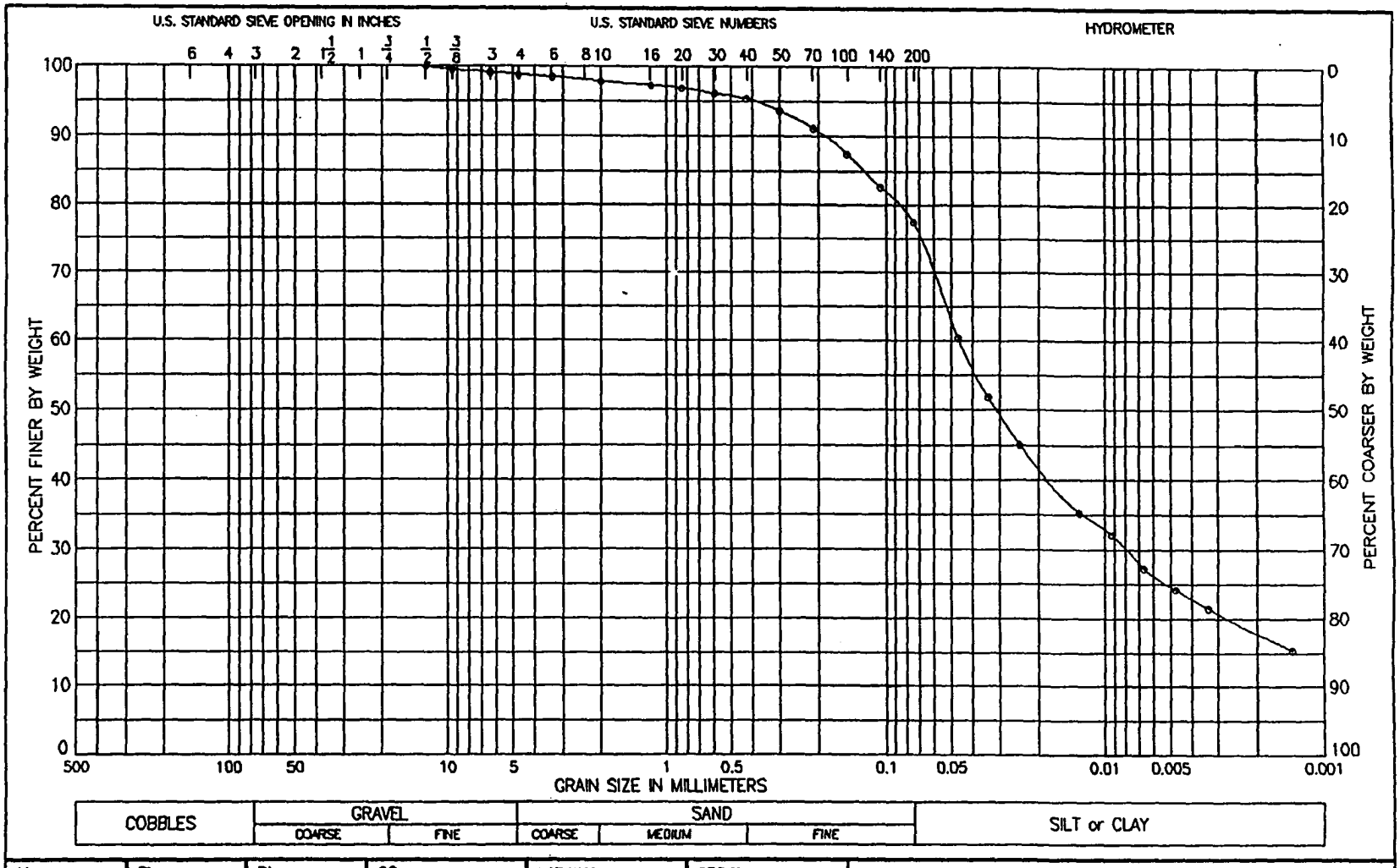

LL	PL	PI	GS 2.70 EST	NAT W,%	ORG,%

CLASSIFICATION
SANDY SILT (ML), GRAY

GRADATION CURVE | LABORATORY USAE WES – STF/GL

PROJECT USARO/WMU

BORING NO. 116-1 SAMPLE NO. 1A

DEPTH/ELEV 19.75-20.0 DATE 02 OCT 96

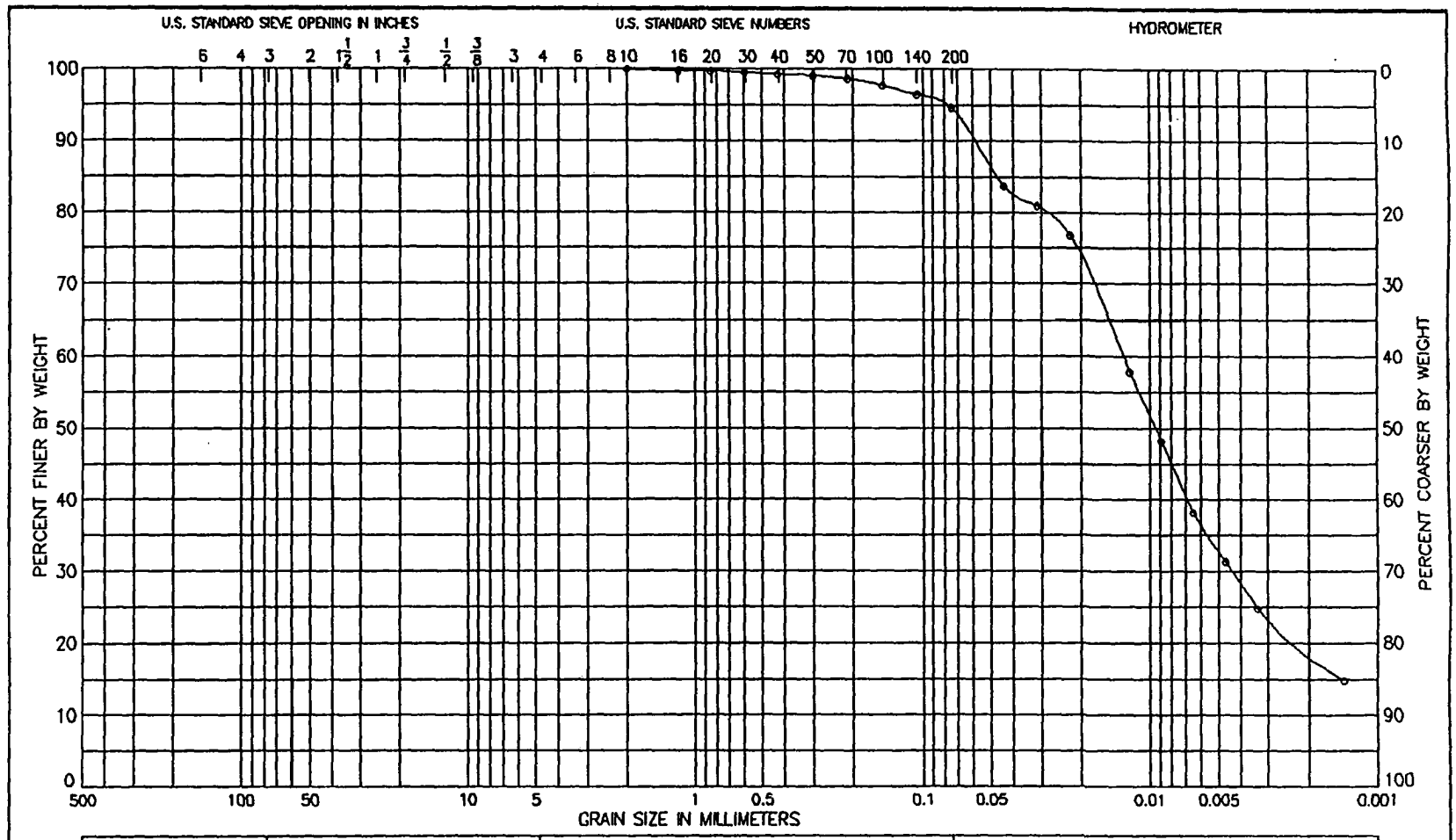

LL	PL	PI	GS	NAT W,%	ORG,%
26	14	12	2.70 EST		

CLASSIFICATION
CLAY (CL), BROWN; WITH SAND

GRADATION CURVE | LABORATORY USAE WES – STF/GL

PROJECT USARO/WMU

BORING NO. WKA-1 SAMPLE NO. 1

DEPTH/ELEV 63-65 DATE 02 OCT 96

Appendix C

Unconsolidated-Undrained Triaxial Test Data From Undisturbed Samples

Till, 80-90% Sw CP-2 #1, 8-10'

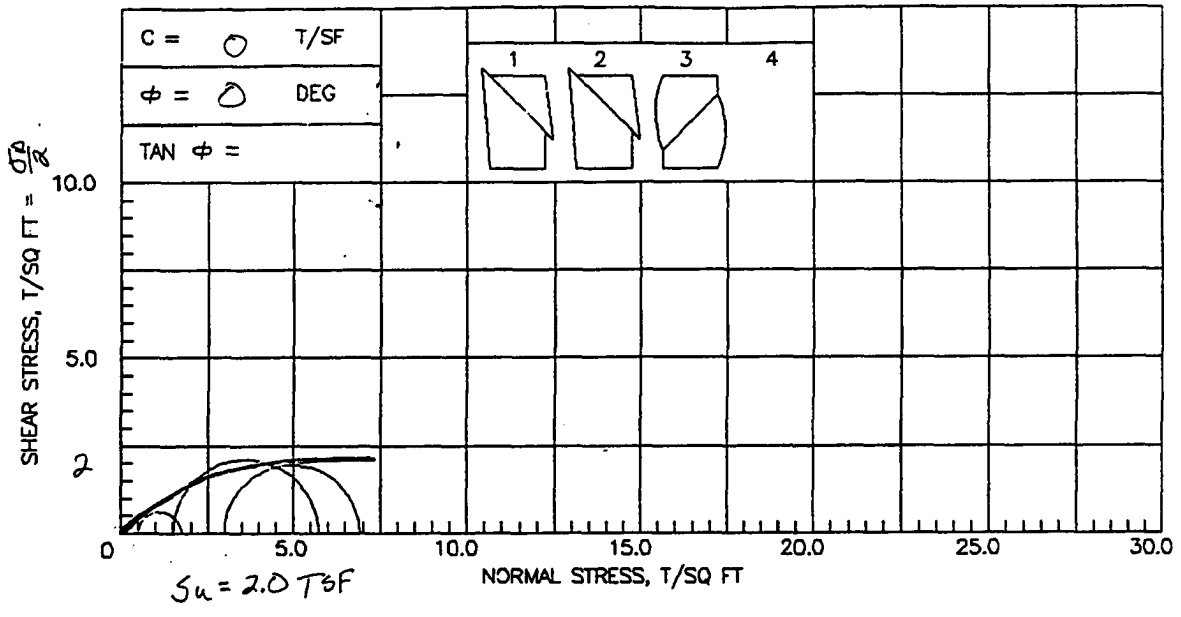

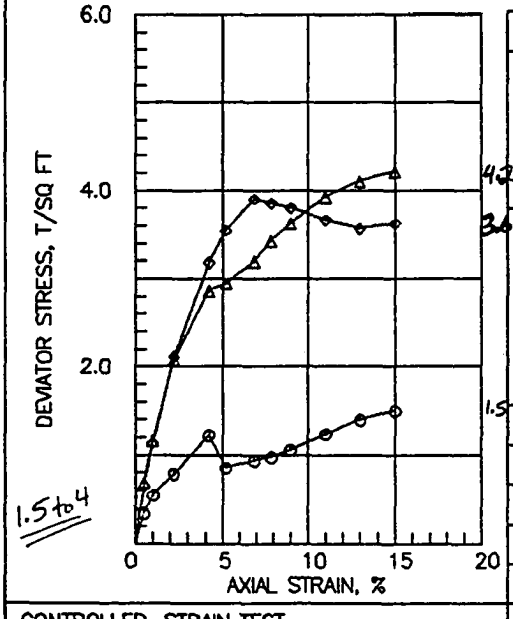

SPECIMEN NO.		○ 1	△ 2	◇ 3	4
INITIAL	WATER CONTENT, %	14.4	15.9	15.1	
	DRY DENSITY, PCF	112.4	113.4	114.9	
	SATURATION, %	77.9	88.3	87.2	
	VOID RATIO	.500	.486	.467	
BEFORE SHEAR	WATER CONTENT, %				
	DRY DENSITY, PCF				
	SATURATION, %				
	VOID RATIO				
	BACK PRESSURE, TSF				
CHAMBER PRESSURE, TSF		.50	1.50	3.00	
MAX. DEV. STRESS, TSF		1.23	4.22	3.91	
TIME TO FAILURE, MIN.		9	73	33	
STRAIN RATE INCR., %					
INITIAL DIAMETER, IN.		1.33	1.34	1.38	
INITIAL HEIGHT, IN.		3.00	3.00	3.00	

CONTROLLED-STRAIN TEST

DESCRIPTION OF SPECIMENS: SANDY CLAY (CL) WITH PEBBLES

LL	PL	PI	GS 2.70 (ESTIMATED)	UNDISTURBED SPECIMEN	Q TEST

REMARKS: Low saturation

σ_{3c} = .5 TSF

PROJECT USARO/WMU

BORING NO. CP2 SAMPLE NO. 1

DEPTH/ELEV 10 TECH. WWM

LABORATORY USAE WES – STF/GL DATE 03 SEP 96

TRIAXIAL COMPRESSION TEST REPORT

Till, 93-100% S_w

CP-2 #3, 53'-55'

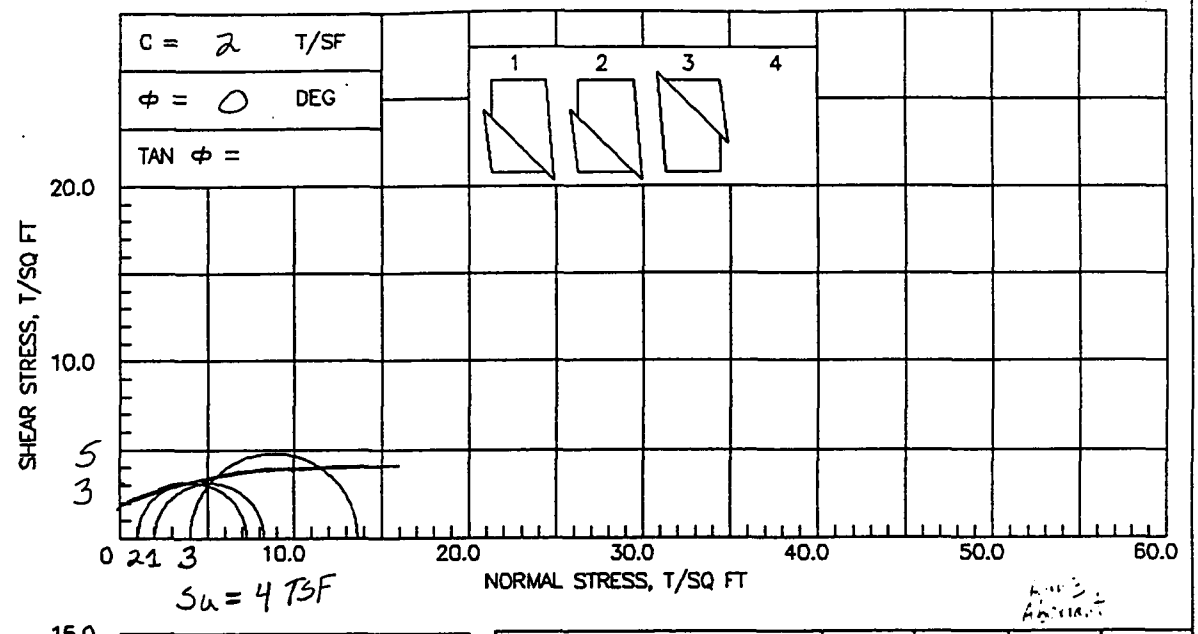

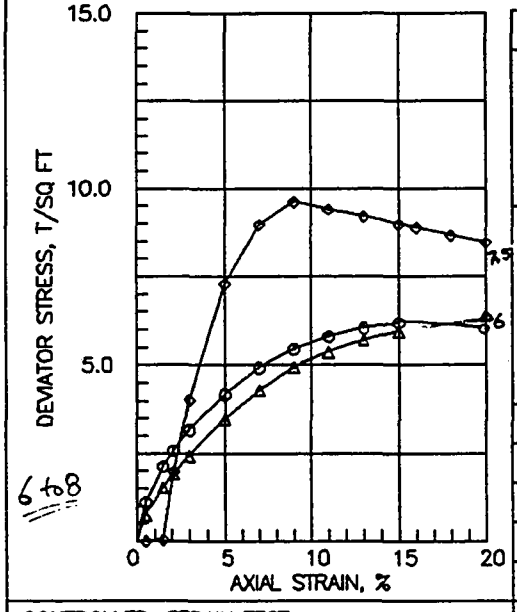

SPECIMEN NO.		○ 1	△ 2	◇ 3	4
INITIAL	WATER CONTENT, %	12.9	12.3	9.3	
	DRY DENSITY, PCF	122.7	125.9	155.5	
	SATURATION, %	93.1	98.2	100+	
	VOID RATIO	.374	.339	.084	
BEFORE SHEAR	WATER CONTENT, %				
	DRY DENSITY, PCF				
	SATURATION, %				
	VOID RATIO				
	BACK PRESSURE, TSF				
CHAMBER PRESSURE, TSF		1.00	2.00	4.00	
MAX. DEV. STRESS, TSF		6.26	6.26	9.63	
TIME TO FAILURE, MIN.		53	60	27	
STRAIN RATE INCR., %					
INITIAL DIAMETER, IN.		1.36	1.36	1.37	
INITIAL HEIGHT, IN.		3.00	3.00	3.00	

CONTROLLED-STRAIN TEST

DESCRIPTION OF SPECIMENS: SANDY CLAY (CL), GREY WITH PEBBLES.

LL	PL	PI	GS 2.70 (ESTIMATED)	UNDISTURBED SPECIMEN	Q TEST

REMARKS: HUGE CLAST IN SPECIMEN 3 OF GREY LI

PROJECT USARO/WMU

σ_{vc} = 3 TSF

BORING NO. CP2	SAMPLE NO. 3
DEPTH/ELEV 53-55'	TECH. WWM
LABORATORY USAE WES - STF/GL	DATE 05 SEP 96

TRIAXIAL COMPRESSION TEST REPORT

Till, 95-100% Sw

CP-2 #2, 18-20'

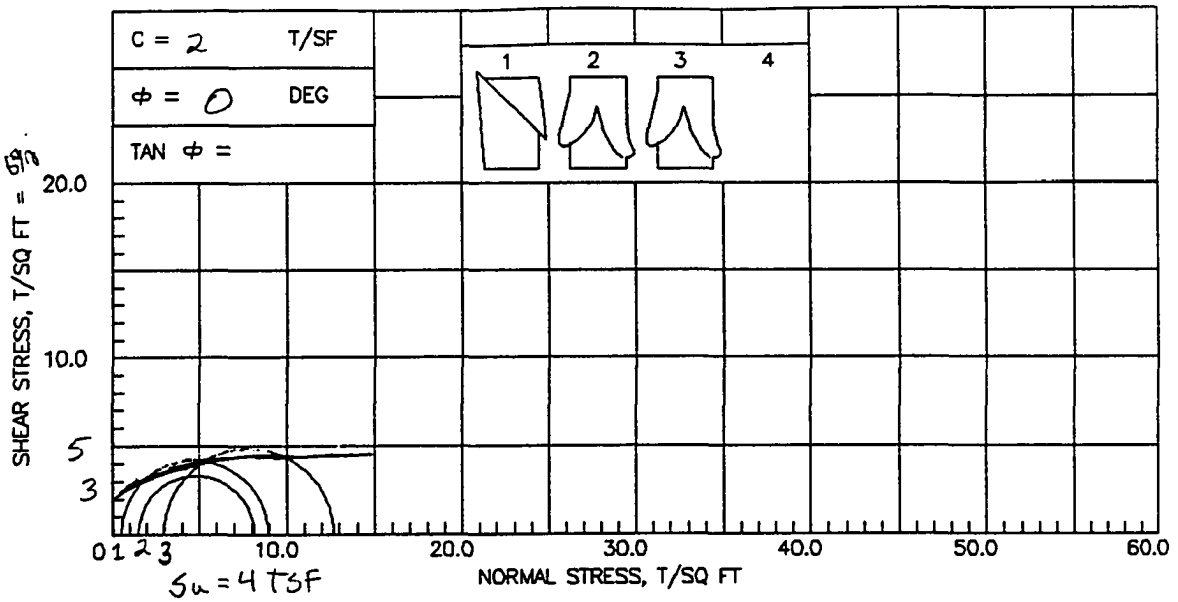

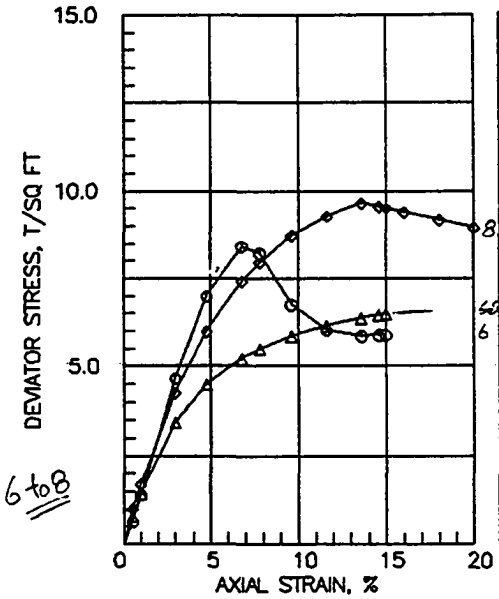

SPECIMEN NO.		○ 1	△ 2	◇ 3	4
INITIAL	WATER CONTENT, %	12.4	12.7	12.9	
	DRY DENSITY, PCF	124.0	124.7	125.1	
	SATURATION, %	93.6	97.1	100+	
	VOID RATIO	.359	.352	.347	
BEFORE SHEAR	WATER CONTENT, %				
	DRY DENSITY, PCF				
	SATURATION, %				
	VOID RATIO				
	BACK PRESSURE, TSF				
CHAMBER PRESSURE, TSF		.50	1.50	3.00	
MAX. DEV. STRESS, TSF		8.44	6.65	9.67	
TIME TO FAILURE, MIN.		20	53	41	
STRAIN RATE INCR., %					
INITIAL DIAMETER, IN.		1.35	1.36	1.36	
INITIAL HEIGHT, IN.		3.00	3.00	3.00	

CONTROLLED-STRAIN TEST

DESCRIPTION OF SPECIMENS: SANDY CLAY (CL), GRAY, PEBBLY

LL	PL	PI	GS 2.70 (ESTIMATED)	UNDISTURBED SPECIMEN	Q TEST

REMARKS: SAMPLE NOT FRACTURED VISIBLY

#1 specimen artificial OCR due to low σ_3

$\sigma_{vc} \approx 1.25$ TSF

PROJECT USARO/WMU

BORING NO. CP2 | SAMPLE NO. 2

DEPTH/ELEV 18-20' | TECH. WWM

LABORATORY USAE WES – STF/GL | DATE 04 SEP 96

TRIAXIAL COMPRESSION TEST REPORT

CP-2 #4, 80-82'

Clay, w/ 1 & 4 also sandy & wet; 99-100% Sw 99-100% except #1

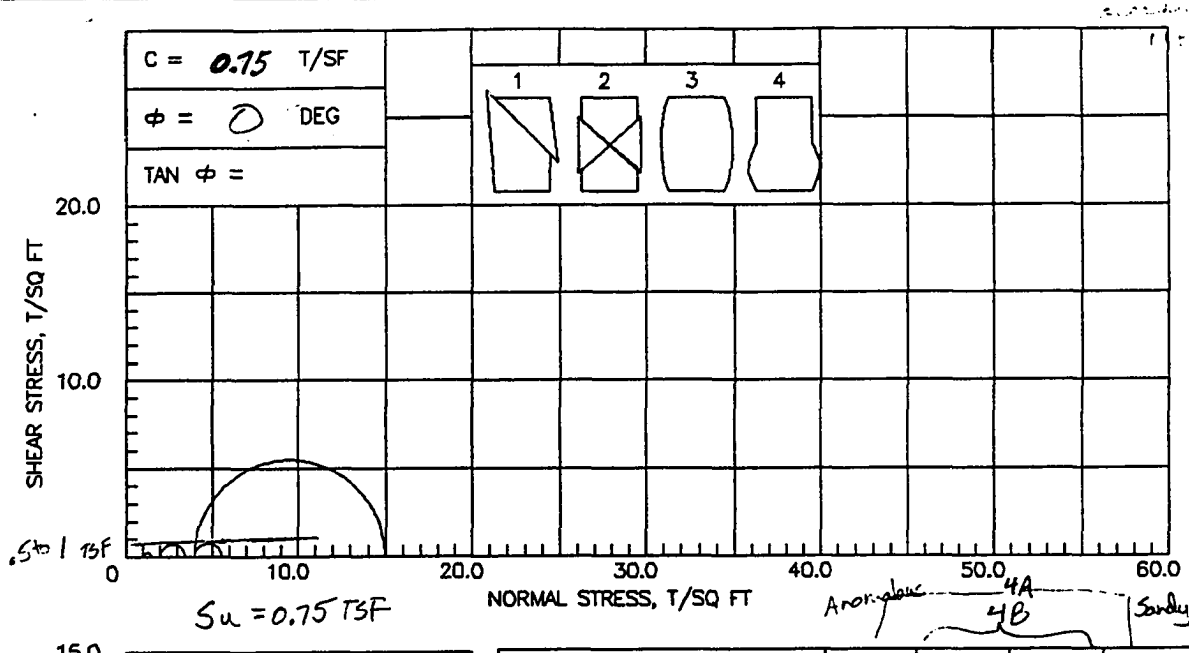

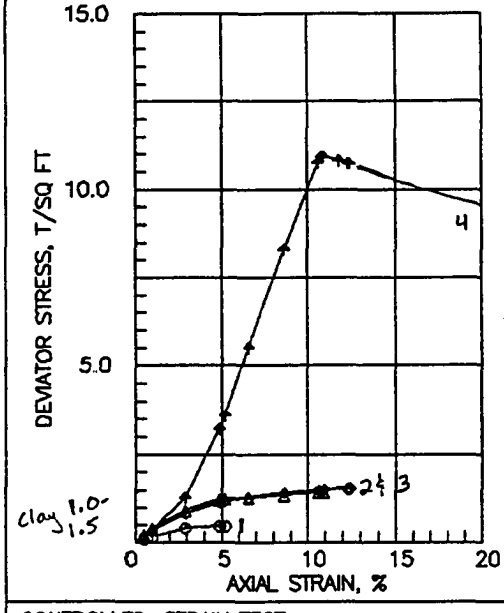

SPECIMEN NO.		○ 1	△ 2	◇ 3	+ 4
INITIAL	WATER CONTENT, %	17.3	17.8	17.6	17.0
	DRY DENSITY, PCF	93.2	113.6	115.4	122.0
	SATURATION, %	57.7	99.5	100+	100+
	VOID RATIO	.809	.484	.461	.382
BEFORE SHEAR	WATER CONTENT, %				
	DRY DENSITY, PCF				
	SATURATION, %				
	VOID RATIO				
	BACK PRESSURE, TSF				
CHAMBER PRESSURE, TSF		1.00	2.00	4.00	4.00
MAX. DEV. STRESS, TSF		.49	1.44	1.56	10.95
TIME TO FAILURE, MIN.		14	31	36	31
STRAIN RATE INCR., %					
INITIAL DIAMETER, IN.		1.48	1.34	1.33	1.29
INITIAL HEIGHT, IN.		3.00	3.00	3.00	2.80

CONTROLLED-STRAIN TEST

DESCRIPTION OF SPECIMENS: SILTY CLAY (CL), GRAY, VERY WET

LL	PL	PI	GS 2.70 (ESTIMATED)	UNDISTURBED SPECIMEN	Q TEST

REMARKS:

$\sigma_{vc} \approx 4$ TSF

PROJECT USARO/WMU

BORING NO. CP2 SAMPLE NO. 4

DEPTH/ELEV 80-82' TECH. WWM

LABORATORY USAE WES - STF/GL DATE 06 SEP 96

TRIAXIAL COMPRESSION TEST REPORT

Fine gr clay, 2&3; Clay & sand 1&4; 92-100% Sw CP-2 #5, 98-100'

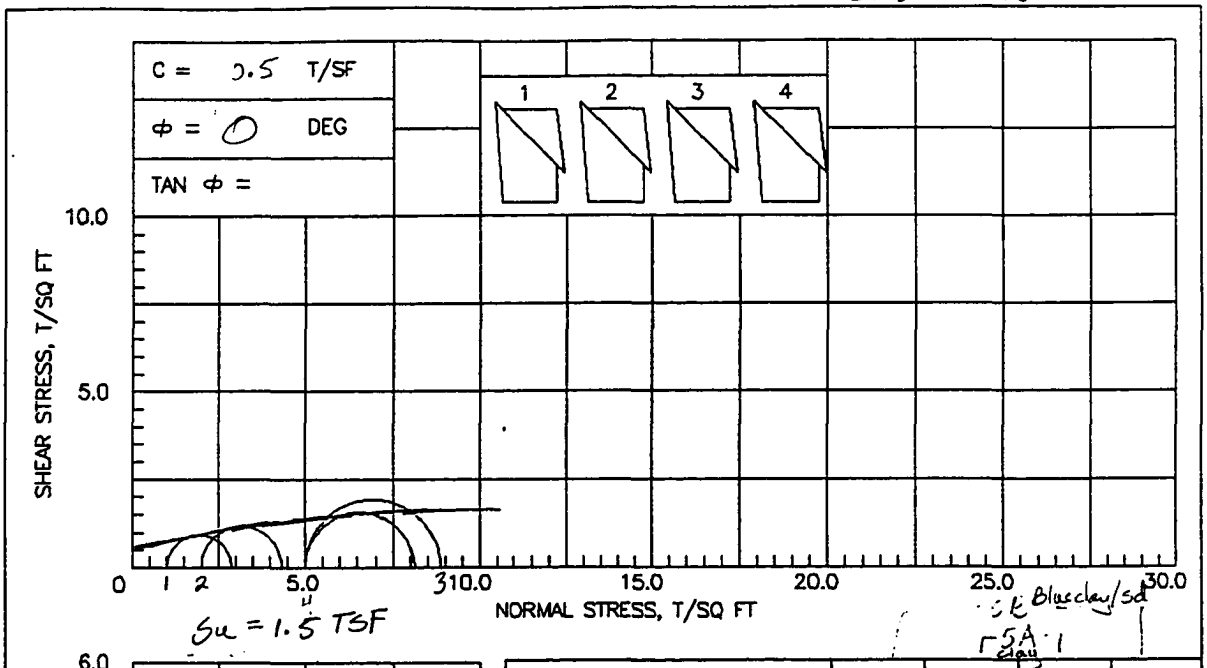

$S_u = 1.5$ TSF

Blue clay/sd

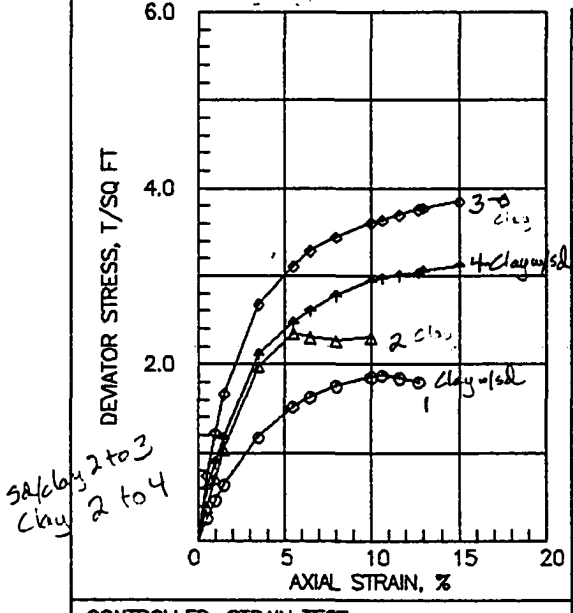

sd/clay 2 to 3
clay 2 to 4

SPECIMEN NO.		○ 1	△ 2	◇ 3	+ 4
INITIAL	WATER CONTENT, %	24.0	21.6	21.8	24.6
	DRY DENSITY, PCF	102.7	105.2	106.7	97.8
	SATURATION, %	100+	96.8	100+	92.0
	VOID RATIO	.641	.602	.579	.723
BEFORE SHEAR	WATER CONTENT, %				
	DRY DENSITY, PCF				
	SATURATION, %				
	VOID RATIO				
	BACK PRESSURE, TSF				
CHAMBER PRESSURE, TSF		1.00	2.00	5.00	5.00
MAX. DEV. STRESS, TSF		1.88	2.35	3.85	3.12
TIME TO FAILURE, MIN.		31	16	44	44
STRAIN RATE INCR., %					
INITIAL DIAMETER, IN.		1.34	1.35	1.35	1.35
INITIAL HEIGHT, IN.		3.00	3.00	3.00	3.00

CONTROLLED-STRAIN TEST

DESCRIPTION OF SPECIMENS: 2 TYPES: 99.33-99.66 IS BLUE-GREY CLAY OVER SAND

LL	PL	PI	GS 2.70 (ESTIMATED)	UNDISTURBED SPECIMEN	Q TEST

REMARKS: OVER BOWN

$\sigma_{vc} \cong 5$ TSF

PROJECT USARO/WMU

BORING NO. CP2 SAMPLE NO. 5

DEPTH/ELEV 98-100 TECH. WWM

LABORATORY USAE WES - STF/GL DATE 07 SEP 96

TRIAXIAL COMPRESSION TEST REPORT

Till, 94-100% Sw

MP-1 #1, 20-22'

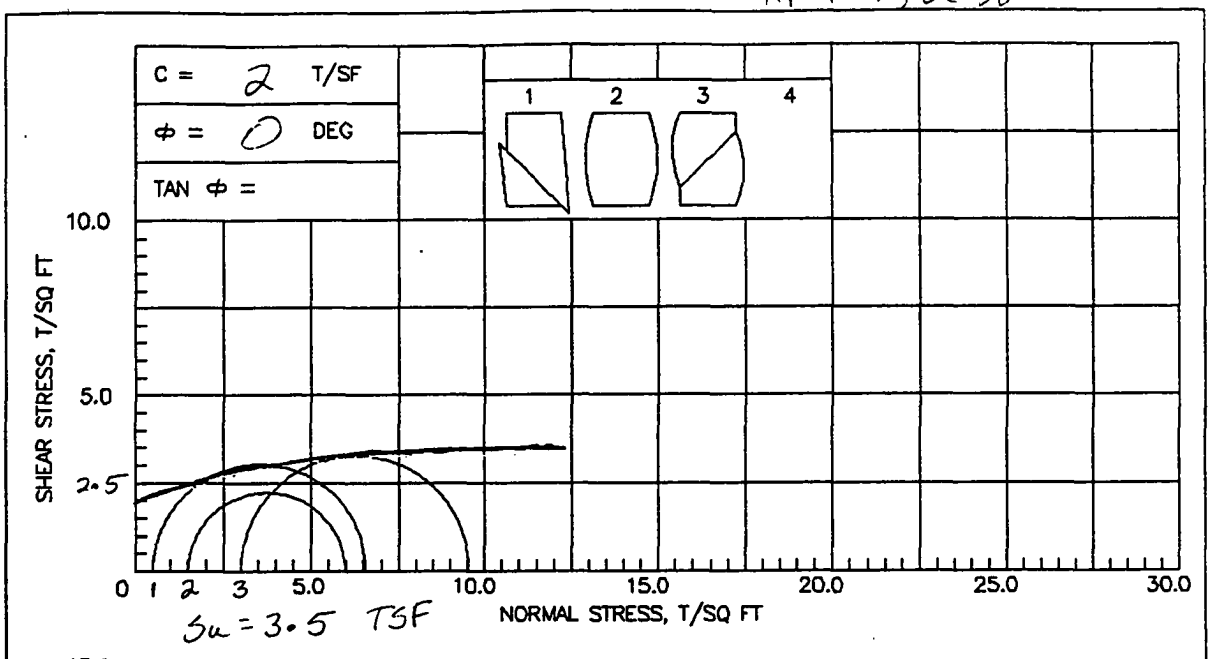

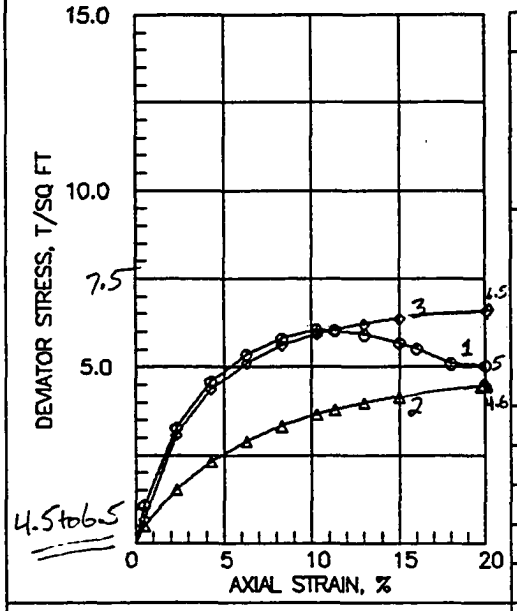

SPECIMEN NO.		○ 1	△ 2	◇ 3	4
INITIAL	WATER CONTENT, %	12.9	13.2	12.7	
	DRY DENSITY, PCF	123.1	123.7	131.7	
	SATURATION, %	94.1	98.4	100+	
	VOID RATIO	.370	.362	.280	
BEFORE SHEAR	WATER CONTENT, %				
	DRY DENSITY, PCF				
	SATURATION, %				
	VOID RATIO				
	BACK PRESSURE, TSF				
CHAMBER PRESSURE, TSF		.50	1.50	3.00	
MAX. DEV. STRESS, TSF		6.05	4.45	6.54	
TIME TO FAILURE, MIN.		30	59	60	
STRAIN RATE INCR., %					
INITIAL DIAMETER, IN.		1.36	1.36	1.37	
INITIAL HEIGHT, IN.		3.00	3.00	3.00	

CONTROLLED-STRAIN TEST

DESCRIPTION OF SPECIMENS: GRAY CLAY TILL (CL), SANDY, PEBBLY, NOT FRACTURE

LL	PL	PI	GS 2.70 (ESTIMATED)	UNDISTURBED SPECIMEN	Q TEST

REMARKS: SPECIMEN 3 HAS LARGE PEBBLE PROTRUDING FROM BASE

σ_{vc} = 1.25 TSF

PROJECT: USARO/WMU

BORING NO. MP1 SAMPLE NO. 1

DEPTH/ELEV 20-22 TECH. WWM

LABORATORY USAE WES - STF/GL DATE 07 SEP 96

TRIAXIAL COMPRESSION TEST REPORT

Clay, fine gr, 99-100% Sw MP-1 #2, 40-42'

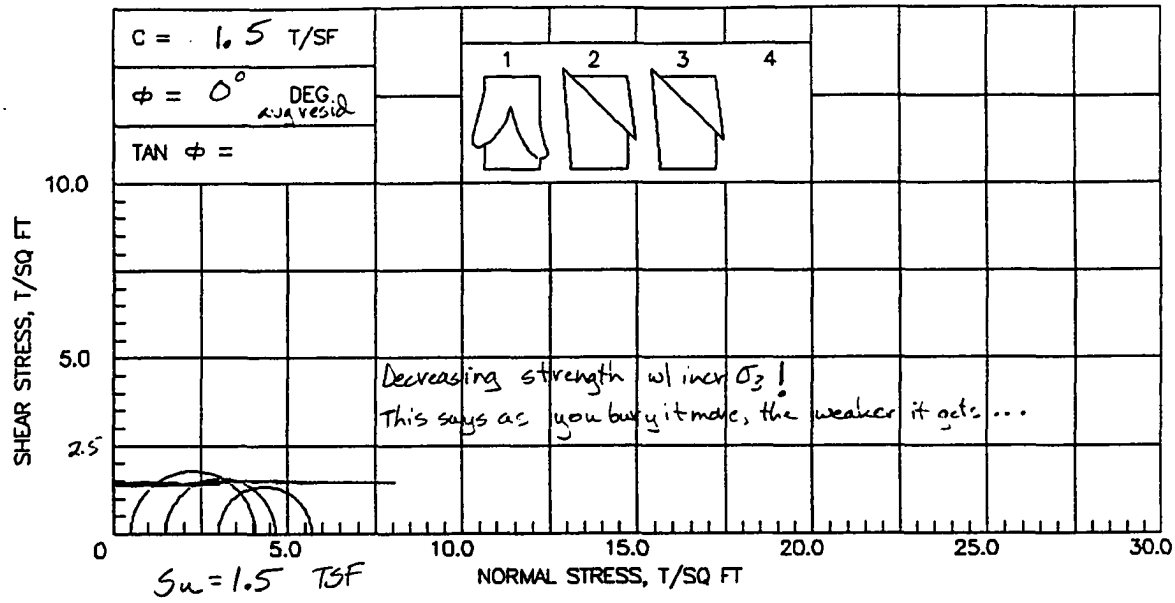

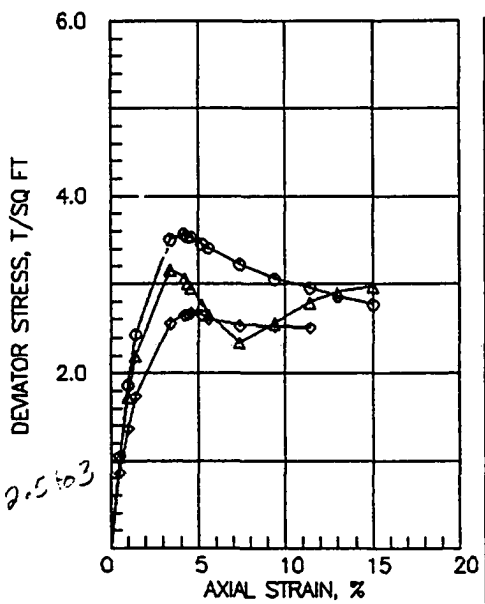

SPECIMEN NO.		○ 1	△ 2	◇ 3	4
INITIAL	WATER CONTENT, %	25.5	25.1	24.1	
	DRY DENSITY, PCF	101.0	101.0	101.8	
	SATURATION, %	100+	100+	99.5	
	VOID RATIO	.668	.669	.656	
BEFORE SHEAR	WATER CONTENT, %				
	DRY DENSITY, PCF				
	SATURATION, %				
	VOID RATIO				
	BACK PRESSURE, TSF				
CHAMBER PRESSURE, TSF		.50	1.50	3.00	
MAX. DEV. STRESS, TSF		3.57	3.16	2.68	
TIME TO FAILURE, MIN.		12	10	14	
STRAIN RATE INCR., %					
INITIAL DIAMETER, IN.		1.35	1.36	1.36	
INITIAL HEIGHT, IN.		3.00	3.00	3.00	

CONTROLLED-STRAIN TEST

DESCRIPTION OF SPECIMENS: CLAY (CL), V. FINE GR, BROWN, PLASTIC

LL	PL	PI	GS 2.70 (ESTIMATED)	UNDISTURBED SPECIMEN	Q TEST

REMARKS: DESCRIBED BY DR KEHEW AS "FINE GR

σ_{3c} = 2.25 TSF

Artificial OCR induced

PROJECT USARO/WMU

BORING NO. MP1 SAMPLE NO. 2

DEPTH/ELEV 40-42 TECH. WWM

LABORATORY USAE WES – STF/GL DATE 08 SEP 96

TRIAXIAL COMPRESSION TEST REPORT

3A Fine or clay (2,3), 98-100% Sw
3B Wet sd & clay (1,4), 77-87% Sw

MP-1 #3, 60-62'

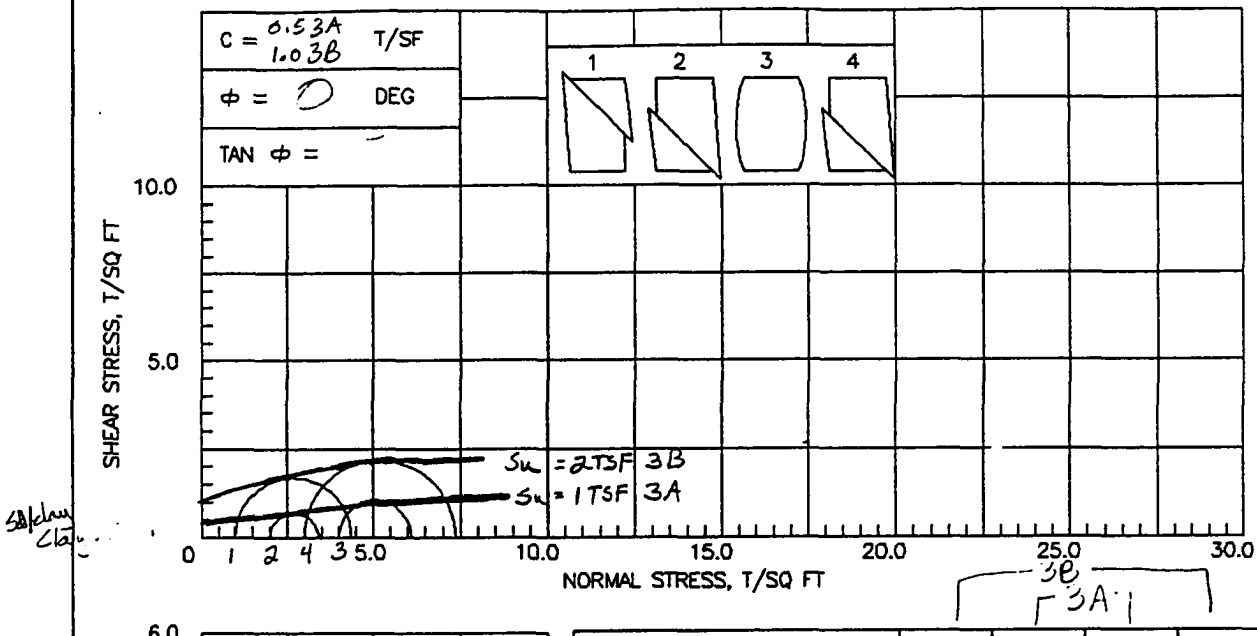

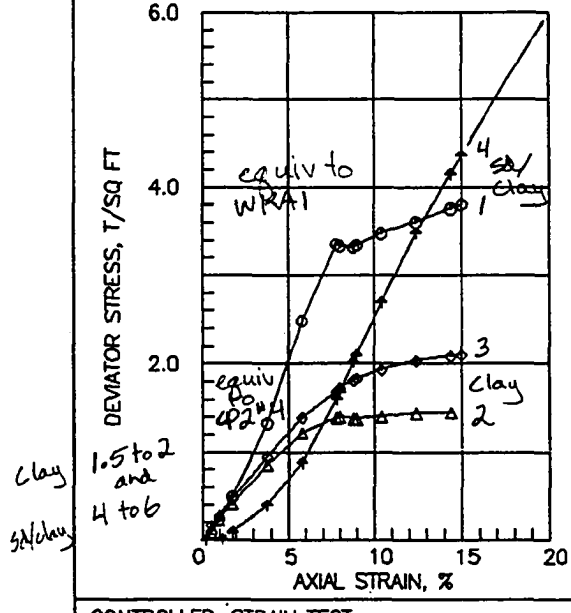

SPECIMEN NO.		○ 1	△ 2	◇ 3	+ 4
INITIAL	WATER CONTENT, %	19.3	25.5	25.5	19.9
	DRY DENSITY, PCF	105.7	99.2	100.9	99.1
	SATURATION, %	87.4	98.3	100+	76.9
	VOID RATIO	.595	.700	.671	.700
BEFORE SHEAR	WATER CONTENT, %				
	DRY DENSITY, PCF				
	SATURATION, %				
	VOID RATIO				
	BACK PRESSURE, TSF				
CHAMBER PRESSURE, TSF		1.00	2.00	4.00	3.00
MAX. DEV. STRESS, TSF		3.36	1.41	2.10	4.37
TIME TO FAILURE, MIN.		22	23	44	44
STRAIN RATE INCR., %					
INITIAL DIAMETER, IN.		1.38	1.37	1.37	1.42
INITIAL HEIGHT, IN.		2.90	3.00	3.00	2.90

CONTROLLED-STRAIN TEST

DESCRIPTION OF SPECIMENS: INTBD SD/CLAY FOR SPEC 1, FINE GR CLAY FOR 2 & 3

LL	PL	PI	GS 2.70 (ESTIMATED)	UNDISTURBED SPECIMEN	Q TEST

REMARKS: SPEC 1 VERY WET, FRAGILE

σ_{VC} = 3.25 TSF

PROJECT USARO/WMU

BORING NO. MP1 SAMPLE NO. 3

DEPTH/ELEV 60-62 TECH. WWM

LABORATORY USAE WES - STF/GL DATE 08 SEP 96

TRIAXIAL COMPRESSION TEST REPORT

Fine gr clay, .00%+ Sw MP-1 #4, 80-82'

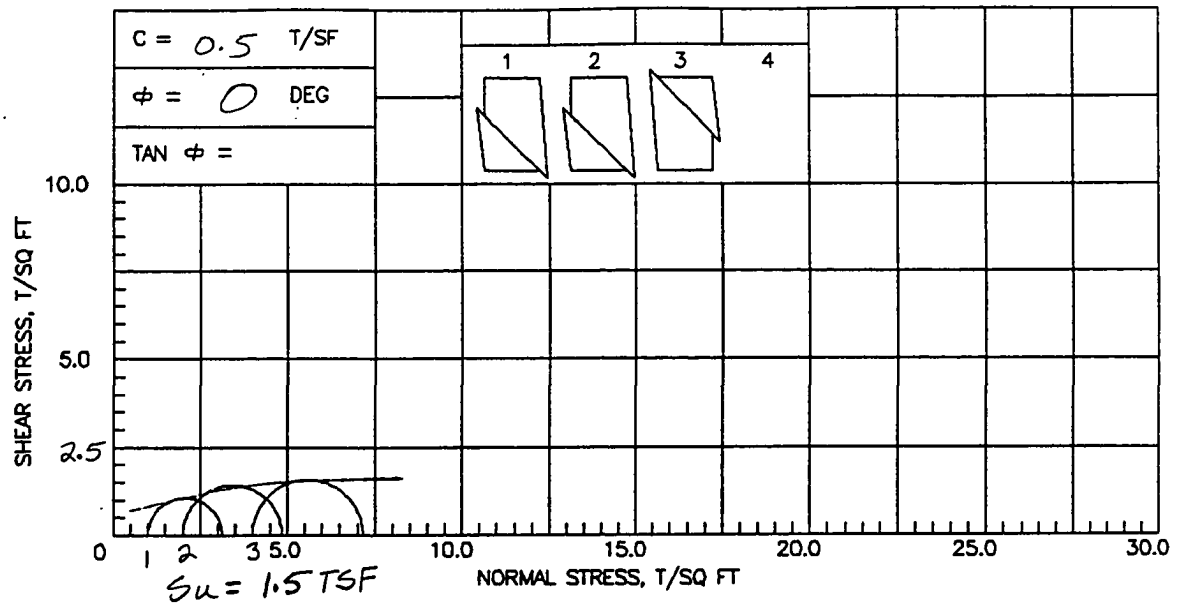

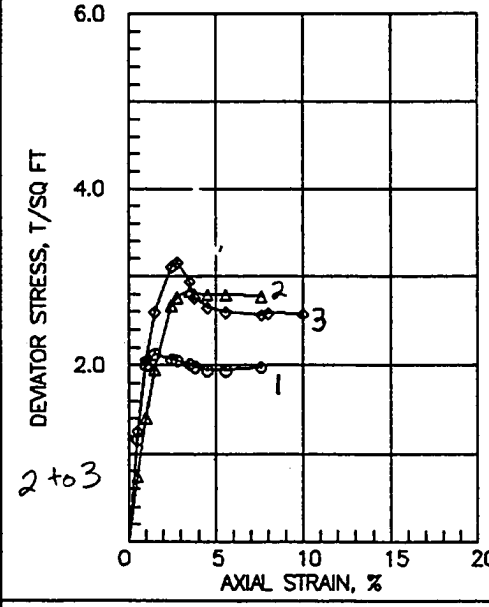

Clay 2 to 3

SPECIMEN NO.		○ 1	△ 2	◇ 3	4
INITIAL	WATER CONTENT, %	26.8	27.2	27.0	
	DRY DENSITY, PCF	98.6	97.4	97.6	
	SATURATION, %	100+	100+	100+	
	VOID RATIO	.709	.731	.727	
BEFORE SHEAR	WATER CONTENT, %				
	DRY DENSITY, PCF				
	SATURATION, %				
	VOID RATIO				
	BACK PRESSURE, TSF				
CHAMBER PRESSURE, TSF		1.00	2.00	4.00	
MAX. DEV. STRESS, TSF		2.13	2.84	3.16	
TIME TO FAILURE, MIN.		5	11	8	
STRAIN RATE INCR., %					
INITIAL DIAMETER, IN.		1.36	1.37	1.37	
INITIAL HEIGHT, IN.		3.00	3.00	3.00	

CONTROLLED-STRAIN TEST

DESCRIPTION OF SPECIMENS: CLAY (CL), BROWN, V FINE GR, PLASTIC, RARE SD LA

LL	PL	PI	GS 2.70 (ESTIMATED)	UNDISTURBED SPECIMEN	Q TEST

REMARKS: SPECIMENS 1 & 3 FROM SAME LIFT

σ_{vc} = 4.25 TSF

PROJECT USARO/WMU

BORING NO. MP1 SAMPLE NO. 4

DEPTH/ELEV 80-82 TECH. WWM

LABORATORY USAE WES - STF/GL DATE 08 SEP 96

TRIAXIAL COMPRESSION TEST REPORT

Fine gr clay, 94-100% Sw MP-1 #5, 95-97' All clay, no

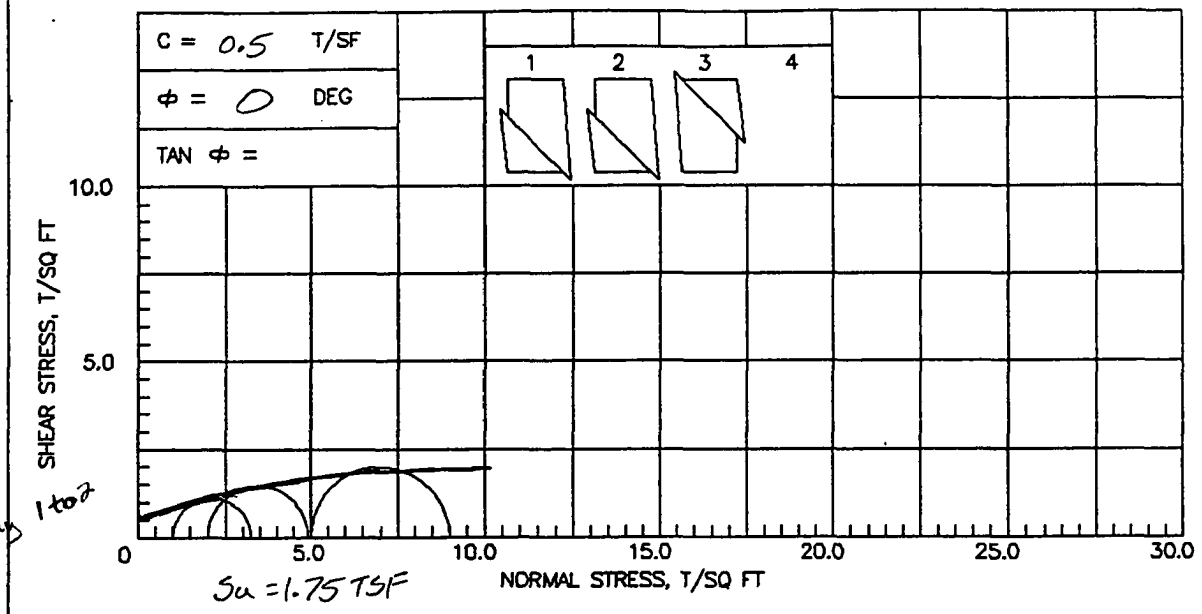

clay 1 to 2

Su = 1.75 TSF

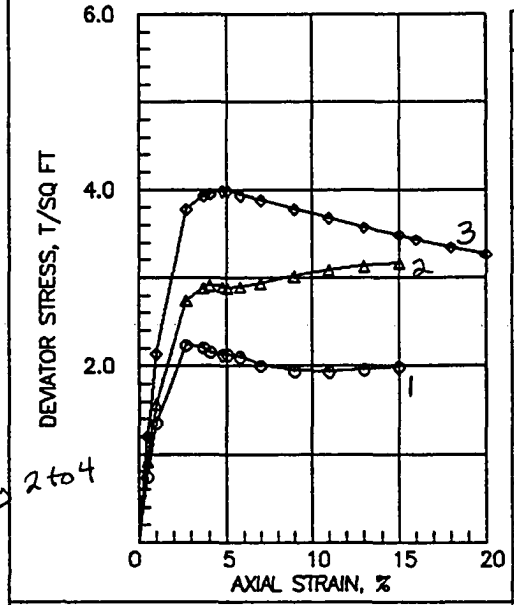

clay 2 to 4

SPECIMEN NO.		○ 1	△ 2	◇ 3	4
INITIAL	WATER CONTENT, %	24.7	24.7	25.4	
	DRY DENSITY, PCF	98.5	100.5	100.0	
	SATURATION, %	93.6	98.7	100+	
	VOID RATIO	.712	.677	.685	
BEFORE SHEAR	WATER CONTENT, %				
	DRY DENSITY, PCF				
	SATURATION, %				
	VOID RATIO				
	BACK PRESSURE, TSF				
CHAMBER PRESSURE, TSF		1.00	2.00	5.00	
MAX. DEV. STRESS, TSF		2.24	2.92	3.99	
TIME TO FAILURE, MIN.		8	12	14	
STRAIN RATE INCR., %					
INITIAL DIAMETER, IN.		1.37	1.37	1.38	
INITIAL HEIGHT, IN.		3.00	3.00	3.00	

CONTROLLED-STRAIN TEST

DESCRIPTION OF SPECIMENS: CLAY (CH), V FINE GR, BROWN W/ SAND SEAMS

LL	PL	PI	GS 2.70 (ESTIMATED)	UNDISTURBED SPECIMEN	Q TEST

REMARKS: SPEC 1 HAS SAND SEAM 1/2" THICK IN 1/16" SAND SEAMS IN MIDDLE. PARTINS

σ_{vc} = 5 TSF

PROJECT USARO/WMU

BORING NO. MP1 SAMPLE NO. 5

DEPTH/ELEV 95-97 TECH. WWM

LABORATORY USAE WES - STF/GL DATE 09 SEP 96

TRIAXIAL COMPRESSION TEST REPORT

Till, 75-88% Sw FA-1 #1, 21-22' No sample [illegible]

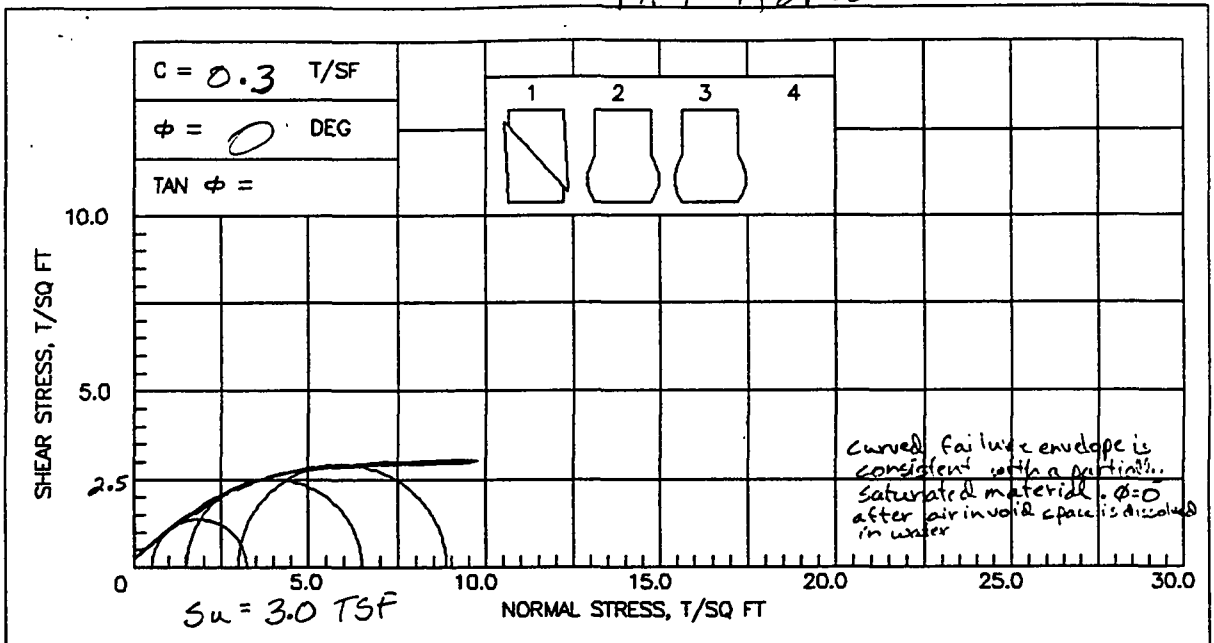

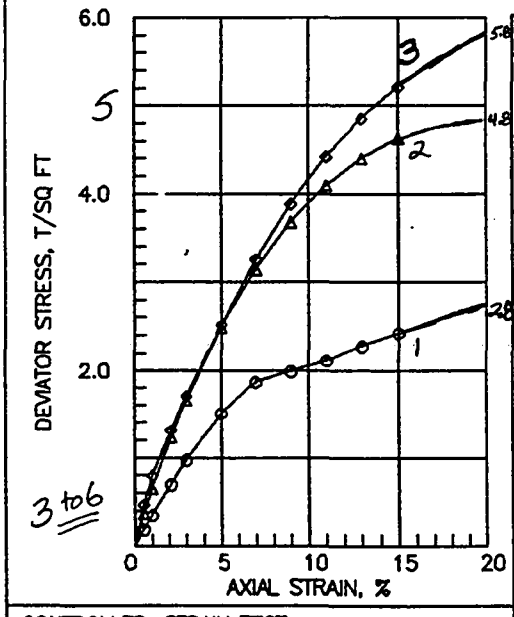

SPECIMEN NO.		○ 1	△ 2	○ 3	4
INITIAL	WATER CONTENT, %	8.3	8.3	8.2	
	DRY DENSITY, PCF	130.2	130.7	134.7	
	SATURATION, %	75.8	77.4	88.5	
	VOID RATIO	.295	.290	.251	
BEFORE SHEAR	WATER CONTENT, %				
	DRY DENSITY, PCF				
	SATURATION, %				
	VOID RATIO				
	BACK PRESSURE, TSF				
CHAMBER PRESSURE, TSF		.50	1.50	3.00	
MAX. DEV. STRESS, TSF		2.75	5.01	5.86	
TIME TO FAILURE, MIN.		55	59	59	
STRAIN RATE INCR., %					
INITIAL DIAMETER, IN.		1.37	1.37	1.38	
INITIAL HEIGHT, IN.		2.80	3.00	2.90	

CONTROLLED-STRAIN TEST

DESCRIPTION OF SPECIMENS: SANDY CLAY TILL (CL), PEBBLY

LL	PL	PI	GS 2.70 (ESTIMATED)	UNDISTURBED SPECIMEN	Q TEST

REMARKS: SPEC 1 EXTENSIVELY REPACKED DURING LIFT

σ_{vc} = 1.25 TSF

PROJECT USARO/WMU

BORING NO. FA1 SAMPLE NO. 1

DEPTH/ELEV 21-22 TECH. WWM

LABORATORY USAE WES - STF/GL DATE 09 SEP 96

TRIAXIAL COMPRESSION TEST REPORT

Sand/clay till (1), 9.2% Sw
Till (2,3), 80-85% Sw

116-1 #1, 18-20'

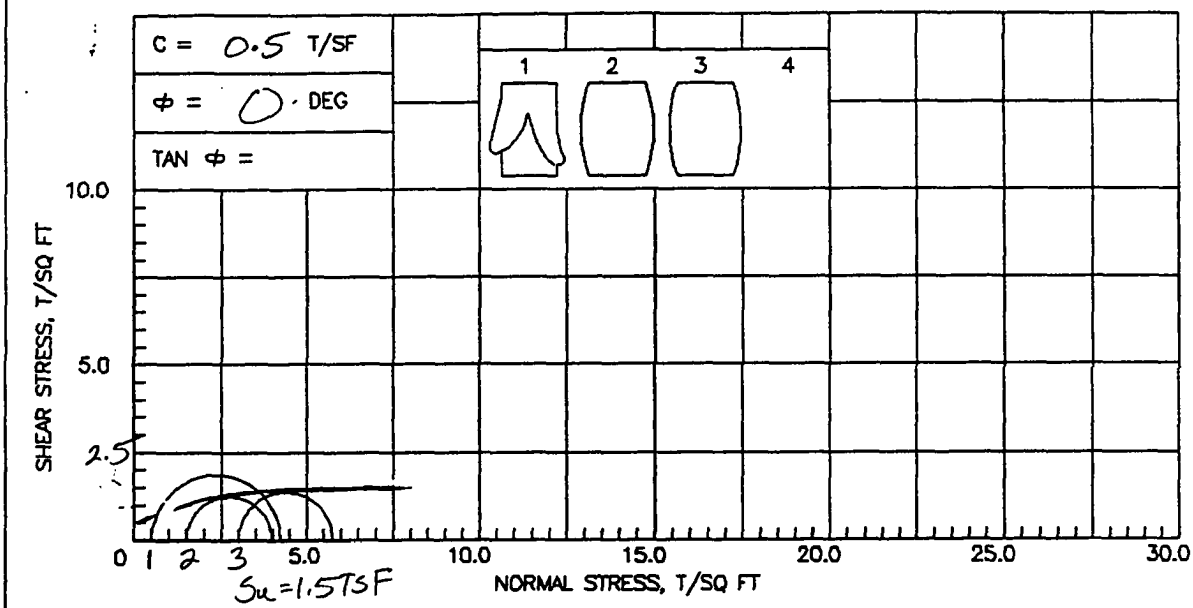

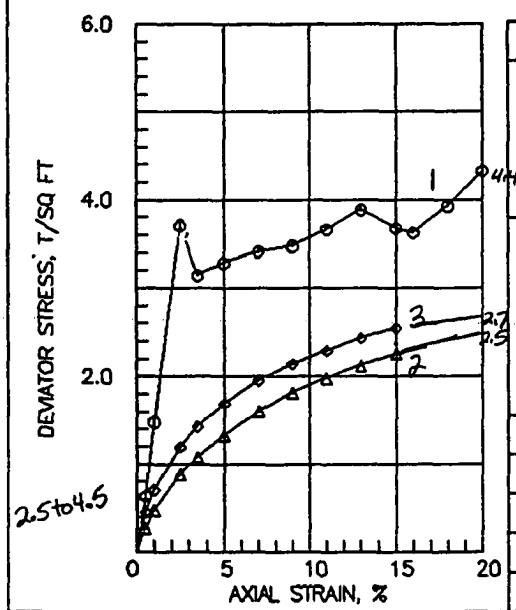

SPECIMEN NO.		○ 1	△ 2	◇ 3	4
INITIAL	WATER CONTENT, %	11.8	14.5	15.4	
	DRY DENSITY, PCF	125.3	113.1	113.4	
	SATURATION, %	92.2	79.8	85.5	
	VOID RATIO	.346	.491	.486	
BEFORE SHEAR	WATER CONTENT, %				
	DRY DENSITY, PCF				
	SATURATION, %				
	VOID RATIO				
	BACK PRESSURE, TSF				
CHAMBER PRESSURE, TSF		.50	1.50	3.00	
MAX. DEV. STRESS, TSF		3.71	2.47	2.75	
TIME TO FAILURE, MIN.		7	58	58	
STRAIN RATE INCR., %					
INITIAL DIAMETER, IN.		1.37	1.37	1.37	
INITIAL HEIGHT, IN.		3.00	3.00	3.00	

CONTROLLED-STRAIN TEST

DESCRIPTION OF SPECIMENS: SPEC 1 IS SAND/CLAY MIX, 2 & 3 ARE CLAY TILL

LL	PL	PI	GS 2.70 (ESTIMATED)	UNDISTURBED SPECIMEN	Q TEST

REMARKS: SPEC 1 WEAK, DIFFICULT TO TRIM – OTH

DISINTEGRATED DURING TRIMMING

PROJECT USARO/WMU

BORING NO. 116 – 1 SAMPLE NO. 1

DEPTH/ELEV 18–20 TECH. WWM

LABORATORY USAE WES – STF/GL DATE 10 SEP 96

TRIAXIAL COMPRESSION TEST REPORT

wet sandy clay (1,2), 97-100% Sw
Fine or clay w/ silt laminae (3,4), 98% Sw

WRA-1 #1, 63-65'

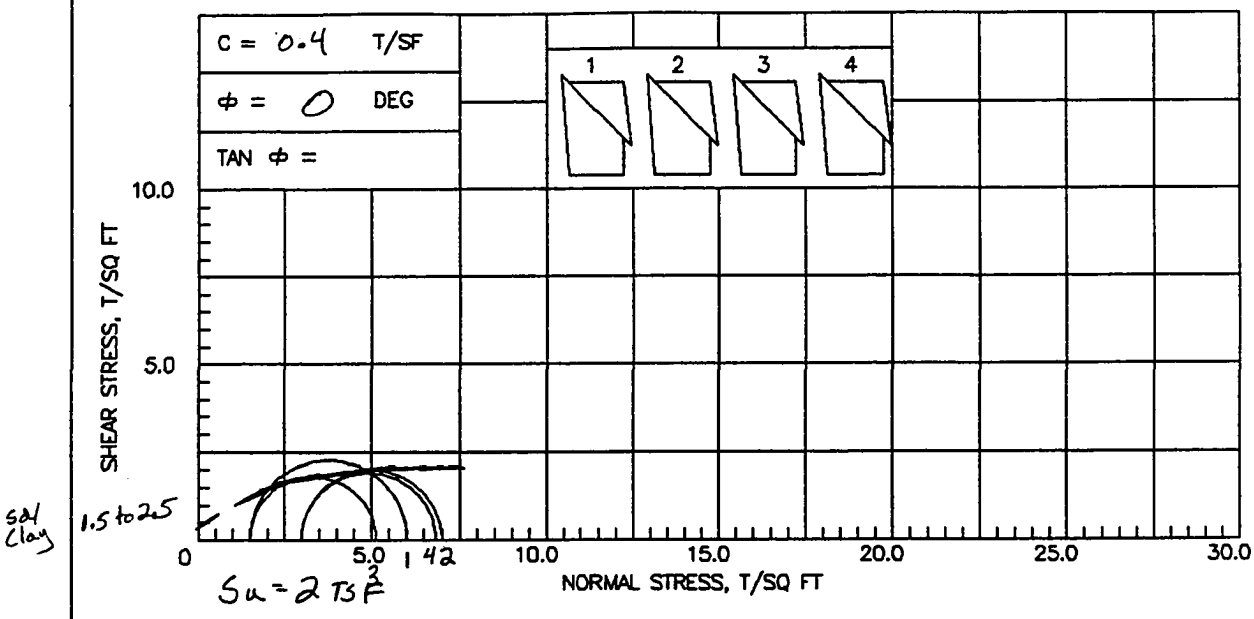

sd/clay 1.5 to 2.5

Su = 2 TSF

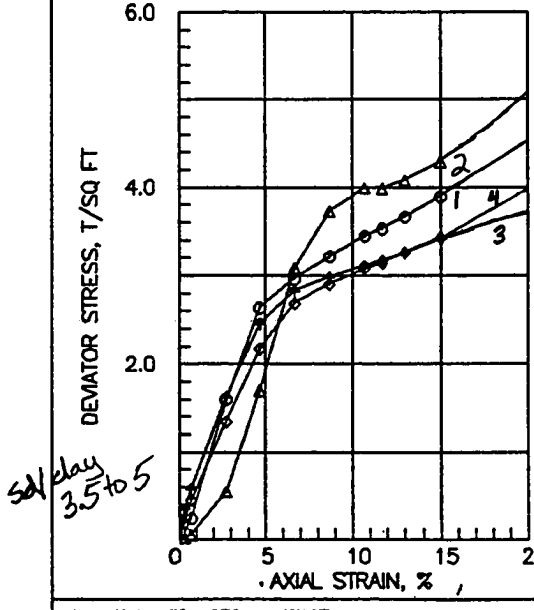

sd/clay 3.5 to 5

SPECIMEN NO.		○ 1	△ 2	◇ 3	+ 4
INITIAL	WATER CONTENT, %	17.9	18.1	19.4	19.5
	DRY DENSITY, PCF	112.4	118.5	109.8	109.9
	SATURATION, %	96.7	100+	97.9	98.6
	VOID RATIO	.499	.423	.536	.534
BEFORE SHEAR	WATER CONTENT, %				
	DRY DENSITY, PCF				
	SATURATION, %				
	VOID RATIO				
	BACK PRESSURE, TSF				
CHAMBER PRESSURE, TSF		1.50	3.00	1.50	3.00
MAX. DEV. STRESS, TSF		? 4.53	4.00	3.63	3.83
TIME TO FAILURE, MIN.		58	30	55	59
STRAIN RATE INCR., %					
INITIAL DIAMETER, IN.		1.41	1.38	1.37	1.37
INITIAL HEIGHT, IN.		2.90	2.90	2.80	3.00

CONTROLLED-STRAIN TEST

DESCRIPTION OF SPECIMENS: SPECS 1 & 2 HAVE 1.5" SAND OVER CLAY

LL	PL	PI	GS 2.70 (ESTIMATED)	UNDISTURBED SPECIMEN	Q TEST

REMARKS: SPECS 3 & 4 ARE LAMINATED FINE GR CL

PROJECT USARO/WMU

σ_{1c} = 3.5 TSF

BORING NO. WKA 1 SAMPLE NO. 1

DEPTH/ELEV 63-65 TECH. WWM

LABORATORY USAE WES - STF/GL DATE 10 SEP 96

TRIAXIAL COMPRESSION TEST REPORT

Appendix D

Consolidated-Undrained Triaxial Test Data From Undisturbed Samples

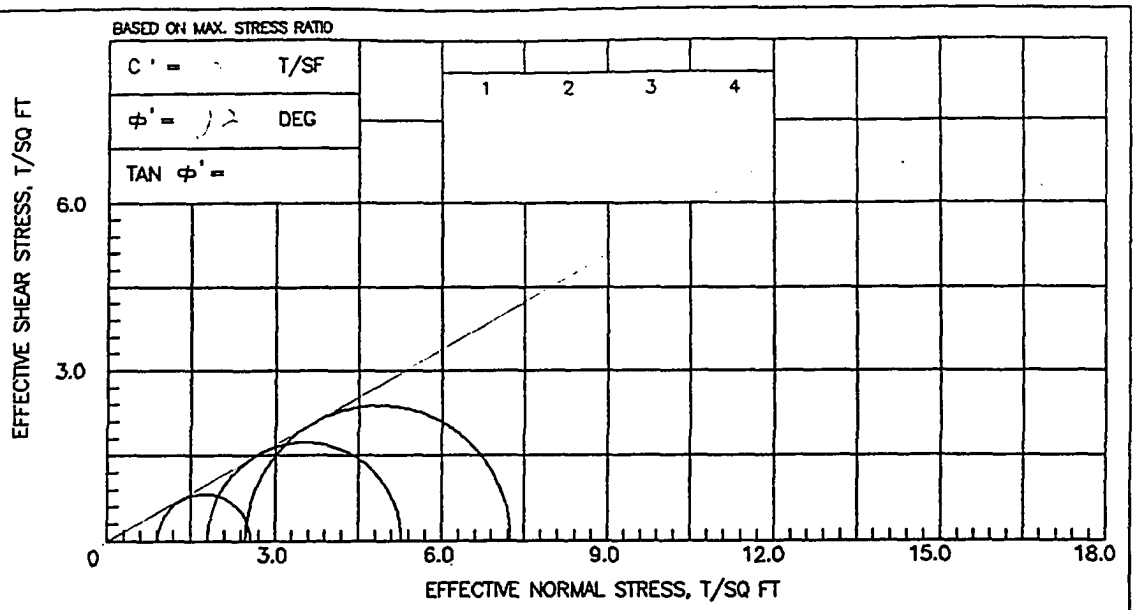

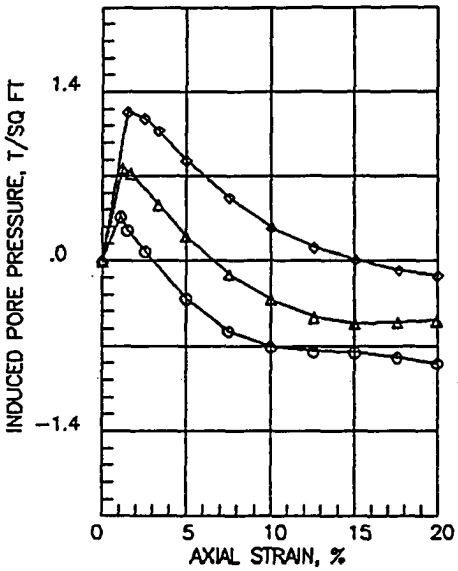

SPECIMEN NO.		○ 1	△ 2	◇ 3	4
INITIAL	WATER CONTENT, %	13.7	13.2	14.1	
	DRY DENSITY, PCF	123.8	125.4	122.6	
	SATURATION, %	100+	100+	100+	
	VOID RATIO	.362	.344	.374	
BEFORE SHEAR	WATER CONTENT, %	14.7	14.0	14.8	
	DRY DENSITY, PCF	125.2	128.2	125.5	
	SATURATION, %	100+	100+	100+	
	VOID RATIO	.346	.315	.343	
	BACK PRESS., TSF	4.32	4.32	4.32	
@ σ_1'/σ_3' MAX	MIN PRIN EFF STRESS, TSF	.92	1.80	2.47	
	DEV. STRESS, TSF	1.65	3.47	4.77	
	TIME TO FAILURE, MIN.	165	321	484	
RATE OF STRAIN, %/MIN		.016	.016	.016	
INITIAL DIAMETER, IN.		1.36	1.36	1.36	
INITIAL HEIGHT, IN.		3.00	3.00	3.00	

CONTROLLED-STRAIN TEST

DESCRIPTION OF SPECIMENS: SANDY CLAY TILL (CL), GRAY

LL 24	PL 14	PI 10	GS 2.70 (ESTIMATED)	UNDISTURBED SPECIMEN	$\bar{R}$ TEST

REMARKS:	PROJECT USARO/WMU	
	R TEST 1, MIAMI PARK	
	BORING NO. MP-1	SAMPLE NO. 1
	DEPTH/ELEV 20-22'	TECH. WWM
	LABORATORY USAE WES - STF/GL	DATE 02 OCT 96
	$\bar{R}$-TRIAXIAL COMPRESSION TEST REPORT	

MP-1 #1, 20-22'

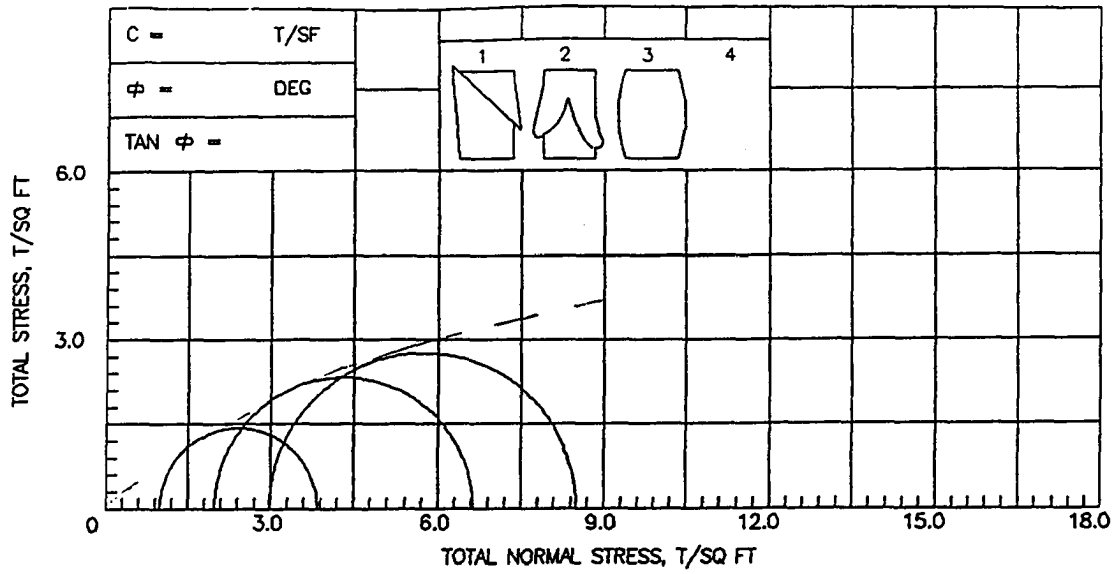

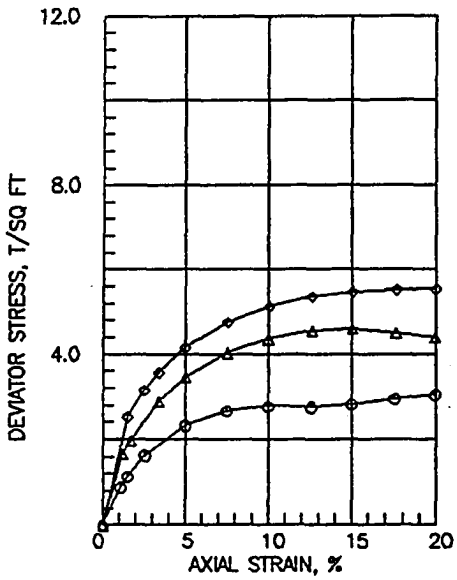

SPECIMEN NO.		○ 1	△ 2	◇ 3	4
INITIAL	WATER CONTENT, %	13.7	13.2	14.1	
	DRY DENSITY, PCF	123.8	125.4	122.6	
	SATURATION, %	100+	100+	100+	
	VOID RATIO	.362	.344	.374	
BEFORE SHEAR	WATER CONTENT, %	14.7	14.0	14.8	
	DRY DENSITY, PCF	125.2	128.2	125.5	
	SATURATION, %	100+	100+	100+	
	VOID RATIO	.346	.315	.343	
	BACK PRESS., TSF	4.32	4.32	4.32	
MIN. PRIN. STRESS, TSF		1.00	2.00	3.00	
MAX. DEV. STRESS, TSF		2.83	4.62	5.49	
TIME TO FAILURE, MIN.		960	965	969	
RATE OF STRAIN, %/MIN		.016	.016	.016	
INITIAL DIAMETER, IN.		1.36	1.36	1.36	
INITIAL HEIGHT, IN.		3.00	3.00	3.00	

CONTROLLED-STRAIN TEST

DESCRIPTION OF SPECIMENS: SANDY CLAY TILL (CL), GRAY

LL 24	PL 14	PI 10	GS 2.70 (ESTIMATED)	UNDISTURBED SPECIMEN	$\bar{R}$ TEST

REMARKS:	PROJECT USARO/WMU	
	R TEST 1, MIAMI PARK	
	BORING NO. MP-1	SAMPLE NO. 1
	DEPTH/ELEV 20-22'	TECH. WWM
	LABORATORY USAE WES - STF/GL	DATE 02 OCT 96
	$\bar{R}$-TRIAXIAL COMPRESSION TEST REPORT	

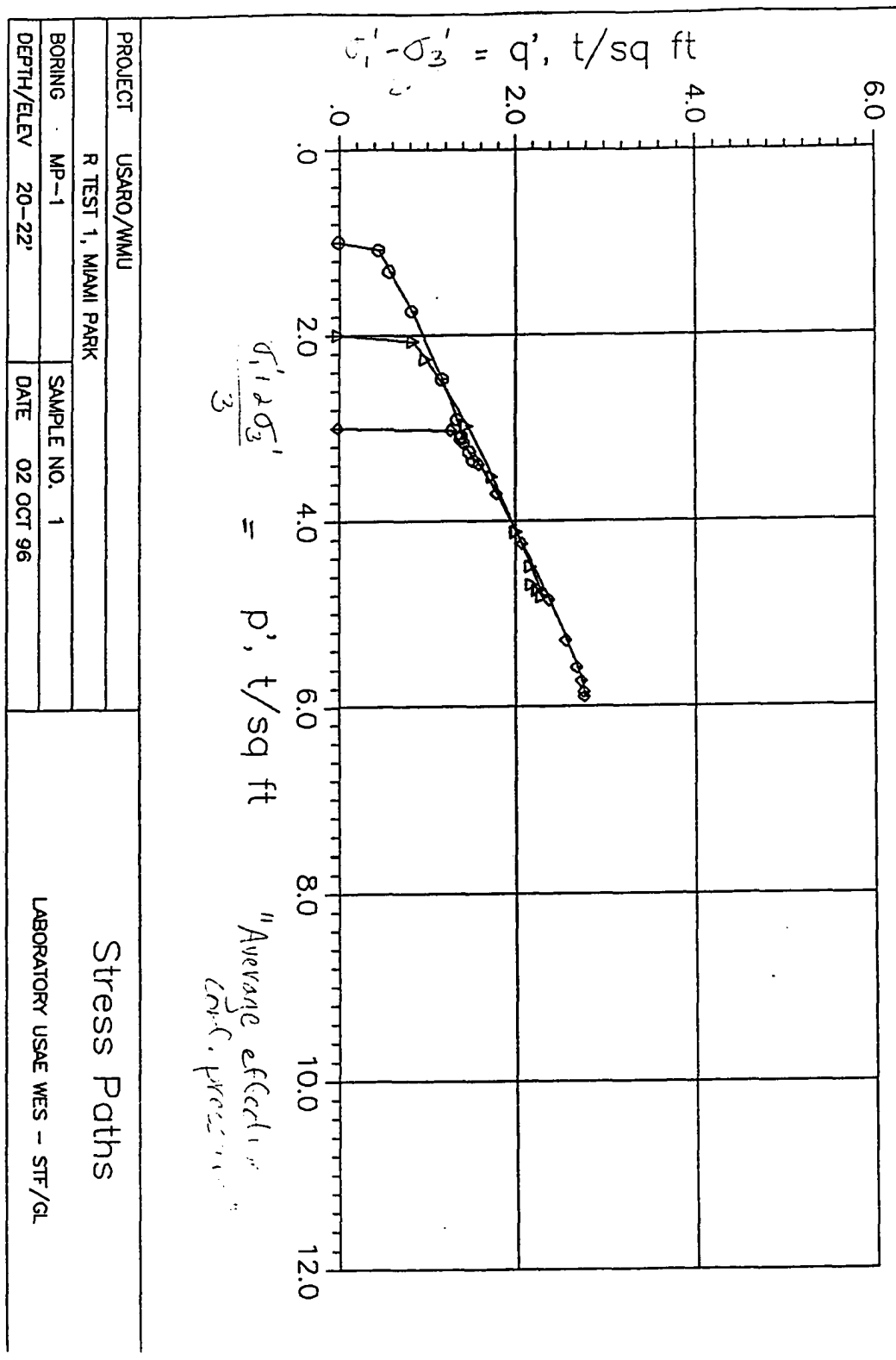

PROJECT USARO/WMU	
R TEST 1, MIAMI PARK	
BORING MP-1	SAMPLE NO. 1
DEPTH/ELEV 20-22'	DATE 02 OCT 96

Stress Paths

LABORATORY USAE WES - STF/GL

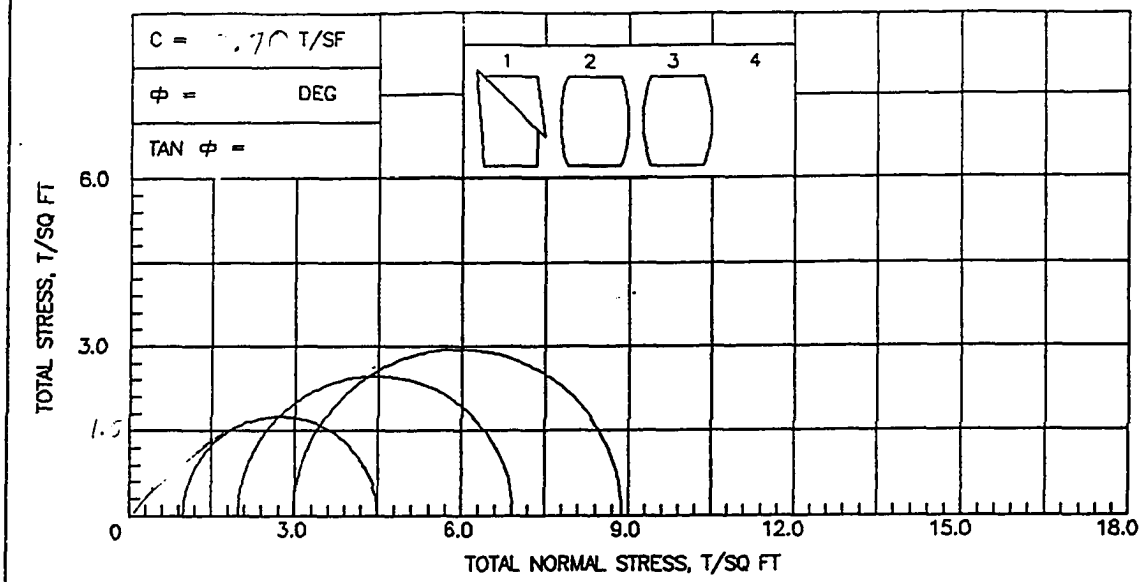

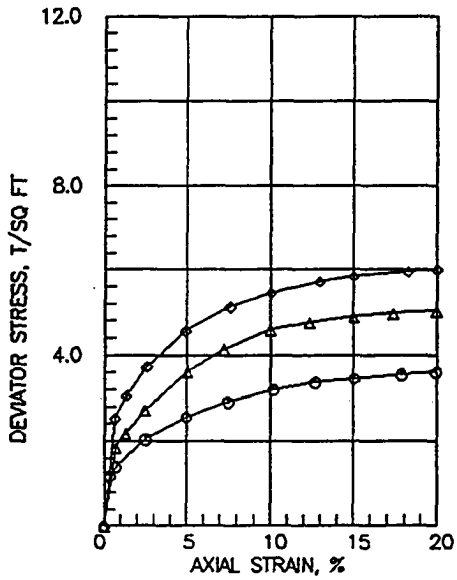

SPECIMEN NO.		○ 1	△ 2	◇ 3	4
INITIAL	WATER CONTENT, %	13.9	14.4	14.1	
	DRY DENSITY, PCF	128.1	122.7	124.0	
	SATURATION, %	100+	100+	100+	
	VOID RATIO	.316	.374	.360	
BEFORE SHEAR	WATER CONTENT, %	16.0	16.2	14.2	
	DRY DENSITY, PCF	133.1	126.3	135.4	
	SATURATION, %	100+	100+	100+	
	VOID RATIO	.267	.335	.245	
	BACK PRESS., TSF	4.32	4.32	4.32	
MIN. PRIN. STRESS, TSF		1.00	2.00	3.00	
MAX. DEV. STRESS, TSF		3.47	4.91	5.86	
TIME TO FAILURE, MIN.		1030	997	1044	
RATE OF STRAIN, %/MIN		.015	.015	.015	
INITIAL DIAMETER, IN.		1.31	1.37	1.36	
INITIAL HEIGHT, IN.		3.00	3.00	3.00	

CONTROLLED-STRAIN TEST

DESCRIPTION OF SPECIMENS: SANDY CLAY TILL (CL), GRAY

LL 25	PL 14	PI 11	GS 2.70 (ESTIMATED)	UNDISTURBED SPECIMEN	$\bar{R}$ TEST

REMARKS:

PROJECT USARO/WMU

R TEST 2, CONSUMERS POWER

BORING NO. CP-2 | SAMPLE NO. 3

DEPTH/ELEV 53-55' | TECH. WWM

LABORATORY USAE WES - STF/GL | DATE 02 OCT 96

$\bar{R}$-TRIAXIAL COMPRESSION TEST REPORT

BASED ON MAX. STRESS RATIO

C ' = T/SF

φ' = 27 DEG

TAN φ' =

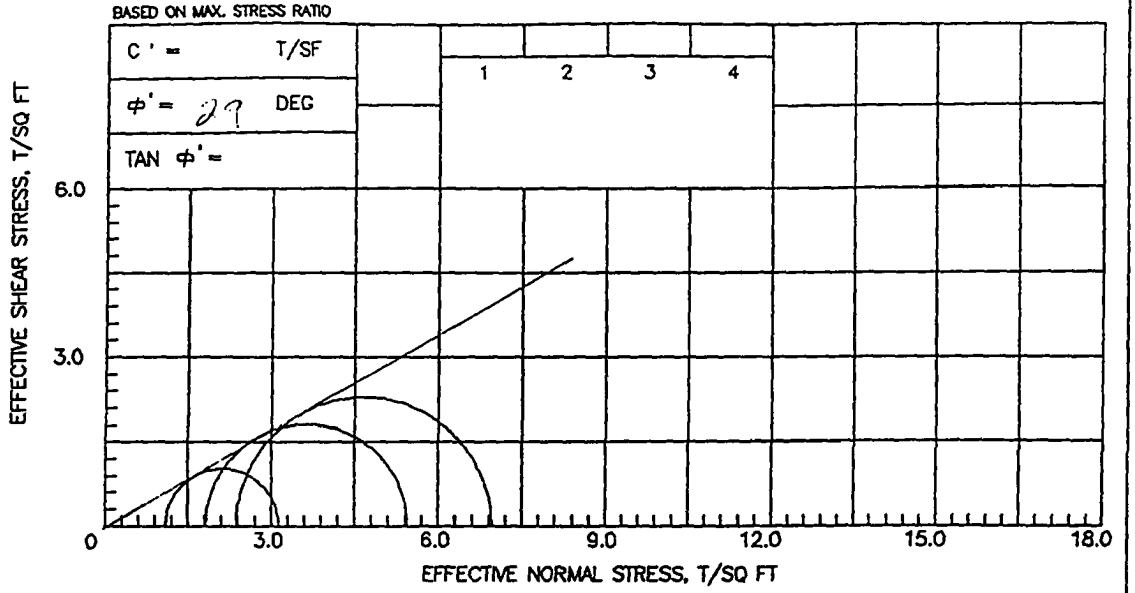

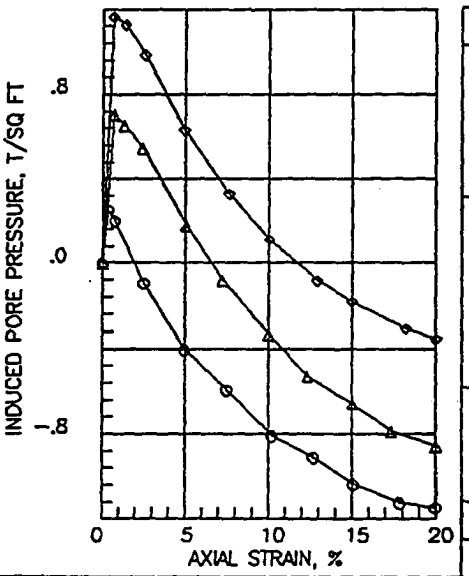

SPECIMEN NO.		⊙ 1	△ 2	◇ 3	4
INITIAL	WATER CONTENT, %	13.9	14.4	14.1	
	DRY DENSITY, PCF	128.1	122.7	124.0	
	SATURATION, %	100+	100+	100+	
	VOID RATIO	.316	.374	.360	
BEFORE SHEAR	WATER CONTENT, %	16.0	16.2	14.2	
	DRY DENSITY, PCF	133.1	126.3	135.4	
	SATURATION, %	100+	100+	100+	
	VOID RATIO	.267	.335	.245	
	BACK PRESS., TSF	4.32	4.32	4.32	
@ σ_1'/σ_3' MAX	MIN PRIN EFF STRESS, TSF	1.09	1.82	2.37	
	DEV. STRESS, TSF	2.05	3.63	4.58	
	TIME TO FAILURE, MIN.	171	333	344	
RATE OF STRAIN, %/MIN		.015	.015	.015	
INITIAL DIAMETER, IN.		1.31	1.37	1.36	
INITIAL HEIGHT, IN.		3.00	3.00	3.00	

CONTROLLED-STRAIN TEST

DESCRIPTION OF SPECIMENS: SANDY CLAY TILL (CL), GRAY

LL 25	PL 14	PI 11	GS 2.70 (ESTIMATED)	UNDISTURBED SPECIMEN	$\bar{R}$ TEST

REMARKS:

PROJECT USARO/WMU

R TEST 2, CONSUMERS POWER

BORING NO. CP-2 SAMPLE NO. 3

DEPTH/ELEV 53-55' TECH. WWM

LABORATORY USAE WES - STF/GL DATE 02 OCT 96

$\bar{R}$-TRIAXIAL COMPRESSION TEST REPORT

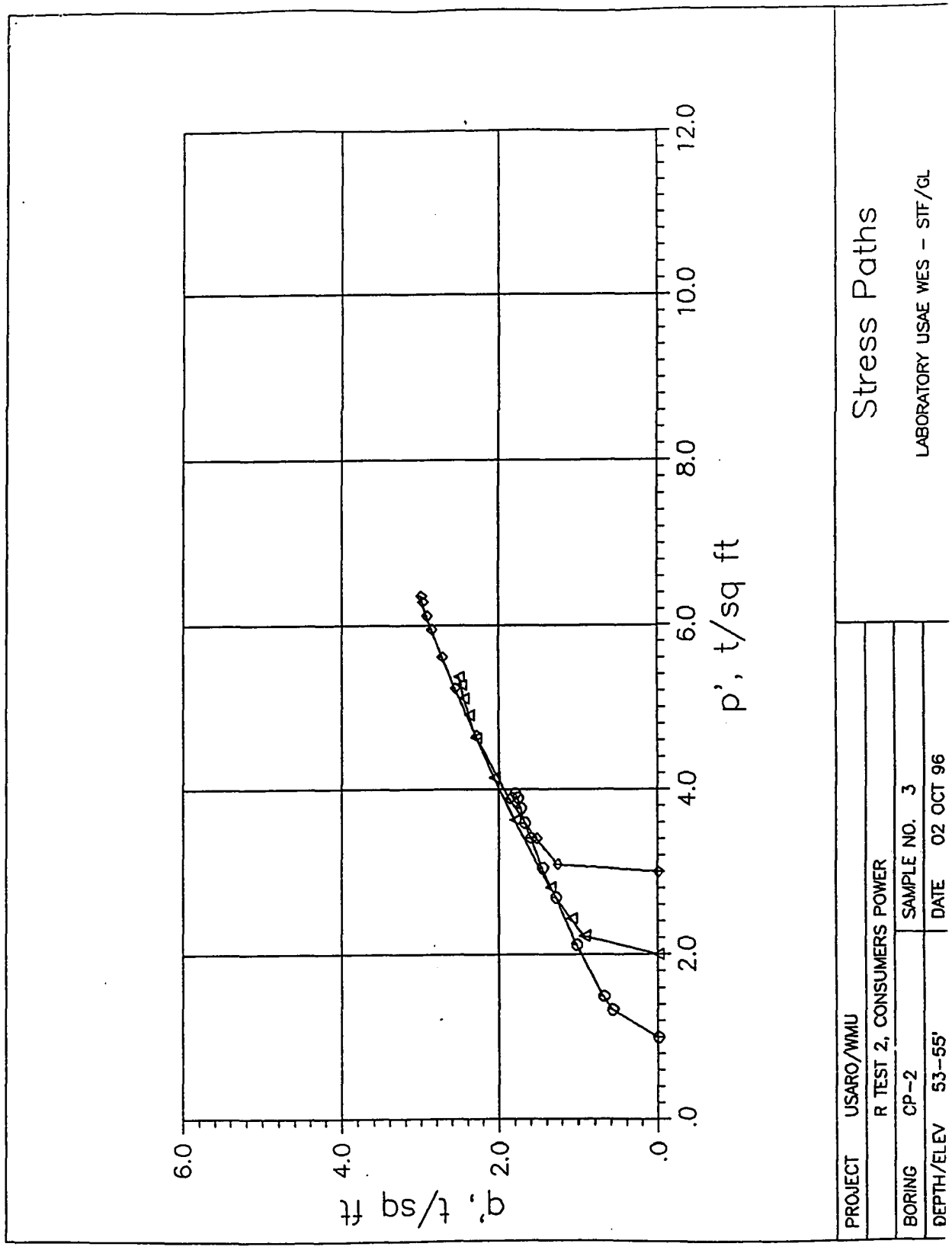

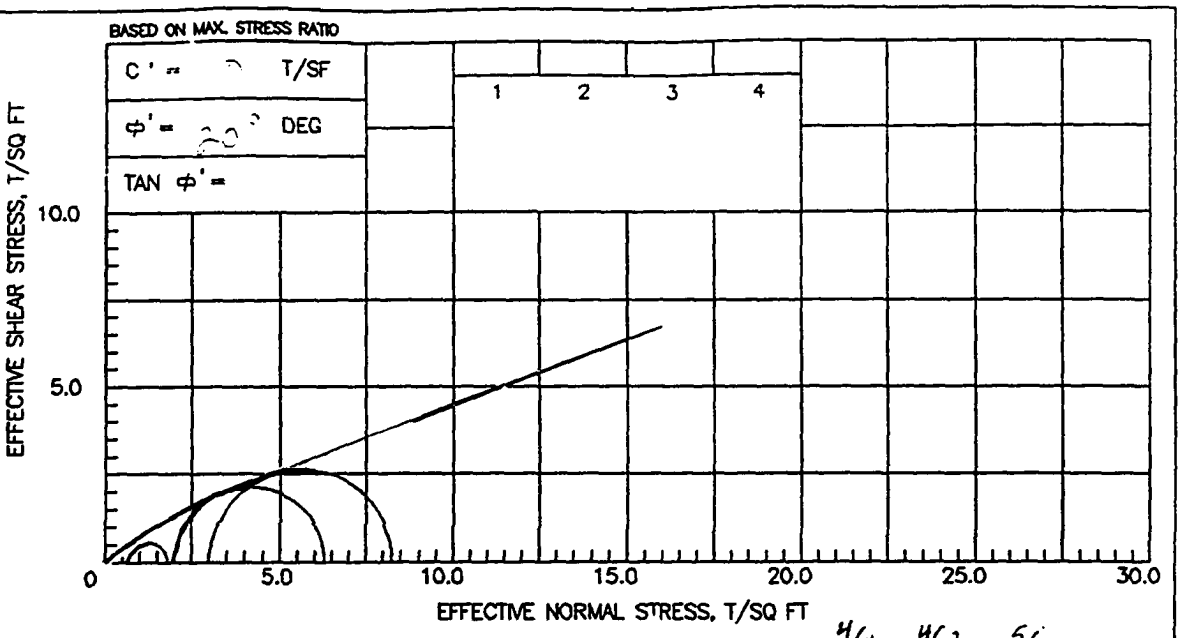

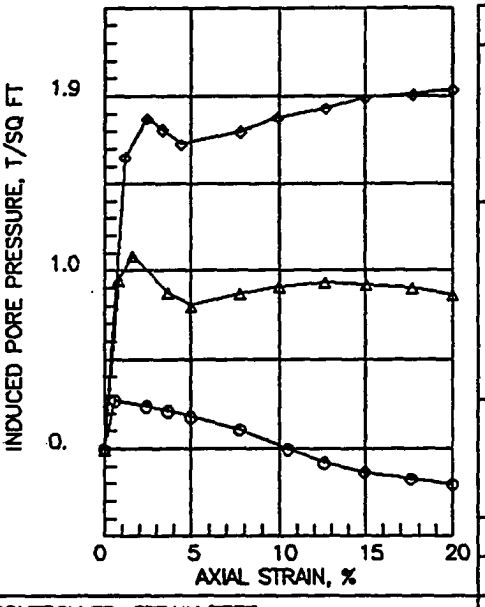

SPECIMEN NO.		○ 1	△ 2	◇ 3	4
INITIAL	WATER CONTENT, %	26.9	27.3	24.7	
	DRY DENSITY, PCF	99.6	97.7	99.6	
	SATURATION, %	100+	100+	96.2	
	VOID RATIO	.693	.725	.693	
BEFORE SHEAR	WATER CONTENT, %	28.1	27.0	25.6	
	DRY DENSITY, PCF	101.0	101.5	102.7	
	SATURATION, %	100+	100+	100+	
	VOID RATIO	.689	.662	.641	
	BACK PRESS., TSF	4.32	4.32	4.32	
@ σ_1'/σ_3' MAX	MIN PRIN EFF STRESS, TSF	.70	2.04	3.01	
	DEV. STRESS, TSF	1.12	4.25	5.25	
	TIME TO FAILURE, MIN.	38	236	214	
RATE OF STRAIN, %/MIN		.016	.016	.016	
INITIAL DIAMETER, IN.		1.35	1.36	1.36	
INITIAL HEIGHT, IN.		3.00	3.00	3.00	

4C1 4C2 5C1

CONTROLLED-STRAIN TEST

DESCRIPTION OF SPECIMENS: CLAY (CL), BROWN, V. FINE GR

LL 48	PL 18	PI 30	GS 2.70 (ESTIMATED)	UNDISTURBED SPECIMEN	$\bar{R}$ TEST

REMARKS:

PROJECT USARO/WMU

R TEST 3, MIAMI PARK

BORING NO. MP-1 SAMPLE NO. 4/5

DEPTH/ELEV 80-82,95-97 TECH. WWM

LABORATORY USAE WES - STF/GL DATE 02 OCT 96

$\bar{R}$-TRIAXIAL COMPRESSION TEST REPORT

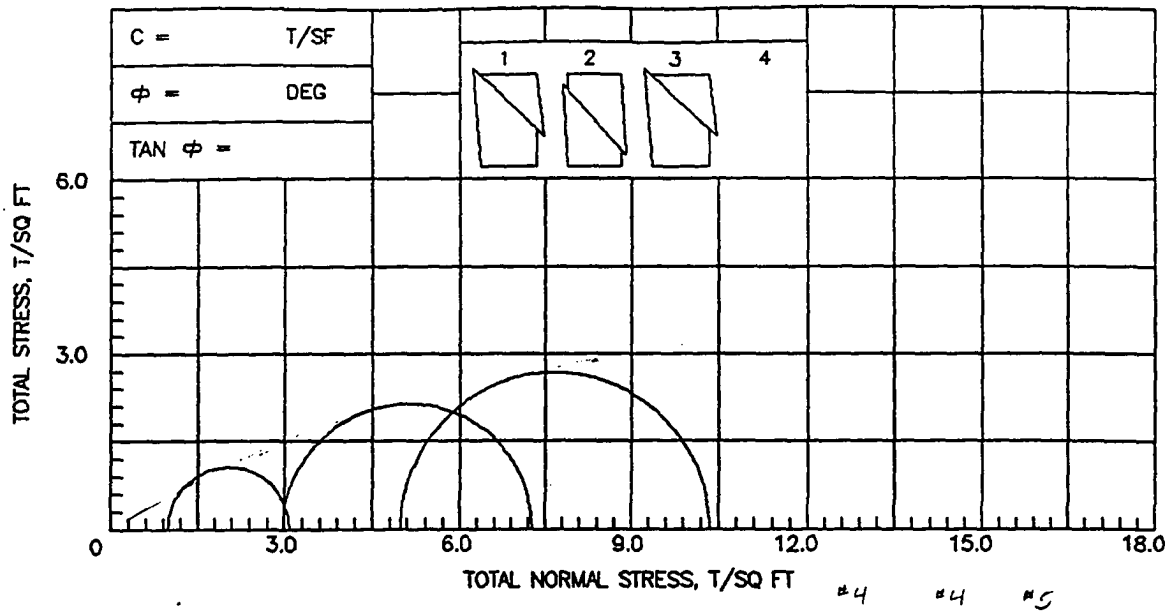

#4 #4 #5

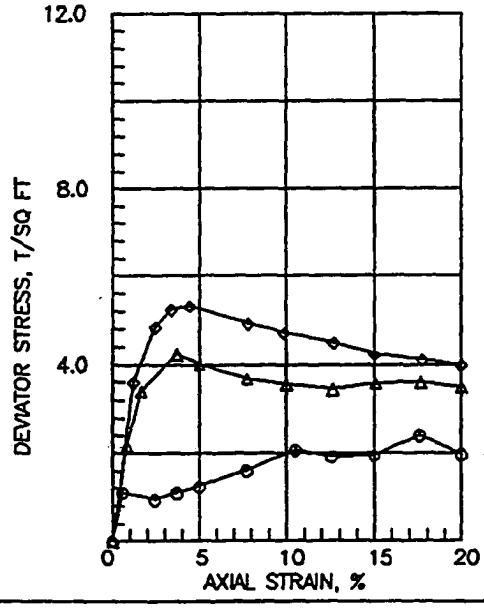

SPECIMEN NO.		⊙ 1	△ 2	◇ 3	4
INITIAL	WATER CONTENT, %	26.9	27.3	24.7	
	DRY DENSITY, PCF	99.6	97.7	99.6	
	SATURATION, %	100+	100+	96.2	
	VOID RATIO	.693	.725	.693	
BEFORE SHEAR	WATER CONTENT, %	28.1	27.0	25.6	
	DRY DENSITY, PCF	101.0	101.5	102.7	
	SATURATION, %	100+	100+	100+	
	VOID RATIO	.669	.662	.641	
	BACK PRESS., TSF	4.32	4.32	4.32	
MIN. PRIN. STRESS, TSF		1.00	3.00	5.00	
MAX. DEV. STRESS, TSF		2.08	4.25	5.33	
TIME TO FAILURE, MIN.		665	236	284	
RATE OF STRAIN, %/MIN		.016	.016	.016	
INITIAL DIAMETER, IN.		1.35	1.36	1.36	
INITIAL HEIGHT, IN.		3.00	3.00	3.00	

CONTROLLED-STRAIN TEST

DESCRIPTION OF SPECIMENS: CLAY (CL), BROWN, V. FINE GR

LL 48	PL 18	PI 30	GS 2.70 (ESTIMATED)	UNDISTURBED SPECIMEN	$\bar{R}$ TEST

REMARKS: Atterburg limits from MP-1 #4 reflect high clay content

PROJECT USARO/WMU

R TEST 3, MIAMI PARK

BORING NO. MP-1 SAMPLE NO. 4/5

DEPTH/ELEV 80-82,95-97 TECH. WWM

LABORATORY USAE WES - STF/GL DATE 02 OCT 96

$\bar{R}$-TRIAXIAL COMPRESSION TEST REPORT

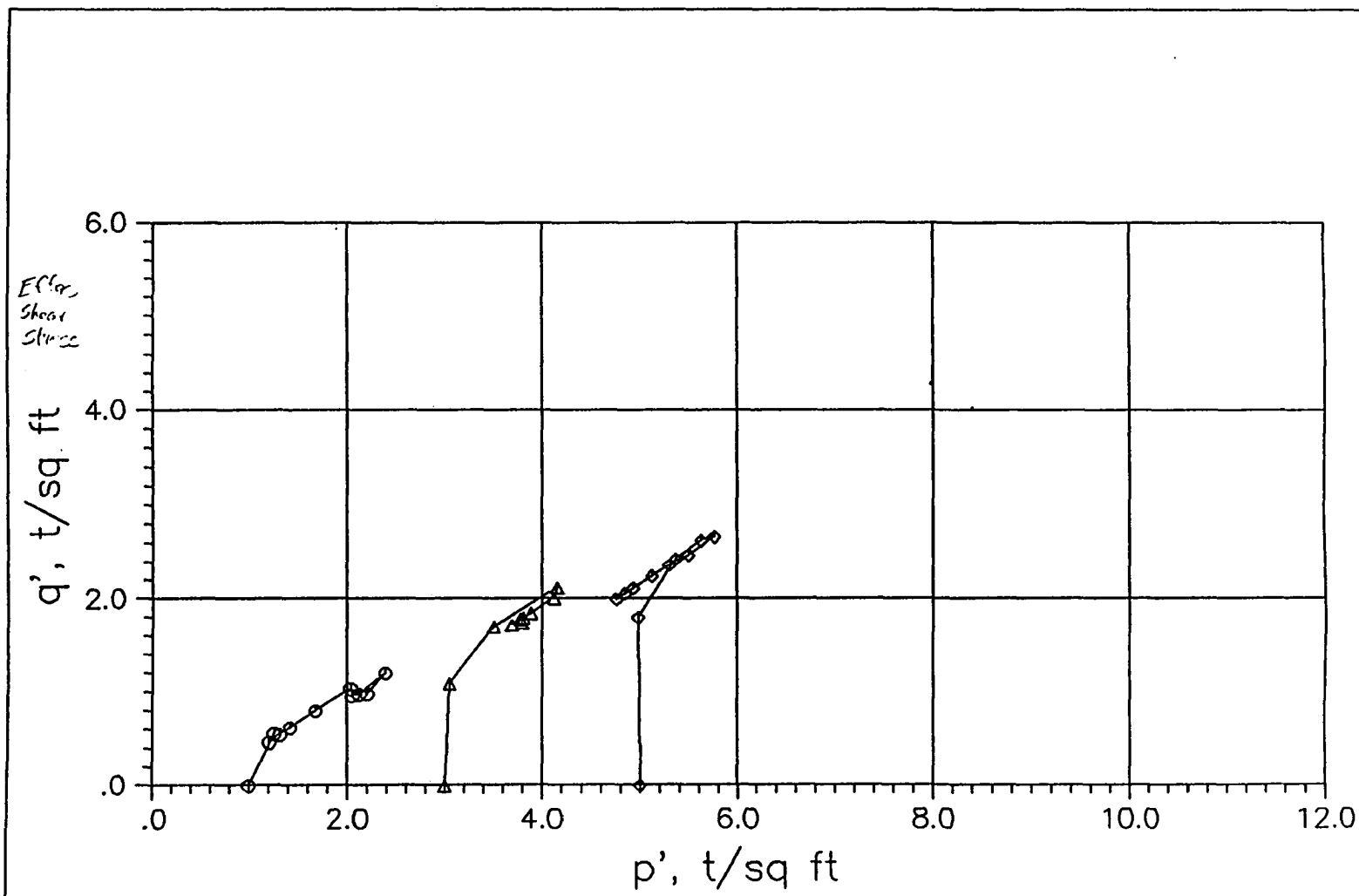

PROJECT	USARO/WMU	
	R TEST 3, MIAMI PARK	
BORING	MP-1	SAMPLE NO. 4/5

Stress Paths

LABORATORY USAE WES – STF/GL

Sd/clay 230

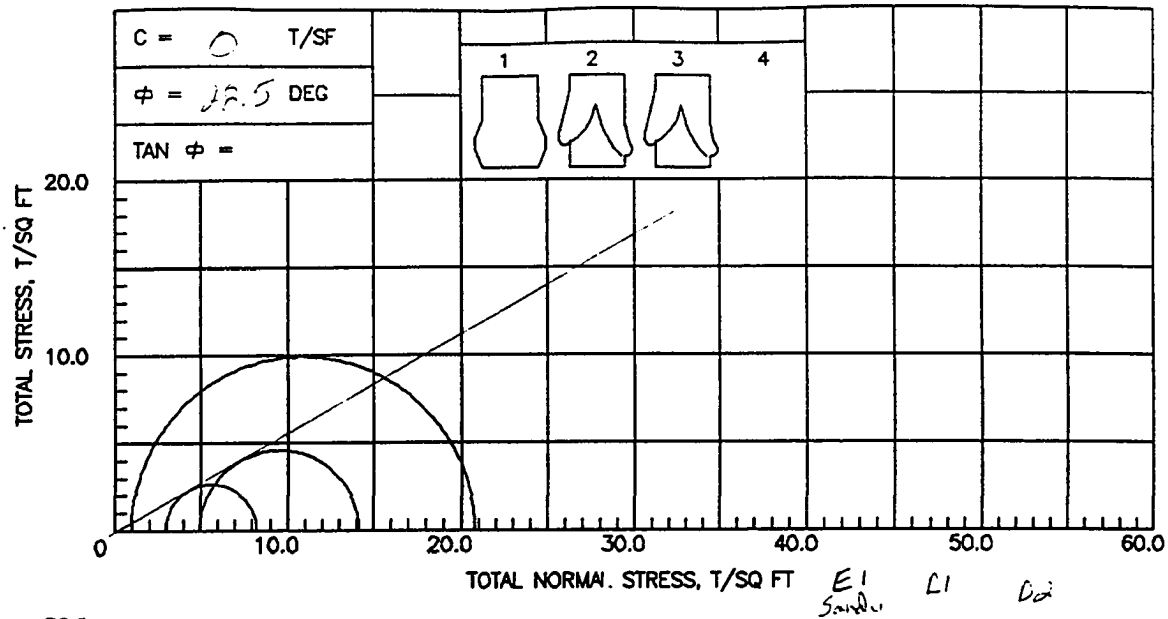

E1 Sandy L1 D2

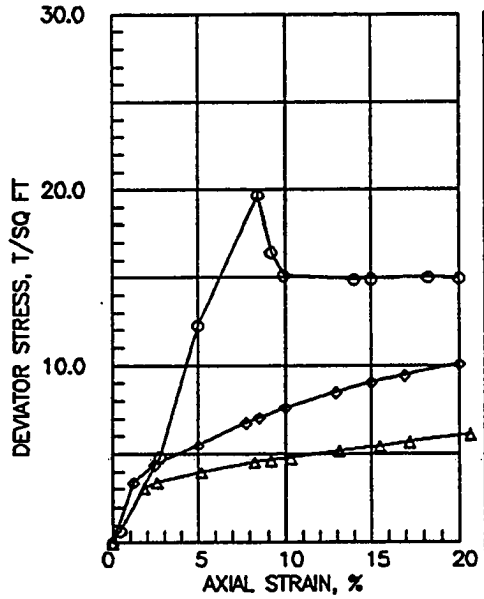

SPECIMEN NO.		○ 1	△ 2	◇ 3	4
INITIAL	WATER CONTENT, %	23.0	23.1	21.8	
	DRY DENSITY, PCF	106.9	104.2	108.2	
	SATURATION, %	100+	100+	100+	
	VOID RATIO	.566	.606	.547	
BEFORE SHEAR	WATER CONTENT, %	18.9	21.6	20.6	
	DRY DENSITY, PCF	107.8	108.3	112.5	
	SATURATION, %	91.6	100+	100+	
	VOID RATIO	.552	.544	.488	
	BACK PRESS., TSF	4.32	4.32	4.32	
MIN. PRIN. STRESS, TSF		1.00	3.00	5.00	
MAX. DEV. STRESS, TSF		19.71	5.20	9.07	
TIME TO FAILURE, MIN.		555	849	1002	
RATE OF STRAIN, %/MIN		.015	.016	.015	
INITIAL DIAMETER, IN.		1.39	1.37	1.34	
INITIAL HEIGHT, IN.		2.69	2.90	2.96	

CONTROLLED–STRAIN TEST

DESCRIPTION OF SPECIMENS: INTERBEDDED SILT/SAND AND FINE GR CLAY, SPEC 1

PARTICULARLY SANDY

From CP-2, 5A

LL 39 | PL 15 | PI 24 | GS 2.68 (ESTIMATED) | UNDISTURBED SPECIMEN | R̄ TEST

REMARKS: Atterburg limits from the LL lift from MP-1 #4 may not reflect this sample

PROJECT USARO/WMU

R TEST 4, MIAMI PARK

BORING NO. MP–1 | SAMPLE NO. 4

DEPTH/ELEV 80–82 | TECH. WWM

LABORATORY USAE WES – STF/GL | DATE 02 OCT 96

R̄–TRIAXIAL COMPRESSION TEST REPORT

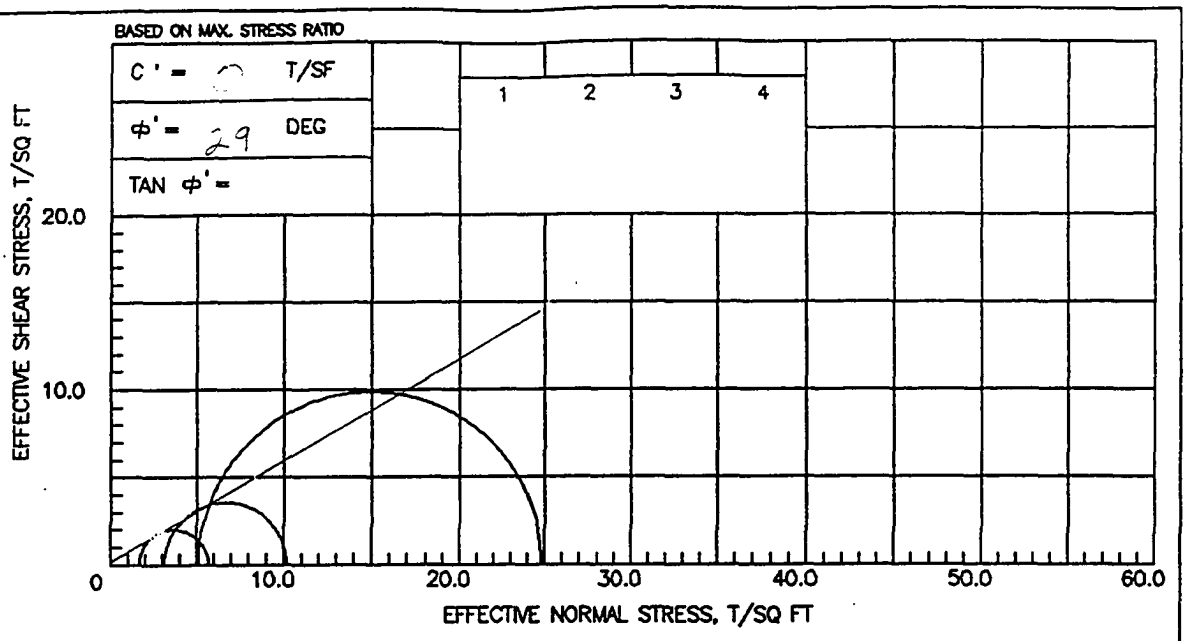

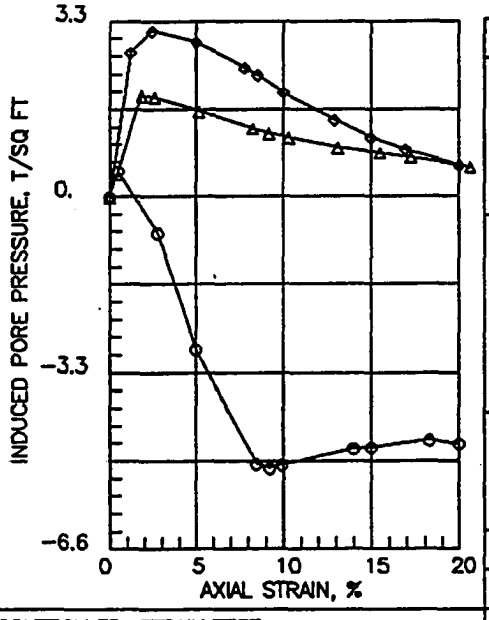

SPECIMEN NO.		○ 1	△ 2	◇ 3	4
INITIAL	WATER CONTENT, %	23.0	23.1	21.8	
	DRY DENSITY, PCF	106.9	104.2	108.2	
	SATURATION, %	100+	100+	100+	
	VOID RATIO	.566	.606	.547	
BEFORE SHEAR	WATER CONTENT, %	18.9	21.6	20.6	
	DRY DENSITY, PCF	107.8	108.3	112.5	
	SATURATION, %	91.6	100+	100+	
	VOID RATIO	.552	.544	.488	
	BACK PRESS., TSF	4.32	4.32	4.32	
@ σ_1'/σ_3' MAX	MIN PRIN EFF STRESS, TSF	5.09	1.68	3.12	
	DEV. STRESS, TSF	19.71	4.00	7.08	
	TIME TO FAILURE, MIN.	555	334	570	
RATE OF STRAIN, %/MIN		.015	.016	.015	
INITIAL DIAMETER, IN.		1.39	1.37	1.34	
INITIAL HEIGHT, IN.		2.69	2.90	2.96	

CONTROLLED-STRAIN TEST

DESCRIPTION OF SPECIMENS: INTERBEDDED SILT/SAND AND FINE GR CLAY, SPEC 1

PARTICULARLY SANDY

LL 18	PL 15	PI 3	GS 2.68 (ESTIMATED)	UNDISTURBED SPECIMEN	$\bar{R}$ TEST

REMARKS: Here appropriate is description of #4 than original #1-1 #1 fine-gr clay w/ [illegible]

PROJECT USARO/WMU

R TEST 4, MIAMI PARK

BORING NO. MP-1 SAMPLE NO. 4

DEPTH/ELEV 80-82 TECH. WWM

LABORATORY USAE WES - STF/GL DATE 02 OCT 96

$\bar{R}$-TRIAXIAL COMPRESSION TEST REPORT

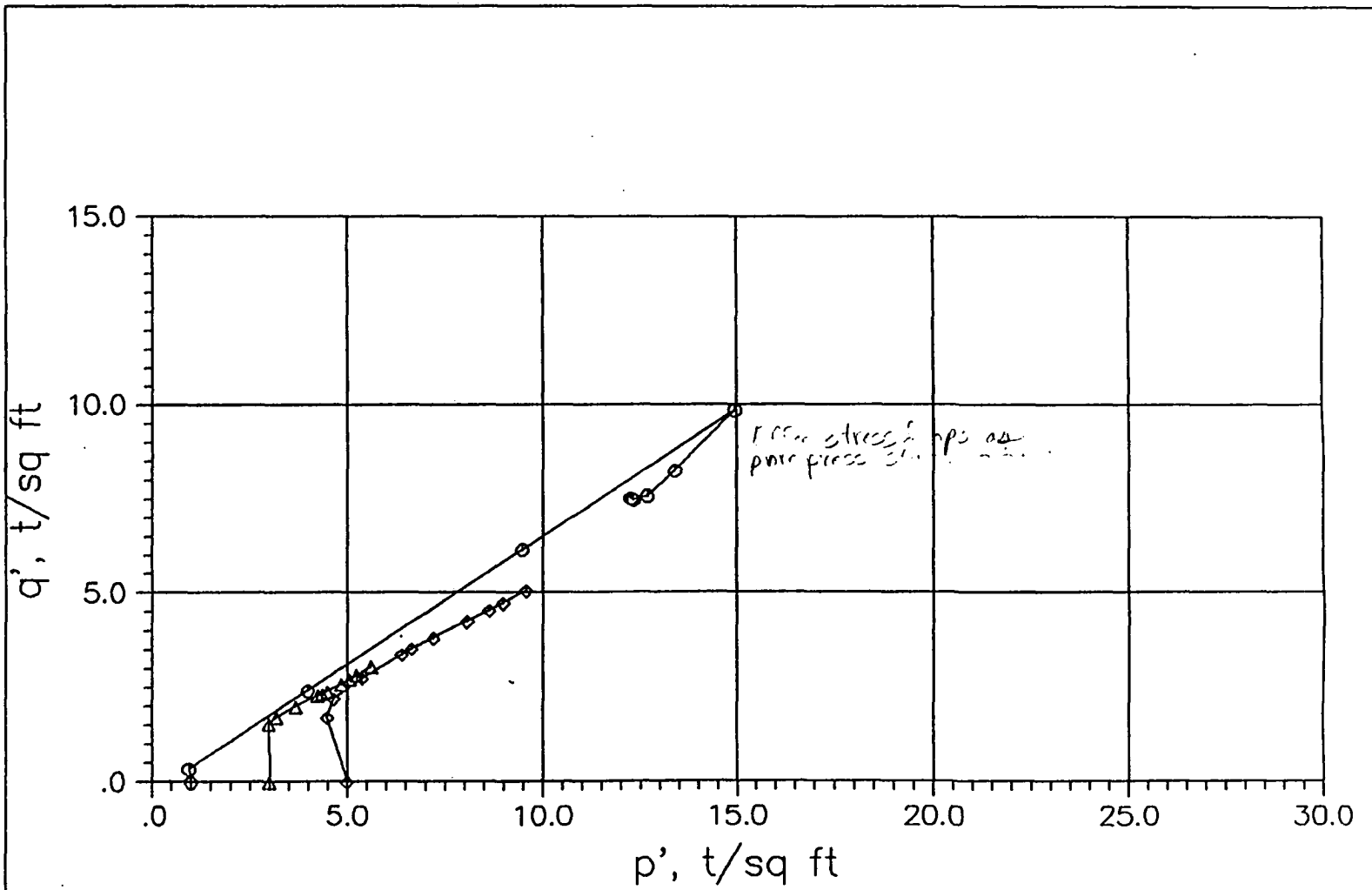

232

PROJECT	USARO/WMU
	R TEST 4, MIAMI PARK
BORING MP-1	SAMPLE NO. 4

Stress Paths

LABORATORY USAE WES – STF/GL

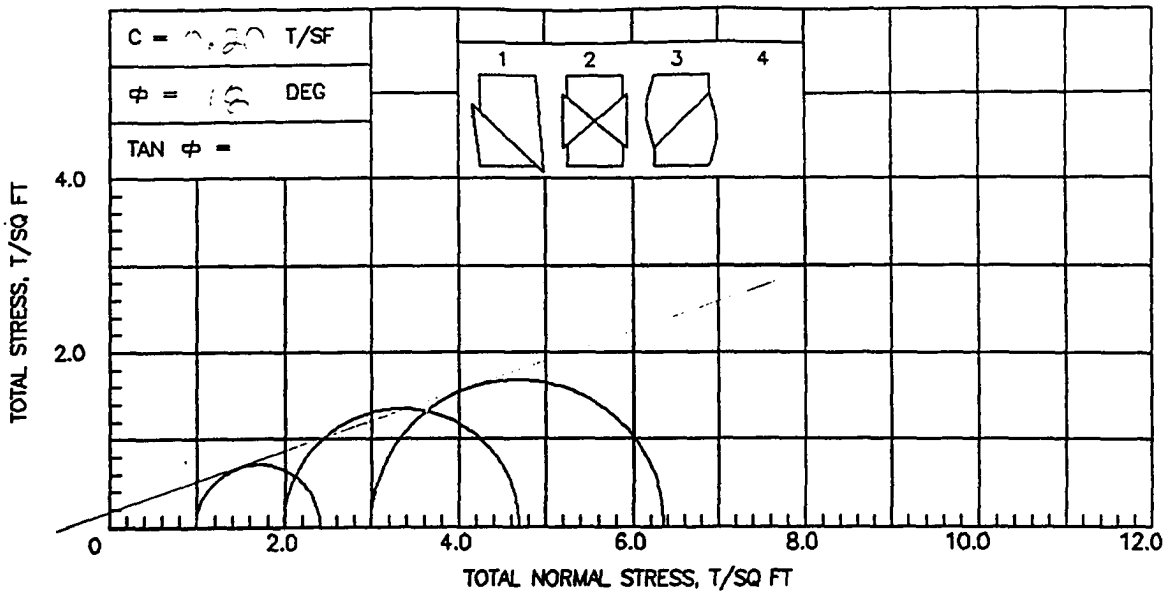

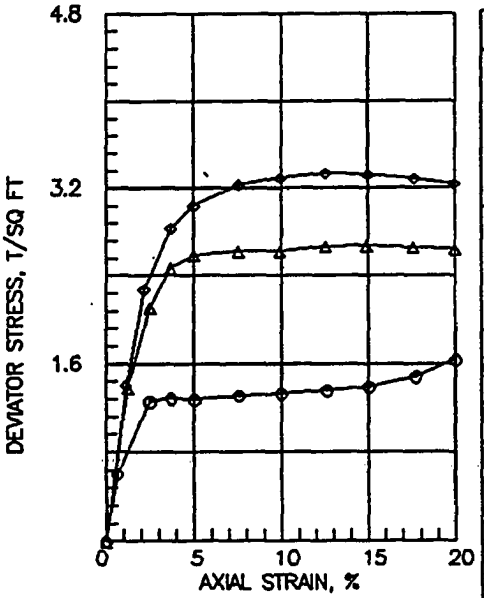

SPECIMEN NO.		○ 1	△ 2	◇ 3	4
INITIAL	WATER CONTENT, %	24.4	28.7	24.8	
	DRY DENSITY, PCF	100.2	101.0	100.2	
	SATURATION, %	96.5	100+	98.2	
	VOID RATIO	.683	.668	.682	
BEFORE SHEAR	WATER CONTENT, %	26.0	25.2	24.9	
	DRY DENSITY, PCF	102.2	104.2	103.6	
	SATURATION, %	100+	100+	100+	
	VOID RATIO	.650	.617	.626	
	BACK PRESS., TSF	4.32	4.32	4.32	
MIN. PRIN. STRESS, TSF		1.00	2.00	3.00	
MAX. DEV. STRESS, TSF		1.39	2.68	3.34	
TIME TO FAILURE, MIN.		960	948	803	
RATE OF STRAIN, %/MIN		.016	.016	.016	
INITIAL DIAMETER, IN.		1.36	1.36	1.36	
INITIAL HEIGHT, IN.		3.00	3.00	3.00	

CONTROLLED-STRAIN TEST

DESCRIPTION OF SPECIMENS: V. FINE GR CLAY (CL), BROWN, TR SAND

LL 41	PL 19	PI 22	GS 2.70 (ESTIMATED)	UNDISTURBED SPECIMEN	$\bar{R}$ TEST

REMARKS:	PROJECT USARO/WMU	
	R TEST 5, MIAMI PARK	
	BORING NO. MP-1	SAMPLE NO. 2
	DEPTH/ELEV 40-42	TECH. WWM
	LABORATORY USAE WES - STF/GL	DATE 02 OCT 96
	$\bar{R}$-TRIAXIAL COMPRESSION TEST REPORT	

BASED ON MAX. STRESS RATIO

C ' = ~ T/SF

φ' = 20 DEG

TAN φ' =

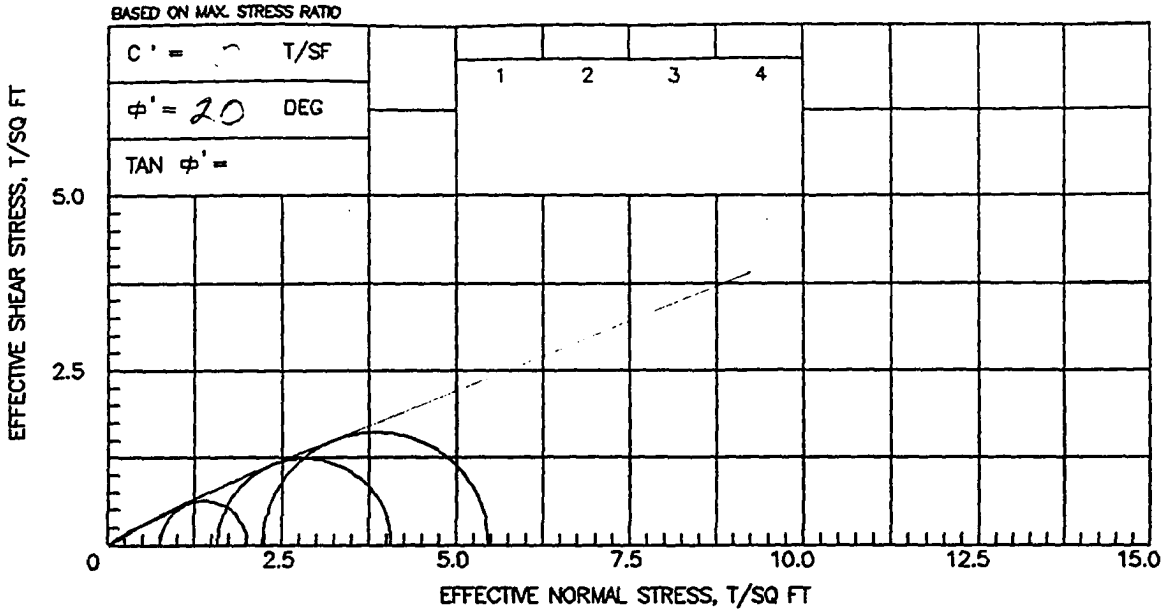

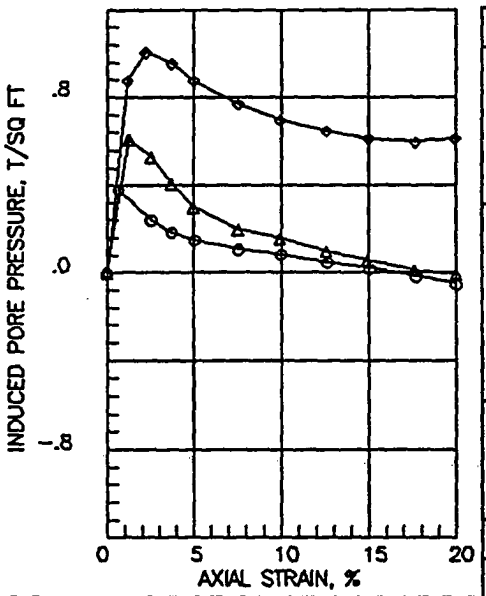

SPECIMEN NO.		⊙ 1	△ 2	◇ 3	4
INITIAL	WATER CONTENT, %	24.4	28.7	24.8	
	DRY DENSITY, PCF	100.2	101.0	100.2	
	SATURATION, %	96.5	100+	98.2	
	VOID RATIO	.683	.668	.682	
BEFORE SHEAR	WATER CONTENT, %	26.0	25.2	24.9	
	DRY DENSITY, PCF	102.2	104.2	103.6	
	SATURATION, %	100+	100+	100+	
	VOID RATIO	.650	.617	.626	
	BACK PRESS., TSF	4.32	4.32	4.32	
σ_1'/σ_3' MAX	MIN PRIN EFF STRESS, TSF	.76	1.59	2.23	
	DEV. STRESS, TSF	1.26	2.47	3.23	
	TIME TO FAILURE, MIN.	159	234	481	
RATE OF STRAIN, %/MIN		.016	.016	.016	
INITIAL DIAMETER, IN.		1.36	1.36	1.36	
INITIAL HEIGHT, IN.		3.00	3.00	3.00	

CONTROLLED-STRAIN TEST

DESCRIPTION OF SPECIMENS: V. FINE GR CLAY (CL), BROWN, TR SAND

LL 41	PL 19	PI 22	GS 2.70 (ESTIMATED)	UNDISTURBED SPECIMEN	$\bar{R}$ TEST

REMARKS:

PROJECT USARO/WMU

R TEST 5, MIAMI PARK

BORING NO. MP-1 SAMPLE NO. 2

DEPTH/ELEV 40-42 TECH. WWM

LABORATORY USAE WES - STF/GL DATE 02 OCT 96

$\bar{R}$-TRIAXIAL COMPRESSION TEST REPORT

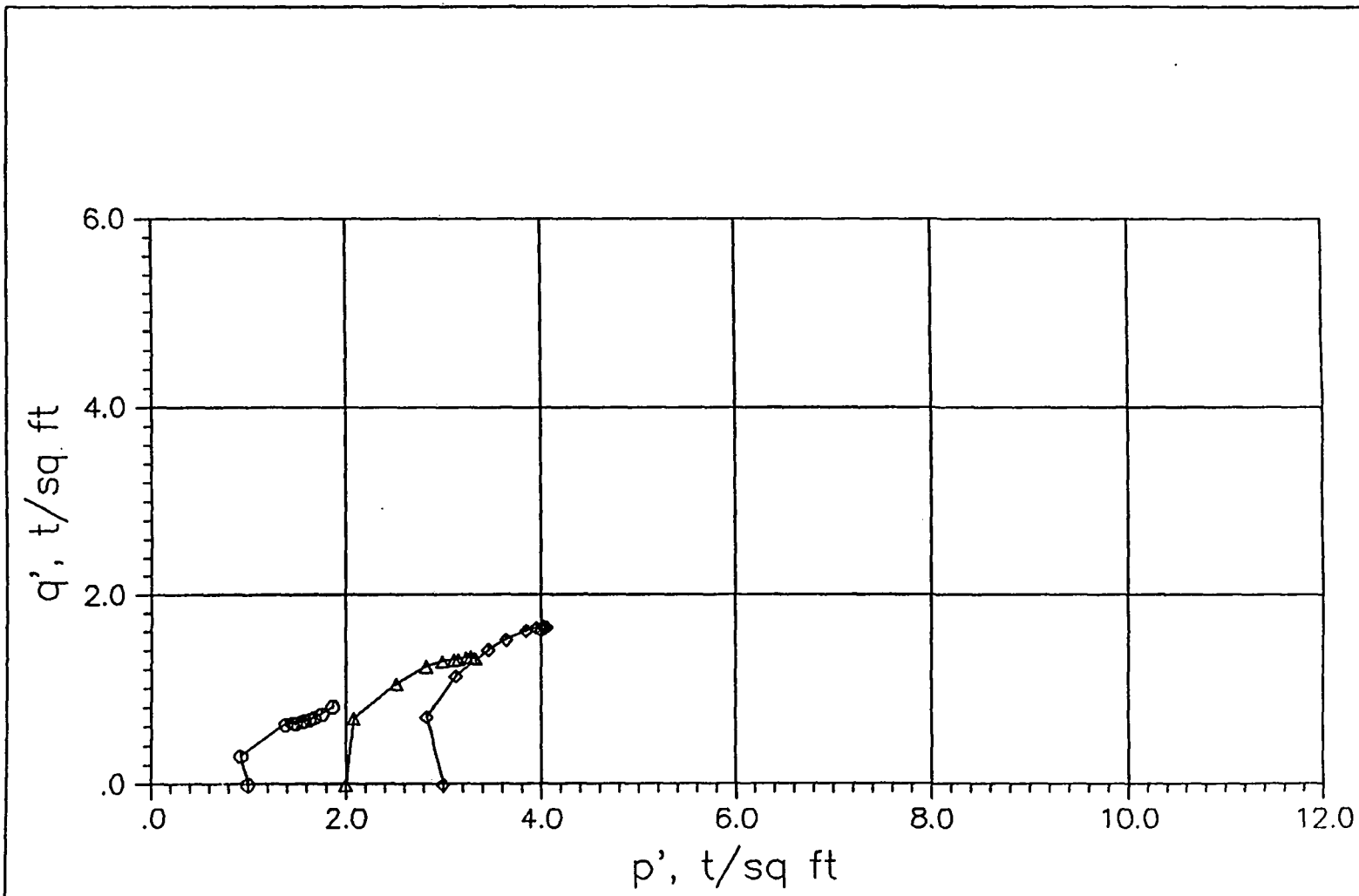

PROJECT	USARO/WMU	
	R TEST 5, MIAMI PARK	
BORING	MP-1	SAMPLE NO. 2
		DATE 02 OCT 96

Stress Paths

LABORATORY USAE WES - STF/GL

Appendix E

Overconsolidation Ratio Data

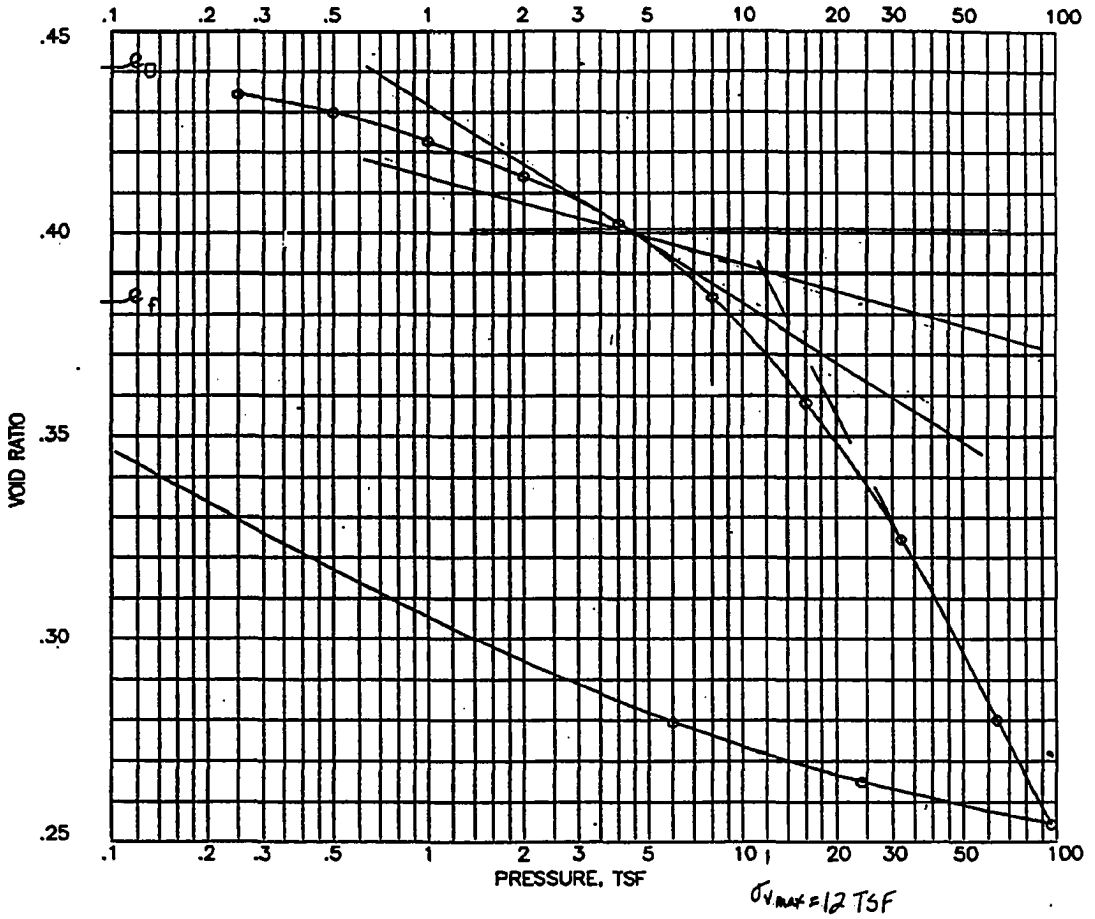

			BEFORE TEST	AFTER TEST
OVERBURDEN PRESSURE, TSF		WATER CONTENT, %	16.4	16.3
PRECONSOL. PRESSURE, TSF		DRY DENSITY, PCF	117.0	121.9
COMPRESSION INDEX		SATURATION, %	100 +	100 +
TYPE SPECIMEN	UNDISTURBED	VOID RATIO	.441	.383
DIA. IN 2.50	HT. IN 1.243	BACK PRESSURE, TSF		
CLASSIFICATION	SANDY SILTY CLAY (CL), GRAY			
LL / PL / PI		PROJECT USARO/WMU		
GS 2.70 (EST)	D_{10}			
REMARKS: $\sigma_{vo} \simeq 1$ TSF, OCR $\simeq 12$		BORING NO. MP1	SAMPLE NO. 1	
		DEPTH/ELEV 20.0–22.0	TECH.	
		LABORATORY USAE WES – STF/GL	DATE 08 OCT 96	
		CONSOLIDATION TEST REPORT		

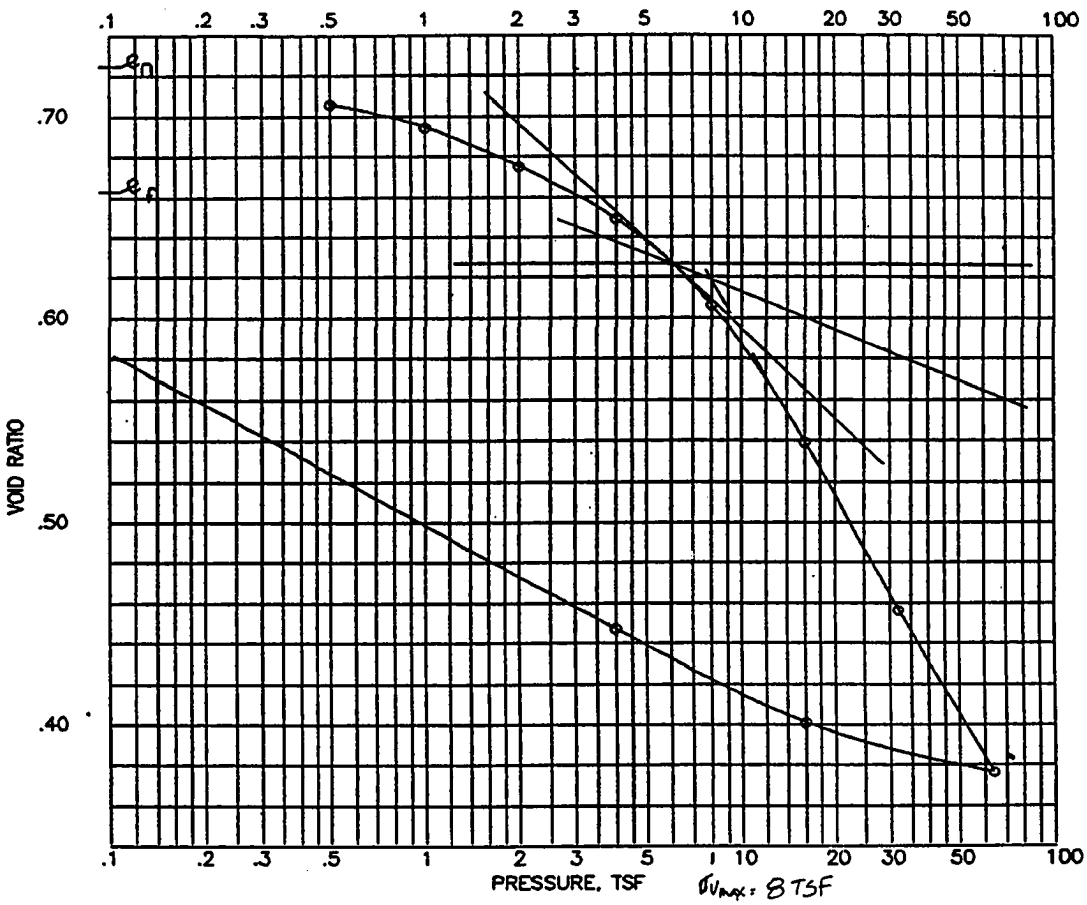

			BEFORE TEST	AFTER TEST
OVERBURDEN PRESSURE, TSF		WATER CONTENT, %	27.6	27.7
PRECONSOL. PRESSURE, TSF		DRY DENSITY, PCF	97.8	101.4
COMPRESSION INDEX		SATURATION, %	100 +	100 +
TYPE SPECIMEN: UNDISTURBED		VOID RATIO	.724	.662
DIA. IN 2.50	HT. IN 1.258	BACK PRESSURE, TSF		
CLASSIFICATION: CLAY (CH), DARK BROWN				
LL	PL / PI	PROJECT: USARO/WMU		
GS 2.70 (EST)	D_{10}			
REMARKS: SWELL PRESSURE = 0.3 TSF		BORING NO. MP1	SAMPLE NO. 2	
$\sigma_{v_0} \simeq 2$ TSF; OCR $\simeq 4$		DEPTH/ELEV 40.0–42.0	TECH.	
		LABORATORY USAE WES – STF/GL	DATE 08 OCT 96	
		CONSOLIDATION TEST REPORT		

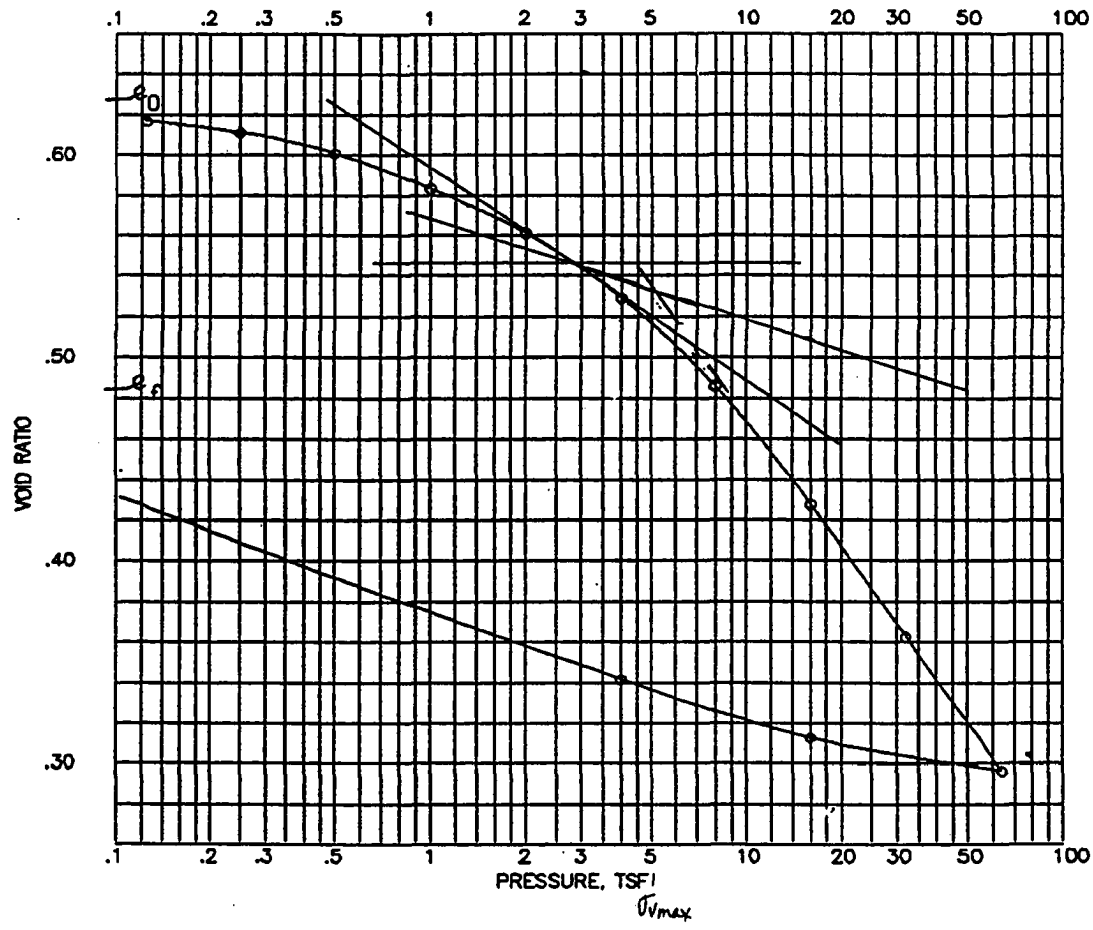

	BEFORE TEST	AFTER TEST
OVERBURDEN PRESSURE, TSF	WATER CONTENT, %	23.6	20.8
PRECONSOL. PRESSURE, TSF	DRY DENSITY, PCF	103.6	113.6
COMPRESSION INDEX	SATURATION, %	100 +	100 +
TYPE SPECIMEN: UNDISTURBED	VOID RATIO	.627	.484
DIA. IN 2.50 — HT. IN 1.276	BACK PRESSURE, TSF		
CLASSIFICATION: CLAY (CH), DARK BROWN			
LL — PL — PI	PROJECT: USARO/WMU		
GS 2.70 (EST) — D_{10}			
REMARKS: $\sigma_{vo} \simeq 4$ TSF. OCR ≃ 1.25 (or NC)	BORING NO. MP1	SAMPLE NO. 4
	DEPTH/ELEV 80.0–82.0	TECH.
	LABORATORY USAE WES – STF/GL	DATE 08 OCT 96
	CONSOLIDATION TEST REPORT	

Appendix F

1938, 1989, and 1996 Airphoto Mosaics

Northern Area – Allegan County

1996 Natural Color Photography

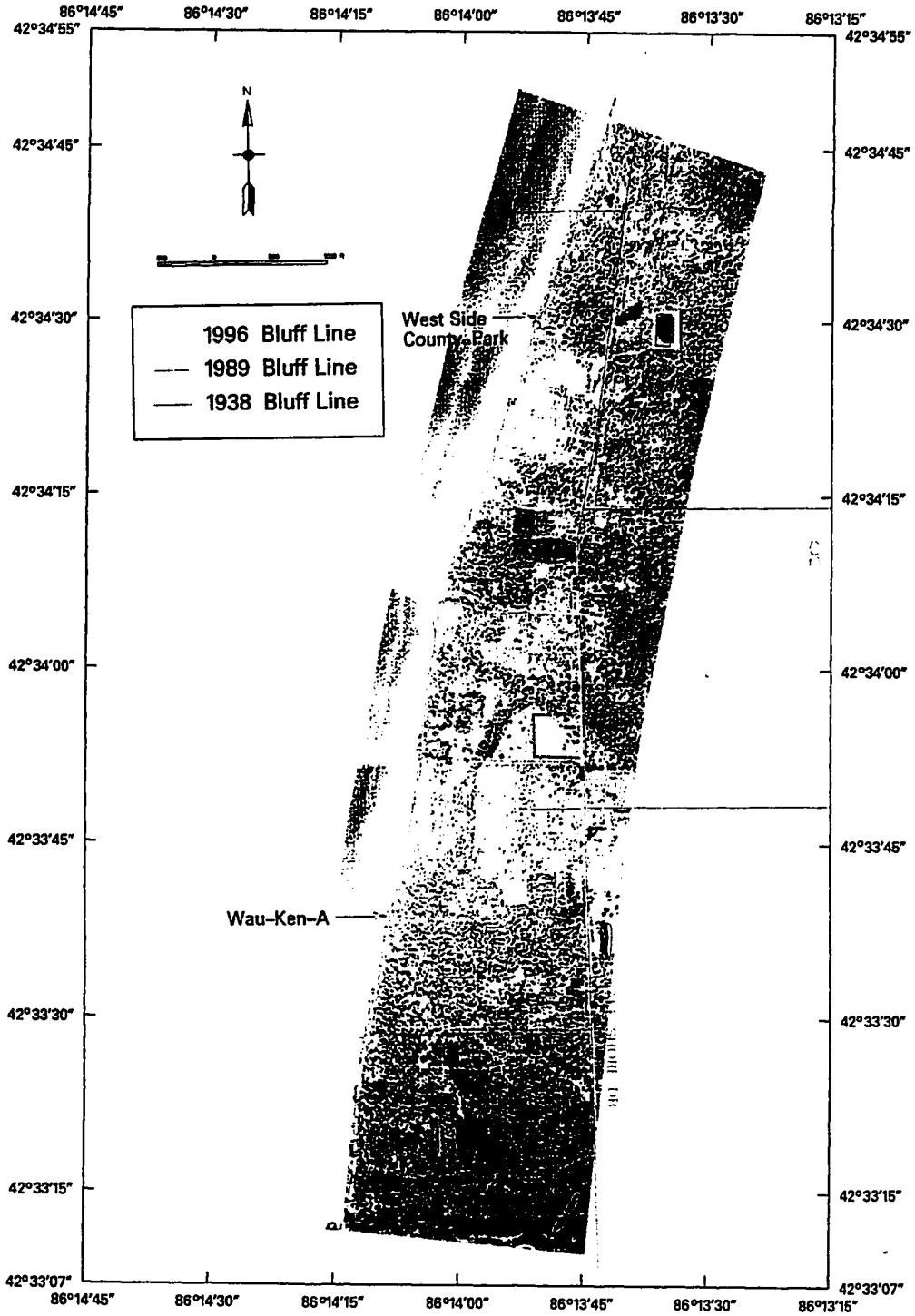

Central Area – Allegan County

1989 Natural Color Photography

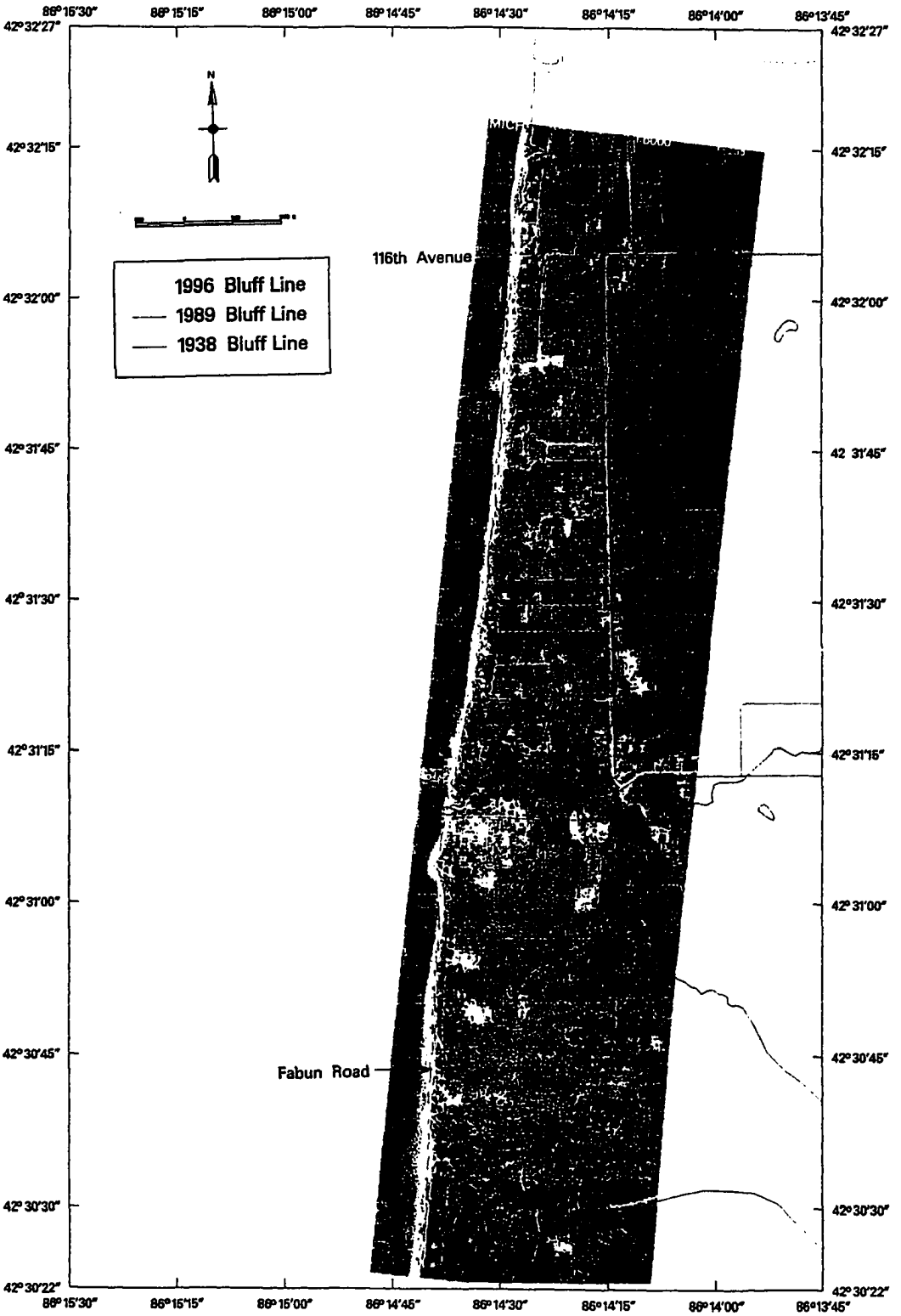

Southern Area – Allegan County

1996 Natural Color Photography

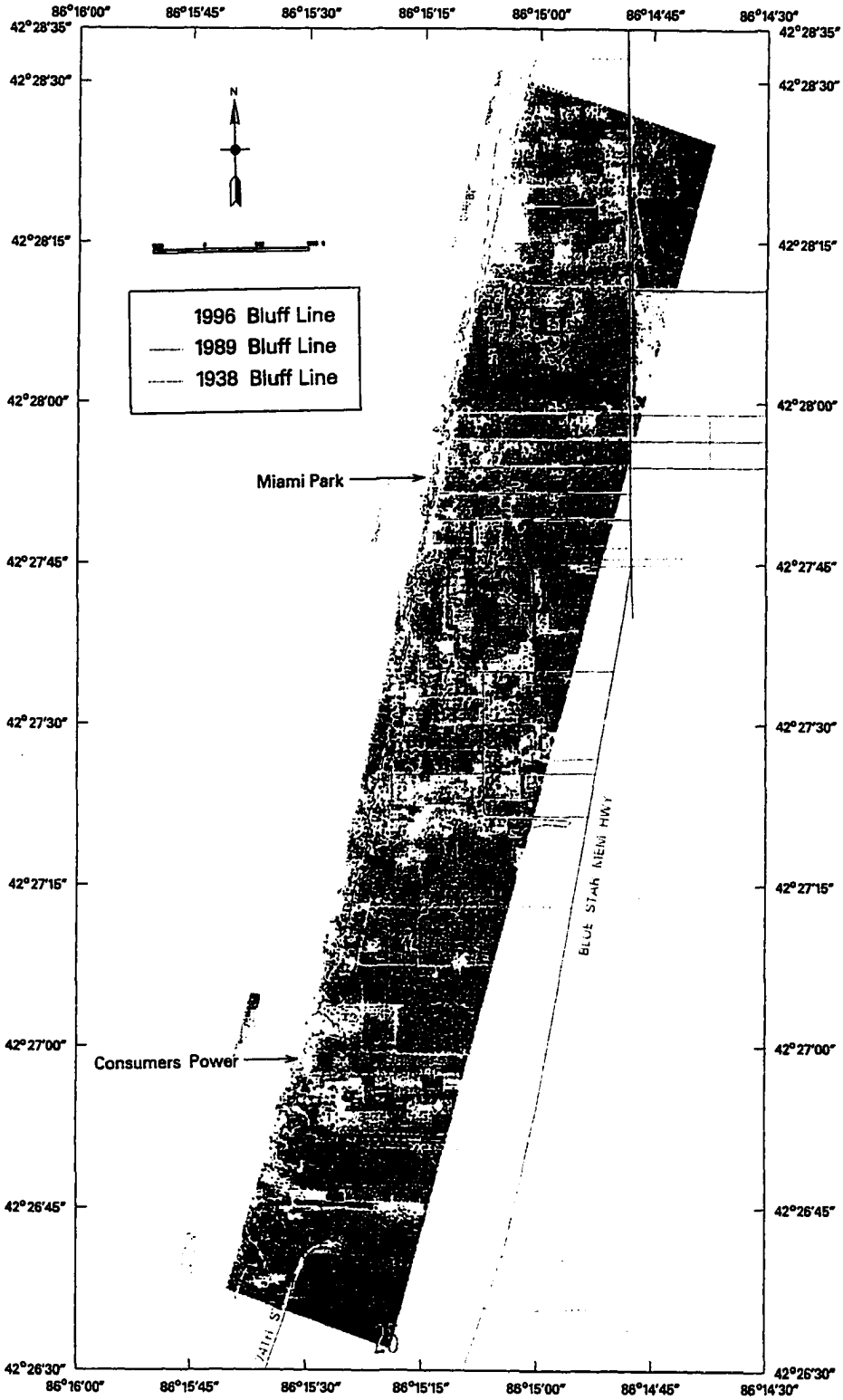

Northern Area – Allegan County

1989 Natural Color Photography

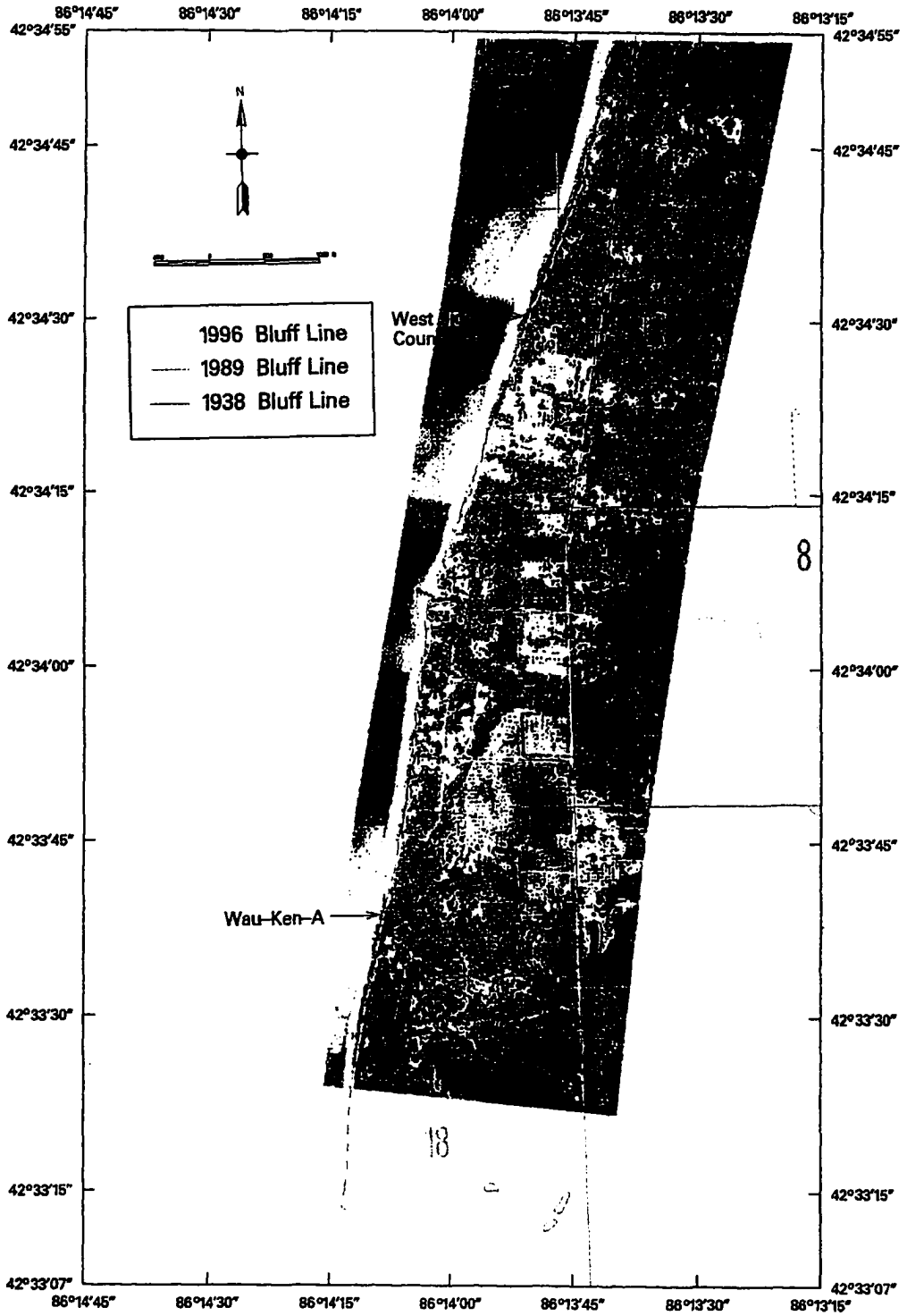

Central Area – Allegan County

1989 Natural Color Photography

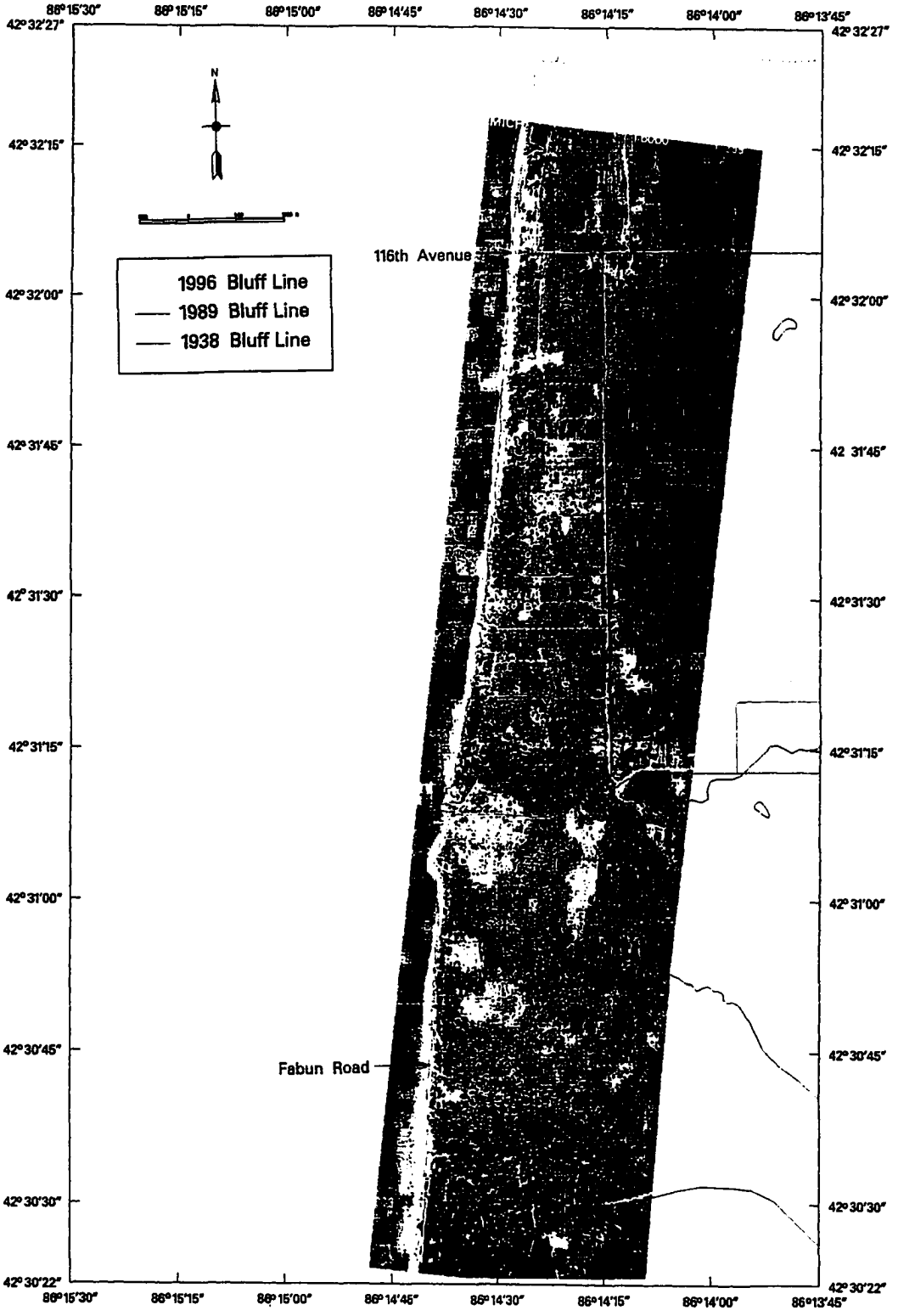

Southern Area – Allegan County

1989 Natural Color Photography

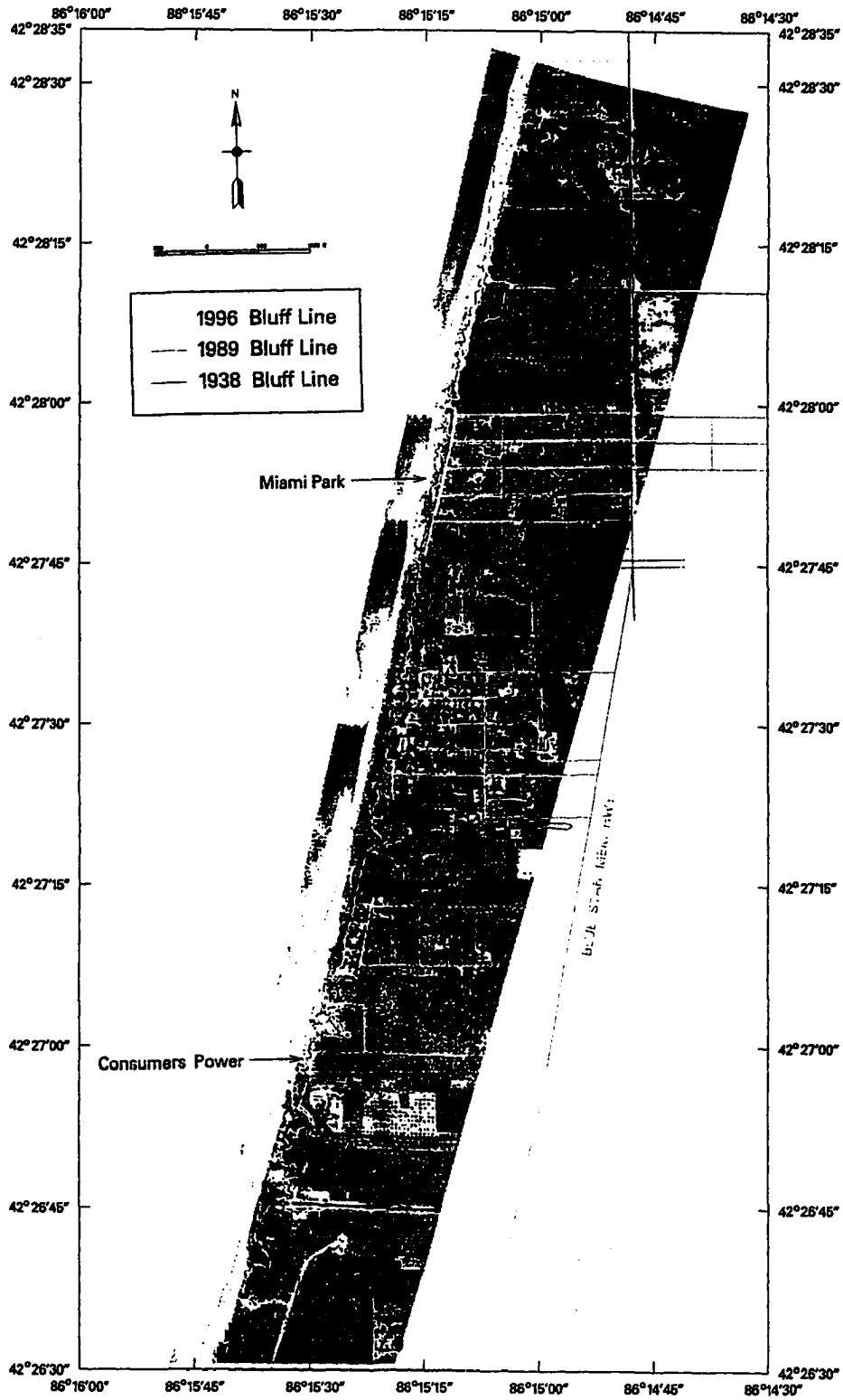

Northern Area – Allegan County

1938 Black and White Photography

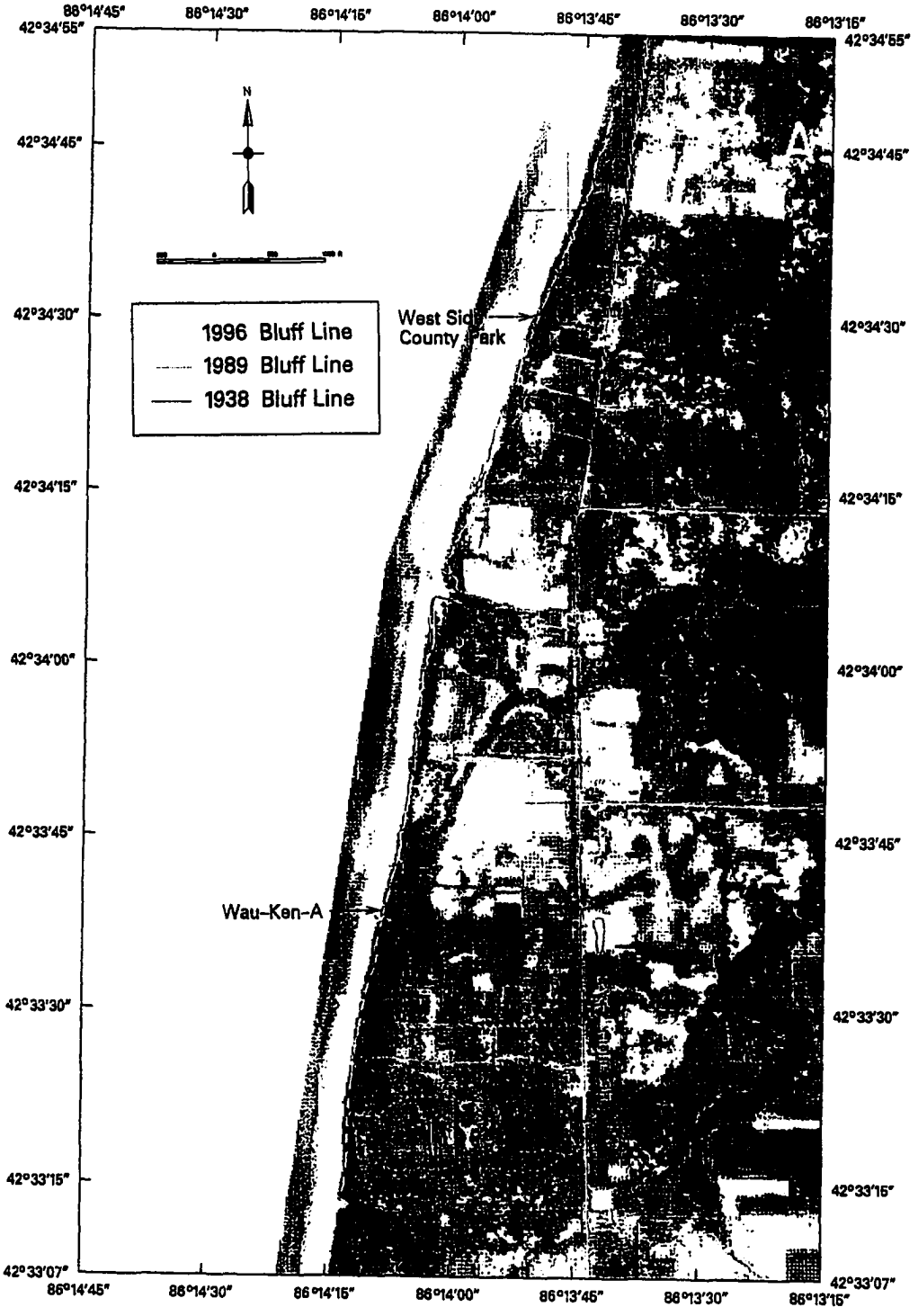

Central Area – Allegan County

1938 Black and White Photography

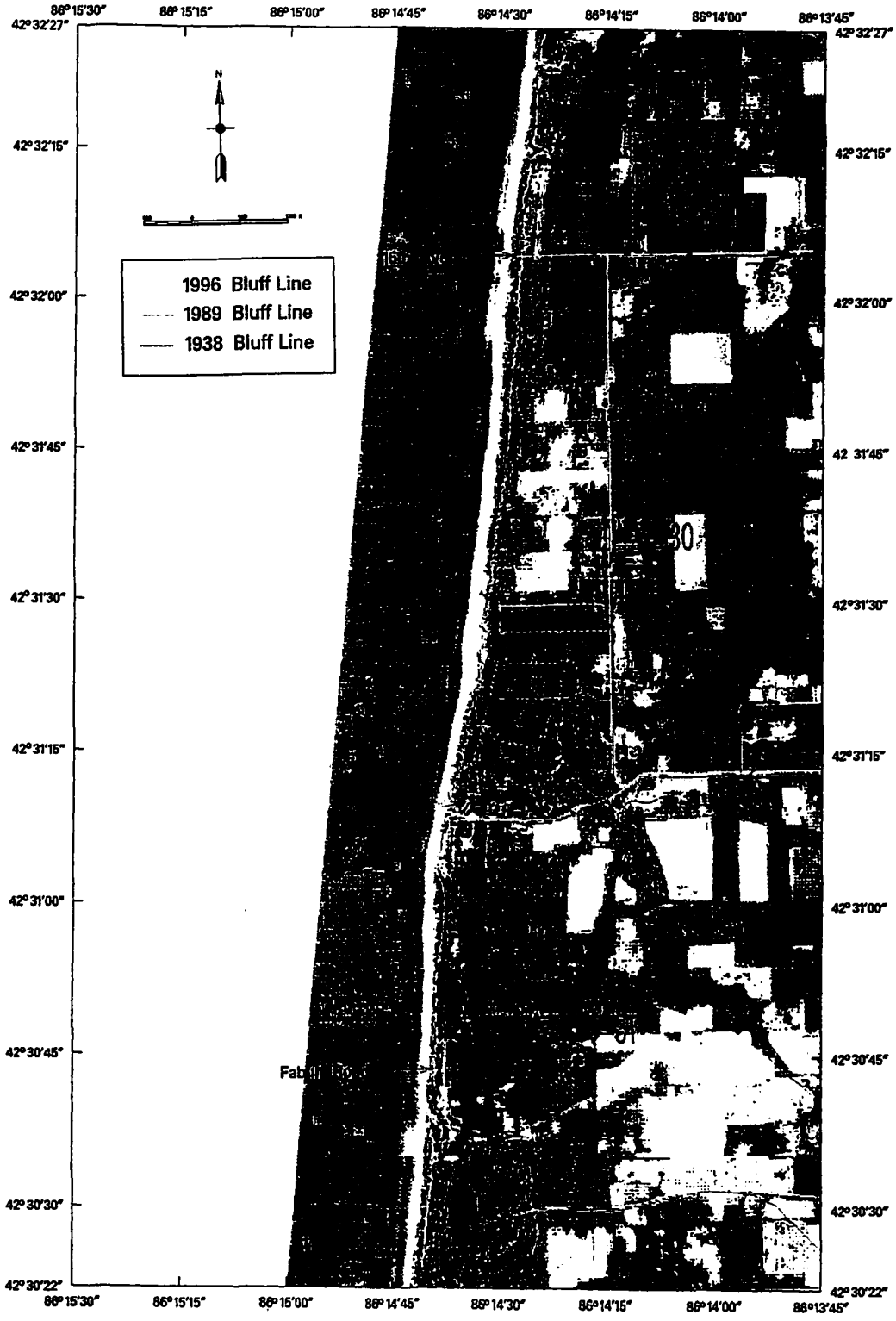

Southern Area – Allegan County

1938 Black and White Photography

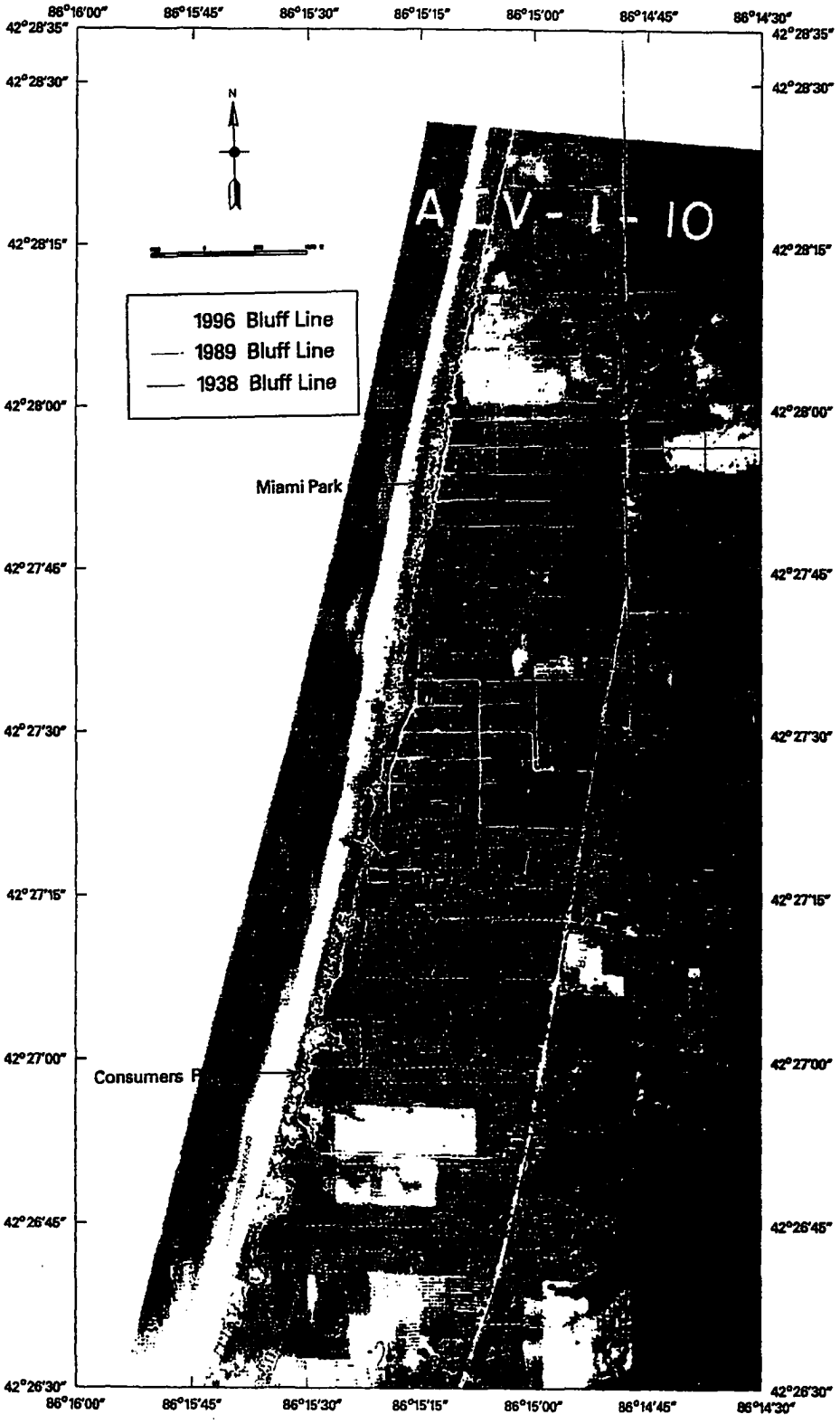

BIBILIOGRAPHY

Anders, F. J., and M. R. Byrnes, 1991, "Accuracy of shoreline change rates as determined from maps and aerial photographs", Shore and Beach, v. 59, pp. 17-26.

Andrews, Edmund, 1870, "The North American lakes considered as chronometers of post-glacial Time", Trans. Chicago Academy of Science, v. II, pp.1-24.

Avery, T. F. and G. L. Berlin, 1985, Interpretation of Aerial Photographs, 4th ed., Burgess, 554 p.

Birkemeier, W. A., 1980, The effect of structures and lake levels on bluff and shore erosion in Berrien County, Michigan 1970-74, CERC Miscelleneous Report 80-2, U. S. Army Corps Engineers, 74 p.

Birkemeier, W. A., 1981, Coastal changes, eastern Lake Michigan, 1970-74, CERC Miscellaneous Report 81-2, U. S. Army Corps Engineers, 89 p.

Bishop, A. W., 1955, "The use of the slip circle in the stability analysis of slopes", Geotechnique, v. 5, pp. 7-17.

Bishop, A. W. and D. J. Henkel, 1962, The Measurements of Soil Properties in the Triaxial Test, Edward Arnold, London, 227 p.

Boyd, G. L., 1992, A descriptive model of shoreline development showing nearshore control of coastal landform change: Late Wisconsinan to present, Lake Huron, Canada, unpublished Ph.D. dissertation, University of Waterloo, 206 p.

Bruun, P., 1962, "Sea level rise as a cause of shore erosion", Journal of Waterways and Harbors Division, ASCE, v. 88, pp. 117-130.

Buckler, W. R., 1973, Bluff Erosion at selected sites along the southeastern shore of Lake Michigan, unpublished M.A. research paper, Michigan State University Dept. of Geography, 61 p.

Buckler, W. R., 1983, "Lake Michigan Bluff Recession", Annals of Association of American Geographers, v. 73, pp. 89-110.

Buckler, W. R., 1987, "High water levels and bluff recession: Lake Michigan's southeast shore", East Lakes Geographer, v. 22, pp. 157-177.

Buckler, W. R. and J. P. LaMoe, 1988, "Bluff crest recession along the southwest shore of southern Michigan", Midwest Friends of the Pleistocene Field Conference Guide, pp. 51-60.

Buckler, W. R. and H. A. Winters, 1975 "Rates of bluff recession at selected sites along the southeastern shore of Lake Michigan", Michigan Academician, v. 8, pp. 179-186.

Casagrande, A.,1936, "The determination of the preconsolidation load and its practical significance", Proc. 1st Int'l. Conf. Soil Mechanics Found. Engr., p. 60

Casagrande, A., 1948, "Classification and Identification of Soils", Trans. ASCE, v. 113, p. 901.

Chamberlin, T. C., 1877, "Geology of Wisconsin", pp. 219-233.

Chapman, J. A., 1996, Predictive Capability of Shoreline Analysis Methods for Lake Michigan Shoreline Slopes, unpublished M.S. thesis, Dept. Civil & Environmental Engineering, University of Wisconsin-Madison, 203 p.

Chase, R. B., 1990, A structural analysis of fractures in clay-rich tills of Southwestern Michigan, Technical Report, Institute of Water Sciences, Western Michigan University, 60 p.

Chase, R. B., W. W. Montomgery, A. E. Kehew, 1996, Degradations of slopes composed of clay-rich till: Relationships between ground-water activity and accelerated mass movements: Geological Society of America Abstracts with Programs, v. 28, no. 7.

Costa, J. E. and V. R. Baker, 1977, Surficial Geology - Building with the Earth, Tech Books, 498 p.

Crowell, M., S. P. Leatherman, and M. K. Buckley, 1991, "Historical shoreline change: Error analysis and mapping accuracy", Journal of Coastal Research, v. 7, pp. 838-852.

Davidson-Arnott, R. D. G., 1986, "Rates of erosion of till in the nearshore zone", Earth Surface Processes and Landforms, v. 11, pp. 53-58.

Davidson-Arnott, R. D. G. and J. Ollerhead, 1995, "Nearshore erosion on a cohesive shoreline", Marine Geology, v. 122, pp. 349-365.

Davis, R. A., 1976, Coastal changes, eastern Lake Michigan, 1970-73, CERC Technical Paper No. 76-16, U. S. Army Corps of Engineers, 64 p.

Davis, R. A., W. G. Fingleton, and P. C. Pritchett, 1975, Beach profile changes: east coast Lake Michigan, 1970-72, CERC Miscellaneous Paper No. 10-75, U. S. Army Corps of Engineers.

Davis, R. A. and W. T. Fox, 1971, Beach and nearshore dynamics in eastern Lake Michigan, Technical Report No. 4, Office of Naval Research, 145 p.

Dean, R. G., 1977, Equilibrium beach profiles: U. S. Atlantic and Gulf Coasts, Technical Report 12, University of Delaware, 45 p.

Dean, R. G., 1983 "Principles of beach nourishment", in Komar, P. D., ed., CRC Handbook of Coastal Processes, CRC Press, 305 p.

Edil, T. B., 1974, Laboratory investigation of the shear strength of two clays from Appleton, Wisconsin, University of Wisconsin Soil Mechanics Lab. Technical Report No. 1.

Edil, T. B., 1975, Laboratory investigation of the shear strength of two clays from Kimberly, Wisconsin, University of Wisconsin Soil Mechanics. Lab. Technical Report No. 2.

Edil, T. B. and P. J. Bosscher, 1988, "Lake shore erosion processes and control", Proceedings of 19th Conference of Int'l Erosion Control Assoc., New Orleans, LA, pp. 1-18.

Edil, T. B. and B. J. Haas, 1980, "Proposed criteria for interpreting stability of lakeshore bluffs", Engineering Geology, v. 16, pp. 97-110.

Edil, T. B. and D. M. Mickelson, 1995, "Overconsolidated glacial tills in eastern Wisconsin", *in* Engineering Properties and Practice in Overconsolidated Clays, Transportation Research Record No. 1479, pp. 99-106.

Edil, T. B., D. M. Mickelson, and L. J. Acomb, 1977, "Relationship of geotechnical properties to glacial stratigraphic units along Wisconsin's Lake Michigan shoreline", *in* Proceedings of Canadian Geotechnical Conference, pp. II-36-54.

Edil, T. B. and L. E. Vallejo, 1977, Shoreline erosion and landslides in the Great Lakes, Wisconsin Sea Grant Advisory Report 15, 7 p.; also *in* Proceedings 9th Int'l Conference Soil Mechanics & Foundation Engineering, Tokyo, Japan, v. II, pp. 51-57.

Edil, T. B. and L. E. Vallejo, 1980, "Mechanics of coastal landslides and the influence of slope parameters", Marine Geology, v. 16, pp. 83-96.

Edris, E. V. Jr., and S. G. Wright, 1992, Users Guide: UTEXAS3 Slope Stability Package, Vol. IV: User's Manual, Instruction Report GL-87-1, USACE, Vicksburg, MS, 203 p.

Farrand, W. R. and D. L. Bell, 1982, Quaternary Geology of Southern Michigan, University of Michigan, Ann Arbor, MI, 1 Plate.

Fellenius, W., 1936, "Calculation of the stability of earth dams", Second Congress on Large Dams, Washington, D.C. v. 4, p. 445.

Gelinas, P. J., 1974, Contributions to erosion studies, Lake Erie north shore, unpublished Ph.D. dissertation, University of Western Ontario, 264 p.

Gelinas, P. J. and R. M. Quigley, 1973, "The influence of geology on erosion rates along the north shore of Lake Erie", Proceedings 16th Int'l Conf. on Great Lakes Research, Int'l. Association for Great Lakes Research, pp. 421-430.

Gephardt, G. D., G. W. Monaghan, and G. J. Larson, 1982, " A mid-Wisconsin event in the Lake Michigan Basin" (abs.), Geological Society of America Abstracts with Programs, v. 14, p. 260.

Gephardt, G. D., G. W. Monaghan, and G. J. Larson, 1983, " Stratigraphic evidence for a significant readvance of the Michigan ice lobe to the Kalamazoo moraine, southwestern Michigan" (abs.), Geological Society of America Abstracts with Programs, v. 15, p. 161.

Goldthwait, James W., 1907, Abandoned shorelines of eastern Wisconsin, Wisconsin Geology and Natural History Survey Bulletin 17, p. 58.

Hands, E. B., 1979, Changes in rates of shore retreat, Lake Michigan, 1967-76, CERC Technical Paper 79-4, U. S. Army Corps Engineers, 71 p.

Hands, E. B., 1980, Prediction of shore retreat and nearshore profile adjustments to rising water levels on the Great Lakes, CERC Tech. Paper 80-7, U. S. Army Corps Engineers, 119 p.

Hands, E. B., 1983, "Erosion of the Great Lakes due to changes in water level" in Komar, P.D., ed., CRC Handbook of Coastal Processes, CRC Press, 305 p.

Hansel, A. K., D. M. Mickelson, A. F. Schneider, and C. E. Larsen, 1985, "Late Wisconsinan and Holocene history of the Lake Michigan Basin", *in* Karrow, P. F., and P.E. Calkin, eds., Quaternary Evolution of the Great Lakes, Geological Association of Canada Spec. Paper 30, pp. 39-53.

Hvorslev, M. J., 1949, Subsurface exploration and sampling of soils for civil engineering purposes, Vicksburg, MS, USACE Waterways Experiment Station, 521 p.

Janbu, N., 1954, Stability analysis of slopes with dimensionless parameters, Harvard Soil Mechanics. Series No. 46.

Jibson, R. W. and J-M Staude, 1991, Bluff recession rates along the Lake Michigan shoreline in Illinois, United States Geol. Survey Open-File Rept 91-583, 16 p.

Johnson, B. L. and C. A. Johnston, 1995, "Relationship of lithology and geomorphology to erosion of the western Lake Superior coast", Journal of Great Lakes Research, v. 21, pp. 3-16.

Kamphuis, J. W., 1983, "On the erosion of consolidated clay material by fluid containing sand", Canadian Journal of Civil Engineering., v. 10, pp. 223-231.

Kamphuis, J. W., 1987, "Recession rate of glacial till bluffs", Journal Waterway, Port, Coastal, and Ocean Engineering, v. 113, pp. 60-73.

Lambe, T. W. and R. V. Whitman, 1969, Soil Mechanics, Wiley and Sons, New York, 553 p.

Law, M. N., K. E. Saunders, D. E. Coleman, J. D. Fisher, R. van Wyngaarden, G. L. Boyd, and C. J. Stewart, 1991, "Using GIS to monitor and predict long-term Great Lakes shoreline erosion", Proc. 1991 Canadian Conference on GIS, Ottawa, pp. 372-386.

Leatherman, S. P., 1983, "Shoreline Mapping: A Comparison of Techniques", Shore and Beach, v. 51, pp. 28-33.

Lillesand, T. M. and R. W. Kiefer, 1994, Remote Sensing and Image Interpretation, 3rd ed., Wiley and Sons, 750 p.

Mayne, P. W., R. D. Holtz, and Mehmet T. Tumay, 1995, "U.S. state of the practice in sampling and strength testing of overconsolidated clays", *in* Engineering Properties and Practice in Overconsolidated Clays, Transportation Research Record No. 1479, pp. 1-16.

McCarthy, D. F., 1993, Essentials of Soil Mechanics and Foundations, 4th ed., New Jersey, Prentice-Hall, 618 p.

McManis, K. L. and D. E. Lourie, 1995, "Issues and techniques for sampling overconsolidated clays", *in* Engineering Properties and Practice in Overconsolidated Clays, Transportation Research Record No. 1479, pp. 7-16.

Meadows, L., G. Meadows, B. Haus, J. Pazdalski, A. Koengeter, 1991, Coastal monitoring program and shoreline evolution model year three: Report to the State of Michigan Department of Natural Resources, University of Michigan Ocean Engineering Lab. Report OEL-9102-LWMD-10C-5.

Mickelson, D. M., L. J. Acomb, T. B. Edil, C. Fricke, B. Haas, D. Hadley, C. Hess, R. Klauk, N. Lasca, and A. F. Schneider, 1977, Shore erosion study technical report, Wisconsin Coastal Management Program, Wisconsin Geological and Natural History Survey, 197 p.

Monaghan, G. W., 1990, "Systematic variation in the clay-mineral composition of till sheets; Evidence for the Erie Interstade in the Lake Michigan basin" Geological Society of America Special Paper 251, pp. 43-50.

Monaghan, G. W., and G. J. Larson, 1986, "Late Wisconsinan drift stratigraphy of the Saginaw ice lobe in south-central Michigan", Geological Society of America Bulletin, v. 97, pp. 324-328.

Montgomery, W. W., R. B. Chase, A. E. Kehew, G. P. Anderson, 1996, "Stability of the Lake Michigan Shore, Allegan Co., Michigan - A Preliminary Hazard Map", Geological Society of America Abstracts with Programs, Denver, CO p 464.

Montgomery, W. W., R. B. Chase, A. E. Kehew, 1996, "Degradation of Slopes Composed of Clay-Rich Till: Relationships Between Ground-Water Activity and Accelerated Mass Movements", Geological Society of America Abstracts with Programs, Denver, CO p. 157.

Montgomery, W. W., R. B. Chase, A. E. Kehew, G. P. Anderson, 1997, "Relationships between lithology, hydraulic head, and shoreline recession on the eastern shore of Lake Michigan", Geological Society of America Abstracts with Programs, Salt Lake City, UT.

Morgenstern, N. R. and V. E. Price, 1965, "The analysis of the stability of general slip surfaces", Geotechnique, v.15.

Muldoon, M. A., K. R. Bradbury, D. M. Mickelson, and J. W. Attig, 1988, Hydrogeologic and geotechnical properties of Pleistocene materials in north-central Wisconsin, Wisconsin Water Resources Center Report 88-03, 58 p.

Nairn, R. B., 1992, Erosion processes evaluation paper - final report, Int'l Joint Commission, Great Lakes - St. Lawrence River Levels Reference Study Board, 165 p.

Philpott, K. L., 1984, "Comparison of cohesive coasts and beach coasts", Coastal Engineering in Canada Conference, Queens University, Kingston, Ontario, pp. 227-224.

Powers. W. E., 1958, Geomorphology of the Lake Michigan Shoreline, Final Report of Project No. NR 387-015, Office of Naval Research 103 p.

Quigley, R. M., and P. J. Gelinas, 1976, "Soil mechanics aspects of shoreline erosion", Geoscience Canada, v. 3, pp. 169-173.

Quigley, R. M., P. J. Gelinas, W. T. Bou, and R. W. Packer, 1977, "Cyclic erosion-instability relationships: Lake Erie north shore bluffs", Canadian Geotechnical Journal v. 14, pp. 310-323.

Raphael, C. N. and E. J. C. Kureth, 1988, "Bluff line recession and economic loss in coastal Berrien Co., Michigan, Institute for Community and Regional Development, Eastern Michigan University, 131 p.

Seibel, E. A., 1972, Shore erosion at selected sites on Lake Michigan and Lake Huron, unpublished Ph.D. dissertation, University of Michigan, 175 p.

Stafford, D. B., and J. Langfelder, 1971, "Air photo survey of coastal erosion", Photogrammetric Engineering, v. 37, pp. 565-575.

Sterrett, R. J., 1980, Factors and mechanics of bluff erosion on Wisconsin's Great Lakes shorelines, unpublished Ph.D. dissertation, University of Wisconsin-Madison, 372 p.

Sunamura, T., 1983, "Processes of sea cliff and platform erosion", *in* Komar, P. D., ed., CRC Handbook of Coastal Processes, CRC Press, 305 p.

Taylor, D. W., 1948, Fundamentals of Soil Mechanics, New York, Wiley and Sons, 700 p.

Terzaghi, K., 1936, "Relation between soil mechanics and foundation engineering", Proceedings of the1st Int'l Conference on Soil Mechanics and Foundation Engineering, v. 3. pp. 13-18.

Terzaghi, K. and R. B. Peck, 1968, Soil Mechanics in Engineering Practice, 2nd ed., New York, Wiley and Sons, 729 p.

United States Army Corps of Engineers, 1986, Laboratory Soils Testing, Engineering Manual EM 1110-2-1906, Washington, D.C.

United States Army Corps of Engineers, 1993, Engineering and Design Slope Stability Manual EM1110-0-1902, Washington D.C. 352 p.

Williams, S. J., K. Dodd, and K. K. Gohn, 1991, Coasts in Crisis, 1991, U.S. Geological Survey Circular 1075, 32 p.